DOCTORAL THESIS

Craniofacial morphology, adaptation, and paranasal pneumatisation in Pleistocene hominins

Buck, Laura

Award date:
2014

Awarding institution:
University of Roehampton

Craniofacial morphology, adaptation, and paranasal pneumatisation in Pleistocene hominins

Laura Tabitha Buck

A thesis in partial fulfilment of the requirements for the degree of PhD

Department of Life Sciences

University of Roehampton

2014

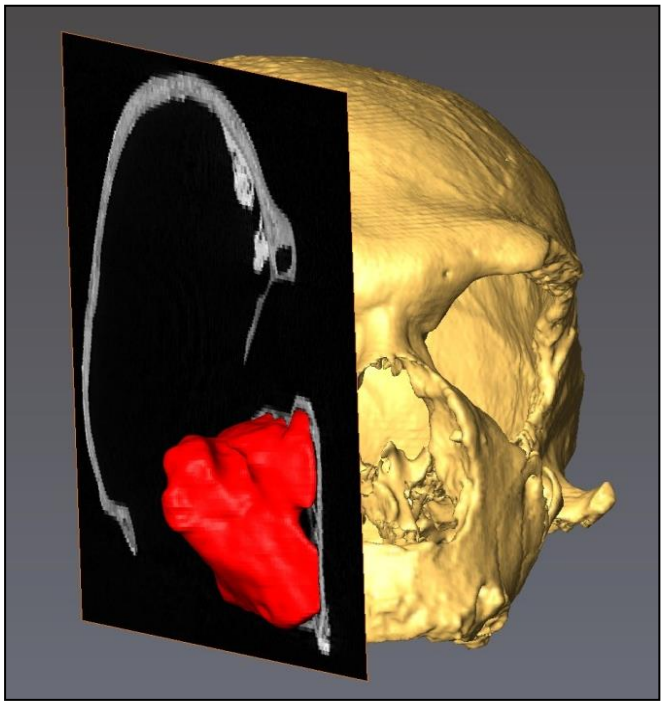

Abstract

Mid-Late Pleistocene species are reported to have sinuses of taxonomic and functional interest. Frontal hyperpneumatisation in *Homo heidelbergensis* is one of few hypothesized autapomorphies of this controversial taxon and Neanderthal sinuses are also said to be distinctively large, resulting from cold adaptation and explaining diagnostic craniofacial morphology. Variation in sinus size within and between populations of recent *H. sapiens* has been described, but has not been quantified. Sinus variables in Mid-Late Pleistocene hominins were investigated to illuminate causes of craniofacial variation and clarify alpha taxonomy, whilst evaluating theories of sinus function and advancing the understanding of adaptation in this group. Sinus volumes were measured from CT data and geometric morphometric methods were used to identify associated shape variables in a large sample of fossil and extant hominins. Relationships were investigated between these sinus variables and taxonomic/population, dietary, and climatic variables. The results demonstrate that the sinuses have no detectable direct function in Mid-Late Pleistocene hominins but they do respond to selective pressures, such as diet and climate, indirectly via craniofacial adaptation. There is also a relationship with neutral population differences in craniofacial morphology, for at least the frontal sinus. These effects are of varying strength, and it is likely that stochastic development also plays a part in determining differences in individual volumes. Inter-taxon comparisons support frontal hyperpneumatisation as a distinctive, perhaps derived, trait in *H. heidelbergensis*, but show that *H. sapiens* has *hypo*pneumatised maxillary sinuses, rather than *H. neanderthalensis* being

*hyper*pneumatised. Whilst the causes of extremely large sinuses in *H. heidelbergensis* remain uncertain, small maxillary sinuses in *H. sapiens* are suggested to result from their derived craniofacial size and morphology. These conclusions build on previous studies to over-turn long-standing but unfounded theories about the pneumatic influences on Neanderthal morphology and the functional nature of sinuses, whilst opening up exciting questions about relationships between strain, climate, pneumatisation, and intraspecific variation.

For Dad, with love and thanks.

Acknowledgements

I would like to thank the University of Roehampton for the studentship that enabled me to conduct this research, attend relevant courses, and present my work at conferences. The Centre for Evolutionary and Ecological Anthropology at the University also generously awarded me subsequent funding for research trips. I am grateful to all the help and support I have received from the Natural History Museum, particularly to Eileen Cox, as a PhD student partly based there. I would like to thank The Primate Society of Great Britain, The Leakey Trust, and the American Museum of Natural History for funding which allowed me to expand my sample. For kind permission and help in collecting my data I would like to thank Robert Kruszynski, Richie Abel, Farah Ahmed, Dan Sykes, Margaret Clegg, and Heather Bonney at the Natural History Museum; Janet Monge and Tom Schoenemann at the University of Pennsylvania; Phillipe Mennecier, Alain Fromment, and Antoine Balzeau at the Musée de l'Homme, Paris; Thomas Koppe at the Ernst-Morritz-Arndt University, Greifswald; Christoph Zollikofer at the University of Zurich; Amelie Vialet and Henry de Lumley at the Institut de Paléontologie Humaine, Paris; Giselle Garcia at the American Museum of Natural History; Giorgio Manzi at Universitá La Sapienza, Rome; Gerhard Weber at the University of Vienna; George Koufos at the Aristotle University of Thessaloniki; Luca Bondioli at the Museo Nazionale Preistorico Etnografico "Luigi Pigorini", Rome; and Andreas Pastoors at the Neanderthal Museum, Mettmann. For useful discussions, methodological help, proof reading, and patience I would like to thank Jane Buck, Rosie Buck, Laura Wilson, Louise Humphrey, Peter Shaw, Kim Plomp,

Emily Lodge, Charlotte Carne, and Julie Lawrence. I am grateful to all my officemates at Roehampton and the Natural History Museum for making most of the last five years so enjoyable, and for helping me through the bits that weren't: Astrid Willener, Emily Lodge, Nienke Alberts, Charlotte Carne, Steph Bird, Laetitia Marechal, James Munro, Shems Morrison, Kati Pourseied, Michael Thorpe, Phil Collins, Paddy Tkaczynski, Damiano Weitowitz, Aleks Trajce, Brenna Hassett, Ali Freyne, Silvia Bello, Ros Wallduck, and Mark Lewis. To Isabelle De Groote, my un-official fourth supervisor, I owe a huge debt for her humour, help, support, and unfailing generosity with her time. I would like to thank all my non-academic friends (Jess Duran and Filipe Da Silva deserve a special mention) and family for their love, support, and patience with me over the last five years, above all, thanks to my parents, without whom none of this would have been possible, nor even conceivable. Finally, I would like to thank Todd Rae, Ann MacLarnon, and Chris Stringer; they have all been fantastic supervisors and I am very grateful for their help, time, and advice throughout. In particular, I would like to thank Todd for his unshakable optimism, understanding, and belief in me over the years.

Contents

List of tables

List of Figures

Chapter 1: Introduction

This is an investigation into one particular aspect of craniofacial morphology - paranasal pneumatisation - in Mid-Late Pleistocene hominins (from approximately 800 to 12 ka [thousand years ago]). There are three broad questions of interest: whether, in this group, sinus size is taxonomically diagnostic, whether it is a determinant of craniofacial shape, and whether sinuses are functional. The relationships between sinus size and craniofacial morphology, and key ecological variables (climate and diet) and neutral evolutionary processes leading to differences between taxa/populations, are explored to address these questions. In this introduction, the reasons for undertaking the study are explained, the existing literature on the subject is described and research questions arising from this literature are stated.

1.I. Why study craniofacial morphology in Mid-Late Pleistocene hominins?

The cranium is the most suitable skeletal element through which to study hominin adaptation because of its functions, the history of its study in palaeoanthropology and the great level of variation seen in craniofacial morphology between closely related hominin species. The cranium is the most complicated skeletal component of the body and this is a reflection of its numerous functions (Lieberman, 1996; Pan & Oxnard, 2002). It houses the organs of smell, hearing, sight, balance and thought,

and it is the main interface between the interior of the body and the exterior world. As a result, it is perhaps the most crucial skeletal component for mediating interactions between the individual and the environment, meaning that it is the most informative skeletal component for reconstructing environment and behaviour. Evidence of diet (e.g., Paschetta *et al.*, 2010); climate (e.g., Beals *et al.*, 1984), vision (e.g., Pearce & Dunbar, 2011), hearing (e.g., Webster, 1966), smell (e.g., Smith *et al.*, 2007b), and encephalisation (e.g., Alba, 2010) may all be found in the cranium and from this information it may be possible to make inferences about less tangible aspects of behaviour such as sociality (Pérez-Barbería *et al.*, 2007), mating system (e.g., Plavcan, 2000), cognitive ability (e.g., Falk *et al.*, 2005), activity pattern (e.g., Kay & Kirk, 2000), and even cultural practices (e.g., Gerszten, 1993; Humphrey & Bocaege, 2008).

Crania have had a particular importance for palaeoanthropology throughout the history of the field. The earliest discoveries of fossil hominins were mainly of cranial material (Gibraltar I, found 1848 [Busk, 1865]; Neanderthal, found 1856 [Busk, 1861]; Cro-Magnon, found 1868 [Lartet, 1868]; '*Pithecanthropus'*, found 1891[Tuner, 1895]; Kabwe, found 1921 [Woodward, 1921]; Taung, found 1924 [Dart, 1925]) and the nineteenth and early twentieth centuries saw a great enthusiasm for the collection of 'exotic' crania (Gould, 1997; Twine, 2002), leading to comprehensive global samples of recent *H. sapiens* crania. This history of palaeoanthropological interest in crania has resulted in a huge body of literature on cranial variation within and between taxa, and thus the cranium is probably the richest source of hypotheses concerning skeletal morphology. There are some very

well preserved Mid-Pleistocene crania (here attributed to *H. heidelbergensis*, the oldest, and thus rarest, of the three taxa which are the focus of the current study – see below), for example Kabwe, Bodo, Petralona, and Arago 21. However, little Mid-Pleistocene hominin postcranial material has been found to date. This means that if one hopes to investigate the taxonomic, functional, or ecological correlates of morphology in Mid-Late Pleistocene hominins, it is most profitable to consider these questions through the lens of the cranium.

The final reason to focus on the cranium to study Pleistocene hominins is that they exhibit a surprisingly wide range of craniofacial morphologies for such closely related species. There are, of course, well-documented postcranial differences between Neanderthals and recent *H. sapiens* (e.g., Trinkaus, 1983; Holliday & Trinkaus, 1991; Churchill, 1998; De Groote, 2011a, b) and between both of these species and *H. heidelbergensis* (e.g., Stringer, 2012c), but these are arguably fewer than those seen between the crania of the three taxa. The cranium is therefore an ideal starting point for investigating the ecological correlates of taxonomic differences in hominin morphology.

1.II. Why study paranasal sinuses?

The paranasal sinuses are air-filled cavities between the inner and outer tables of the cranial bones, lined with mucous membrane (Gray, 1997). Each is recognised by the position of its ostium, the hole by which mucous drains into the nasal cavity, and each is named for the bone it most commonly pneumatises (Rae, 2008) (Figure 1). There are four types of sinus in hominins: frontal, maxillary, sphenoidal, and

ethmoid. Maxillary and sphenoidal sinuses are present in all hominoids, whilst the frontal and ethmoid sinuses are only found in hominids (Rae, 2008). The frontal, maxillary, and sphenoidal sinuses are investigated in this thesis; the ethmoid sinuses are small air bubbles in such a fragile bone that they are rarely preserved, even in recent specimens. For this reason many previous researchers have also avoided studying them (see for example, Tillier, 1975), and there is little on the subject in the literature. This thesis seeks to clarify the differences in sinus morphology within and between Mid-Late Pleistocene hominin taxa, the relationships between sinus size and craniofacial morphology and the relationship between both these variables and ecological/neutral factors. This will provide evidence useful in evaluating competing taxonomic theories for Pleistocene hominins, the explanations of species' diagnostic craniofacial morphology, and selective pressures in recent *Homo* evolution. It will simultaneously shed light on the potential functions of the sinuses themselves, a question that has occupied biologists for centuries (Blaney, 1990; Marquez, 2008).

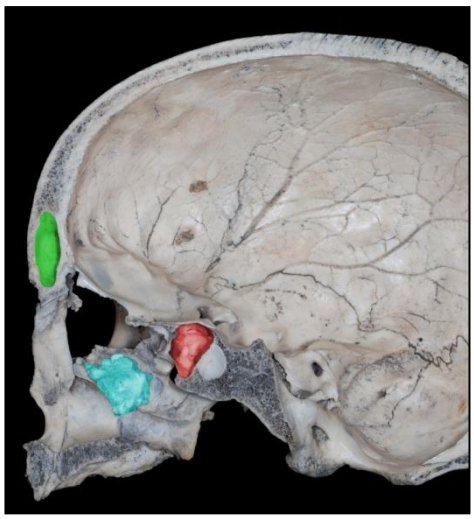

Figure 1: Recent *H. sapiens* cranium dissected sagittally. The sinuses of interest in the current study are coloured post-hoc, green: frontal sinus; blue: maxillary sinus; red: sphenoidal sinus. Photo courtesy of C. Coleman.

1.II.a. Are there population/taxonomic differences in paranasal pneumatisation?

In the Mid-Late Pleistocene, there is considerable diversity in the genus *Homo*. There is evidence for perhaps seven distinct taxa (e.g., Stringer, 1985), although taxonomic divisions and phylogenetic affinities are much disputed. *Homo erectus, H. neanderthalensis,* and *H. sapiens* are generally accepted species designations; *H. heidelbergensis* (in one incarnation or another – see below) is accepted by many (Stringer, 2012c; Buck & Stringer, 2014), whilst *H. floresiensis*, *H. antecessor*, and the Denisovans are still known only from very limited material and so are to a greater extent controversial. The foci for this thesis are *H. heidelbergensis*, *H. neanderthalensis*, and *H. sapiens*; *H. heidelbergensis* is the probable last common ancestor of the other two taxa (e.g., Stringer, 2012c). These three species have been central to theories of hominin sinus function and, conversely, sinus morphology has been used as an explanation for taxon-diagnostic morphology, and even as a justification for the species hypodigm, in the case of *H. heidelbergensis* (e.g., Stringer, 2012c).

The focal taxa in the current species have distinctive craniofacial morphology, as described below. If it is accepted that *H. heidelbergensis* is a valid taxon (see below), it is differentiated from *H. erectus* by its expanded upper cranial vault and increase in endocranial capacity, specialisations of the temporomandibular joint, a vertical lateral border to the piriform aperture, reduced total facial prognathism, and a more derived palatal anatomy (Rightmire, 2001; Stringer, 2012c). The complex of neurocranial features that diagnose *H. neanderthalensis* include a large, long, low

cranium, expanded nuchal region with occipital bunning (Brose & Wolpoff, 1971; Vandersmeersch, 1985) and a suprainiac fossa (Stringer, 1985a; Tattersall & Schwartz, 2006; Balzeau & Rougier, 2010). Facial characteristics include swept-back zygomatics; a great degree of mid-facial prognathism (Stringer, 1985a); a flat or convex intraorbital region (Hublin, 1998); large, continuous, double-arched supraorbital tori (Stringer, 1985a; Tattersall & Schwartz, 2006); a large piriform aperture and large anterior dentition (Brose & Wolpoff, 1971; Stringer, 1985a; Klein, 1999; Tattersall & Schwartz, 2006). Independently, these features are not unique to Neanderthals, but they are each most frequent in this taxon and, in concert, demarcate Neanderthal morphology as different from that of any other taxon (Hublin, 1998). *H. sapiens* is characterised by a globular cranial vault, increased basicranial flexion, enlarged middle cranial fossa, lengthened anterior cranial fossa, an anteroposteriorly short midface, vertical forehead, presence of a canine fossa, and a true chin (Lieberman, 1998; 2008; Lieberman *et al.*, 2002, Stringer, 2002a; Stringer, 2012d; Pearson, 2008; Stringer & Buck, 2014).

1.II.a.i. Paranasal pneumatisation in Homo heidelbergensis

The nature of sinus morphology in *H. heidelbergensis* is important because the alpha taxonomy and phylogeny of these Mid-Pleistocene hominins has been keenly debated for many years (Stringer, 1983, 1985a, 2002b, 2012c; Rightmire, 1996, 1998, 2008; Harvati, 2007; Mounier, 2009; Friess, 2010a; Buck & Stringer, 2014) so much so that the ‘muddle in the middle’ (Butzer & Isaac, 1975) has become somewhat of a cliché. Mid-Pleistocene hominins include specimens such as Bodo, Kabwe (Broken Hill), Elandsfontein, Ndutu and Eyasi from Africa, and European

fossils such as Vertesszöllös, Petralona, Boxgrove, Arago, Bilzingsleben, Ceprano, and Mauer (Rightmire, 1998). These hominins share primitive features with *H. erectus* (*sensu lato*) but they also share derived traits with later Pleistocene specimens. This has led many researchers to group them together in the Euro-African species designation *H. heidelbergensis* (Stringer, 1985a, 2012c; Rightmire, 1996, 1998, 2008, 2013; Harvati, 2007; Mounier *et al.*, 2009). There are also Asian fossils, such as Dali and Jinniushan (China), that potentially form part of this group (Stringer, 2012c), but since none of them were available to study for this thesis, only the African and European fossils have been considered.

The African material, such as Kabwe, resembles European specimens such as Petralona in many respects, including the degree of postorbital constriction, shape of the nasal aperture and temporal squamae, the proportions of the occipital region and the endocranial volume (Rightmire, 2008). Arago and Petralona can be grouped together, despite differences in frontal, maxillary and nasal morphology, due to decreased total prognathism, but increased midfacial prognathism, lack of buttressing, increased cranial height, and distinctive parietal arch shape (Stringer, 1985a). If one agrees that the material from Africa and Europe forms a cohesive group that includes Arago, the traits shared between Arago and the type specimen, the Mauer mandible (Schoetensack, 1908), allow this taxon to be named *H. heidelbergensis* (Rightmire, 2008; Mounier, 2009). There may also be traits of the mandible that are autapomorphies for this group, justifying the elevation of this group to species level (Mounier *et al.*, 2009). Supporters of this Euro-African species have suggested that there is less difference between the purported *H. heidelbergensis*

specimens than between Upper Palaeolithic and recent *H. sapiens* (van Vark, 1995; Stringer, 2002b; Mounier *et al.*, 2009), or within *H. erectus* (*sensu lato*) (Rightmire, 2008).

Critics of the Euro-African hypothesis argue that Neanderthal traits present in European Mid-Pleistocene specimens are evidence of an ancestor-descendent relationship between *H. heidelbergensis* and Neanderthals to the exclusion of the African Mid-Pleistocene hominins (Rosas & Bermúdez de Castro, 1997; Manzi, 2004; Carbonell *et al.*, 2008; Friess, 2010a). In this scenario, similarities between African and European Mid-Pleistocene hominins are merely symplesiomorphies and *H. heidelbergensis* is not a direct *H. sapiens* ancestor (Rosas & Bermúdez de Castro, 1997; Manzi, 2004; Carbonell *et al.*, 2008; Friess, 2010a). Others claim that to suggest that Euro-African *H. heidelbergensis* gave rise to both Neanderthals and *H. sapiens* underestimates the complexity of the hominin fossil record, which they feel supports an interpretation of a more speciose phylogeny (Manzi, 2004). Those who see the earlier European material, such as Gran Dolina (Atapuerca), as distinct have proposed the species *H. antecessor* based on a primitive hominin morphology combined with supposed incipient Neanderthal traits (Manzi, 2004; Carbonell *et al.*, 2008). *H. heidelbergensis* is then hypothesised to be the daughter species of *H. antecessor*, which later formed a chronospecies with Neanderthals in Europe. In this scenario, *H. sapiens* is thought to have evolved in Africa (either by anagenesis or cladogensis, depending on the author) from *H. antecessor* via *H. rhodesiensis*, the species created by Woodward (1921) based on Kabwe (e.g., Mallegni *et al.*, 2003). Supporters of the Euro-African *H. heidelbergensis* hypothesis reject the idea that the

high level of similarity between the European and African groups can be explained away as symplesiomorphies and point to the way in which specimens such as Petralona and Kabwe group together in morphometric, quantitative analyses, as well as through qualitative examination (Stringer, 1983, 2002b; Rightmire, 1996, 1998, 2008; Mounier, 2009; Mounier *et al.*, 2009; Friess, 2010a).

Given the level of debate surrounding the grouping of these fossils, any morphological trait, such as distinctive paranasal pneumatisation, that can be used to assign group membership is potentially useful to its resolution and, since most of the Mid-Pleistocene fossil material is cranial, taxonomy must be established on the basis of craniofacial characters. The presence and size of paranasal sinuses has been used in the systematic evaluation of several species (Rae, 1999; Farke, 2010) and large sinuses have been proposed as a distinctive trait for *H. heidelbergensis* (Seidler *et al.*, 1997; Prossinger *et al.*, 2003; Stringer, 2012c). Thus, investigating the size and level of variation in the pneumatisation of these specimens has the potential to clarify their taxonomy.

1.II.a.ii. Paranasal pneumatisation in Homo neanderthalensis

Neanderthal crania have been characterised as being hyperpneumatised (Busk, 1861; Blake, 1864; Brose & Wolpoff, 1971), a condition that has been used as an explanation for some of their diagnostic craniofacial morphology. The large supraorbital tori of Neanderthals have been said to result from their large frontal sinuses (Coon, 1962; Wolpoff, 1999), and the ‘inflated’ mid-face, which projects and lacks a canine fossa, has been attributed to large maxillary sinuses (Coon, 1962). The

assertion that Neanderthal sinuses are large has also been used to underpin some key theories for sinus function in hominins, as discussed below. Recent work, however, suggests that the key assumption upon which these theories rest may not be correct if the size of the cranium is taken into account (Zollikofer *et al.*, 2008; Rae *et al.*, 2011). Some sinuses have been shown to scale isometrically with craniofacial size in hominoids (Rae & Koppe, 2000), and it seems that Neanderthals may fit in with this general pattern. The two studies which have questioned the hyperpneumatisation of Neanderthals (Zollikofer, *et al.*, 2008a; Rae, *et al.*, 2011) were restricted to fairly small samples, both of fossils and of recent *H. sapiens*. The time is ripe, therefore, to test the assumption of Neanderthal hyperpneumatisation with a more comprehensive sample, as in the current study.

1.II.a.iii. Paranasal pneumatisation in Homo sapiens *(within the taxon and between populations)*

It has been stated that sinuses are particularly variable in *H. sapiens* compared to other species (Buckland-Wright, 1970; Seidler, *et al.*, 1997; Vinyard & Smith, 1997). In the context of theories that *H. sapiens* was able to adapt to novel niches and colonise new territory in part due to an unusually plastic phenotype (Wells & Stock, 2007; Stock, 2008; Stock & Buck, 2010), the presence of greater level of pneumatic variation in *H. sapiens* is an interesting assertion, and one that addressed below by comparison with closely related species. If *H. sapiens* does indeed show greater intraspecific variation than other taxa, this may suggest it has lower levels of canalisation (relaxed selection), perhaps enabling greater plastic flexibility to the environment (Waddington, 1942; Flatt, 2005; Buck *et al.*, 2010). Below, paranasal

sinus variation within *H. sapiens, H. neanderthalensis,* and *H. heidelbergensis* is measured and compared to assess their relative intraspecific homogeneity.

1.II.b. Do paranasal sinuses have a function?

The existence human paranasal sinuses has been appreciated since at least the second century AD (Keir, 2009). Surprisingly for a macroscopic cranial component, however, there is still little known about whether they have any function, or about the correlates of their size and shape. In fact, sinuses have been described as "the last frontier in craniofacial biology" (Marquez, 2008). This lack of understanding is not for want of attention; over the past several hundred years, many explanations have been suggested for hominin sinus function (for reviews, see Blaney, 1990; Marquez, 2008; Keir, 2009). Some theories are eccentric than others, such as the idea that the sinuses acted as buoyancy aids during a hypothetical aquatic phase in hominin evolution (Rhŷs Evans, 1992), or that the sinuses act as resonating chambers to help the voice carry (Howell, 1917). The former lacks any real evidence beyond the circumstantial (Rae & Koppe, 2014).The latter can be discounted as species with loud voices can have very small sinuses and vice versa, the physical properties of the sinuses would actually make them poor resonators, and people who have undergone sinus surgery to fill their sinuses for clinical reasons do not report differences in their voices (Blaney, 1990). Other theories are more plausible, but not well supported. It has been suggested that the sinuses serve to protect the skull from blows (Ravosa *et al.*, 2000), partly based on the observation that bovids, some of which ram heads as part of mating or defensive behaviour, often have large sinuses (Negus, 1954). However, a comprehensive study employing CT data of bovid sinuses from sixty-two

species found no significant relationship between the size or complexity of the sinuses and head-ramming behaviour (Farke, 2010). Despite some evidence to refute them (see below), two further hypotheses for sinus function remain widely debated in the literature: that sinuses serve to disperse strain from mastication, and that sinuses are a climatic adaptation (e.g., Preuschoft *et al.*, 2002; Holton *et al*., 2013) As described below, both hypotheses for sinus function have particular relevance for Pleistocene hominins and it are evaluated in the current thesis.

1.II.b.i. Are the paranasal sinus types homologous?

In general, the literature on sinus function refers to the sinuses as a group, implicitly assuming that they are functionally and developmentally homologous. In fact, there is evidence that this is not the case. The number and type of sinuses is not a constant and during the course of primate evolution, sinuses have been lost and regained independently (Rae *et al.*, 2002; Rae, 2008), which suggests at least some degree of functional heterogeneity, or at least modularity. This is also supported by Tillier's (1975) observation of a lack of covariation in sinus size between sinus types within individuals. In the current thesis, the sinuses are considered separately and their individual relationships with ecological and taxonomic variables are compared to assess the case for homology.

1.II.b.ii. Masticatory functional explanations for paranasal sinuses

The hypothesis that sinuses are adaptations to mitigate the stress/strain of chewing has proved popular in recent years, with this cause invoked to explain large sinus

volumes in hominins and other primates (Bookstein *et al.*, 1999; Wolpoff, 1999; Prossinger *et al.*, 2000; Preuschoft *et al.*, 2002). Though the mechanism behind the adaptive nature of large sinuses is not explicit, it is implied that larger sinuses enable resistance to higher masticatory stresses/strains, a hypothesis linked to architectural theory suggesting that thin shelled, curved walled spaces are biomechanically well-suited to the dissipation of forces, balancing the requirements of strength and weight. Thus, the expectation is that high dietary stress/strain will lead to large sinuses (e.g., Bookstein *et al.*, 1999).

In terms of the frontal sinus in primates, there is evidence against this expectation due to low strains levels in the upper face. It has been shown repeatedly that the majority of strain from chewing affects only the maxillary region, particularly the muscle attachment areas and alveolar region (Endo, 1965; Ross & Metzger, 2004; Kupczik *et al.*, 2009; Tückmantel *et al.*, 2009; Chalk *et al*., 2011). Yet even pneumatisation in regions subject to masticatory stress/strain does not conform to the pattern implied by this hypothesis; i.e., that high stresses/strains lead to large sinuses. Cranial adaptation to hard-object feeding in capuchin monkeys does not lead to differences in maxillary pneumatisation when compared to congeners with a softer diet (Rae & Koppe, 2008), nor is there any relationship between maxillary sinus volume and diet-adapted cheek dentition in *Macaca mulatta* or *M. fascicularis* (Marquez & Laitman, 2008). In the current thesis, sinus variables are compared between large samples of Pleistocene hominins with distinctive diets diets resulting in differing masticatory stresses/strains to evaluate the claimed link between high dietary stress/strain and large sinus volume.

1.II.b.iii. Climatic functional explanations for paranasal sinuses

A long-favoured explanation for paranasal pneumatisation is that sinuses are an adaptation to climatic pressures. This theory seems to be well-established in the public imagination, and it is the explanation for sinus function frequently given by medical doctors and dentists (pers. obs.). It has been hypothesised that large sinuses are a cold-adaptation, assumed to condition (warm and moisten) inspired air and to protect the brain from cooling via the well-vascularised sinus epithelium (Coon, 1962; Wolpoff, 1999). This theory is at odds with the evidence, however. Maxillary and frontal sinus volumes amongst the cold-adapted Inuit actually show a negative correlation with temperature or with inferred temperature from latitude (Koertvelyessy, 1972; Shea, 1977). This relationship is seen in other species, too; Japanese macaques (Rae *et al.*, 2003) and rats in experimentally controlled climates (Rae *et al.*, 2006) both exhibit smaller maxillary sinuses with colder temperatures. Furthermore, it has been argued that the size of sinus ostia means that the rate of gaseous exchange between the nasal cavity and sinuses is too low for efficient air conditioning (Negus, 1954; Blaney, 1990).

The idea of sinuses as a cold-adaptation has been linked especially to Neanderthals (Coon, 1962; Churchill, 1998; Wolpoff, 1999). The assumption that Neanderthals have large sinuses (see above) has formed part of the paradigm of Neanderthals as a hyper-glacial species, which has been dominant in anthropology for many decades (c.f. Rae *et al.*, 2011). It is obviously a circular argument to state that Neanderthals have large sinuses, so sinuses must be a cold-adaptation, whilst simultaneously arguing that Neanderthals must be cold-adapted because they have large sinuses. In

fact, the available information suggest that sinuses are relatively small in cold-adapted mammals (see above). If this is the case, large sinuses cannot be a cold-adaptation in Neanderthals, even if they are a cold-adapted species, which is currently in question (Stewart, 2004; 2005; Hublin & Roebroeks, 2009; Rae *et al*., 2011). Recent research also suggests that, if cranial size is taken into account, Neanderthals do not have larger sinuses than recent humans (Zollikofer *et al.*, 2008; Rae, *et al.*, 2011).

The converse climate theory, that the sinuses aid in cooling the blood supply to the brain in hot climates by optimising evaporation from the expanded mucous membrane surface area, has received less attention (but see Dean, 1988; Irmak *et al.*, 2004; Rae & Koppe, 2004). This would lead to the expectation of larger sinuses in hotter temperatures, which fits the Inuit and (non-human) mammal evidence, but which also falls foul of the slow exchange rate of air through sinus ostia (Blaney, 1990), and does not fit the Neanderthal theory, if they can be assumed to have lived largely in cold climates (Churchill, 1998). The theory is also contrary to the evidence of studies that have found larger sinuses in European recent *H. sapiens* than in African recent *H. sapiens* (Fernandez, 2004b).

It is not necessary to invoke a direct climatic cause for the change in sinus volume; it is possible that differences in sinus size that seemingly correlated with climate, such as those described above, are actually a secondary product of changes in the morphology of the nasal apparatus or other facial regions with which sinus growth may be integrated (Hylander, 1975; Shea, 1977; Rae *et al.*, 2003; Holton, *et al.*, 2013,

see also below). In the current thesis, paranasal pneumatisation is compared between a large sample of recent *H. sapiens* and fossil hominins (including a sample of *H. neanderthalensis* from different inferred climates) to assess the plausibility of the sinuses as a thermoregulatory mechanism (either conditioning or cooling air) and to assess potential differences in the relationship between pneumatisation and climate between taxa.

1.II.b.iv. Paranasal sinuses as spandrels

The absence of a consensus on sinus function and the evidence against the causal theories of diet, phylogeny and climate has led some (e.g., Lund, 1988) to conclude that sinuses have no function of their own, but are spandrels in the sense of Gould and Lewontin (1979). It is suggested that sinuses passively expand into space made available by different growth trajectories in neighbouring craniofacial units; different shaped crania leading to different sinus morphology (Moss & Young, 1960; Shea, 1977; Blaney, 1990; Vinyard & Smith, 1997; Zollikofer *et al.*, 2008). If this is the case, sinus size should be correlated primarily with craniofacial shape, rather than ecological variables such as diet or climate. These spatial hypotheses are supported by correlations between the size of the sinuses and various craniofacial indices, including measures of craniofacial size (Lund, 1988; Koppe *et al.*, 1999b; Rae & Koppe, 2000; Farke, 2010) and the angle between the face and brain (Seidler *et al.*; 1997, Zollikofer *et al.*, 2008). The clinical literature is another source of support, recording cases where the inner table of the frontal bone has been displaced inwards, following atrophy of the brain, and the resulting space between the (normal appearing) external table and the internal table has become pneumatised (Moss &

Young, 1960). In fact, the very variability of the sinuses may speak to their lack of function, as it would be expected that a functional structure would be subject to selective pressures to optimise it for that function, or canalisation to maintain optimal performance, which would lead to homogeneity within species (O'Higgins *et al.*, 2006; Buck *et al.*, 2010).

It seems counter-intuitive that sinuses would have been maintained over evolutionary history without some positive benefit, as they certainly have a cost: sixteen percent of Americans suffer from sinusitis annually (Lundberg, 2008), a rate that is likely to be similar in other industrialised countries. Bone growth inside the sinus cavities, resulting from severe sinusitis, shows that the incidence of the disease was high in some populations even in prehistoric times (Roberts, 2007). This must have been detrimental to fitness before the advent of modern medicines and would be expected to result in selection against pneumatisation. Although it seems unlikely that sinuses would have been maintained without positive selection, they could have evolved neutrally and been subsequently optimised to maintain the balance between weight and strength (Zollikofer *et al.*, 2008) or have been exapted for some adaptive function. One possible candidate for exaption is nitric oxide (NO) production (Keir, 2009). The epithelium lining the paranasal sinuses produces large amounts of NO (Marquez *et al*., 2002; Lundberg, 2008). This gas is also produced by the nasal epithelium, but at lower levels. NO has a vasodilatory effect, which is thought to increase pulmonary oxygen uptake when it (the NO) is inhaled from the nose and sinuses. It is also likely to have a disease-resistance function, stimulating ciliary activity and inhibiting the growth of pathogens (Marquez *et al*., 2002; Lundberg,

2008). Appealing as this explanation is, the non-human primate fossil record shows that some sinuses have been lost and regained several times in different species (Kuykendall & Rae, 2008; Rae, 2008), so it is hard to argue that any purported function, be it NO production or something else, is vital. Furthermore, this hypothesis does not account for the level of variation in sinus volume within and between groups. In the current thesis, the non-functional, spandrel explanation for pneumatisation is treated as the null hypothesis against which the evidence for dietary and climatic adaptation is evaluated. By comparing the strengths of direct relationships between ecological and behavioural variables and sinus variables, and of the indirect relationships, between sinus-related craniofacial morphology and ecological/behavioural variables, the plausibility of the status of sinuses as spandrels is assessed.

1.II.c. Does pneumatisation influence craniofacial morphology, or vice versa?

If the sinuses are functional, selective pressure for greater/smaller sinus volume could contribute to craniofacial morphology, as suggested for Neanderthal midfacial prognathism (Coon, 1962). Conversely, if sinuses are spandrels, as suggested above, their morphology would depend on the shape of the crania they pneumatise. Craniofacial form is subject to myriad selective pressures due to its multiple functions (e.g., Lieberman, 1996; Pan & Oxnard, 2002), and also to plastic change during an organism's lifetime (Antón, 1996; Larsen, 1997; Goodship & Cunningham, 2001; Pearson & Lieberman, 2004; Pucciarelli *et al.*, 2006; von Cramon-Taubadel, 2009b). Two of the factors with the greatest influence on hominin

craniofacial morphology are diet and climate, but there is also evidence that much of craniofacial shape is neutrally determined (see below). The way in which these factors affect shape is also dependent on the way in which cranial regions are related to one another and the degree to which regions with different functions are free to vary independently (Moss & Young, 1960; Moss, 1962). These three determinants of craniofacial morphology (and thus potential correlates of sinus morphology) are investigated in the current thesis.

1.II.c.i. The influence of masticatory stress/strain on craniofacial morphology

Differences in masticatory strain have been shown to affect craniofacial shape in *H. sapiens*, non-human primates and other mammals (Wolpoff, 1968; Larsen, 1997; Pucciarelli *et al.*, 2006; Paschetta, *et al.*, 2010). This is as a combination of inherited differences in phenotype, due to selection over the course of generations (Viguier, 2004; von Cramon-Taubadel, 2009b), and the result of plastic change over the course of an individual's lifetime as a result of cumulative mechanical strain leading to bone functional adaptation (Antón, 1996; Larsen, 1997; Goodship & Cunningham, 2001; Pearson & Lieberman, 2004; Pucciarelli *et al.*, 2006; Ruff *et al*., 2006; von Cramon-Taubadel, 2009b). Of course, the two mechanisms interact, genetic disposition to plastic adaptation may also be selected for over generations.

One case where the impact of diet on craniofacial morphology has been much studied is the Neolithic transition to agriculture; it has been shown that the softer diets of agriculturalists (inclusions of grit/stones notwithstanding), particularly the

reliance on processed grains, led to changes in craniofacial shape, particularly a reduction in the lower face, palate, and attachment regions of the masticatory muscles, such as the masseter and temporalis (González-José *et al.*, 2005; Sardi *et al.*, 2006; Paschetta *et al.*, 2010). Greater bone thickness, strengthening the cranium, is likely to be present in regions, such as muscle attachments, experiencing greatest strain in populations with harder diets (González-José *et al.*, 2005; Sardi *et al.*, 2006; Paschetta *et al.*, 2010). The overall shape of the cranium is also likely to be optimised to strain, where dental loading is a selective pressure; for example, it has been argued that the relatively flat faces of Inuits are a response to the need to minimise bending strains produced by anterior dental loading, which is greater in a projecting mid-face (Wang *et al*., 2010). Thus, if the sinuses are spandrels, but are affected by local influences on craniofacial shape, one might expect masticatory strain to affect craniofacial shape, which would in turn lead to differences in sinus morphology, with, for example, flat faces in Inuit adapted to high anterior dental loading leading to smaller sinuses.

Strain from the use of the teeth has not only been held accountable for some of the differences between the morphology of recent *H. sapiens* populations; it also has been proposed that diagnostic Neanderthal craniofacial morphology, specifically the midfacial projection, lack of canine fossa and swept back zygomatic arches, is the result of high levels of stress on the anterior dentition in this taxon as well (Coon, 1962; Smith, 1976b; Rak, 1986; Demes, 1987; Trinkaus, 1987; Klein, 1999). If true, high levels of biomechanical stress/strain on the Neanderthal mid-face would lead to large, 'inflated' maxillae, which could lead to larger maxillary sinuses, given the

greater scope for opportunistic pneumatisation. The idea that Neanderthal mid-facial morphology is an adaptation to high levels of stress/strain on the teeth arises from comparisons of Neanderthal crania with evidence of dental stress seen in Inuit crania (Hylander, 1975). There are ethnographic accounts of paramasticatory behaviour in the Inuit, which results in some of the same skeletal indications of unusual stresses as seen in Neanderthal crania: large size of the anterior teeth, mandibular robusticity and marked masticatory muscle attachments, frequency of pathology in the temporomandibular joint, and (in Neanderthals) the presence of microstriae that seem to indicate the drawing of a blade across the teeth (usually hypothesised to have resulted from the use of the jaws as a vice) (Coon, 1962; Hylander, 1975; Smith, 1976a; Klein, 1999). Although the mechanisms by which anterior dental loading is supposed to have led to the Neanderthal face shape are disputed, the many theories of this nature may be grouped together as anterior dental loading hypotheses (ADLH) (O'Connor *et al.*, 2005).

Some supporters of ADLH hold that Neanderthal craniofacial shape demonstrates morphological reorganisation to withstand the high stresses/strains of paramastication (Rak, 1986; Demes, 1987). Other proponents state that selection for large anterior dentition is the primary cause of Neanderthal craniofacial shape, with other changes following as a secondary response (Smith, 1976a; Smith, 1976b; Trinkaus, 1986; Trinkaus, 1987). The ADLH as a group are questioned by those who suggest that Neanderthal mandibular structure itself precludes the generation of the kind of forces that would be necessary to produce their morphology (Antón, 1994; O'Connor *et al.*, 2005).

An alternative to the ADLH, which still focuses on biomechanical strains as shapers of Neanderthal craniofacial morphology, suggests that the indisputably heavy wear on *H. neanderthalensis* incisors reflects repetitive use, rather than abnormally high strains (Ungar *et al.* 1997; O'Connor *et al.*, 2005). Results from finite element analyses on a macaque model, however, conclude that repeated incisal biting could help explain the flat faces seen in Inuits, but is unlikely to have been efficient in prognathic Neanderthals (Wang *et al.*, 2010). The conclusion that orthognathic Inuit faces are an adaptation to repetitive use of the anterior dentition supports Hylander's (1975) earlier work, and also reflects what is seen in macaques with different diets (Antón, 1996). Thus, the relationship between Neanderthal tooth use and craniofacial morphology is still uncertain, but this does not affect the utility of such hypotheses for the purposes of the current thesis. It is not the aim of the current work to answer outstanding questions regarding the masticatory shaping of particular, diagnostic hominin craniofacial traits. Rather, it is to ascertain if masticatory strain is a key factor in the determination of hominin craniofacial morphology, which could affect sinus volume.

1.II.c.ii. The influence of climate on craniofacial morphology

As described above, some climatic theories of sinus function suggest that variation in volume may be a secondary response to a primary adaptation of facial morphology to climate. Climate is known to be a major selective pressure on hominin cranial shape; in fact, adaptation to extremely cold temperatures is thought by some to be the only non-neutral signal in population differences in recent *H. sapiens* craniofacial morphology (Roseman, 2004; Roseman & Weaver, 2004). In *H. sapiens*,

neurocranial shape and size seem to vary with climate in accordance with Bergmann's Rule. Crania are more brachycephalic and larger in cold climates in order to minimise heat loss (Beals *et al.*, 1984), albeit perhaps only in populations living at extremely low temperatures (Roseman & Weaver, 2004; Harvati & Weaver, 2006b; Relethford, 2010; Foster & Collard, 2013). A flatter face and more brachycephalic neurocranium result in less disjunction between the two cranial modules and thus less space for the frontal sinus to pneumatise, if it is indeed an opportunistic spandrel (Zollikofer *et al*. 2008). Nasal apparatus shape also seems to be affected by climatic selection, being correlated with variables of both temperature and humidity (Carey & Steegmann, 1981; Franciscus & Long, 1991; Betti *et al.*, 2010; Noback *et al.*, 2011; Evteev *et al.* , 2013). It is logical that the means of taking in air should be affected by climate, as inspired air must be warmed and moistened to avoid damaging the respiratory tissues and to enable the proper functioning of the nasal cilia and mucosa, whilst expired air can be a substantial source of heat and moisture loss (Carey & Steegmann, 1981). As suggested by Rae *et al*. (2003) for Japanese macaques and Shea (1977) for Inuits, a climatic requirement for a wider nasal cavity could result in reduced space for the development of maxillary sinuses. However, as with neurocranial size and shape, the relationships between nasal apparatus shape and climate seem to be driven by a few cold-adapted groups (Roseman & Weaver, 2004; Betti *et al.*, 2010).

Parallel to climate-induced intra-*H. sapiens* craniofacial shape differences, there is an established paradigm of interpreting Neanderthals as a hyper-cold-adapted species inhabiting a glacial niche (Coon, 1962; Trinkaus, 1981; Holliday, 1997; Wolpoff,

1999), which has led to the adaptionist explanation of Neanderthal craniofacial morphology as a series of responses to climatic pressures. Increased prognathism has been seen as an adaptation to increase the distance between the respiratory apparatus and arteries serving the brain, thus reducing the cooling effect of inspired air on the cranial blood and delicate cerebral tissues (Coon, 1962; Brose & Wolpoff, 1971; Wolpoff, 1999), whilst the large nasal aperture has been attributed to the need to warm and condition air (Coon, 1962; Churchill, 1998; Wolpoff, 1999). Increased prognathism would lead to the potential for larger maxillary sinuses, whilst a large nasal aperture could limit maxillary sinus size.

The evidence from laboratory experiments in animals does not support the hypothesis that the Neanderthal craniofacial shape is a cold-adaptation; an experiment raising rats at cold temperatures found smaller crania, anterosuperiorly shifted naso-maxillary complexes, narrower nasal apertures, more globular neurocrania, and shorter, broader zygomatics in test animals compared to the controls (Steegmann & Platner, 1968; Rae *et al.*, 2006). These changes are very similar to the morphology of cold-adapted recent *H. sapiens* (see above); they are the reverse of characteristic Neanderthal morphology. In recent years, evidence has begun to accumulate that questions the widely accepted belief of *H. neanderthalensis* as a glacial specialist. *H. neanderthalensis* migration in and out of Europe seems to coincide with climatic changes, with populations increasing in warmer times and contracting when temperatures decreased (van Andel *et al.*, 2003; Stewart, 2004). There is also little difference between Neanderthal and Aurignacian *H. sapiens* in terms of their preference for climate or their tolerance of wind chill and snow cover

(Davies & Gollop, 2003; van Andel *et al.*, 2003). Numbers and locations of later *H. sapiens* sites actually suggest a preference for colder climatic conditions than those at Neanderthal sites (Davies & Gollop, 2003; Stewart, 2004; Hublin & Roebroeks, 2009). These data suggest that, not only is it unlikely that all Neanderthal craniofacial morphology can be explained simply as an adaptation to climate, but that the paradigm of Neanderthals as hyper-polar (Holliday, 1997) itself cannot be accepted without question.

In the current thesis, relationships between climatic variables (measures of temperature/precipitation and grouping based on palaeoclimatic reconstructions) and sinus-related craniofacial morphology are analysed in all hominin taxa to ascertain whether these supposedly key determinants of craniofacial shape can be shown to have an indirect effect on sinus morphology, which (in the absence of a direct relationship with sinus morphology) would strengthen the case for the spandrel hypothesis.

1.II.c.iii. Neutral effects on craniofacial morphology

Neutral theories for differences in craniofacial morphology between Pleistocene hominin species can be treated as a null hypothesis to counter selective explanations and avoid adaptionist thinking. If variation in craniofacial morphology is neutrally patterned and sinuses are spandrels, sinus volume would be expected to correlate with craniofacial shape, but no relationship would be found between craniofacial morphology and ecological variables. In comparisons between neutral genetic distances and phenotypic distances, the variation between recent *H. sapiens* and *H.*

neanderthalensis may be best explained by genetic drift acting in isolated populations (Weaver *et al.*, 2007; Weaver, 2009). This conclusion is supported by studies using population genetics, which also suggest that genetic drift is probably a key factor in much of the evolution of the genus *Homo (*Ackerman and Cheverud, 2004). Ackerman and Cheverud (2004) hypothesise that this may reflect a transition to more isolated populations following a geographic expansion in stem *Homo*. In recent *H. sapiens*, it has also been postulated that genetic drift and population history may account for the majority of craniofacial differences between geographically (Roseman, 2004; Roseman & Weaver, 2004; Relethford, 2010), and chronologically (Brewster *et al*., 2014) separated, populations. In the current thesis this null hypothesis is applicable at different taxonomic levels, both between species, and between populations of recent *H. sapiens*. In this study the relationships between sinus variables and diet/climate are assessed against neutral expectations for sinus volume, and sinus-related craniofacial, morphology. Neutral and adaptive processes are not mutually exclusive and in any real-world situation the mechanisms leading to a particular morphology are likely to be complex; however, the consideration of the key agent operating on sinus volume in isolation is useful to unpick the reasons for the differences between groups.

1.II.c.iv. Functional modules and integration in craniofacial morphology

How the cranium is affected by any agency depends partly on how different regions are inter-linked; most traits are integrated to differing levels at both a genetic and phenotypic level (Cheverud, 1982). It is unrealistic to treat a phenotype as a mosaic

of discrete traits because any trait under consideration may change as a result of selection on another region with which it is integrated. One example is the Neanderthal 'chignon', which has been suggested as a Neanderthal autapomorphy. 'Hemi-buns' seen in some European Upper Palaeolithic groups (e.g., the Mladeč material) have therefore been interpreted as evidence of hybridisation (Frayer, 1997). However, geometric morphometric analyses show that neurocranial shape is highly integrated and thus 'hemi-buns' are not an independent trait (Gunz & Harvati, 2007). Gunz and Harvati (2007) found that 'hemi-buns' occur in *H. sapiens* populations from all parts of the worlds at low frequencies, and they appear to be homologous with those of Neanderthals; both are a response to the shape of the neurocranium, to an anterosuperiorly placed temporal and a flat parietal region, rather than evidence of shared genetic material (Gunz & Harvati, 2007). For the purposes of investigating craniofacial shape related to sinus morphology, the problems associated with integration can be overcome, to a degree, by considering the cranium as a whole. One of the advantages of the geometric morphometric methods used in the current thesis (see Section 2.III.) is that shape differences in all parts of the studied shape can be considered simultaneously, as opposed to the traditional methods of comparing individual characteristics (Stringer & Buck, 2014).

Modularity can be seen as the flipside of integration and the extent to which different parts of the cranium can alter is determined by the balance between the two (Bastir & Rosas, 2005). A degree of modularity is likely to be advantageous, because selection can work on the optimisation of one character without affecting the cranium as a whole (Bastir & Rosas, 2005). Moss and Young (1960) first

popularised the idea that the cranium is a matrix of different functional components each adapted to a different task: vision, speech, respiration etc., and each responding to different selective pressures. These functional modules often cross traditional, bone-based boundaries (Moss & Young, 1960). The maxilla, for example, is formed of relatively independent modules related to the orbits, nose, teeth and sinuses (Moss Salentijn, 1997). This is illustrated by the fact that failure to develop, or pathology, in one of these regions may leave the others untouched (Moss & Young, 1960; Moss, 1962). Zollikofer *et al*. (2008) drew on Moss and Young's ideas to suggest that large frontal sinuses in hominids are opportunistic spandrels enabled (although not necessitated) by a disjunction between growth trajectories in the neurocranial module, responding to growth in the brain, and the orbital module, responding to growth in the visual system. This hypothesis is further explored in the current thesis by examining three sinuses (frontal, maxillary and sphenoidal) and their relationships to external factors in a far larger sample of hominins.

1.III. Research questions

The relationships between sinus variables (variables of sinus size and craniofacial shape associated with sinus morphology) and comparative variables (variables of diet, climate, and taxonomic/population attribution) are investigated in an attempt to address the following questions:

1.III.a. RQ1: Are there population/ taxonomic differences in sinus variables?

RQ1.a: Are there differences in sinus variables between populations of recent *H. sapiens*?

RQ1.b: Are there differences in sinus variables between Mid-Late Pleistocene taxa?

RQ1.c: Are the sinuses homologous across type?

1.III.b RQ2: Are there interactions between masticatory stress/strain and sinus variables?

Are there differences in sinus variables between groups (across taxa) experiencing different levels of masticatory stress/strain?

1.III.c. RQ3: Are there interactions between climate and sinus variables?

RQ3.a: Are there differences in sinus variables between populations of recent *H. sapiens* experiencing different climates?

RQ3.b: Are there differences in sinus variables between groups (across taxa) experiencing different climates?

Chapter 2: Materials and methods

2.I. Materials

2.I.a. Computed tomography

The data used in this thesis consist of computed tomography (CT) scans of crania, whether partial or complete, still living, dry, or fossilised (for details of scans, see Appendix 2). CT is an X-ray attenuation-based imaging technique analogous to combining many traditional radiographs to digitally recreate a three dimensional (3D) volume of an object (Zollikofer *et al.*, 1998; Abel *et al.*, 2012). CT data have many advantages: they allow non-destructive visualisation of internal structures (such as sinuses) and protect delicate original fossils from repeated handling. Data can be sent in digital format, rather than the researcher being required to visit the institution where each specimen is housed; this allows the compilation of a sample that would be logistically difficult. Because one continues to hold the source of measurement/shape analysis data (the CT scans themselves), it is possible to revisit them to check measurements or landmarks, or to try new methods/conduct new tests based on preliminary analyses. CT data are also perfect for combining volumetric measurement and 3D landmark geometric morphometric methods (GMM), as in the current study. This study fits into a fast-expanding body of research using geometric morphometrics in palaeoanthropology (e.g., Zollikofer *et al.*, 2008; Harvati and Weaver, 2006a, b) and, likewise, a well-established tradition of using CT scans to visualise skulls, particularly to analyse interior features such as the sinuses (e.g., Seidler *et al.*, 1997; Baab and McNulty, 2009).

Potential drawbacks of the use of CT data include the potential costs of scanning and the computer power and memory needed to run CT analysis software, which itself is often expensive. If one is using data collected by someone else (data sharing being one of the advantages of CT data) the combination of data types may also be an issue. The main division in the types of CT data used in palaeoanthropology is between data collected on microCT and medical CT scanners. These types of scanner work in slightly different ways: in a medical CT scanner, the patient (or specimen) remains stationary and the X-ray source and detector panel spin around them collecting images; in a microCT scanner, it is normal for the source and detector to remain stationary whilst the specimen rotates. The relevant difference, however, is in the resolution of the scan. All the microCT scans in the current sample were conducted on a Metris X-Tek HMX ST 225 CT scanner (Nikon®), and microCT scans in the sample have an isometric voxel size of around $0.13mm^3$. The medical CT scans in the sample are from various sources (see Section 2.I.b.) and the resolutions of the scans vary; in some of the earlier scans, slice thickness can be up to 1mm. This difference could be problematic in the measuring of very small structures. However, it should not prevent the comparison of relatively large structures, such as sinuses, since this resolution is sufficient to visualise and measure the pneumatisation. Although the resolution in one dimension may mean that the thin walls delineating a sinus may not be visible in that plane, the greater resolution in the other planes (and interpretation of the view from all three planes) allows for sufficiently precise measurement, and measurement error in collecting sinus volumes is low, even when using medical CT data (see Section 2.II.b.). There is no greater

intra-sample variation in medical CT scanned data than microCT data (see Section 4.I.a.i.), suggesting that differences in data sources has not contributed to the distribution of variation in the results.

2.I.b. Sample

The sample was intended to maximise the number of fossil taxa and the number of specimens from each taxon, and to obtain the best possible geographic spread of recent *H. sapiens* samples, reflecting the range of intraspecific variation within the species. Limiting factors included the availability of CT data of specimens, completeness of preservation (especially of fossils), and the time consuming nature of data collection. Data were obtained from commercial databases of CT data (e.g., the Digital Archives of Fossil Hominoids, University of Vienna; NESPOS), purchased directly from their home institutions (National Museums of Kenya), or supplied freely by the holders of the data. The sample consists of recent *H. sapiens*, early *H. sapiens*, *H. heidelbergensis*, *H. neanderthalensis*, and *H. erectus* (for definitions, see Section 2.IV.c.i.). Only adult crania were used; adult status was taken from institution records and confirmed by checking that the third molar (where present) was erupted to occlusion and/or the spheno-occipital synchondrosis (where present) was fused. Pathological crania were avoided where possible; where no alternatives were available (as for the fossil sample), pathological crania were used only as long as the pathology did not appear to alter morphology in the regions of interest. The source and details for each population and/or specimen is reported below (Section 2.I.b; Appendix 1).

Figure 2: Map showing mean location for all recent *H. sapiens* groups and sites for each fossil in sample (for details see below). Black circles: recent *H. sapiens*, white circles: early *H. sapiens*, black stars: *H. neanderthalensis*, black squares: *H. heidelbergensis*, black pentagon: *H. erectus*.

2.I.b.i: Recent H. sapiens *sample*

In this section, the recent *H. sapiens* sample is broken down by population and a summary is given of each population composition (complete details are given in Appendix 1). Justification is given for the population grouping, subsistence classification, and climatic category used in this thesis, along with any other relevant information. For definition and method for calculating subsistence and climate categories see Section 2.IV.b. and 2.IV.c. respectively. For a summary of the sample details, see Table 1.

Whilst each recent *H. sapiens* sample was chosen to include both males and females, it was not possible to obtain exactly equal numbers without compromising sample size. Butaric *et al*. (2010) have shown that, at least in recent *H. sapiens*, there is no sexual dimorphism in relative maxillary sinus volumes, but this is not known for the other sinus types. There were generally more males available, probably for historical reasons; for example some of the crania came from prisoners (ORSA database), and some populations had no reliable sex information available. Postcrania were not available (since only scans of the crania were obtained) and no attempt was made to sex individuals based on cranial characteristics, since these are very variable between populations and, as they are largely based on levels of robusticity, decisions about sex might bias the sample. Sex is unknown for the fossil sample, thus sexing the recent sample would not completely avoid potentially confounding sex issues.

China

The Chinese sample consists of ten individuals from the Morton Collection obtained via the Open Resource Scan Archive (ORSA) database administered by the

University of Pennsylvania. The biographical information available from ORSA records that there are seven males and two females aged 25 to 60 years (for more details see Appendix 1). Known locations are shown on the map below (Figure 2). Manchuria is an area of northeast China of variable size depending on interpretation (Perdue, 1998). For the purposes of this thesis, the approximate centre of Manchuria was used to obtain the latitude and longitude used for climate calculations. No information is known about the date of the specimens, but Morton was collecting between the 1820s and 1851, when he died (Gould, 1997), so the specimens must be older than the latter date.

Source

Medical CT obtained from ORSA, courtesy of Janet Monge and Tom Schoenemann, University of Pennsylvania. For details of all CT scans, see Appendix 2.

Climate category

For the definitions of climate categories and details of the methods used to calculate climate variables here and throughout this section, see Section 2.IV.c.ii. Due to the size and geographic complexity of China, combining the specimens from all the known locations (plus the unknown location specimens) results in climate estimations which do not reflect the level of variation within the group. There is a clear geographic division between the five individuals from southeastern China (Guangzhou, Ningbo, and Shanghai), the central location assigned to unknown location individuals, and the northeastern individual from Manchuria. The Chinese sample of ten is therefore divided into two groups of five for the climate analyses

only: group 1: China (cool), the Manchurian and central individuals, and group 2: China (warm), the southeastern individuals (see Table 1).

Climate – China (cool): Mean annual temperature (MAT) of 8.67 °C; Mean annual precipitation (MAP): 554.04 mm/yr. This group is classified as Temperate.

Climate – China (warm): MAT of 19.04 °C, MAP of 1694.4 mm/yr. This group is classified as Hot/Wet.

Subsistence

For the definitions of subsistence groups here and throughout this section, see Section 2.IV.b.i. Since agriculture in China was established by 7000 BP (Zhao, 2011), it is assumed that the much more recent individuals in this population would have had a diet based on farmed foods. They are therefore classified as depending on domestic species (DOM).

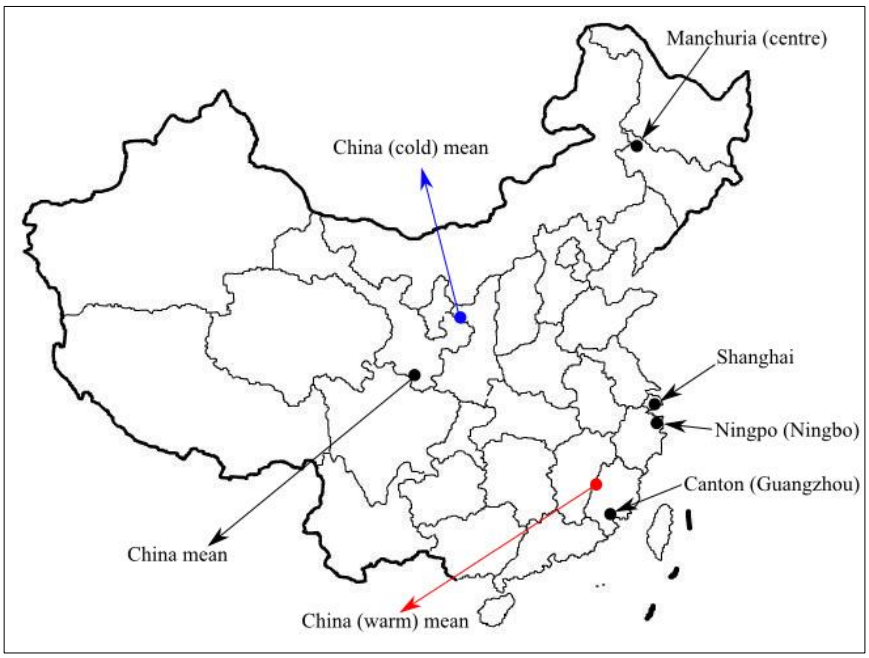

Figure 3: Approximate known locations for Chinese specimens, China mean (used for individuals with no known provenance), and mean locations for China (warm) and China (cold) groups (which are used to calculate climate variables). For latitudes and longitudes, see Table 1. Map adapted from blank map freely available from Wikicommons (www.wikicommons.org).

Greenland

The Greenland sample consists of seven Greenland Inuit from the Natural History Museum (London) collection (for more information see Appendix 1). There are three males and three females; age is recorded only as "adult". Known locations are shown on the map below (Figure 4). Biographical information is taken from information collated by Robert Kruszynski (Anthropology Curator at the Natural History Museum, London) from the Museum catalogues and archives. Most of the sample was originally donated to the Oxford University Museum by the explorer Edward Whymper in 1869 on his return from the Arctic and was later transferred to the Natural History Museum. This provides a minimum age for the sample.

Source

MicroCT collected by the author with permission from Robert Kruszynski, Farah Ahmed, and Margaret Clegg, Natural History Museum, London.

Subsistence

Traditionally the Greenland Inuit were foragers (Nansen, 1893). Staple foods were meat and fish; almost any meat would be eaten, especially in times of hardship. Vegetable food was scarce and seasonal (Nansen, 1893). Because of the date of the sample, it is most likely the specimens would have mainly followed a traditional diet and therefore this population is classified as Forager.

Climate Category

MAT for the Greenland Inuit is -7.68°C and MAP is 559.44mm/yr, therefore the population is classified as Cold/Dry.

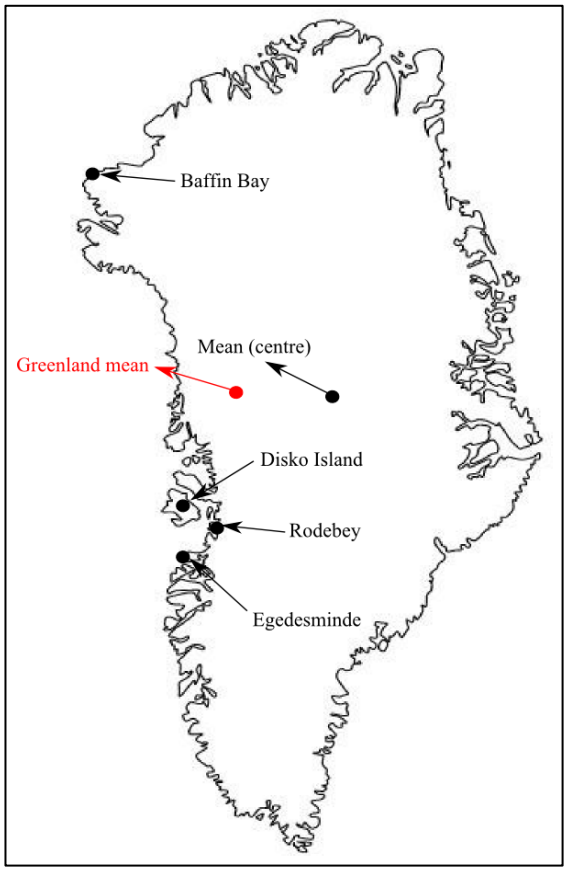

Figure 4: Approximate known locations for Greenland specimens. 'Mean (centre)' location was used for individuals of no known provenance. Greenland (mean) is mean of all locations used to calculate weather data. For latitudes and longitudes, see Table 1. Map adapted from blank map freely available from Wikicommons (www.wikicommons.org).

Hawaii

The Hawaiian sample consists of eleven adult crania (six females and five males) from Hawaii and Oahu Islands (see Figure 5) collected in the nineteenth century by European inhabitants of the Hawaiian Islands (for more details see Appendix 1). The specimens must therefore be at least nineteenth century, but may be much older, as some of the crania were collected from sepulchral caves and others from ancient burial grounds. The biographical information was supplied by Margaret Clegg (Head of Human Remains, Natural History Museum, London) from the Museum catalogues and archives.

Source

MicroCT scans courtesy of Robert Kruszynski, Farah Ahmed, and Margaret Clegg, Natural History Museum, London.

Subsistence

The Hawaiian Islands were traditionally divided into small villages and gardens. Pork was an important part of the diet; the staple was taro. Gardens, irrigated fields, and fish farms were tended in "intense cultivation" (Stannard, 1989: 27, McGregor, 2007). As horticulturalists, the Hawaiian individuals are classified as depending on domesticated species (DOM).

Climate category

The Hawaiian sample has a MAT of 25.3°C and an MAP of 591.60mm/yr and is thus classified in the Hot/Wet climate group.

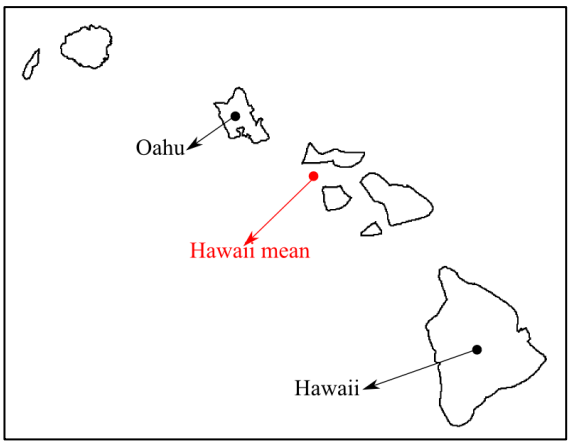

Figure 5: Map showing Hawaiian archipelago. Approximate centres of islands were used for locations recorded as Hawaii or Oahu. Hawaii mean: mean of all specimens' locations, which is used to calculate climate data. For latitudes and longitudes, see Table 1. Map adapted from blank map freely available from Wikicommons (www.wikicommons.org).

India

The Indian sample consists of twelve individuals from the Morton Collection held at University of Pennsylvania. According to ORSA records there are seven males and five females aged between 25 and 40 (for more details see Appendix 1). Known locations are shown on the map below (Figure 6). The known location sample is from what was historically Bengal; the region is now split into West Bengal and Bangladesh. No information was available regarding the date of the specimens beyond the fact that, as part of Morton's collection, they must have been collected prior to 1851 (Gould, 1997).

Source

Medical CT obtained from ORSA, courtesy of Janet Monge and Tom Schoenemann, University of Pennsylvania.

Subsistence

The origin of Indian agriculture (including crops and domesticated animals) is dated to approximately 7000 BP (Fuller, 2006), thus the Indian sample is categorised as depending on domesticated species (DOM category).

Climate

The MAT for the sample from India is 30.76°C and the MAP is 2034.36mm/yr. The sample is therefore classified as having a Hot/Wet climate.

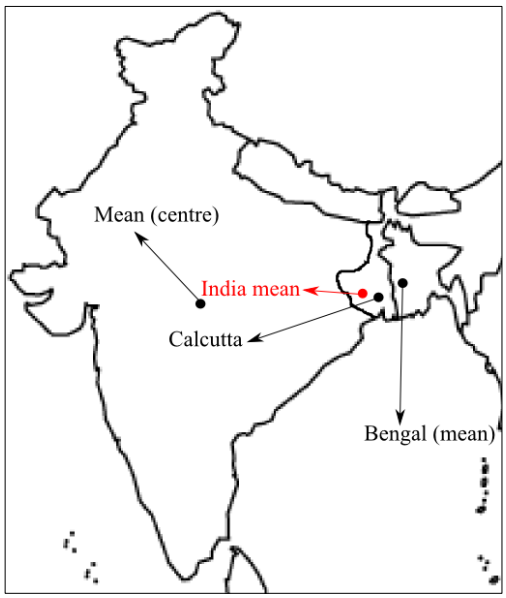

Figure 6: Map showing India/Bengal. Known location, approximate centre of India [Mean (centre) – used for specimens marked only "India"] and approximate centre of Bengal shown (used for specimens marked only "Bengal"). India mean: mean of all individual's locations, which is used to calculate climate data. For latitudes and longitudes, see Table 1. Map adapted from blank map freely available from Wikicommons (www.wikicommons.org).

Lithuania

The Lithuanian sample consists of 14 Lithuanian individuals from two archaeological sites: Alytus, a small medieval town in southern Lithuania (Jankaukas, 1998), and Plinkaiglais, a Middle Iron Age (fifth to sixth century) population from Central Lithuania (Palubeckaité, 2001) (see Figure 7). Sex is unknown, but all individuals were defined as adult based on the fusion of the spheno-occipital synchondrosis and the eruption to occlusion of the third molar (where present) (for more details see Appendix 1).

Source

Medical CT courtesy of Thomas Koppe, Ernst-Morritz-Arndt University, Greifswald.

Subsistence

For both Middle Iron Age and Medieval Lithuanians subsistence was based on agriculture (Jankaukas, 1998; Palubeckaité, 2001). Therefore the Lithuanian sample is classified as consuming domesticated species (DOM).

Climate category

The MAT for the two sites in Lithuania is 6.59°C and the MAP 676.26mm/yr, thus the Lithuanian sample is classified in the Temperate climate category.

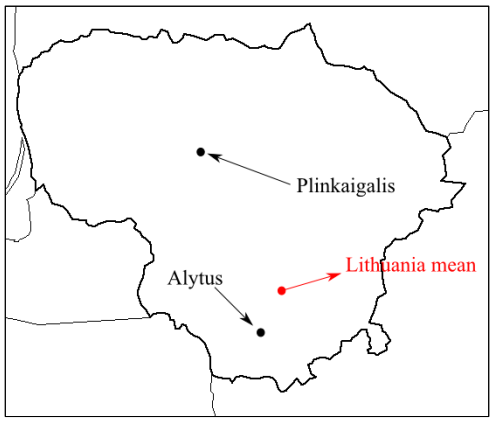

Figure 7: Locations of Lithuanian sites. Lithuania mean: mean for all specimens, which is used for climate calculations. For latitudes and longitudes, see Table 1. Map adapted from blank map freely available from Wikicommons (www.wikicommons.org).

Mexico

The Mexican sample consists of nine Mexicans from the Morton collection, and one from the Wistar collection obtained via ORSA (for more details see Appendix 1). Known locations are shown on the map below (Figure 8). In the ORSA database, some of the individuals are recorded as being Otomi (Otomie), Tlahuica, and Pame (Pames). These are extant indigenous ethnic groups in Mexico, although the same names are also given to ancient groups. Some of the sample is recorded as coming

from Tezcuco (Tetzcoco), an archaeological site of a city founded by the Chichimeca (Chechemeca) in the 11th or 12th centuries (Hicks, 1982). The "ancient tombs of Tacuba and Otumba", cited by Morton as the location of origin for some of his collection (Morton, 1839: 230), seem to be of Aztec origin. The beginnings of the Aztec civilisation date to the 12th century, and it came to an end with Spanish conquest in the 1500s. Thus the dates for the entire Mexican sample are likely to be between the 1000s and 1850s (when Morton died – see above).

Source

Medical CT obtained from ORSA, courtesy of Janet Monge and Tom Schoenemann, University of Pennsylvania.

Subsistence

Intensive agriculture began in Mexico around 7000 BP (Zizumbo-Villarreal & Colunga-GarcíaMarín, 2010), and given the most likely dates for the individuals in the Mexico sample, they are most likely to have relied on domesticated species (DOM category).

Climate category

The MAT for the Mexican specimens is 18.34°C and the MAP is 696.06mm/yr. Thus the sample is classified as a Hot/Wet climate category.

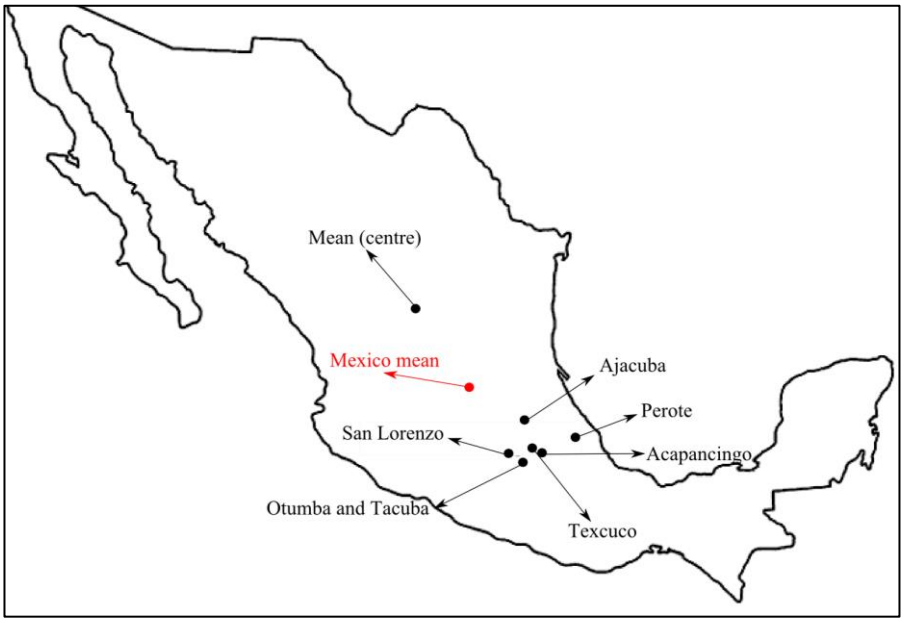

Figure 8: Map showing known Mexican locations and mean (approximate centre of Mexico) used for those of no known location. Mexico mean: mean of locations for all individuals. For latitudes and longitudes, see Table 1. Map adapted from blank map freely available from Wikicommons (www.wikicommons.org).

North Africa

The North African sample is composed of seven Iberomaurusians from Afalou Bou-Rhummel (Algeria) and Grotte des Pigeons, Taforalt (Morocco) (see Figure 9). The crania are housed at the Institut de Paléontologie Humain, Paris. The sample includes three specimens from Afalou and four from Taforalt. Age and sex are unknown, but all individuals were adult, as judged by the eruption of the third molar (where present) and/or the closure of the spheno-occipital synchondrosis (for more details see Appendix 1).

The Iberomaurusian was an epipalaeolithic microlithic bladelet industry spread widely along the Mediterranean coast of the Maghreb (Barton *et al.*, 2013). Grotte des Pigeons, Taforalt is a cave in the Beni-Snassen mountains in north-eastern Morocco. It was first excavated by Roche between 1944 and 1977 (Barton *et al.*,

2013). The human remains are dated to 14-15 ka (Barton, *et al.*, 2013; Humphrey *et al.*, 2014). Afalou Bou-Rhummel rockshelter is situated to the east of Algiers, between the towns of Bedjaïa and Jidjel. It was discovered in 1927 by Arambourg and excavated 1928-30 (Balzeau & Badawi-Fayad, 2005). The human remains have not been directly dated, but, based on stratigraphy, are aged between approximately 13.5 and 11.2 ka, or slightly older (Balzeau & Badawi-Fayad, 2005; Humphrey *et al.*, 2012).

Source

Medical CT courtesy of Amelie Vialet and Henri de Lumley, Institut de Paléontologie Humaine, Paris.

Subsistence

The Iberomaurusian is described as an epipalaeolithic forager culture with subsistence based on hunted animals, land snails, and gathered plants, such as pine nuts and acorns (Barton *et al.*, 2013; Humphrey *et al.*, 2014). Thus the North African population is classified as part of the Forager category.

Climate category

The North African sample is largely pre-Holocene, the two constituent sites also have potentially different dates (see above) and the climate was extremely variable at the time the individuals from Afalou and Taforalt lived (Lisiecki & Raymo, 2005). For these reasons, continuous climatic estimates based on recent data are likely to be inaccurate for these specimens and so the North African population is excluded from

continuous climatic analyses performed on only the recent *H. sapiens* sample (Section 6.I.). This is despite the fact that they are morphologically and taxonomically recent *H. sapiens* (Barton *et al.*, 2013) and are chronologically part of that group for the purposes of this thesis (see Section 2.IV.a.i.). There is, however, sufficient evidence of the palaeoclimate at Taforalt and Afalou to place them in climate categories with reasonable confidence and, therefore, to include them in analyses of differences between climate categories in the full sample (Section 6.II.).

Taforalt

Grotte des Pigeons, Taforalt is broadly coeval with the first part of Greenland interstadial 1 (Marine Isotope Stage [MIS] 1), a relatively warm, humid time for this region (Cacho *et al.*, 2001; Fletcher & Sánchez-Goñi, 2008; Barton *et al.*, 2013). Since the beginning of the Holocene, global $\delta^{18}O$ levels have decreased, indicating a warmer, more humid climate (Lisiecki & Raymo, 2005). The area around Grotte des Pigeons today would be classified as Dry (estimated annual precipitation, based on weather station data, as for other recent *H. sapiens* (see Appendix 3), is 323.28mm/yr). During the time at which the Taforalt individuals lived it would have been drier, based on $\delta^{18}O$ levels. It is therefore reasonable to put Taforalt in the Dry climate category for this thesis. Sánchez-Goñi *et al.* (2002) found that in late Pleistocene interstadials in the Mediterranean minimum temperatures were similar to those found today, and today Taforalt would have an annual mean temperature of 17.02°C; thus, it is reasonable to place the Taforalt sample in the Hot/Dry group.

Afalou

The Afalou remains are probably slightly younger than those from Taforalt. Dated to at least 13.5-11.2 ka, this time period includes interstadial phases but also the severe Younger Dryas stadial (YD). The YD was a dry, cool period, during which desert vegetation in the Mediterranean expanded its range (Fletcher & Sánchez-Goñi, 2008). Globally the YD is dated to 12.9-11.5 ka Cal BP (Meyer *et al.*, 2010). Before the YD, during MIS 1 (Cacho *et al.*, 2001; Fletcher & Sánchez-Goñi, 2008), and after the YD as the climate approached the Holocene climatic maximum (Cacho *et al.*, 2001), the humidity at Afalou is likely to have been similar to the MIS 1 of Taforalt (classified here as Dry), since they are geographically very close. During the YD, the Mediterranean was even more arid (Fletcher & Sánchez-Goñi, 2008). Thus the Afalou remains can be classified as Dry, if a palaeoclimate analogous to that at Taforalt (classified as Dry) is the most humid likely condition for Afalou.

During the most extreme low temperatures of the YD, sea surface temperatures dropped by 3-4 °C (Cacho *et al.*, 2001). Sea surface temperatures have been shown to be a robust proxy for land air temperatures in the Mediterranean (Bar-Matthews *et al.*, 2003). Therefore, if the temperatures prior to the YD can be assumed to be at least as warm as at present (see above), then the coldest temperature during the date range for Afalou would have been a MAT estimate of 14.78 °C (based weather station data – see Appendix 3). This is just below the cut-off for the Hot climate group (>15°C, see Section 2.IV.c.i.). Marine core evidence from the Alboran Sea (between Spain and Morocco), however, shows that the YD here was shorter than in other regions (Cacho *et al.*, 2001). In the Alboran Sea, the YD lasted only

approximately 700 years, with an abrupt warming phase (temperatures increasing by about 3.3°C every 55 years) beginning at ~12.3 ka and reaching the warmest temperatures in the last 25 ka at around 10.9 ka (Cacho, *et al.*, 2001). Thus, the extreme cold and aridity of the YD would only have been experienced in Afalou for approximately 700 years out of the approximately 2,300 years of the dating range for the human remains. Given that the MAT estimate of 14.78 °C is suggested for the very lowest temperature in the date range, and the YD is thought to have lasted less than a third of the time in question, a Hot classification for Afalou, as for Taforalt, seems most reasonable. The whole North African sample is therefore classified as Hot/Dry.

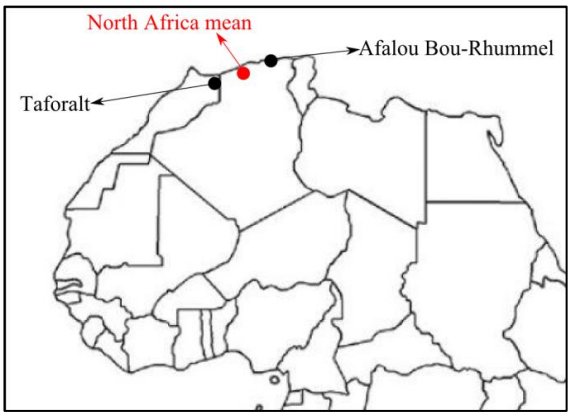

Figure 9: Location of Taforalt, Morocco and Afalou Bou Rhumel, Algeria. North Africa mean: mean of locations for all individuals. For latitudes and longitudes, see Table 1. Map adapted from blank map freely available from Wikicommons (www.wikicommons.org).

Peru

The sample comprises ten Peruvians from the Morton collection obtained via ORSA. There are five males and five females, aged 30 to 60 years (for more details see Appendix 1). The ORSA records cite many of the remains as originating from Pachacamac, an archaeological site comprising an urban centre inhabited from about

100 BC to the Spanish conquest at 1553 (Michczynski *et al.*, 2007). Several of the other specimens are recorded as being Toltec; the Toltec civilisation lasted from around 950 to 1150 AD (Diehl, 1993). The entire Peruvian sample is therefore likely to date from between 100 BC and 1553 AD. Known locations are shown on the map below (Figure 10).

Source

Medical CT obtained from ORSA, courtesy of Janet Monge and Tom Schoenemann, University of Pennsylvania.

Subsistence

Food production in Peru began with the domestication of crops from approximately 9000 BP (Piperno, 2011), therefore, given the approximate dates of the specimens, this sample is classified as part of the domesticated consumers (DOM) category.

Climate category

The MAT for the Peruvian sample is 18.84°C and the MAP is 198.36mm/yr, thus the sample is classified as part of the Hot/Dry climate category.

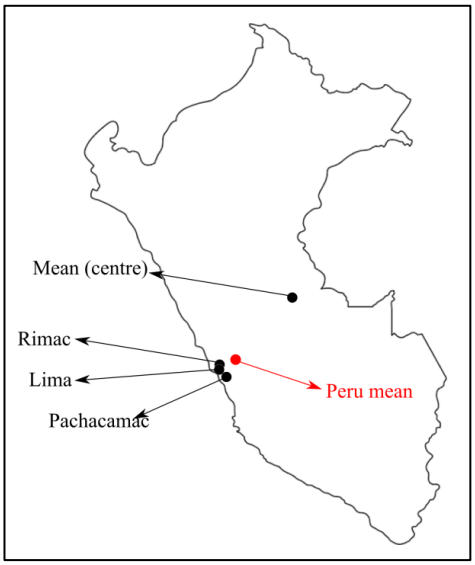

Figure 10: Known locations for Peruvian sample and mean (centre) location used for climate classification when specific location is unknown. Peru mean: mean of location for each individual used to calculate climate variables. For latitudes and longitudes, see Table 1. Map adapted from blank map freely available from Wikicommons (www.wikicommons.org).

Russia

The Russian sample consists of four individuals from the Morton collection obtained via ORSA. According to the ORSA records, there is one male and three females aged between 40 and 65 years, three are recorded as being Tchukchi (Chuckchi), and one Kalmuck (Kalmyk) (for more details see Appendix 1). Locations are shown on the map below (Figure 11). No information was available regarding the date of the specimens, but as above, they must be pre-1851 to be part of Morton's collection (Gould, 1997).

Source

Medical CT obtained from ORSA, courtesy of Janet Monge and Tom Schoenemann, University of Pennsylvania.

Subsistence

The Chuckchi are traditionally (this was still the case when Bogoras conducted his fieldwork at the beginning of the twentieth century) divided into Reindeer Chuckchi and Maritime Chuckchi based on their subsistence method (Bogoras, 1904-9; Kerttula, 2000). It is not known from which group the individuals in the current sample came. There is, however, evidence that this split is not complete (Bogoras, 1904-9; Kerttula, 2000). Originally, according to the Chuckchi, their people lived in coastal regions and had a mixed subsistence pattern, hunting marine mammals, as well as herding some reindeer. Indeed at the beginning of the twentieth century, Bogoras (1904-9) writes that many camps of Reindeer Chuckchi had small herds only, and supported themselves largely by seal hunting. He also records (Borogas, 1904-9: 71) that the domestication of the Chuckchi reindeer was "imperfect...milking is impossible; and the reindeer are difficult to manage even in harness, and are unable to endure prolonged and regular service". Despite their herding, the Reindeer Chuckchi were described as semi-maritime people, who disliked getting too far away from the sea, and who had a taste for seal meat, whale blubber and skin. Even for the reindeer-herding Reindeer Chuckchi, fishing and gathering on tundra subsidised herded reindeer meat (Kerttula, 2000). As it is not known which Chuckchi group the sample belonged to, as the Chuckchi reindeer were only semi-domesticated, as both groups still depended for a large amount of their diet on wild resources, as domesticated vegetable foods do not form any major part of the diet, and given the presumed date of the specimens, the Chuckchi are categorised in the Forager group.

The Kalmyks are traditionally nomadic pastoralists, herding goats, sheep, and camels and living mainly off their milk and meat (Mataskovna Gouchinova, 2006). This type of subsistence does not fit neatly into the broad categorisation of domesticated species consumers (DOM) versus Foragers used in this thesis (see Section 2.IV.b.ii.). Although the animals herded by the Kalmyks are domesticated, the absence of vegetable foods in their diet separates them from most other DOM groups. The processed domesticated vegetable foods relied on by most agriculturalists and horticulturalists are the dietary element likely to result in lower dietary strain in these groups compared to hunter-gatherers (González-José, *et al.*, 2005; Sardi *et al.*, 2006; Paschetta *et al.*, 2010), a difference that may not be seen in pastoralists. It would be interesting to see if pastoralists form an intermediate group between Foragers and DOM in analyses of masticatory shape, but since there is only one pastoralist individual in this sample, this specimen was instead excluded from dietary analyses (Chapter 5) to avoid obscuring a possible shape difference between the two dietary samples.

Climate

The Russian sample has a MAT of-5.18°C and a MAP of 437.82mm/yr, the Russian sample is therefore classified in the Cold/Wet group.

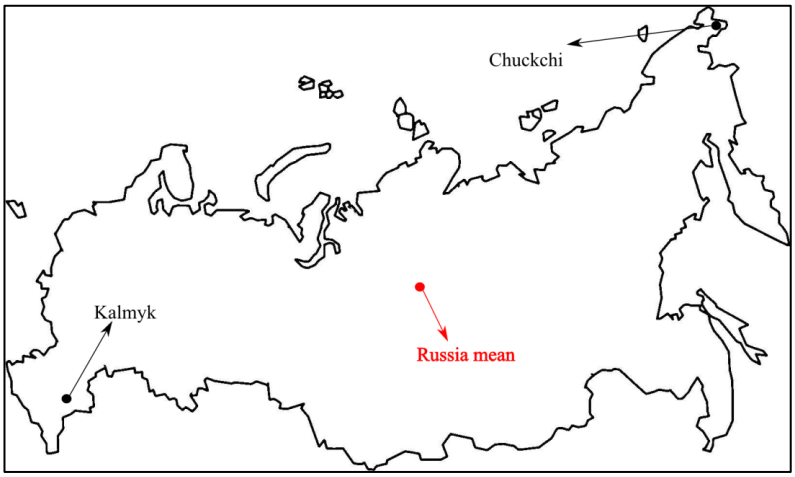

Figure 11: Approximate locations for Russian sample of Kalmycks and Chuckchi. Russia mean: mean location for all individuals used to calculate climate variables. For latitudes and longitudes, see Table 1. Map adapted from blank map freely available from Wikicommons (www.wikicommons.org).

Tasmania

The Tasmanian sample consists of eight individuals from collections at the Natural History Museum, London. Three individuals are male (or probably male), two female, and three are of unknown sex. All are recorded as "adult" in the Museum catalogue (for more details see Appendix 1). For those specimens where such information is available, crania are recorded as having been donated in the mid- to late-1800s, providing a minimum age. Known locations are shown on the map below (Figure 12). Biographical information was provided by Margaret Clegg, Head of the Human Remains Unit (HRU) at the Natural History Museum, from the Museum catalogue and archives.

Source

MicroCT scans courtesy of Robert Kruszynski, Farah Ahmed, and Margaret Clegg, Natural History Museum, London.

Subsistence

The Tasmanians were traditionally foragers, eating mainly terrestrial and marine animal foods (Clark, 1983; Plomley, 1983; Reynolds, 2006). Plant foods generally contributed less than animal foods, but this varied with season (Clark, 1983; Plomley, 1983). Given their early date, the Tasmanians in the current sample are classified as part of the Forager subsistence group.

Climate category

Tasmania has an MAT of 13.47°C and an MAP of 686.34mm/yr, it forms part of the Temperate climate group.

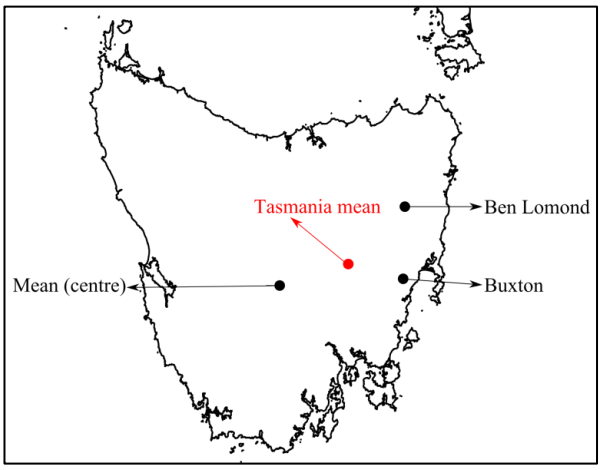

Figure 12: Approximate locations for Tasmanian specimens' possible provenances and mean location used where provenance is not given. Tasmania mean: mean of all locations for all individuals used to calculate climate variables. For latitudes and longitudes see Table 1. Map adapted from blank map freely available from Wikicommons (www.wikicommons.org).

Torres Straits Islands

The Torres Straits Islands (TSI) are over 100 islands set in the narrow (not much more than 150km wide) stretch of water between Cape York in northern Australia, and the southwest coast of Papua New Guinea (Lawrence & Reeves Lawrence,

2004). The Torres Straits Islands sample consists of 14 adult individuals. Where such details exist, the Natural History Museum archives record that the crania were collected between the 1840s and 1880s, providing a minimum age for the specimens. Of the individuals with biographical information, two are possible females, and four of unknown sex (for more details see Appendix 1). All individuals are recorded as "adult". Known locations are shown on the map below (Figure 13). Biographical information is from Margaret Clegg, as above.

Source

MicroCT courtesy of Robert Kruszynski, Farah Ahmed, and Margaret Clegg, Natural History Museum, London

Subsistence

Of the specimens' islands of origin (where known), Mabuiag, Nagir (Nagheer), Moa (Banks Island) and Muralŭg (Prince of Wales Island) are western islands and Erub (Darnley) is an eastern island (see Appendix 1 and Figure 13). The western islands are rocky, with sparse vegetation, whilst the eastern islands support rich vegetation (Haddon, 1935; Lawrence & Reeves Lawrence, 2004). These different environments led to differences in the traditional subsistence strategies; there was an east to west subsistence gradient within the islands. Pre-contact, the western islanders were organised into mobile bands of foragers, whereas the eastern islanders inhabited hamlets and villages and practiced mixed foraging and horticulture (Lawrence & Reeves Lawrence, 2004). Given the ethnographic information, and their relatively early date, the western TS islanders are categorised as Foragers. The eastern

islanders are excluded from the dietary strain analyses (Chapter 5) as their diet is likely to have been more mixed.

Climate category

The MAT for the Torres Straits Islanders in the sample is 28.28°C and the MAP is 4995.12mm/yr. The group is therefore classified in the Hot/Wet climate group.

Ethnographical note

Head hunting was commonly practised among the TS islanders in pre-contact times, particularly in the western islands (Haddon, 1935). The heads of slain enemies were kept as trophies and, in some regions (mainly the western islands) raiding parties were initiated for this very purpose; Haddon (1935) reports that there was raiding and trade in heads as far afield as New Guinea. These practices make it difficult to know if the crania in the sample actually came from individuals who lived on the islands where they were found. Four crania were found in a trophy cave on Mabuiag, but the Museum archive documents suggest they would in fact have come from an enemy group of the Mabuiag islanders, probably Moa islanders (Museum archives, courtesy of M. Clegg). However, as Moa is still a western island, that would not affect the dietary strain analyses on the basis of differences in subsistence strategy.

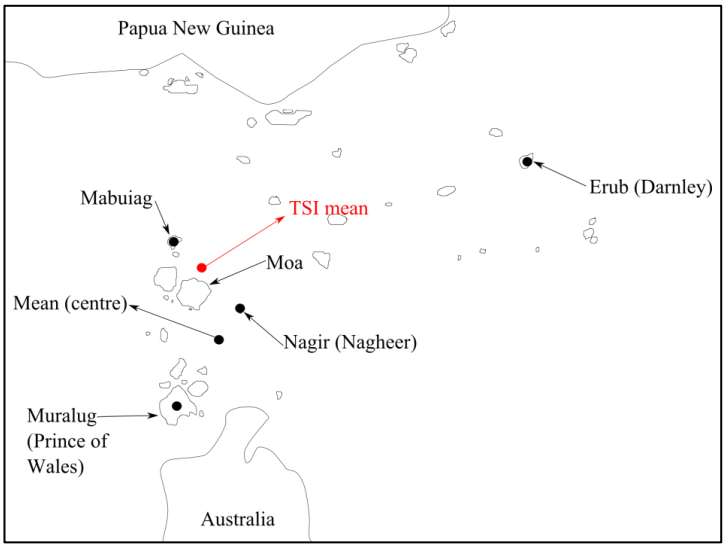

Figure 13: Torres Straits Islanders locations for known provenance individuals and mean location used for individuals of unknown provenance. TSI mean: mean of all locations of all individuals used to calculate climate variables. For latitudes and longitudes, see Table 1. Map hand-drawn in Inkscape (Harrington, 2004-5), copied from Google Maps (www. google.com/maps).

Western Africa

The Western African sample consists of 13 individuals (ten Liberians, two Nigerians, and one Angolan) from the Morton Collection, obtained via ORSA. According to ORSA records, there are ten males and three females aged between 25 and 50 years (for more details see Appendix 1). No information was available regarding the date of the specimens except that they must be pre-1851 (see above) (Gould, 1997). Known locations are shown on the map below (Figure 14).

Source

Medical CT obtained from ORSA, courtesy of Janet Monge and Tom Schoenemann, University of Pennsylvania.

Subsistence

Agriculture began in Western Africa at least 3000 BP (Manning, 2010) with several plant species independently domesticated in that region (Harlan, 1971). Since none of the tribal groups included in this study (see Appendix 1) are reported to be foragers (Lee & Hitchcock, 2001, Mitchell, 2006), the Western African sample are classified as DOM.

Climate category

With an MAT of 25.41°C and an MAP of 4029mm/yr, the Western African population is classified as Hot/Wet.

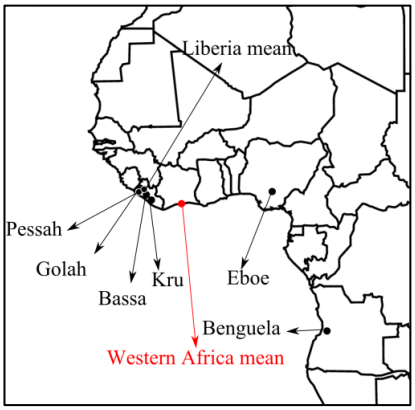

Figure 14: Approximate locations for known provenance individuals in Western African sample labelled by tribal group (see Appendix 1), and mean Liberian location for individual for whom there is no greater detail. West Africa mean: mean of all locations for all individuals used to calculate climate variables. For latitudes and longitudes see Table 1. Map adapted from blank map freely available from Wikicommons (www.wikicommons.org).

Western Europe

The Western European sample consists of twelve contemporary Western Europeans, nine males and three females. Two are from the Netherlands, four from Norway/Sweden, two from Hannover, two from Pommern, and two are unspecified

Germans (for more information see Appendix 1). Known locations are shown on the map below (Figure 15). The two Germans are held at the Institut für Humangenetik und Anthropologie, Freiburg, all other specimens are held at the Anatomisches Institut, University of Leipzig.

Source

Medical CT from contemporary (possibly extant) individuals freely obtained from NESPOS (www.nespos.org).

Subsistence

This is a recent Western European population. They are thus classified as relying on domesticated species (DOM category).

Climate category

For the specimens in the Western Europe sample the MAT is 7.9°C and the MAP is 577.5 mm/yr. Therefore the sample is classified as part of the Temperate group.

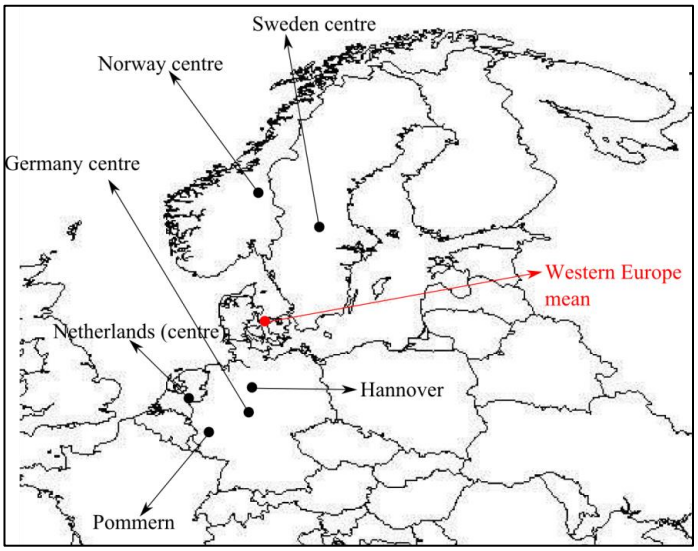

Figure 15: Approximate locations for known provenance individuals in Western Europe sample. Western Europe mean: mean of locations for all individuals used to calculate climate variables. For latitudes and longitudes, see Table 1. Map adapted from blank map freely available from Wikicommons (www.wikicommons.org).

Table 1: Summary of recent *H. sapiens* sample (n = 132, for further details, see Appendix 1) details and climate variables. For calculation of climate variables see Section2.IV.c.i. . For justification for climate categories, see Section 2.I.b.i. MAT: mean annual temperature, maxTemp: maximum monthly temperature; minTemp: minimum monthly temperature; MAP: mean annual precipitation; maxPrecip: maximum monthly precipitation; maxPrecip: maximum monthly precipitation.

Population	Specific location where known	Latitude of known location	Longitude of known location	Mean latitude for population	Mean longitude for population	MAT (°C)	maxTemp (°C)	minTemp (°C)	MAP (mm/year)	maxPrecip (mm/month)	minPrecip (mm/month)	Climate category
China (cool)	Manchuria	45°52'N	123°53'E									
	Mean (centre)	34°31'N	103°89'E	36°55'N	107°82'E	9	19	-3	554	113	4	Temperate
China (warm)	Guangzhou	23°13'N	113°26'E									
	Ningbo	29°87'N	121°54'E									
	Shanghai	31°23'N	121°47'E	26°10'N	116°56'E	19	28	9	1694	297	45	Hot/Wet
Greenland	Baffin Bay	78°67'N	-71°57'E									
	Disko Island	69°82'N	-53°43'E									
	Egedesminde	68°71'N	-52°87'E									
	Rodebay	69°33'N	-50°97'E									
	Mean (centre)	75°58'N	-39°55'E	73°32'N	-49°64'E	-8	5	-21	229	29	9	Cold/Dry
Hawaii	Hawai'i	19°58'N	-155°53'E									
	O'ahu	21°43'N	-157°99'E	20°93'N	-157°32'E	23	24	22	592	92	7	Hot/Wet
India	Bengal (mean)	23°21'N	88°95'E									
	Calcutta	22°57'N	88°36'E									
	Mean (centre)	20°96'N	78°22'E	22°73'N	87°11'E	25	31	20	2034	336	3	Hot/Wet
Lithuania	Alytus	54°40'N	24°46'E									
	Plinkaigalis	55°41'N	23°66'E	54°62'N	24°29'E	7	18	-5	676	81	31	Temperate
Mexico	Ajacuba	20°09'N	-99°12'E									
	San Lorenzo	20°47'N	-100°72'E									
	Perote	19°56'N	-97°24'E									
	Acapancingo	18°91'N	-99°22'E									

	Otumba & Tacuba	19°46'N	-99°19'E								
	Tezcuco	19°53'N	-98°53'E								
	Mean (centre)	23°63'N	-102°50'E	20°94'N	-100°24'E	19	22	15	696	110	6	Hot/Wet
North Africa	Afalou, Algeria	36°7'N	5°53'E									
	Taforalt, Morocco	34°48'N	-2°24' E	35°59'N	1°65'E	-	-	-	-	-	-	Hot/Dry
Peru	Lima	-12°08'N	-76°87'E									
	Pachacamac	-12°19'N	-76°85'E									
	Rimac	-12°03'N	-77°04'E									
	Mean (centre)	-9°80'N	-74°36'E	-11°92'N	-76°62'E	19	22	15	198	33	0	Hot/Dry
Russia	Chuckchi Peninsula	66°16'N	-175°14'E									
	Kalmykia	46°57'N	45°77'E	61°26'N	-119°91'E	-5	17	-27	438	57	16	Cold/Wet
Tasmania	Buxton	-42°32'N	148°.30'E									
	Ben Lommond	-41°54'N	147°67'E									
	Mean (centre)	-42°36'N	146°67'E	-42°22'N	147°00'E	13	17	10	686	71	44	Temperate
Torres Straits	Erub	-9°39'N	142°59'E									
	Mabuiag	-9°96'N	142°18'E									
	Mŭralug	-10°68'N	142°18E									
	Nagheer	-10°25'N	142°48'E									
	Mean (centre)	-10°40'N	142°36'E	-10°09'N	142°29'E	28	28	25	4995	416	6	Hot/Wet
Western Africa	Bassa (Liberia)	4°78'N	-8°4'E									
	Benguela (Angola)	-12°80'N	13°91'E									
	Eboe (Nigeria)	5°35'N	6°64'E									
	Golah (Liberia)	7°23'N	-10°81'E									
	Krooman (Liberia)	4°70'N	-7°51'E									
	Pessah (Liberia)	7°04'N	-10°92'E									

	Liberia (centre)	6°43'N	-9°43'E	4°53'N	-5°33'E	25	27	24	4029	651	20	Hot/Wet
Western Europe	Hannover, Germany	52°38'N	9°73'E									
	Pommern, Germany	50°17'N	7°27'E									
	Germany (centre)	50°93'N	10°24'E									
	Netherlands (centre)	52°27'N	5°58'E									
	Norway/ Sweden (centre)	64°59'N	16°30'E	55°82'N	10°90'E	7.9	16	0	578	66	31	Temperate

2.I.b.ii: Fossil sample

In this section, the fossil sample (early *H. sapiens, H. neanderthalensis, H. heidelbergensis,* and *H. erectus*) is detailed along with date, taxonomic attribution (where disputed), subsistence strategy, and climate assigned to each specimen and justification for these assignments, plus any other relevant information. For definition of subsistence and climate, categories, and taxonomic definitions see Section 2.IV.b.i. and 2.IV.c.i. respectively. For summary see Table 2.

Note on subsistence

As they predate agriculture, all the fossils are included in the Forager subsistence group (see Section 2.IV.b.i.).

Homo erectus

The *H. erectus* sample consists of two specimens from Koobi Fora in Kenya.

KNM-ER 3883

This specimen is dated to between 1.5 and 1.65 Ma (million years) (Antón, 2002).

KNM-ER 3733

This specimen is dated to approximately 1.78 Ma (Antón, 2002).

Source

Both medical CT purchased from the National Museums of Kenya.

Climate category

Palaeoenvironmental reconstructions analysing the distribution of ^{13}C-^{18}O bonds in palaeosol carbonate isotopes in the Turkana Basin (Koobi Fora is in the Turkana Basin) show that the local climate has been very hot and dry for most of the last four million years (Passey *et al.,* 2010). The results indicate that at the time of soil carbonate formation soil temperatures were typically > 30 °C, and often > 35 °C, which is similar to what occurs today. These soil temperatures result from high air temperatures and solar heating of the soil surface. Given that the air temperatures needed to achieve these temperatures with a forested habitat (more humid environment) are extremely rare, as are the amounts of precipitation needed to sustain such forest at similar temperatures, a hot arid environment, as seen today, is most likely (Passey *et al.*, 2010). A detailed study using fossil mammal assemblages as environmental indicators in the region also suggests a dry, savannah ecosystem was in place from approximately 2.5 Ma onwards (Hernández Fernández & Vrba, 2006). Hernández Fernández and Vrba (2006) estimate that the annual precipitation for the two stratigraphic layers at Koobi Fora of interest, OKT (1.39-1.64 Ma) and KBS (1.64-1.88 Ma), are 357mm/yr and 292mm/yr respectively. The Koobi Fora specimens are therefore categorised as Hot/Dry.

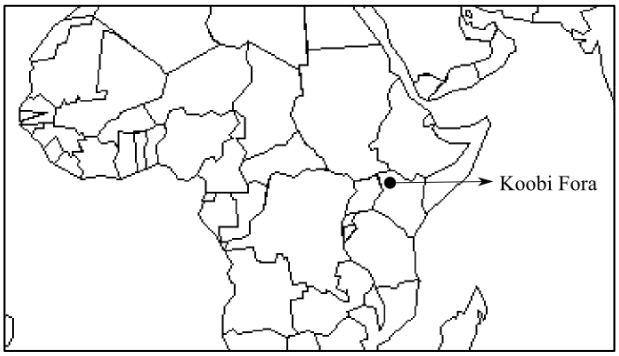

Figure 16: Site of *H. erectus* provenance. Koobi Fora: Kenya. For more details, see text. Map adapted from blank map freely available from Wikicommons (www.wikicommons.org).

Homo heidelbergensis

Bodo

The Bodo cranium was found in the Middle Awash Valley of Ethiopia in 1976. It is dated to approximately 600 ka using chronostratigraphic methods (Clark *et al.*, 1994).

Source

Medical CT purchased from the Digital Archives of Fossil Hominoids, University of Vienna.

Climate category

Palaeotemperature reconstructions from Middle Pleistocene Africa are very rare, perhaps because humidity levels have always been more variable and had more effect on ecosystems, whilst the more constant temperature has generated less interest. However, the ~74 ka Lake Malawi geochemical proxies for lake surface temperature (TEX_{86}), which are thought to be close to mean annual air temperatures, show that during cold stages (glacials), mean temperatures did not drop below 20°C

(Woltering *et al.*, 2011). Although the date of this proxy is much younger than the approximate date for Bodo, it seems reasonable to conclude that during the relatively warm, interglacial stage of MIS 15, Bodo would have certainly fulfilled the criteria for the Hot climate category.

Mediterranean sapropels (marine deposits of organic matter resulting from increased riverine run-off during periods of high precipitation) suggest a green Sahara period (i.e., wetter conditions, with MAP of 500-1000mm/yr) at 600 ka (Larransoaña *et al.*, 2013). The majority of that range places Bodo in the Wet category (MAP > 550mm/yr for hot climates, see Section 2.IV.c.i.). This was also a time of growth in East African lakes (an indicator of regional palaeoclimate), suggesting a wetter climate (Schultz & Maslin, 2013: 2). Bodo is therefore placed in the Hot/Wet climate category.

Ceprano

Ceprano is a site in Italy, southeast of Rome. The hominin calvaria that takes its name from the site was found in 1994. Based on geological and palaeobiological evidence Ceprano is dated to the interglacial of MIS 11, 430-385 ka (Manzi *et al.*, 2010).

Source of data

Medical CT courtesy of Giorgio Manzi, Universitá La Sapienza, Rome.

Taxonomic attribution

It has been suggested that Ceprano is more primitive than other member of the *H. heidelbergensis* hypodigm, and that it is more *H. erectus*-like in many aspects of its morphology (Bruner & Manzi, 2005; Mounier *et al.*, 2011; Rightmire, 2013). In fact, due to its more primitive features, Ceprano has been posited as the ancestral species for *H. heidelbergensis* (Manzi *et al.*, 2001; Stringer, 2002b; Bruner & Manzi, 2005; Mounier, *et al.*, 2011), despite its relatively young date of 430-385 ka (Manzi *et al.*, 2010). Given its date, and the current lack of any other species at that point for which there is greater evidence for an attribution (Bruner & Manzi, 2005; Mounier *et al.*, 2011), Ceprano is here included provisionally in *H. heidelbergensis* and its relative position in the analyses is considered in order to ascertain whether this is a reasonable assignation for the fossil.

Trauma

There is reactive bone growth, perhaps due to trauma, visible on ectocranial surface of Ceprano's right browridge, but there is no sign that this affected the frontal sinus or anything else other than the immediate cortical bone (Bruner & Manzi, 2005).

Climate category

Based on the over-lapping present day climatic tolerances of amphibians and reptiles found in different layers of the Gran Dolina (Atapuerca, Spain) site, Blain *et al.* (2009) predict that at the start of level TD10 (late Middle Pleistocene) MAT was 12.56°C and MAP was 981mm/yr. Current climatic indices from the Gran Dolina site are: MAT: 9.9°C and MAP: 572 mm/yr. For Ceprano, the MAT is 15.46°C and

the MAP is 761.23 mm/yr. If the same warmer, moister trend in northern Spain can be applied to the rest of southern Europe, the differences between current and projected past temperatures for Gran Dolina can be used to calculate plausible climatic ranges for Ceprano. This results in an estimated MAT of 18.12°C and MAP of 1170.23 mm/yr. This is well over the Hot/Wet climate threshold; Ceprano is therefore placed in this category.

Kabwe (Broken Hill) 1

This specimen was found by lead miners in a cave in Broken Hill, Northern Rhodesia (now Kabwe, Zambia) in 1921 (Woodward, 1921). It is currently dated to the Middle Pleistocene, between approximately 700 and 300 ka using faunal analogies, palaeomagnetography and sedimentation rates (Klein, 1973). However, it is undergoing new ESR dating which is likely to show that Kabwe dates to ~250-300 ka (Stringer, 2011, 2012b) and that is the date used in the current study.

Source

Medical CT courtesy of Robert Kruszynski and Farah Ahmed, Natural History Museum, London.

Pathology

Kabwe exhibits lesions on its temporal region, two of which are possibly pathological, the others of which are most plausibly explained by postmortem trauma (Montgomery *et al.*, 1994). The lesions to the squamous temporal and petrosal temporal do not affect the shape of the cranium, and the damage to the mastoid is not

so great that it was not possible to digitise the landmark mastoidale (see Section 2.III.c.i.). Kabwe also has several abscesses resulting from severe dental caries (Montgomery *et al.*, 1994), but these are not extensive enough to affect any of the regions landmarked or the paranasal sinuses.

Climate category

As described above, TEX_{86} temperature records show that during cold stages (glacials) including the last glacial maximum (LGM) and the peak cold period previous to that (MIS 4), mean temperatures in Malawi did not drop below 20°C (Woltering *et al.*, 2011). The World Bank (based on data 1960 to 1990) now gives Malawi an average temperature range of 17.6 to 24.4°C and Zambia an annual temperature range of 17.1 to 24.7°C (WBG, 2013), suggesting that the two countries experience similar temperatures. From this, it seems reasonable to conclude that even during the glacial stage of MIS 8, Kabwe would have been warmer than the palaeoreconstructions for Malawi and, thus, fulfilled the criteria for the Hot climate category. West African, North African and Arabian Sea dust records correlate with East African Rift lake level data, suggesting that lake presence can indicate wet/arid periods for the whole of Africa, including Zambia (Schultz & Maslin, 2013). Kabwe is dated to a non-lake period, suggesting aridity (Schultz & Maslin, 2013). This fits with its position in glacial MIS 8, which has been shown by West African palynolgical analyses to be relatively arid (Jahns *et al.*, 1998). It seems that, as a whole, glacial periods were drier than interglacials in Africa (Dupont, 2011); therefore, Kabwe is placed in the Hot/Dry climate category.

Petralona

The Petralona cranium was found in Petralona Cave, near Thessaloniki, Greece. Due to the lack of preserved *in situ* sediments, it has been difficult to date (Stringer, 1983). Based on fauna, the cranium is thought to be between approximately 350 and 730 ka, but there is some debate over whether the fauna and the hominin fossil are associated, and the date of the hominin cranium is thought to be far nearer the former, possibly about 400 ka (Stringer, 1983). Based on ESR dating of flowstone thought to have bracketed the cranium, it is dated to a much younger 150-200 ka (Grün, 1996), but there is some question as to exactly where the ESR samples came from; therefore, this date is not entirely secure. As the potential age range (150-700 ka) covers many changes in climate, for the purposes of this thesis the approximate mid-point of this range, the ~400 ka suggested by Stringer (1983), is used.

Source

Medical CT courtesy of Gerhard Weber, University of Vienna and George Koufos, Aristotle University of Thessaloniki.

Climate category

As described for Ceprano, Blain *et al.* (2009) predict, for the Gran Dolina site, that the climatic range from the late Middle Pleistocene is: MAT: 12.56°C and MAP: 981mm/yr. The current climatic indices for the site of Petralona were calculated as described for the recent *H. sapiens* sample. The MAT is 16.10°C and MAP is 442.83mm/yr. If the same warmer, moister trend seen in northern Spain at Gran Dolina can be applied to the rest of southern Europe, the differences between current

and projected past temperatures for Gran Dolina can be used to calculate plausible climatic variables for Petralona: MAT: 18.3°C and MAP: 799.3 mm/yr. These estimations classify Petralona in the Hot/Wet climate category. If the cranium is younger than 400 ka, as suggested by Grün (1996), at approximately 200 ka, this would still date Petralona to a relatively warm stage (the MIS 7 interglacial), and so would be unlikely to change the fossil's climate category.

Steinheim

The Steinheim cranium was discovered in 1933 in a gravel pit near Steinheim, Germany (Berckheimer, 1933). On geological evidence, Steinheim is dated to either ~250 ka or > 300 ka, but the latter is more commonly accepted, placing Steinheim in interglacial MIS 9 (Street *et al.*, 2006).

Source

Medical CT purchased from the Digital Archives of Fossil Hominoids, University of Vienna.

Taxonomic attribution

Steinheim is an enigmatic fossil, showing affinities with both Mid Pleistocene *H. heidelbergensis* and Neanderthals (Stringer, 1974, 1994, 2012c; Rightmire, 1998; Tattersall, 2007). It is variably placed in one of the two taxa by different authors (e.g., Friess, 2010a, b, Harvati *et al.*, 2010; Stringer, 2012c). In any case, the non-linear, accretory process by which *H. heidelbergensis* seems to have evolved into *H. neanderthalensis* in Europe (e.g., Hublin, 2007) makes it hard to draw a line between

these two taxa. In the current study, the fossil is preliminarily placed in *H. heidelbergensis*, due to its relatively early date and its effect on the results is examined and discussed in Sections 4.II.a.ii. and 7.I.b.i.

Distortion

Steinheim has suffered some postmortem distortion (e.g., Prossinger *et al.*, 2003), yet this is not so severe as to preclude its regular inclusion in morphological studies (e.g., Dean *et al.*, 1998; Tattersall, 2007; Rightmire, 2008, 2013; Friess, 2010a, b, Harvati, *et al.*, 2010). The specimen is a key part of any study of Mid Pleistocene morphology, because of its age and combination of characteristics. In the current study, it is included despite its distortion, but its position in analyses is scrutinised to see if its possibly unnatural shape affects the results.

Climate category

During interglacials, the area around Steinheim would have been covered with thick deciduous forest, suggesting this was not an arid climate (van Andel & Tzedakis, 1996; Dennell *et al.*, 2011). Kühl and Litt (2007) reconstruct the temperature of the Holsteinian interglacial (which they interpret as being MIS 9) as being roughly between 0 and -10°C in the coldest month and 15-20°C in the warmest month. This gives an MAT of 5°C and places Steinheim in the Temperate climate category.

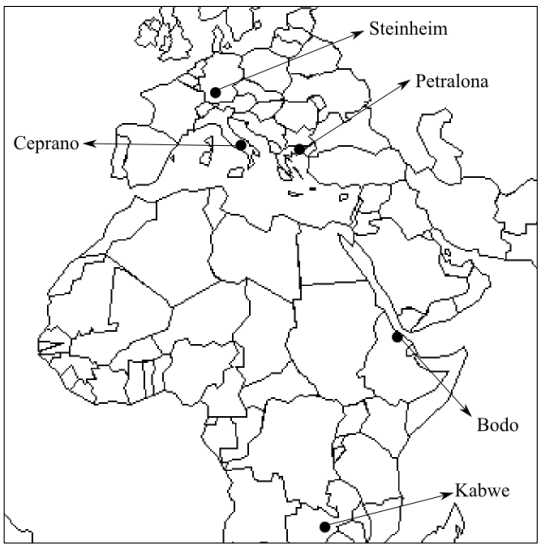

Figure 17: Locations for *H. heidelbergensis* specimens. Steinheim: Germany; Petralona: Greece; Ceprano: Italy; Bodo: Ethiopia; Kabwe: Zambia. Map adapted from blank map freely available from Wikicommons (www.wikicommons.org).

Homo neanderthalensis

Forbes' Quarry (Gibraltar 1)

The Neanderthal cranium from Forbes' Quarry was discovered at the north end of the rock of Gibraltar in 1848 (Busk, 1865). The stratigraphic provenance of the Forbes' Quarry cranium is unknown and the Pleistocene sediments that were presumably present at the quarry have now been removed, meaning that there is no exact date for the cranium. Neanderthal remains from Vanguard's and Gorham's Caves on Gibraltar have been dated to over 42 ka and as recent as 30 ka, respectively (Bronk Ramsey *et al.*, 2002; Finlayson *et al.*, 2006; Stringer *et al.*, 2008), some of the latest Neanderthals in Europe, which may provide a minimum date for Forbes' Quarry. Unpublished data place the Forbes' Quarry specimen slightly older, at about 50 ka (Stringer, pers. comm.). This date corresponds to early MIS 3.

Source

Medical CT, courtesy of Robert Kruszynski and Farah Ahmed, Natural History Museum, London.

Climate category

Climate reconstructions suggest that during the Pleistocene the climate of Gibraltar remained Mediterranean in type with slightly cooler temperatures, but also shorter dry periods (Blain *et al.*, 2013). For the Mousterian levels of Gorham's Cave, the bottom of which has yielded the date of >32-30 ka (Finlayson *et al.*, 2006), the estimated MAT is 16.1°C and the estimated MAP is 763mm/yr (Blain *et al.*, 2013). These climate indices would place Gorham's Cave in the Hot/Wet climate category. The bottom of the Mousterian levels at Gorham's Cave dates to over 31 ka (Bronk Ramsey *et al.*, 2002), making the whole Mousterian sequence slightly younger than the most likely date for Forbes' Quarry (around 50 ka). The Gorham's dates come from after the European climate had begun to deteriorate into a colder, more arid part of MIS 3 towards the LGM (Lisiecki & Raymo, 2005; Douka *et al.*, 2013). Following this line of reasoning, Forbes' Quarry would come from a warmer and wetter climate than Gorham's Cave (if anything), thus it seems reasonable to place Forbes' Quarry in the Hot/Wet category.

Guattari (Monte Cicero)

The Guattari cranium from Monte Cicero, southern Italy, is dated to 51-57 ka using U series and ESR dating on calcite encrustations on associated faunal remains (Schwarcz *et al.*, 1991).

Source

Medical CT obtained via NESPOS courtesy of Luca Bondioli, Museo Nazionale Preistorico Etnografico "Luigi Pigorini", Rome.

Climate category

The time period for Guattari corresponds to the beginning of the interglacial MIS 3 (Lisiecki & Raymo, 2005). This was the warmest part of MIS 3, but was still cooler than the previous interglacial, MIS 5 (Lisiecki & Raymo, 2005). According to OIS 3 Project climate modelling (Barron *et al*., 2004), using both warm and cold phase estimates, the site of Monte Cicero at this time is estimated to have experienced an MAT of 8°C. Based on this estimation, Guattari is placed in the Temperate climate category.

Krapina 3

The Neanderthal remains from Krapina in northern Croatia are dated to ~130 ka using ESR (Rink *et al*., 1995). This time period corresponds to the beginning of MIS 5 (sub-stage MIS 5e), an interglacial, or to the MIS 6/5e boundary (Gaudzinski, 2004; Caspari & Radovčić, 2006).

Source

Medical CT obtained via NESPOS courtesy of Andreas Pastoors, Neanderthal Museum, Mettmann.

Climate category

MIS 5e was a warm, temperate and stable interglacial, which led to the spread of mixed, temperate forest over much of Europe (Gaudzinski, 2004; Willis & MacDonald, 2011). Temperatures were similar to today, maybe 1-2°C warmer (Caspari & Radovčić, 2006), and there were probably lower levels precipitation than at present (Willis & MacDonald, 2011). Current climate indices for Krapina are: MAT of 8.40°C and MAP of 911.1mm/yr. If the above estimate of temperature is correct (Caspari & Radovčić, 2006), Krapina in MIS 5e would have a MAT of 9.40-10.40°C, which would make it part of the Temperate climate category.

La Chapelle-aux-Saints 1

La Chapelle-aux-saints Cave is in the Corrèze department of central France. ESR dating of associated faunal tooth enamel dates the La Chapelle Neanderthal skeleton to ~ 50 ka (Grün & Stringer, 1991). This corresponds to mid MIS 3 (Lisiecki & Raymo, 2005).

Source

Medical CT courtesy of Phillipe Mennecier, Alain Fromment, and Antoine Balzeau at the Musée de l'Homme, Paris.

Climate category

Palaeoclimate modelling (Barron, *et al.*, 2004) suggests that at around 50 ka, a relatively cold part of MIS 3 (Lisiecki & Raymo, 2005), in La Chapelle-aux-Saints

MAT would have been 5°C. La Chapelle is therefore classified as part of the Temperate category.

La Ferrassie 1

La Ferrassie Cave is in the Dordogne department of southwest France. The La Ferrassie 1 Neanderthal remains are dated to 75 – 60 ka using chronostratigraphy (Pettitt, 2002). This corresponds to MIS 4 (Lisiecki & Raymo, 2005).

Source

Medical CT courtesy of Phillipe Mennecier, Alain Fromment, and Antoine Balzeau at the Musée de l'Homme, Paris.

Climate category

The dating of La Ferassie corresponds to a time period encompassing a transition from an early glacial warm period (~70 ka), through a transitional period to the MIS 4 glacial maximum (66-58 ka) (Lisiecki & Raymo, 2005). Although for the majority of the time period La Ferrassie would have had a deteriorating, or cold climate, to be conservative both the warm and cold estimates for the site were taken from Barron *et al.* (2004). The warm phase temperatures would give an estimated MAT of 7°C, which would lead to a classification of Temperate, but the cold phase temperatures (more likely given the range of dates) and the mean of the cold and warm phases (MAT estimates of 2°C and 4.5°C respectively) both place La Ferassie in the Cold category. Warm phase annual precipitation is estimated at 365-1314mm/yr and cold phase estimates are 365-1168mm/yr (Barron, *et al.*, 2004). Since all these estimates

are above the threshold for Wet in Cold climates, La Ferrassie is classified as originating from a Cold/Wet climate.

La Quina H5

La Quina Cave is near the village of Villebois-Lavalette, department of Charente, southwestern France. The Neanderthal fossils are dated to 75-48 ka using chronostratigraphy (Pettitt, 2002, 2011), perhaps most likely to the beginning of glacial MIS 4 (71-57 ka) (Maureille & Tillier, 2008).

Source

Medical CT courtesy of Phillipe Mennecier, Alain Fromment, and Antoine Balzeau at the Musée de l'Homme, Paris.

Climate category

The earlier part of this time period was in an early glacial warm phase (~70 ka); the climate then deteriorated into the glacial maximum ~66 ka, which then developed into a warmer phase (Lisiecki & Raymo, 2005). Thus, it is difficult to say much with confidence about the climate at the time the La Quina H5 individual was alive. However, regardless of whether La Quina was living a warm, or a cold phase climate, it would still be placed in a Temperate category (based on Barron *et al.*'s (2004) climate modelling). The warm phase estimate gives an MAT of 7°C and the cold phase gives an MAT of 5°C.

Neanderthal (Feldhofer Grotto) 1

The type specimen for *Homo neanderthalensis*, from the Neandertal Valley in western Germany from which the species takes its name, is dated to ~40 ka using direct AMS radiocarbon dating (Schmitz *et al.*, 2002). This corresponds to mid MIS 3 (Lisiecki & Raymo, 2005).

Source

Medical CT courtesy of Christoph Zollikofer, University of Zurich.

Climate category

The date for Neanderthal falls in a transitional phase between a warmer phase ending ~44 ka and the deterioration into the LGM starting at ~37 ka (Lisiecki & Raymo, 2005). A general deterioration over this time means perhaps the climate for Neanderthal is likely to have been more similar to the LGM. Taking both the warm and cold phase OIS 3 Project models (Barron *et al.*, 2004) into account, the Neanderthal site would have had an MAT of -1°C. The MAP is estimated as 828mm/yr (Barron *et al.*, 2004). Neanderthal is therefore classified as part of the Cold/Wet category.

Tabun C1

The Tabun remains come from the Muharet et-Tabun cave in Israel. The C1 skeleton is dated to 138-106 ka (with 122 ka the most probable date) using ESR and Th/U series spectrometric analysis (Grün & Stringer, 2000). The oldest part of this time

period is the very tail end of glacial MIS 6, and most of the range is in interglacial MIS 5 (Lisiecki & Raymo, 2005).

Source

Medical CT courtesy of Robert Kruszynski and Farah Ahmed, Natural History Museum, London.

Climate category

140-110 ka is a time of much environmental change according to $\delta^{18}O$ levels, from a cold trough between 140-130 ka to a warm peak between 130-120 ka (Lisiecki & Raymo, 2005). In contrast to higher latitudes, where temperature is the most influential driver of climate change in the Pleistocene, in the Levant it is the amount of precipitation (Frumkin *et al.*, 2011). Interglacials were wetter than glacials in the Levant, as shown by speleothem deposition, $\delta^{18}O$ composition and palaeolake levels (Frumkin *et al.*, 2011). Fumkin *et al.* (2011) reconstructed the Levantine climate as warm and dry for the time period of Tabun C1. The very low levels of speleothem deposition at this time can be interpreted as precipitation <400mm/yr; therefore, Tabun is placed in the Hot/Dry climate category, in agreement with Frumkin and colleagues (Frumkin, *et al.*, 2011).

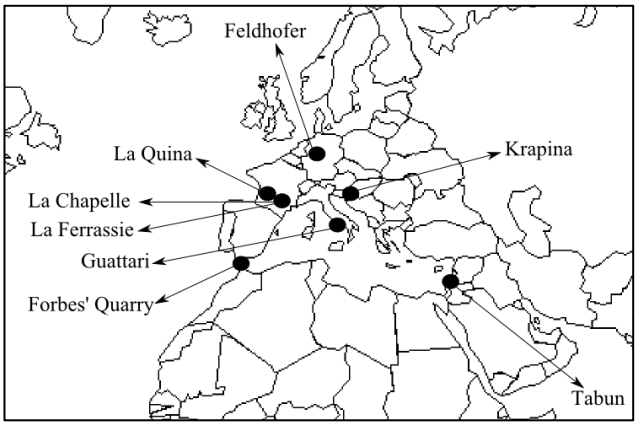

Figure 18: Locations for *H. neanderthalensis* sample. Feldhofer (Neanderthal): Germany; Krapina: Croatia ; La Quina, La Chapelle, and La Ferrassie: France; Guattari: Italy; Forbes' Quarry: Gibraltar. Map adapted from blank map freely available from Wikicommons (www.wikicommons.org).

Early *H. Sapiens*

Cro-Magnon 1, 2 and 3

The three adult burials from Cro-Magnon are dated to ~30 ka. They were found in a rock shelter in the Dordogne, France in 1868 (Movius, 1969).

Source

Medical CT data courtesy of Phillipe Mennecier, Alain Fromment, and Antoine Balzeau, Musée de l'Homme, Paris.

Climate category

The dates for Cro-Magnon correspond to a cold phase in Europe at the end of MIS 3 (Lisiecki & Raymo, 2005; Douka *et al.*, 2013). Palaeoclimatic modelling (Barron, *et al.*, 2004) for the LGM cold phase predicts an MAT of 2°C and an MAP of 720mm/yr. The Cro-Magnon specimens are therefore placed in the Cold/Wet climate category.

Mladeč 1

The Mladeč remains from the Czech Republic are some of the oldest *H. sapiens* in Europe. They are dated to ~37.5-34.75 ka using calibrated AMS radiocarbon dating (Douka *et al.*, 2013).

Source

Medical CT purchased from the Digital Archive of Fossil Hominoids, University of Vienna.

Climate category

This time period largely coincides with a relatively warm stage in MIS 3 (Lisiecki & Raymo, 2005; Douka *et al.*, 2013). Using Barron *et al.*'s (2004) warm phase reconstruction, this estimates MAT of 6°C. Based on this estimation, Mladeč is classified as having come from a Temperate climate.

Ngaloba (LH18)

This partial cranium is from Laetoli in Tanzania. It was found by a team led by Mary Leakey in 1976 (Magori & Day, 1983). The Ngaloba fossil is dated to 150-120 ka by analogy with the Ndutu beds at Olduvai Gorge (Magori & Day, 1983; McBrearty & Brooks, 2000).

Source

Medical CT purchased from the Digital Archive of Fossil Hominoids, University of Vienna.

Climate category

As described above for Kabwe and Bodo, Woltering *et al.* (2011) suggest that even during very cold glacial maxima, the average annual temperature in Malawi did not fall below 20°C. Based on data from 1900-2009, the World Bank puts current Malawi MAT at 21°C (WBG, 2013); using data from the same source, Tanzania has an MAT of 23.2°C. Given that Tanzania is now warmer than Malawi, and there is no reason to think that this was otherwise in the past, it seems unlikely that Ngaloba would have experienced annual temperatures below the cut off point for inclusion in the Hot temperature category.

The period between 150-120 ka was climatically variable (Lisiecki & Raymo, 2005). It is therefore difficult to tell exactly what the precipitation levels were like during the Ngaloba individual's lifetime. Laetoli is part of Blome *et al.*'s (2012) 'East African region' and during the time period for Ngaloba, the synthesis suggests wet conditions were more common than arid ones in that region. It was relatively wet ~145 to 120 ka, whereas it was arid only ~150-145 ka (Blome *et al.*, 2012). Blome *et al.* (2012) show that Africa was wetter than today during previous wet periods. Tanzania today has a MAP level of 1071mm/year (WBG, 2013), which is above the threshold for a Wet classification in this thesis. If most of the time period in question is thought to be wetter than at present, this would most likely place Ngaloba in the Hot/Wet category.

Singa

The Singa cranium from Sinjah, eastern Sudan was discovered in 1924 (Schwartz & Tattersall, 2002). It is dated to a minimum age of 131-135 ka (the end of MIS 6) by U/Th mass spectrometry and ESR on sediments from the inside of the cranium (McDermott *et al.*, 1996).

Source

The fossil was microCT scanned at the Natural History Museum, London, by the author, with permission from Robert Kruszynski and Farah Ahmed.

Pathology

The Singa fossil exhibits some pathology in the parietal and temporal regions (Stringer, 1979; Spoor & Stringer, 1998). However, Singa is only included in the frontal sinus volume analyses and this region is not affected by pathology.

Climate category

Woltering *et al.* (2011) suggest that, even during very cold glacial maxima, the average annual temperature in Malawi did not fall below 20°C. Given that today Malawi has an annual temperature range of 17.6 to 24.4°C, whilst Sudan has an annual temperature range of 20 to 32.99 °C (WBG, 2013), one can conclude that Sudan is warmer than Malawi, and was most likely so in the past, due to its latitude and geography, which have not changed over the time period in question. Originating at the very end of a glaciation, when climate was beginning to warm (leading up to the MIS 5 interglacial) it seems likely that Singa would have

experienced annual temperatures above the cut off point for inclusion in the Hot category.

It is suggested that during Lake Naivasha's high stand at ~139-133 ka, the surrounding region would have received 11-28% more precipitation than at present (Trauth *et al.*, 2003); although this is further south than Singa, both fall within Blome's (2012) 'East African region'. If Trauth *et al.*'s (2003) predictions are used on present day Sudanese precipitation values (WBG, 2013), Singa would have had an estimated MAP of 520mm/yr. The time period also falls outside Larransoaña *et al.*'s (2013) green Sahara periods, which are clustered around 80, 105, and 125 ka, supporting the idea than Singa would have inhabited a fairly dry environment, thus Singa is placed in the Hot/Dry category.

Skhul 5

The Skhul material was discovered in the Mugharet es-Skhul in the Mount Carmel range, Israel in 1931-2 (Schwartz & Tattersall, 2002). Part of the assemblage (which represents at least ten individuals), Skhul 2, 5 and 9, is dated as a whole to 130-100 ka using ESR, U series, and thermoluminescence analyses (Grün *et al.*, 2005). However, it has been argued that Skhul 9 is older than the other two fossils, as suggested by its morphology and lower stratigraphic position (Stringer, 1996). If this is the case, a better date for Skhul 2 and 5 is 117-88 ka (Grün, *et al.*, 2005).

Source

Medical CT obtained via NESPOS courtesy of Harvard University., Mettmann.

Climate category

A date of 130-88 ka puts Skhul 5 in MIS 5, a period of some climatic variation covering sub-stages 5.5 to 5.4. There is a very warm peak ~ 130-120 ka, followed by a deterioration in climate by ~110 ka and several smaller subsequent variations 110-80 ka (Lisiecki & Raymo, 2005). A palaeoclimate estimate for Israel for the interglacial of 85 ka, based on speleothem and foraminifera isotope ratios, gives an MAT of ~20°C and an MAP of ~350 mm/yr (Bar-Matthews, *et al.*, 2003). Since, according to the $\delta^{18}O$ curve of Lisiecki and Raymo (2005), this would have been the coolest, driest period in the 13-88 ka possible window for Skhul 5, the climate would have been warmer and wetter, if anything. Skhul can therefore be confidently placed in the Hot climate category. As for the Tabun remains from nearby, Skhul 5 is placed in the Dry category based on Frumkin *et al.*'s (2011) speleothem data. Therefore, Skhul 5 is categorised as originating from a Hot/Dry climate.

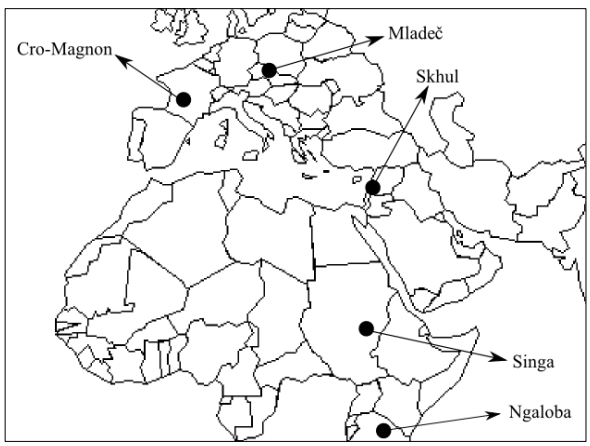

Figure 19: Locations of early *H. sapiens* sample. Cro-Magnon: France, Mladeč: Czech Republic, Skhul: Israel, Singa: Sudan, Ngaloba: Tanzania. For more details see text. Map adapted from blank map freely available from Wikicommons (www.wikicommons.org).

Table 2: Summary of fossil sample. For sources of dates, see text. For calculation of climate categories, see Section 2.IV.c.i; for justification of categories, see Section 2.I.b.ii. All longitudes and latitudes from Google Maps Lat/Long finder (http://www.doogal.co.uk/LatLong.php).

Taxon	Specimen	Site	Country	Assigned date (ka)	Latitude	Longitude	Climate category
Homo erectus	KNM-ER 3883	Koobi Fora	Kenya	1650-1500	4°18'N	36°13'E	Hot/Dry
	KNM-ER 3733	Koobi Fora	Kenya	1780	4°18'N	36°13'E	Hot/Dry
Homo heidelbergensis	Bodo	Bodo	Ethiopia	~ 600	12°11'N	42°09'E	Hot/Wet
	Ceprano	Ceprano	Italy	430-385	41°32'N	13°30'E	Hot/Wet
	Kabwe	Kabwe	Zambia	300-250	-14°23'N	28°23'E	Hot/Dry
	Petralona	Petralona	Greece	~400	40°22'N	23°9'E	Hot/Wet
	Steinheim	Steinheim an der Merr	Germany	300-337	48°97'N	9°28'E	Temperate
Homo neanderthalensis	Forbes' Quarry	Forbes' Quarry	Gibraltar	50-30	36°14'N	-5°35'E	Hot/Wet
	Guattari	Monte Cicero Cave	Italy	57-51	41°24'N	13°10'E	Temperate
	Krapina 3	Krapina Cave	Croatia	~130	46°16'N	15°87'E	Temperate
	La Chapelle 1	La Chapelle-aux-Saints Cave	France	~50	44°59'N	1°43'E	Temperate
	La Ferrassie 1	La Ferrassie Rockshelter	France	75-60	44°57'N	0°56'E	Cold/Wet
	La Quina H5	La Quina Cave	France	75-48	45°51'N	0°29'E	Temperate
	Neanderthal 1	Feldhofer Cave	Germany	~40	51°13'N	6°57'E	Cold/Wet
	Tabun C1	Mugharet et-Tabun Cave	Israel	138-106	32°74'N	35°15'E	Hot/Dry
Early *H. Sapiens*	Cro-Magnon 1	Cro Magnon	France	~30	44°56'N	1°0'E	Cold/Wet
	Cro-Magnon 2	Cro Magnon	France	~30	44°56'N	1°0'E	Cold/Wet
	Cro-Magnon 3	Cro Magnon	France	~30	44°56'N	1°0'E	Cold/Wet
	Mladeč 1	Mladeč	Czech Republic	~37.5 – 34.75	49°42'N	17°1'E	Temperate
	Ngaloba	Laetoli	Tanzania	150-120	-3°22'N	35°19'E	Hot/Wet
	Singa	Singa	Sudan	131-135	13°10'N	33°57'E	Hot/Dry
	Skhul 5	Mugharet es-Skhul Cave	Israel	130-100	32°63'N	34°96'E	Hot/Dry

2.II: Methods – Measuring sinus volume

There are several possible ways of measuring sinus size, including volume, surface area, and greatest extent superiorly/laterally. In the current thesis it was decided to measure sinus volume because it has been measured most often in previous studies with a bearing on the same research questions (e.g., Shea, 1977; Rae *et al.*, 2003, 2006, 2011; Balzeau & Grimaud-Hervé, 2006; Zollikofer *et al.*, 2008; Butaric *et al.*, 2010, Holton *et al.*, 2013) and, thus, the results from the current thesis will be comparable with most of the relevant literature. Most theories for sinus function, with the notable exception of theories suggesting sinuses aid the dissipation of heat (see Introduction), are based on differences in the size of the sinus hollow (i.e., its volume), rather than the surface area of the hollow. Using CT data is also an effective, repeatable, accurate way of measuring sinus volume (see below), whereas measuring extent on CT data is fraught with problems of orientation (see Section 2.II.c.). Similarly, the correlates of sinus shape are not addressed in this thesis, because the great majority of the literature on possible sinus functions does not consider shape and also because, given the complex shape of the sinuses (particularly the frontal sinus), their lack of homologous landmarks, and their extreme variability between individuals, there is not yet a method of proven accuracy for analysing sinus shape. This is something that should be addressed in future work.

Note on controlling for family-wise error inflation – the use of Bonferroni corrections

Performing many successive statistical tests as part of a single analysis (as described below) inflates the chance of obtaining a type I error, the chance of obtaining a

significant result where none exists because there is a small probability of this happening in each of the tests ($\leq 5\%$ if $\alpha = 0.05$, as is usual within anthropology; Field, 2009). This possibility is often accounted for by using a Bonferroni correction ($\alpha = 0.05/n$) to reduce the α threshold relative to the number of tests performed. Reducing the α in this way, however, also reduces the power of the test and increases the chance of getting a type II error, i.e., real, significant results not being detected (Field, 2009). Corrections such as the Bonferroni tend to be over-conservative and make it very hard to detect small effects from large numbers of variables, particularly when samples are small (Hammer *et al.*, 2001; Moran, 2003; Nakagawa, 2004). Amongst statisticians, there is considerable movement to reject the use of Bonferroni corrections, especially in non-experimental situations (Moran, 2003; García, 2004; Nakagawa, 2004; Garamszegi, 2006). The route taken by the current thesis is to compare and discuss the significance from analyses with multiple comparisons both with and without Bonferroni corrections, in conjunction with effect sizes, ordinations of the data, and trends between comparisons, in order to make reasoned conclusions about which results may be due to increased family-wise error and which reflect real results (Moran, 2003; García, 2004; Garamszegi, 2006).

2.II.a. Method for sinus volume measurements

2.II.a.i. Segmentation and measurement

Sinuses were segmented out manually from cranial CT scans by selecting the desired region, CT slice by CT slice, in AVIZO 5.0/6.3/7 (FEI Visualization Sciences Group, Burlington, MA, USA). The sum of the selected areas in each slice was then designated as a single material and the volume of this material was calculated using a

measurement tool in AVIZO (see Figure 20). The volumes of both the right and left frontal sinuses were taken (indeed, there is often no simple demarcation between the two), except where one side was broken, and the volume was recorded as the sum of both sides, or the only side present multiplied by two, in the few instances where only one side was measurable. Both left and right maxillary sinuses were measured in the same way, as was the sphenoidal sinus.

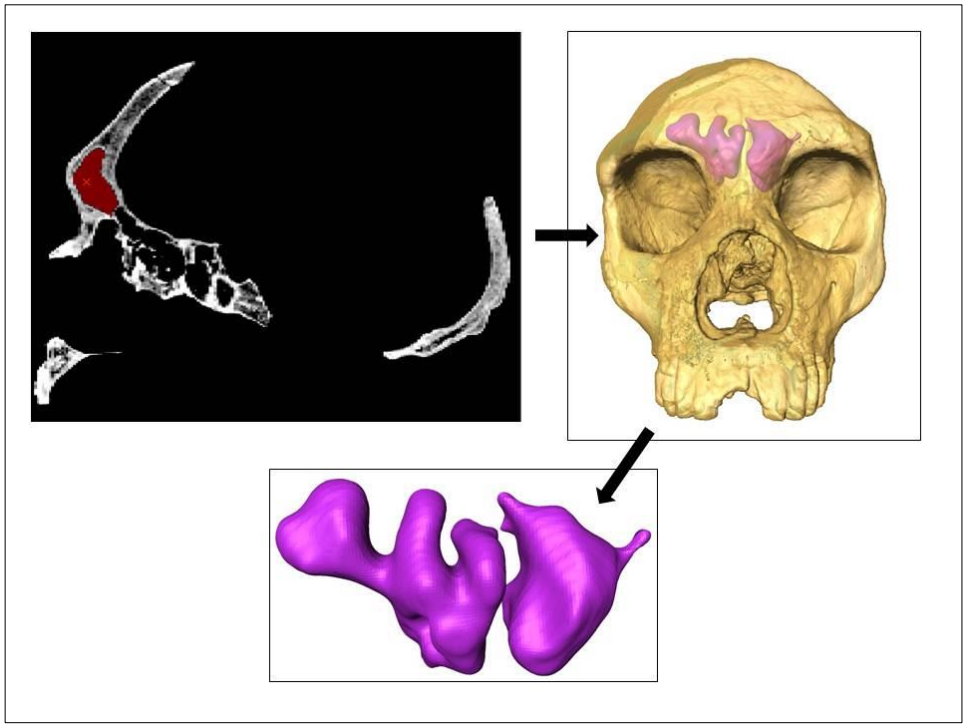

Figure 20: Segmentation for measurement of frontal sinus volume from CT slices using AVIZO (Forbes' Quarry, *H. neanderthalensis*).

2.II.a.ii. Standardising volume measurements for size

Sinus size has been shown to scale with craniofacial size in *H. sapiens* and other hominoids (Lund, 1988; Koppe *et al.*, 1999a, b; Holton *et al.*, 2011, Rae, *et al.*, 2011; although see Butaric *et al.*, 2010). Therefore, to look at meaningful (non-isometric) differences in volume, measurements must be standardised. Centroid size (see Section 2.III.b.) is one appropriate measure of size, as it is a three-dimensional

measure, appropriate for the standardisation of a volume. A centroid size's quality, however, depends on the number and distribution of landmarks used to calculate it and using enough landmarks to obtain a good measure of centroid size on fragmentary specimens is problematic. This problem is compounded by the fact that the most fragmentary specimens are fossil species, which also have the smallest sample sizes, making it even more neceesary to include all available individuals. In the current sample, if only the landmarks which are preserved on the entire sample were used, centroid size would be computed using only four landmarks. These landmarks are all clustered around the supraorbital region and so would not give a good measure of overall craniofacial size.

A landmark set for the calculation of centroid size was devised to include the maximum sample with the minimum number of landmarks to cover the entire cranium (see Table 3 and Figure 21). Despite the low number of landmarks, they are not all preserved in 75% of the fossils (100% *H. erectus*, 86% early *H. sapiens*, 75% *H. neanderthalensis*, and 50% *H. heidelbergensis*; see Appendix 4). The recent *H. sapiens* sample is less badly affected (14% do not preserve landmark set), since they are better preserved, in general.

Table 3: Landmarks used to calculate centroid size to standardise sinus volume/surface area. For full landmark set see Table 9.

Landmark (LM)	LM number in full landmark set	LM number in sinus metric set
Bregma	1	1
Glabella	2	2
Frontomalare temporale	15	3
Porion	22	4
Lambda	28	5
Orale	45	6

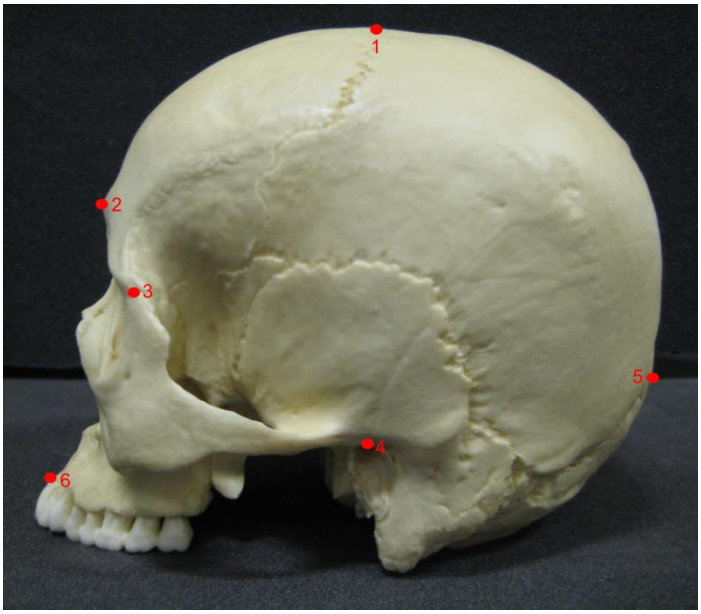

Figure 21: Landmarks used in centroid size calculation. 1: bregma, 2: glabella, 3: frontomalare temporale, 4: porion, 5: lambda, 6: orale. Photo by the author.

In a previous study a simple linear measurement of bi-frontomalare temporale breadth was used as a proxy for cranial size to standardise sinus volume (Rae *et al.*, 2011). The use of just half this measurement (glabella to right frontomalare temporale) holds the same information and would enable all crania in the current sample to be included. A comparison was made between centroid size (CS) calculated based on the landmark set above and on glabella to frontomalare temporale (G-FMT) measurement. The 3D measurement tool was used in AVIZO to take a measurement from G to right FMT and G-FMT measurements were cubed in

order to enable direct comparison with volumetric measures. Pearson's correlation tests were run between relative sinus volumes calculated using CS and using G-FMT^3. Here, and throughout, significant results are reported in detail; non significant results are not reported in detail and should be taken as having a p value of > 0.05. The results from the comparison of size standardisation with CS and with G-FMT^3 (Table 4) show very strong, highly significant (and robust to Bonferroni corrections) relationships between relative frontal and sphenoidal sinus volumes calculated using the two measures of size. The relationship for maxillary sinus volumes, although still robust, has a smaller r value. However, given the number of specimens that would have to be excluded if CS were used to measure size, the relationship was judged to be strong enough, and G-FMT^3 was used to standardise all sinus volumes.

Table 4: Results from Pearson's correlation tests comparing standardised relative sinus volumes calculated with centroid size and with glabella-right frontomalare temporale measurement cubed. All correlations remain significant if a Bonferroni correction is applied.

Sinus	r value	p value
Frontal	0.98	<0.001
Maxillary	0.71	<0.001
Sphenoidal	0.95	<0.001

Allometry

Standardising sinus volumes by a measure of cranial size, for example a linear measurement from glabella to frontomalare temporale, should remove the effect of cranial size (to the extent that the metric successfully measures cranial size – see above), such that the volumes show relative, rather than absolute volume. Similarly, General Procustes Analysis superimposition removes size differences between landmark configurations as part of geometric morphometric analyses (see Section 2.III.b.). Neither method removes the effect of allometric differences, however.

Allometry is shape difference associated with, or caused by, size. An obvious example of allometric shape difference is the differences in limb-trunk proportions between an adult and a young child; the size of the two is different, but so is the associated shape, such that a child skeleton and an adult skeleton can be differentiated, even if size is not known. In order to test for allometry in sinus variables (relative sinus volume and sinus volume shape parameters – SVSPs – see Section 2.III.c.) the natural log (ln) of the relative volumes/SVSP scores (following standard practice for examining allometry in biology, see for example LaBarbera, 1989) were regressed against the ln transformed centroid size (see Section 2.III.b.) calculated from the relevant sinus-specific landmark set, using reduced major axis regression in PAST (Hammer *et al*., 2001). Reduced major axis regression was used because it assumes error in both variables. The residuals from significant regression analyses were then taken to be a size-free, allometry-free measure of the sinus variable and were used in subsequent analyses as such.

2.II.a.iii. Bilateral asymmetry in maxillary sinus volumes

Not all specimens preserve both maxillary sinuses, but in those that do, the two sides are very similar in size and shape, supporting Tillier's finding that the maxillary sinus is the least variable of all the sinus types (Tillier, 1975). A paired t-test was performed to test for a significant difference between the volumes on the right and left sides in the current sample; the result was not significant. There is also a very strong correlation between right and left side volumes ($n = 101$, $r = 0.92$, $p < 0.001$). Since there seems to be very little bilateral asymmetry in maxillary sinuses, it was decided that in subsequent analyses only the side most commonly preserved would

be used. Since the fossil sample size is necessarily much smaller than that of recent *H. sapiens*, it was judged that the benefit of having two extra Neanderthals with left sinuses preserved (see Table 5) outweighed the benefit of having three more recent *H. sapiens* with the right side preserved. Therefore, the left maxillary sinus was used in all subsequent analyses of maxillary sinus volume where present, and was substituted with the right where necessary.

Table 5: Bilateral preservation of maxillary sinuses.

Group	Right maxillary sinus present	Left maxillary sinus present
H. erectus	0	0
H. heidelbergensis	2	2
H. neanderthalensis	1	3
Early *H. sapiens*	2	2
Recent *H. sapiens*	110	107
Total	**115**	**114**

2.II.b. Error test for method of measuring sinus volumes

To ensure that the method of measuring sinus volume was precise, the three sinus types (frontal, maxillary, and sphenoidal) were sectioned out of the same recent *H. sapiens* cranial CT data five times with at least one day elapsing between measurements. These measurements were then compared and error was calculated following White and Folkens (2005).

Table 6: Results (cm^3) for five repetitions of sinus volume measurement and percentage error.

Replication	Frontal	Maxillary	Sphenoidal
1	7.6	17.2	14.5
2	7.8	16.9	14.6
3	7.4	16.7	14.8
4	7.6	16.7	14.6
5	7.8	18.4	14.6
Mean	**7.6**	**17.2**	**14.6**
Standard deviation	**0.2**	**0.7**	**0.1**
% error	**1.8**	**2.9**	**0.7**

The measurement errors are low for each sinus; all are below 5% (see Table 6). The cranium used is reasonably complete and may therefore be easier to measure accurately than some of the more broken specimens (a reasonably intact specimen was chosen in order to perform all the sinus measurements on the same individual). However, the medial wall of the maxillary sinus was quite broken, which is reflected in the higher level of error in the volume for that sinus, as was part of the anterior sphenoid. This damage resulted in the need to estimate the position of the margins of the sinus for numerous slices, so the low level of error is reassuring. The scan is also a conventional (medical) CT scan, rather than a microCT scan, so the level of resolution is not as high as for some other individuals. For these reasons, it was felt that these error tests demonstrated the method to be sufficiently precise.

2.II.c. The study of paranasal sinuses in fossil and extant hominins by Anne Marie Tillier – a critique

The most complete study of hominin sinuses to predate this thesis was conducted by Tillier (Tillier, 1975, 1977). Tillier studied intra-population and inter-population variation, and the relationship between morphological and climatic variation and

sinus size, in three groups of extant humans. She considered the frontal, maxillary, and sphenoidal sinuses and was interested in whether the different types of sinus covary. She did not consider the ethmoid sinus, stating that it was very difficult to measure and rarely preserved. Tillier also studied a sample of hominin fossils with the additional aim of evaluating taxonomic and climatic theories for extinct hominin sinus size. This section summarises the Tillier's findings and evaluates her method, explaining why the same method was not employed for the current study and why the results are not directly comparable.

2.II.c.i. Tillier's methods

Tillier collected data on two samples, one of extant *H. sapiens* and one of fossil hominins. The extant *H. sapiens* data were collected with the aim of studying intra-population variation and covariation in sinuses. The sample consisted of three populations: French, Australian, and Inuit. The French sample was intended to test for sexual dimorphism in sinus size and bilateral asymmetry. The Australian sample was chosen, because of their high incidence of supraorbital tori, to test the relationship between supraorbital morphology and frontal sinus morphology. The Inuit sample was chosen for their assumed cold-adaptation. All three groups of recent *H. sapiens* were analysed for covariation between sinus types. The taxonomic terms used by Tillier for her fossil sample have fallen out of favour due to revisions in dating and resulting species attributions. Tillier's sample included "Archanthropiens": presumed older Pleistocene fossils such as Broken Hill (Kabwe), Saldhana (Elandsfontein), Petralona, Tautavel (Arago), Ehringsdorf, Saccopastore, Forbes' Quarry, Solo Man, '*Pithecanthropus'* (Indonesian *H. erectus*), and

'*Sinathropus'* (*H. erectus* from Zhoukoudian); the younger "Paleoanthropiens", which included Neanderthals (according to her definition) and African fossils such as Jebel Irhoud, and a small number of Central and Western European Upper Palaeolithic *H. sapiens*, including Obercassel, Chancelade, Mladeč, and Combe Capelle.

For the extant sample, Tillier took radiographs in four standardised orientations chosen to view each sinus from multiple viewpoints. She then took a series of linear measurements of the sinuses on tracings of the radiographs using a planimeter. She did not standardise the measurements for cranial size. This means that the method fails to take into account allometric shape differences, a possible issue addressed in the current thesis. The means, coefficients of variation within groups, coefficients of correlation between sinuses, and standard errors were calculated, and t-tests were performed to test for significant differences. In addition to the quantitative measurements, the sinuses were categorised into types based on their size and extent. Some fossils Tillier was able to radiograph herself, and so could control the orientation and x-ray parameters as for the extant sample. For other fossil specimens, she had to rely on existing radiographs, where she had no control over the orientation. In some cases, no radiographs existed and she was not able to take any, having to examine the external appearance of the specimen, or even a cast. She also collated data from published accounts, when other sources were not available. As many as possible of the sinus measurements were taken on the fossil sample, depending on preservation and/or the availability of suitable radiographs. As with the extant sample, these measurements were not standardised for cranial size.

2.II.c.ii. Critique of Tillier's methods

When Tillier conducted her study, radiography was the only available way to visualise the interior of a cranium non-destructively. There are however, limitations to her methodology, precluding its direct comparison with CT data such as that used in the current study, which seeks to overcome these limitations as far as possible using the methodological and technological advances now available. A radiograph compresses the entire specimen into one plane; it can thus be difficult to make out the shape of a structure with a variable shape, such as a frontal sinus. It may also be difficult to distinguish internal structures through highly mineralised fossil bone, as commented on by Tillier (1977) for, for example, Forbes' Quarry and Skhul 5. For this reason, Tillier decided to measure only the region of the frontal sinus above the tops of the orbits, rather than the entire sinus. This was standard practice at the time (e.g., Vlček, 1967; Koertvelyessy, 1972; Hanson & Owsley, 1980), but means that individuals with small sinuses may be erroneously dismissed as having no frontal sinus. It may also explain why Tillier (1975) found only a very small cell for the frontal sinus of Mladeč, whereas from the CT data it is easy to see a reasonably sized sinus. Tillier also disagrees substantially with previous work by Vlček (1967) on the size of the sinuses in many of the fossils they both measured; e.g., Saccopastore, Forbes' Quarry, La Ferrassie, La Chapelle, La Quina, and Krapina E. This may be due to the high level of estimation necessary on occasion when interpreting a radiograph.

Tillier did not standardise her measurements to take into account the effect of cranial size. All other things being equal, larger crania have larger sinuses in both *H. sapiens*

and other hominoids (Lund, 1988; Koppe *et al.*, 1999a, b; Holton *et al.*, 2011; Rae, *et al.*, 2011). This does not tell us anything specific about the effects of taxonomy, shape, or ecology on the sinus. Therefore comparisons between individuals, and particularly between taxa, in her work must be made with caution.

In the current study, it was originally intended to recreate Tillier's method using CT data (this is possible in AVIZO software), to take some of her measurements on the current sample and combine the two sources of data extending the fossil sample size considerably. However, although Tillier may have been very precise in orientating her sample when taking her own radiographs, she was not able to do this for the majority of the fossil taxa. Some of the sample no longer exists [for example, the '*Sinanthropus*' material from Zhoukoudian, which was lost during the Second World War (Oakley *et al.*, 1967)], and it seems from Tillier's thesis (Tillier, 1975) that other material was not available to her to study. For this reason, as well as the use of different types of data (measuring directly on specimens, or even casts), the results from her fossil sample are likely to be much less reliable than those she collected from her extant sample. Using the method of orientation Tillier describes virtually with CT data, it was not possible to obtain the same measurements (or within a reasonable margin of inter-observer error) on those fossil specimens present in both samples. It was concluded that this was due to the lack of standardisation of orientation in the radiographs in the fossils, and because of the inherent distortion of measuring from a radiograph. As charged x-ray particles leave their source they spread out, with the effect that structures further from the source appear relatively larger than those near it, which can make measurements taken directly on

radiographs unreliable, phenomenon known as the parallax effect (Morvan *et al.*, 2011). This problem is compounded if specimens not set a standardised distance from the x-ray source (and thus experience the parallax effect to different extents) are compared. There also seems to be some ambiguity in Tillier's work over whether the right side referred to in a measurement is the viewer's right side, or the specimen's right side. Given the problems with combining Tillier's quantitative data with those from the current study, it was decided that Tillier's results could only be used for a qualitative comparison with the current data.

2.III: Methods: Geometric morphometric shape analyses

2.III.a. Shape analysis using geometric morphometric methods

Shape is defined as the geometric properties of an object once size, position, and orientation have been removed; form refers to shape plus size (O'Higgins, 2000). Geometric morphometric methods (GMM) are a suite of methods that enable quantitative three dimensional (3D) shape analysis based on landmark data, which preserve geometry and allow useful ordination and visualisation of shape differences (Klingenberg, 2013). GMM operate in a specific shape space (Kendall's shape space), the properties of which are well-understood, allowing for statistical analyses to be performed on shape differences (O'Higgins, 2000). The methods can also be used to generate shape variables for analysis with ecological or taxonomic variables (Singleton, 2004, 2005; McNulty, 2005; De Groote *et al.*, 2010). Here, GMM are used to decompose total shape variation into a set of shape variables showing only the variation in craniofacial shape associated with the different sinus volumes; these

are then used in subsequent analysis with other variables (Singleton, 2004, 2005; McNulty, 2005; De Groote *et al.*, 2010).

2.III.b. A description of geometric morphometric methods

In this section, the geometric morphometric methods used in this thesis are explained in general before their specific use in particular analyses is detailed in Section 2.III.c. The GMM used in this thesis are those currently and frequently used in the fields of biology and anthropology (e.g., Cobb & O'Higgins, 2007; Gunz & Harvati, 2007; Cardini & Elton, 2008; Baab *et al*., 2009; von Cramon-Taubadel, 2009, 2011; Friess, 2010a; Harvati *et* al., 2010; Harvati & Hublin, 2010; Paschetta, 2010; De Groote, 2011a, b; Noback *et al.*, 2011; Gómez-Robes *et al.*, 2012; Almécija *et al*., 2013; Holton *et al.*, 2013; Ingicco *et al.*, 2014; Kenyhercz *et al*., 2014; Klingenberg & Marugán-Lobón, 2014). It is recognised that the method choices and limitations (e.g., the numbers of landmarks used, metrics used for size correction, sample sizes and compositions, palaeoclimate and dietary reconstructions) could influence the results and these issues are discussed where relevant in the Results and Discussion chapters.

Landmarks

The 3D coordinates of landmarks are the raw data on which GMM are performed. Landmarks for use with GMM should be points which have biological homology and are repeatable between specimens (Bookstein, 1991). These have been classified into three types of decreasing reliability. Type I landmarks are points of juxtaposition of different tissues, and are the most homologous and easiest to

replicate between specimens. In terms of a cranium, an example might be the intersection of two sutures at right angles, such as the coronal and sphenoidal. Type II and III landmarks are also referred to as pseudolandmarks, since they are inferred and based on geometric homology, rather than biological homology. An example of a type II landmark would be the extreme point of a curve. Type III landmarks, such as a point furthest from a structure, are deficient in at least one of their three coordinates, meaning that they can be located consistently to a surface or an outline, but not to a precise location (Markus *et al.*, 1996).

General Procrustes analysis

Configurations of landmarks must be placed into the same coordinate system so that differences in landmark coordinates reflect only differences in specimen shape; this is achieved by superimposition. General Procrustes Analysis (GPA) (Gower, 1975) is the most commonly used superimposition technique in modern GMM (e.g., Harvati & Hublin, 2012; Gómez-Robes *et al.*, 2012; Almécija *et al*., 2013; Holton *et al.*, 2013; Ingicco *et al.*, 2014; Kenyhercz *et al*., 2014; Klingenberg & Marugá-Lobón, 2014). This method superimposes specimens so that their landmark configurations are as close as possible by removing differences in size, position, and orientation, and in doing so, places them in Kendall's shape space. Differences in position and orientation are removed by reducing the squared, summed distance between each configuration and a reference configuration iteratively until a minimum summed squared distance is reached. Size is removed by scaling all configurations to the same centroid size. Centroid size is the square root of the sum of the squared distances from all landmarks in a configuration to their centre

(centroid). During GPA, shapes are fitted to the first shape entered into the analysis, and then to the mean shape, until iterations fail to achieve a closer fit. The new coordinates obtained after GPA are shape coordinates, which are used for subsequent analyses, such as Principal Components Analysis (PCA). GPA can be problematic if variation in landmarks veers too far from isotropy (equal variation in every direction), which may occur if the error around landmarks is large compared to their distance from each other in the mean shape, or if there is excessive variation in one particular landmark. However, if the data are tightly clustered around the mean shape, as should be the case for intraspecific comparisons, or comparisons of closely related taxa (as here), the data should be close to isotropy (Klingenberg & Monteiro, 2005).

Tangent projection

GPA superimposition means that Euclidean statistics cannot be used, since Kendall's shape space is curved (Dryden & Mardia, 1993; Le & Kendall, 1993; Kent, 1994). To avoid this problem, the data can be projected into a Euclidean space tangent to Kendall's shape space. This can be imagined as analogous to the way a cartographer projects the globe onto a two-dimensional map (O'Higgins & Jones, 1998; O'Higgins, 2000). Points representing variation in shape configurations are then given as coordinates on a multidimensional plane, and thus Euclidean mathematics can be used. PCA can be used to project coordinates into tangent space (Dryden & Mardia, 1993; Kent, 1994). For biological shapes, which are relatively similar, and so are close together in Kendall's shape space (for example intra-generic comparisons, such as those in this thesis), tangent projection make almost no

difference to the relative relationships between shapes (O'Higgins & Jones, 1998; O'Higgins, 2000).

Principal components analysis

In addition to achieving tangent projection, principal components analysis reduces the overall variance in a dataset into a series of successive, variance-optimised, orthogonal, linear variables whilst preserving elative positions between specimens. Each PC explains successively less of the variation in the sample, as shown by the associated eigenvalues, which represent the variance associated with each PC and sum to total variance in the sample. The method is used in this thesis to partition shape differences in the sample into orthogonal shape variables that can be analysed with other variables, such as sinus volume (e.g., O'Higgins & Jones, 1998; Singleton, 2004, 2005; McNulty, 2005; Reddy, 2005; Gunz & Harvati, 2007; Baab *et al*., 2010; De Groote, 2011a, b).

2.III.c. Identification of sinus volume shape parameters using geometric morphometric methods

To ascertain whether there are relationships between craniofacial shape and paranasal sinus size, GMM were used to partition total shape differences between specimens into individual shape vectors, which were then tested for relationships with sinus volumes (see also Chapter 3). The resulting shape variables, designated sinus volume shape parameters (SVSPs), were used in subsequent analyses with taxonomic/population history, dietary strain, and climatic variables to determine if

they are related to sinus-related shape. It was not the intention of this thesis to study total craniofacial shape differences between individuals or groups, but to focus only on those aspects of shape differences alone that are related to sinus volume. By comparing direct relationships between comparative variables (taxonomy/population history/diet/climate) and sinus volume, to indirect relationships between these comparative variables and sinus volume-associated craniofacial shape, the intention was to clarify if differences in sinus volume contribute to differences in craniofacial shape, or the reverse.

2.III.c.i. Landmarks

The landmarks used in the current study were chosen to provide good coverage of the whole cranium; both splanchnocranium and neurocranium. It was also considered necessary to include landmarks on different functional modules, e.g., optic and respiratory (see Introduction). Both masticatory and non-masticatory regions were sampled, because the dispersal of biomechanical strains is considered a possible sinus function (e.g., Preuschoft, *et al.*, 2002) and mastication is known to affect the shape of the cranium via phenotypic plasticity (Plavcan, 2001, 2002; Wood & Lieberman, 2001; Lieberman *et al.*, 2004; Pucciarelli *et al.*, 2006; von Cramon-Taubadel, 2009b; Paschetta, *et al.*, 2010). Therefore, one might therefore expect differences in the relationships with paranasal pneumatisation between these regions. Care was also taken to ensure the region of the cranium pneumatised by each of the sinuses was well covered by the landmark set. Type I and type II landmarks were preferentially chosen over type III landmarks for their greater reliability and biological information (see Section 2.III.b.). Counter to the need to accurately

capture cranial shape were concerns to minimise the problem of missing data for fragmentary specimens (particularly fossils) (see Appendix 4) and the consideration of time taken to digitise each specimen, since a large sample was desirable to represent global recent *H. sapiens* variation. The first of these issues was addressed by using both the full landmark set as described below, and also a smaller sinus-specific landmark set for each of the three sinus types, which focused mainly on the region pneumatised by that sinus. This is explained in Chapter 3, but since the smaller landmark sets are all subsets of the full landmark set, the method and error tests described below (Section 2.III.c.i. to 2.III.c.iv.) apply to them all.

The landmarks in the current study were chosen from a larger set created by von Cramon Taubadel (2009) (see Table 7 and Figures 22 to 24). Landmarks from von Cramon Taubadel (2009) were used because she synthesised experimental, observational, and developmental research on strain to separate her landmarks into masticatory and non-masticatory sets. This satisfied one of the key requirements of the landmark set for the current study; that both masticatory and non-masticatory regions were included, and the difference between the two had been validated. In her 2009 study, von Cramon Taubadel used her full landmark data in a GMM study using Morphologika software (O'Higgins & Jones, 1998) to show that the masticatory regions of *H. sapiens* crania are more variable than the non-masticatory regions. This shows that these landmarks are successful in capturing biologically relevant shape differences in a similar type of study to the current thesis.

Table 7: Landmarks taken from von Cramon-Taubadel (2009b). Lat: lateral; inf: inferior; sup: superior; pos: posterior; ant: anterior.

Number	Name	Definition
1	Bregma	Point where coronal & sagittal sutures intersect
2	Glabella	Most anterior point on frontal bone
3	Nasion	Point of intersection of nasofrontal suture & midsagittal plane
4	Infranasion	Point of intersection of nasofrontal, nasomaxillary, & maxillofrontal sutures
5	Dacryon	Point of intersection of frontolacrimal & lacrimomaxillary suture
6	Nasiospinale	Point where line drawn between inferior-most points of nasal aperture crosses midsagittal spine.
7	Nariale	Most inferior point on lower rim of nasal aperture
8	Alare	Most lateral point on nasal aperture taken perpendicular to nasal height
9	Prosthion	Most anterior point on maxillary alveolar process between two central incisors
10	C/P3	Most inferior external point between maxillary canine (C) and first pre-molar (P3)
11	Supraorbital notch	Point of greatest projection of notch into orbital space, taken on medial side of notch
12	Frontomalare orbitale	Point where zygomaticofrontal suture crosses orbital margin
13	Zygoorbitale	Point where zygomaticomaxillary suture intersects with inferior orbital margin
14	Frontotemporale	Point on frontal bone where temporal line reaches its most anteromedial position
15	Frontomalare temporale	Most lateral point on zygomaticofrontal suture
16	Zygion	Most lateral point on surface of zygomatic arch
17	Zygomaxillare	Most inferoanterior point on zygomaticomaxillary suture
18	Mastoideale	Most inferolateral point on mastoid process
19	Molars (pos)	Most inferoposterior point on external maxillary alveolus (posterior to M3)
20	Zygotemporale (inf)	Most inferior point on zygomaticotemporal suture
21	Zygotemporale (sup)	Most superior point on zygomaticotemporal suture
22	Porion	Most superior point on margin of external auditory meatus
23	Sphenozygomatic (pos)	Most inferoposterior point on the sphenozygomatic suture
24	Stenion	Most medial point on sphenosquamosal sutures
25	Krotaphion	Most posterior extent of sphenoparietal suture
26	Coronospenoidale	Intersection of coronal suture and sphenoid
27	FRED	Point of intersection of frontozygomatic, zygomaticosphenoid, & sphenofrontal sutures
28	Coronale	Most lateral point on coronal suture
29	Asterion	Point where lambdoid, parietomastoid & occipitomastoid sutures meet
30	Lambda	Point where sagittal & lambdoid sutures intersect.
31	Opisthocranion	Most posterior midline point, which lies at the farthest chord length from Glabella
32	Inion	Point where superior nuchal lines merge in external occipital protuberance
33	Opisthion	Point where posterior margin of foramen magnum intersects midsagittal plane
34	Foramen magnum (lat)	Most lateral point on margin of foramen magnum
35	Basion	Point where anterior margin of foramen magnum intersects midsagittal plane
36	Occipitocondyle	Most inferolateral point on occipital condyle

	(lat)	
37	Occipitocondyle (ant)	Most inferoanterior point on occipital condyle
38	Styloidmastoid foramen	Most inferoanterior, point on styloidmastoid foramen
39	Jugular (lat)	Most inferolateral point on margin of jugular foramen
40	Jugular (med)	Most inferomedial point on margin of jugular foramen
41	Sphenobasion (lat)	Most inferolateral point on sphenooccipital synchondrosis
42	Carotid canal (lat)	Most lateral point on carotid canal
43	Carotid canal (med)	Most medial point on carotid canal
44	Hormion	Point of attachment of vomer & sphenoid bones
45	Foramen ovale (pos)	Most posterior point on foramen ovale
46	Foramen ovale (ant)	Most anterior point on foramen ovale
47	Alveolon	Point where interpalatal suture intersects line joining posterior margins of alveolar process
48	Ectomolare	Most lateral point on outer surface of alveolar margin of maxilla
49	Orale	Point of intersection on palate with line tangent to posterior margins of central incisor alveoli
50	Palatomaxillare (lat)	Most lateral point on palatomaxillary suture

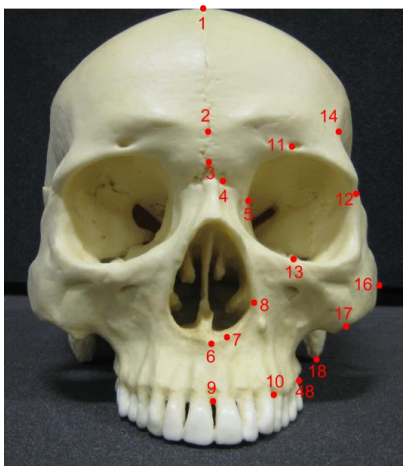

Figure 22: Full landmark set in norma frontalis. Numbers correspond to Table 7. Photo by the author.

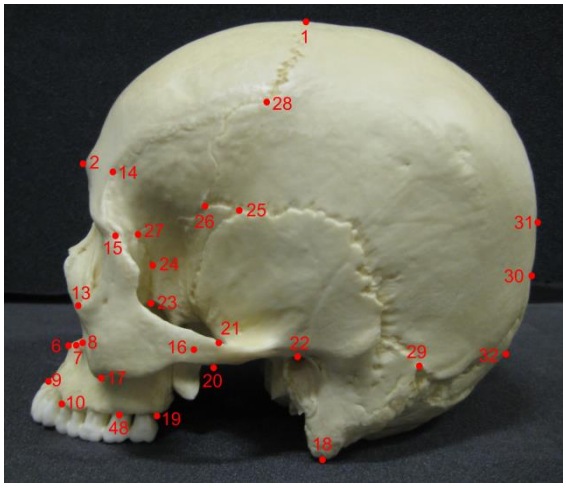

Figure 23: Full landmark set in norma lateralis. Numbers correspond to Table 7. Photo by the author.

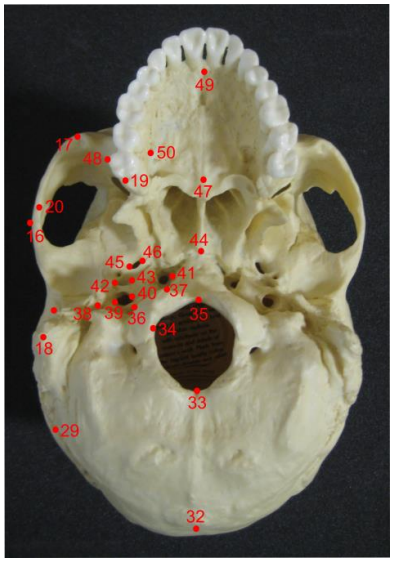

Figure 24: Full landmark set in norma basalis. Numbers correspond to Table 7. Photo by the author.

Landmarks were digitised on virtual reconstructions of crania created from CT data in AVIZO using a built-in digitising routine. The coordinates were exported as a text file for use in Morphologika and PAST software. Only one half of the cranium was digitised, in order to remove noise from individual asymmetry. Morphologika is able to mirror all data to match it to the side (right or left) of the first configuration input, thus although the left side was digitised where there was no difference in

preservation, the right was substituted if better preserved. This allowed reasonable fossil sample sizes to be included.

2.III.c.ii. Shape analysis

In Morphologika, a General Procrustes Analysis (GPA) was performed to superimpose the data for each analysis, and then a PCA was run (see Section 2.III.b.). The eigenvalues, eigenvectors (see Appendix 5), and centroid sizes from PCA analyses were exported. PC scores were tested for correlation with sinus volumes to identify shape related to sinus volumes (SVSPs). Correlation tests, rather than regression analyses, were used to identify SVSPs to avoid making assumptions about dependent and independent variables. Shape change along SVSP was modelled (see Section 2.III.c.iii.).

Number of PCs used in analyses

The decision of how many PCs to investigate was made based on the visualisation of scree-plots (see Figure 25) generated in PAST and on the eigenvalue output from the PCA in Morphologika (see Chapter 3). Eigenvalues reflect the amount of variance represented by each successive PC in a PCA; thus, one can use their relative size to make a decision about what cumulative percentage of variance is sufficient to describe the data. Scree-plots graph the percent of variation explained by the eigenvalues for each PC and show which PCs are likely to be of interest; where the line on the graph flattens out the eigenvalues can be seen to tail off, meaning that further PCs explain very little additional variance (Figure 25). The red line (Figure 25) indicates the eigenvalues expected under a random model (the Broken Stick

model), PCs with eigenvalues under this line may be considered non-significant. Scree-plots and eigenvalues are given in the relevant section for each landmark set analysis to justify the number of PCs used.

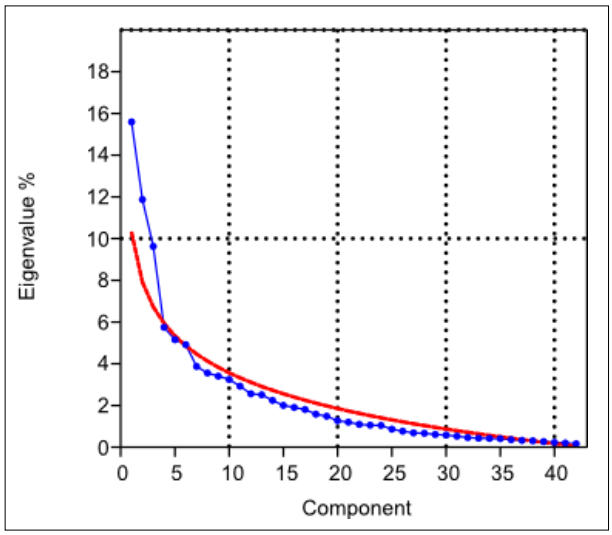

Figure 25: An example of the type of scree-plot (generated in PAST) used to visualise which principal components contain substantial information in GMM analyses. Blue line: eigenvalues for each PC, red line: broken stick model (see text). In this case, PCs after the sixth would probably not be of interest.

2.III.c.iii. Visualising shape differences

Morphologika supports the graphical representation of landmark configurations as wireframes defined by linking pairs of landmarks with straight lines (O'Higgins & Jones, 1998). Wireframes need not include all landmarks, and indeed it may compromise visualisation to do so. These schematic representations facilitate visualisation, but it must be remembered that the landmarks themselves are the data points, the lines between them hold no additional information (O'Higgins & Jones, 1998). Wireframes of any specimen in the sample can be viewed and any point along the PC can be modelled as a hypothetical wireframe to visualise the shape change represented by that vector. When analysing the shape changes represented by

SVSPs, Morphologika was used to model SVSP PCs from the lowest extreme to the highest extreme on that PC to observe the shape change described by the vector. For the full landmarks set (see Chapter 3) rthis required creating separate wireframes in norma frontalis, lateralis, and basalis for clarity; it is necessary to view shape change from several different orientations when considering 3D shape changes, as the 2D nature of visualisation on a screen can be misleading if a landmark moving in more than one direction simultaneously is viewed from any single orientation. The software performs warping along PCs by calculating the location of landmarks in a configuration represented by any point in the PCA by adding the product of the eigenvectors of the PCs of interest to the mean configuration, whilst all other PCs are held constant (O'Higgins & Jones, 1998; O'Higgins, 2000; Lockwood *et al.*, 2002). By changing the software settings to numbered points, rather than wireframes, the movements in the individual landmarks themselves were also scrutinised from different viewpoints to ascertain how shape changes observed in the wireframe were actually achieved.

In describing shape changes, it is crucial to compare configurations (such as those from either extreme of an SVSP) in the same orientation, as the same shape will appear different in slightly different orientations (a perennial problem with 2D visualisation of a 3D object), confounding interpretations of shape change. Wireframes shown in norma lateralis were standardised by orientating the mean shape in the Frankfurt Horizontal. Wireframes shown in norma frontalis were standardised by ensuring the midline between bregma and glabella was straight. Wireframes shown in norma basalis were standardised by ensuring the midline was

vertical (Figure 26). Although it is still possible that there would be slight differences between orientations in separate comparisons using these methods, in Morphologika it is not possible to change the orientation of a wireframe whilst exploring the shape space (warping the configuration along a PC to compare shape), thus there is obligate internal consistency within comparisons. Diagrams showing shape changes were produced by copying Morphologika output (wireframes) into Inkscape (Harrington, 2004-2005) to visualise shape changes and produce figures. Guides and the 'ctrl' function were used to maintain the ratio of images to ensure comparisons between different shape configurations were performed without distortion or resizing.

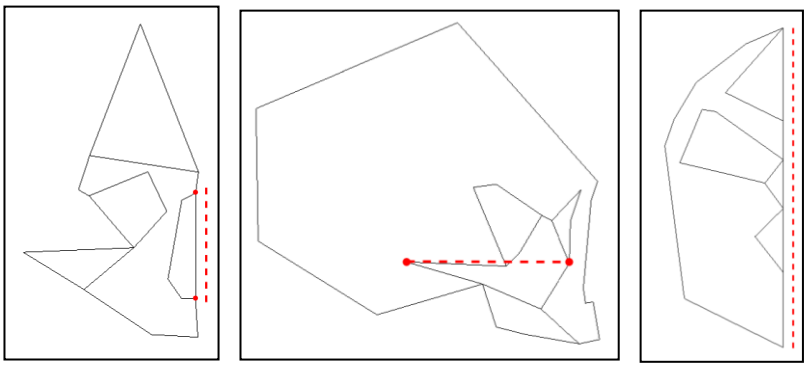

Figure 26: Examples of how wireframes were kept in standard orientation using full landmark set wireframes. Left: standard orientation used for wireframes shown in norma frontalis: mean shapes were orientated so that the line between nasion and nasiospinale was vertical. Middle: standard orientation wireframes shown in norma lateralis: mean shapes were orientated in the Frankfurt Horizontal (horizontal line between porion and zygoorbitale). Right: standard orientation for wireframes shown in norma basalis: the midline was kept vertical.

2.III.c.iv. Error tests for geometric morphometric methods of identifying sinus volume shape parameters

To test the error in the digitising of the CT data, a single cranium was digitised five times with at least a day elapsing between each digitisation session. The same individual as used in the sinus volume error tests was chosen as it is of medium

resolution and has all landmarks preserved (see Section 2.II.b.). For each repetition, a virtual reconstruction was generated from the raw data and all 50 landmarks were digitised on one side only. Landmarks were exported into Morphologika (O'Higgins & Jones, 1998) and GPA and PCA were performed (see Section 2.III.c.ii.). Procrustes aligned coordinates were exported as text from Morphologika. For each repetition, each landmark was compared with the centroid of that landmark for all repetitions, and the Mahalanobis distance was calculated in PAST. The mean Mahalanobis distance from each landmark repetition to the centroid for that landmark was calculated; the Mahalanobis distance is used to avoid the assumption of independence between landmarks. This shows the relative amount of error in each landmark (McNulty, 2005). A percentage error for each landmark (see Table 8) was calculated by summing the distances across repetitions for each landmark, dividing this by the total sum of all distances for all landmarks, and multiplying the result by 100% (McNulty, 2005). Any landmarks with an error greater than 5% were judged to be too error-prone and were discarded from subsequent analyses (see Table 9).

Table 8: Results from error test of digitising landmarks. Table shows percent error for each landmark. Red shading indicates error percentages above the chosen 5% tolerance limit, grey shading indicates two landmarks found to be error-prone between specimens. For explanation of landmarks see Table 7.

Landmark	Percent error
bregma	2.09
glabella	2.66
nasion	1.37
infranasion	1.17
dacryon	4.69
nasiospinale	1.50
nariale	1.19
alare	1.49
prosthion	2.93
C/P3	1.20
supraorbital notch	0.58

frontomalare orbitale	1.27
zygoorbitale	3.72
frontotemporale	3.94
frontomalare temporale	1.72
zygion	3.23
zygomaxillare	1.13
mastoidale	2.26
molars pos	2.86
zygotemporale inf	1.22
zygotemporale sup	0.91
porion	1.40
sphenozygomatic	0.81
stenion	1.17
krotaphion	2.57
coronosphenoidale	1.68
FRED	1.97
coronale	2.76
asterion	1.25
lambda	1.46
opisthocranion	6.05
inion	2.49
opisthion	1.53
foramen magnum lat	1.71
basion	1.26
occipitocondyle lat	7.88
occipitocondyle ant	0.92
stylomastoid foramen	1.02
jugular lat	2.12
jugular med	1.20
sphenobasion lat	1.08
carotid canal lat	1.32
carotid canal med	1.46
hormion	1.17
foramen ovale pos	1.48
foramen ovale ant	1.15
ectomolare	1.26
alveolon	1.23
orale	1.24
palatomaxillare lat	4.24

Two landmarks, Opisthocranion (31) and Occipitocondyle (lat) (36) (see Table 7 and Figure 24), showed greater than the 5% error threshold and so were judged to be insufficiently precise and were removed from subsequent analyses. Two further landmarks, Stenion (24) and Coronale (28) (see Table 7 and Figure 23), were found during data collection to be very variable between specimens, to the point that it appeared that they were not homologous points on different individuals. These two landmarks were also removed from all subsequent analyses, resulting in a configuration of 46 landmarks in the full landmark set. Since the landmarks removed are not clustered in one region, and there are still sufficient landmarks to satisfy the landmark criteria defined above (Section 2.III.c.i.), the removal of these error-prone landmarks should not negatively affect the results from this study. The landmarks were renumbered to reflect the removal of these landmarks, and are shown in Table 9.

Table 9: Full landmark set, post-error test. Numbers are as referred to in full landmark set analyses in the rest of the thesis. Landmarks taken from von Cramon-Taubadel (2009b). Lat: lateral; inf: inferior; sup: superior; pos: posterior; ant: anterior. Descriptions as in Table 7 and Figures 22 to 24.

Landmark	Number	Landmark	Number
Bregma	1	Krotaphion	24
Glabella	2	Coronosphenoidale	25
Nasion	3	Fred	26
Infranasion	4	Asterion	27
Dacryon	5	Lambda	28
Nasiospinale	6	Inion	29
Nariale	7	Opisthion	30
Alare	8	Foramen magnum lat.	31
Prosthion	9	Basion	32
C/p3	10	Occipitocondyle ant.	33
Supraorbital notch	11	Stylomastoid foramen	34
Frontomalare orbitale	12	Jugular lat.	35
Zygoorbitale	13	Jugular med.	36
Frontotemporale	14	Sphenobasion lat.	37
Frontomalare temporale	15	Carotid canal lat.	38
Zygion	16	Carotid canal med.	39
Zygomaxillare	17	Hormion	40
Mastoidale	18	Foramen ovale pos.	41
Molars pos	19	Foramen ovale ant.	42
Zygotemporale inf.	20	Alveolon	43
Zygotemporale sup.	21	Ectomolare	44
Porion	22	Orale	45
Sphenozygomatic pos.	23	Palatomaxillare lat.	46

Once the error-prone landmarks were removed, the matrix of Mahalanobis distances between error test repetition configurations and sample configurations was recalculated. Conditional formatting of the Mahalanobis distance matrix was used to compare distances between all sample configurations all error test configurations to ascertain whether any of the distances between sample configurations was as small as those between error test repetitions (Lockwood, *et al.*, 2002). None were. The distances between the sample configurations and between the error test repetitions were then compared using a Mann Whitney U test (because of non-parametric

distributions) in SPSS 19.0 (IBM Corp., 2010). The distances between the error test repetitions were found to be highly significantly smaller than those between sample configurations (Mann Whitney U: U = 38.00, Z = -5.46, p = <0.001). These results were interpreted as meaning that intra-observer error in landmark collection was small compared to differences between individuals and therefore unlikely to bias the results.

2.IV. Methods: Relating sinus variables to taxonomic/population history, dietary, and climatic variables

In this section the methods used to explore relationships between sinus variables and other possible factors affecting sinus volume/craniofacial morphology are explained. First the methods used in taxonomic and population history analyses (results in Chapter 4) are detailed, then those for masticatory strain analyses (results in Chapter 5), and then for climate analyses (results in Chapter 6). In each case, the methods used for relating the sinus volume, and then the methods used for relating the sinus volume shape parameters (SVSPs), to the non-sinus variables are given.

2.IV.a. RQ1: Relating sinus variables to population/ taxonomic history variables

One of the major aims of this thesis was to establish whether the paranasal sinuses differ between Pleistocene hominin taxa and, if so, whether this could account for

differences in craniofacial shape, as has been suggested historically. Much of the variation in craniofacial morphology between populations of recent *H. sapiens* seems to differ based on population history (i.e., accumulation of neutral differences that reflect time since population division), thus it is of interest to ascertain, if there are population differences in sinus volumes or in SVSPs, whether they reflect population phylogeny. To assess theories that *H. sapiens* is hyperplastic, tests were carried out to show whether sinuses are more variable within recent *H. sapiens* than within other taxa, and to investigate sinus functional homology, differences in intra-group variation in sinuses types were examined. Sinus volumes for each sinus were measured and standardised for size to produce measures of relative sinus volume as described in Section 2.II. and SVSPs were identified as described in Chapter 3. Species designations for the sample were assigned as described in Section 2.IV.a.i. and Table 10; the population groupings are recorded in Section 2.I.b.i. The sample for each analysis is given at the start of the relevant section in Chapter 3.

2.IV.a.i. Quantifying population history

Geographic distance has been shown to be a reliable proxy for neutral genetic differences that reflect population history (Manica *et al.*, 2005; Ramachandran *et al.*, 2005). Therefore, in order to analyse the effects of population history on recent *H. sapiens*, a matrix of geographic distances was calculated for all populations following the methods described in Smith *et al.* (2007a). Great circle distances were calculated using Google Maps Distance Calculator (http://www.daftlogic.com/projects-google-maps-distance-calculator.htm) between mean latitude/longitudes for each population (as used to calculate climate variables).

A series of waypoints was used to constrain the distances and to prevent routes that involved long sea crossings (Smith *et al.*, 2007a). The way points used were Anadyr, Russia; Cairo, Egypt; Istanbul, Turkey; Phnom Phenh, Cambodia; and Prince Rupert, Canada (Ramachandran *et al.*, 2005; Smith *et al.*, 2007a).

2.IV.a.ii. Potentially problematic population groupings

As individuals from some parts of the world are less well represented in the CT data collections available for study (or less available for CT scanning), it was necessary in some cases to combine individuals from relatively large geographical regions in order to preserve reasonable sample sizes (see Section 2.I.b.i. for population breakdown). Populations of most concern for this reason are China, Russia, Western Europe, and Western Africa. If individuals are unrepresentative of their population they might confuse analyses based on differences between populations, or analyses which are intended to test the effect of population history. It also potentially leads to group means of climate variables that are unrepresentative of some, or all of the individuals in the group. The effect of grouping geographically disparate specimens together in these potentially problematic groups is considered and discussed in the relevant results chapters; Chapter 4 for population differences and Chapter 6 for relationships with climatic variables.

2.IV.a.iii. Taxonomic definitions

Table 10: Fossil specimen taxonomic designations used in this thesis.

Species	Specimen
H. erectus	KNM-ER 3733
	KNM-ER 3883
H. heidelbergensis	Bodo
	Ceprano
	Kabwe
	Petralona
	Steinheim
H. neanderthalensis	Forbes Quarry
	Guattari
	Krapina 3
	La Chapelle
	La Ferrassie
	La Quina
	Neanderthal
	Tabun C1
Early *H. Sapiens*	Cro-Magnon 1
	Cro-Magnon 2
	Cro-Magnon 3
	Mladeč
	Ngaloba
	Singa
	Skhul 5

H. sapiens

Here and throughout, "recent *Homo sapiens*" is defined as *H. sapiens* less than 30,000 years old; "early *H. sapiens*" are those from between 150-30 ka following the rationale of Stringer and Buck (2014).

H. neanderthalensis

Despite evidence for Neanderthal introgression in the genomes of recent *H. sapiens* (Green *et al.*, 2010; Sanchez-Quinto *et al.*, 2013; Prüfer *et al.*, 2014), Neanderthals are treated here as a separate species from *H. sapiens*; i.e., *H. neanderthalensis*. It is

not uncommon for closely related species to be able to interbreed to some extent (Jolly *et al.*, 1997; Jolly, 2001, 2009), and levels of morphological difference between Neanderthals and *H. sapiens* are greater than those seen between many closely related species; subsuming the two into one species would result in a level of variation in excess of other primate species (Tattersall & Schwartz, 1998, Harvati, 2003, Harvati *et al.*, 2004, Stringer, 2012a).

H. heidelbergensis

H. heidelbergensis is a disputed category, as discussed in the Introduction. In the analyses that follow, *H. heidelbergensis* is defined following Stringer (2012c); that is to say as a Euro-African, Middle Pleistocene species. Stringer (2012c) also cautiously includes Asian material in his hypodigm, but unfortunately no Middle Pleistocene Asian fossils were available for analysis.

H. erectus

The definition of *H. erectus* used here is *H. erectus* (*sensu lato*) following Rightmire (e.g., Rightmire, 1998, 2008); that is to say a widespread, long-lasting, polytypic species found in both Europe and Africa.

Some fossil specimens are of particularly uncertain taxonomic attribution within these taxonomic definitions (e.g., Ceprano); this is discussed where appropriate in Sections 4.II.a.i. and 7.I.b.i.

2.IV.a.iv. Relating sinus volume to population/taxonomic history variables

Boxplots

Ordinations of the data were produced to visualise differences between groups. In this section and throughout, boxplots are used to show differences between groups. These are produced in SigmaPlot 12.0 (Systat Software, 2013); the box displays 25th to 75th percentiles of the data and the median, the whiskers show the 10th to 90th percentile, and the 5th and 95th percentiles are shown as circles.

Differences in relative sinus volume between populations/taxa of recent *H. sapiens*

Given the small sample size for the fossil groups, the distribution of their sinus volumes is unknown. The very unequal size of the samples for different groups is also likely to cause problems with parametric statistics. For this reason, non-parametric permutation tests, ANOSIMs (analysis of similarity), were performed using PAST software to ascertain differences in sinus volumes and SVSP PC scores (see below) between taxa and populations. An ANOSIM is analogous to an ANOVA in that it compares differences within and between groups (Hammer *et al.*, 2001). Distances are converted into ranks and the test statistic R gives a measure of dissimilarity, with more positive numbers (up to 1) showing greater difference (Hammer *et al.*, 2001). Euclidean distances were used with the default of 9999 permutations for these ANOSIM analyses.

Mantel tests using Euclidean distances were run in PAST to test for relationships between population history, as measured by the geographic distance matrix between populations, and matrices of differences between individuals in sinus variables in populations of recent *H. sapiens*.

Variation in relative sinus volume

The amount of variation in sinus volume within populations/taxa of recent *H. sapiens* was investigated by calculating coefficients of variation (CV) (Rightmire, 2008; Buck, *et al.*, 2010; Stock & Buck, 2010). Due to small sample sizes, Sokal and Rolf's (1995) correction was applied to the normal measurement of CV to produce a measurement of V*. The mean coefficient of variation for each group was calculated.

Covariation in sinus volumes

As not all the relative sinus volumes are normally distributed, non-parametric pair-wise comparisons of sinus volumes were carried out. This method was chosen rather than a single multivariate analysis, which would have inherently controlled for the inflation of the family-wise error rate, because this allowed the use of a larger sample in each analysis.

2.IV.a.v. Relating SVSPs to population/ taxonomic history variables

The same method was followed for populations of recent *H. sapiens* and hominin taxonomic groups . Data were graphed to visualise separation between populations

of recent *H. sapiens* and between taxa on SVSPs. The PC scores of SVSPs were then tested to see if there were significant differences between groups (O'Higgins & Jones, 1998; Singleton, 2004, 2005; McNulty, 2005; Reddy *et al.*, 2005; Gunz & Harvati, 2007; De Groote *et al.*, 2010; De Groote, 2011b) using ANOSIM. The Analysis of single PCs with variables of interest is a well established GMM (see studies cited above), has been successfully used to study the relationship between sinus volume and craniofacial shape (Zollikofer *et al*., 2008), and provides perhaps the simplest to interpret results in shape analysis. However, it is noted that the use of single PCs here, and throughout the current study, may lead to underestimations of relationships, since each individual PC is required to meet the chosen significance level, whereas when many are tested simultaneously, by using multivariate methods such as partial least squares (e.g., Noback et al., 2011), the cumulative significance is tested. The effects of using these two different methods could be explored in future work.

Cluster analysis on group means using Euclidean distances and unweighted pair group averages (UPGA) in PAST was used to create a dendrograms of difference in PC scores of SVSPs for each population of recent *H. sapiens*. These dendrograms (which are not phylogenetic trees) were used to facilitate visualisation of which groups were most similar in terms of the morphology described by SVSPs. Cluster analysis can be problematic, in that it will create groups even if none exist. Combined with ordination techniques such as PCA and statistical tests, however, it can be an effective way of visualising results, if one does not over-state the evidence

and equate morphological closeness on an SVSP to phylogenetic closeness (Harvati *et al.*, 2004).

2.IV.b. RQ2: Relating sinus variables to masticatory stress/strain

The dissipation of dietary strains is one hypothesis for sinus function, and mastication has also been shown to affect craniofacial morphology through plastic bone remodelling. The possible extreme use of the anterior dentition, in particular, is of interest, as it has been invoked as an explanation for the very different craniofacial morphologies of both *H. neanderthalensis* and recent *H. sapiens* Inuits (see Introduction). The methods described in this section are used to generate GMM shape variables as proxies for masticatory stress/strain and categorise the sample by subsistence strategy in order to assess relationships between masticatory stress/strain and sinus variables and investigate the plausibility of these hypotheses.

2.IV.b.i. Differences in sinus variables between groups with different subsistence strategies

Biomechanical-loading-induced bone growth in the direction of strain has been shown experimentally and comparatively in the cranium (as well as postcranial skeleton) for a variety of vertebrate species (Larsen, 1997; Goodship & Cunningham, 2001; Lieberman *et al.*, 2004; Pearson & Lieberman, 2004; Ross & Metzger, 2004; Pucciarelli *et al.*, 2006; Ruff *et al.*, 2006; Stock, 2006; Gomez *et al.*, 2007; Shaw & Stock, 2009). The masticatory apparatus has been shown to be

particularly plastic and shows adaptation to different dietary regimes (Plavcan, 2001, 2002; Wood & Lieberman, 2001; Lieberman, *et al.*, 2004, Pucciarelli *et al.*, 2006; Paschetta *et al.*, 2010) The food of agriculturalists is generally softer than that of foragers, rendering it easier to chew, and also requiring less chewing time (González-José *et al.*, 2005; Sardi *et al.*, 2006; Paschetta *et al.*, 2010). Agriculturalists therefore experience less dietary strain than foragers and will also demonstrate different shapes in their masticatory regions. If, as implied by previous studies, sinus volume is an adaptation to masticatory stress/strain, sinuses should be larger in foragers than in agriculturalists, a hypothesis tested below. If there are dietary differences in SVSPs, but not volumes themselves, this would show that there is only an indirect relationship between masticatory stress/strain and sinus volume, supporting the spandrel hypothesis.

The complete sample for this study comprises a range of populations with different subsistence strategies (see Section 2.I.b.i. for justification of sample classification), but, for simplicity, the sample has been divided into just two groups, hunter-gatherers (the Forager category) and those who largely rely on domesticated species (the DOM category), to reflect differences in masticatory strain as described above. The latter lumps together small scale horticulturalist/farmers, such as the indigenous Hawaiians, and intensive agriculturalists, such as recent Western Europeans. Because DOM reliance on processed vegetable foods contributes most to the softer nature of their diet (González-José *et al.*, 2005; Sardi *et al.*, 2006; Paschetta *et al.*, 2010), and these two groups are likely to be more similar to one another than either is to Forager groups. It might also be argued that marine and terrestrial foragers

experience quite different biomechanical loading patterns, but here they are treated as a single group to preserve reasonable sample sizes (see also González-José *et al.*, 2005). The classification of groups in the sample is detailed in Table 11 below. The breakdown of the sample numbers used in the masticatory landmark analyses is shown in Table 42.

Table 11: Classification of sample into Forager or consumer of domesticated species (DOM) groups. Justification for classification given in Section 2.I.b.i.

Group	Dietary classification
Chinese	DOM
Hawaiians	DOM
Indians	DOM
Lithuanians	DOM
Mexicans	DOM
Peruvians	DOM
Western Africans	DOM
Western Europeans	DOM
Greenland Inuit	Forager
Iberomaurusians	Forager
Russians	Forager
Tasmanians	Forager
Torres Straits Islanders	Forager
Early *H. sapiens*	Forager
H. neanderthalensis	Forager
H. heidelbergensis	Forager

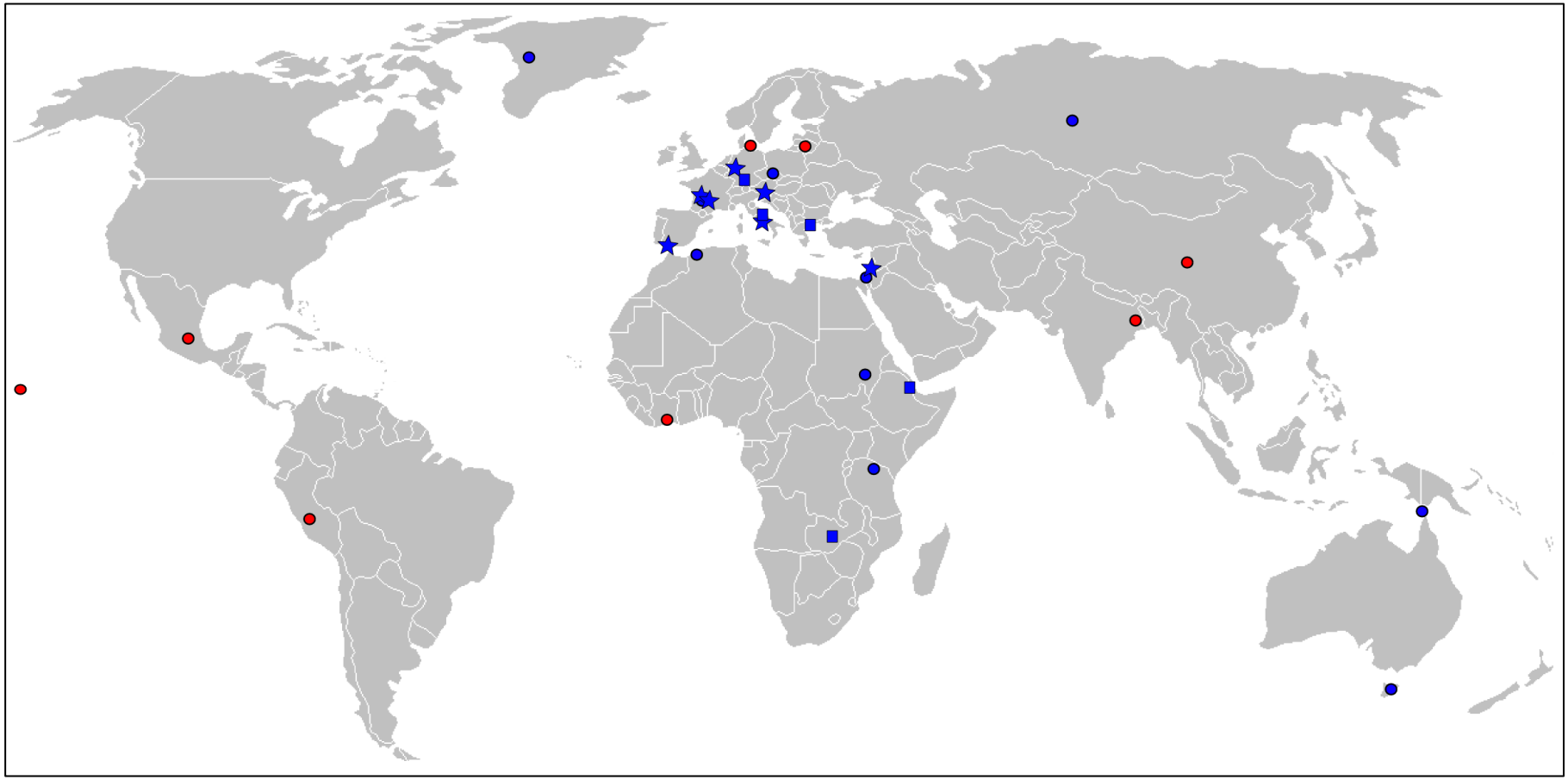

Figure 27: Map showing sample by subsistence. Red: DOM, blue: Forager. Circles: *H. sapiens*, stars: *H. neanderthalensis*, squares: *H. heidelbergensis* (for details, see text).

T-tests were used to test for significant differences in relative sinus volumes and SVSP PC scores between subsistence groups.

2.IV.b.ii. Identification of masticatory stress/strain-related shape variables

Foragers and agriculturalists can be separated in analyses of the size and/or shape of masticatory regions, and this is assumed to be due to differences in mastication-induced plastic growth resulting from different levels of strain caused by the masticatory muscles under different dietary regimes (González-José *et al.*, 2005; Sardi *et al.*, 2006; Paschetta *et al.*, 2010). In the current thesis, a landmark set devised by Paschetta *et al.* (2010) and GMM were used to generate shape variables that separate populations with different subsistence strategies based on temporalis muscle shape (masticatory shape parameters: MSPs). Since the temporalis is a key masticatory muscle, its size and position (and the resulting changes in force and efficiency) should reflect the stresses inherent in any particular diet. The shape of the temporalis region in any individual will reflect the shape of the temporalis (Paschetta *et* al., 2010).MSPs were then analysed to investigate possible relationships between sinus variables and temporalis muscle shape, and to determine if greater dietary stress/strain is associated with larger relative sinus volumes and/or the craniofacial morphology associated with larger sinus volume. GMM were used in shape analyses of the masticatory landmark set as described above (Section 2.III.c.ii.). Results from GMM analyses and generation of MSPs are described in Chapter 5.

Landmark set used to generate masticatory shape parameters

Paschetta *et al*. (2010) compared the craniofacial shapes between foragers, horticulturalists and intensive farmers. They hypothesised that the largest differences between groups would be in the attachment regions of the masticatory muscles, and used GMM to analyse shape differences in these regions. The results show that the best discriminator between subsistence types is their temporal fossa landmark set. This landmark set was designed to reflect the transverse cross-section of the temporal fossa, which indicates the size of the temporalis muscle, and the extension and orientation of the muscle on the vault, which are indicative of the size, shape, and position of the temporalis muscle (see Figure 28) (Paschetta, *et al.*, 2010). The temporalis muscle is the most powerful muscle in the human body (Lieberman, 2011) (and hence the most likely to cause plastic bone growth) resulting in likely shape change in the cranium. In the current study, the landmarks from Paschetta *et al*.'s (2010) temporal fossa subset (see Table 12), which had been shown to separate their sample based on subsistence strategy, were used to generate MSPs to distinguish shape differences in the sample associated with subsistence pattern and associated masticatory strain.

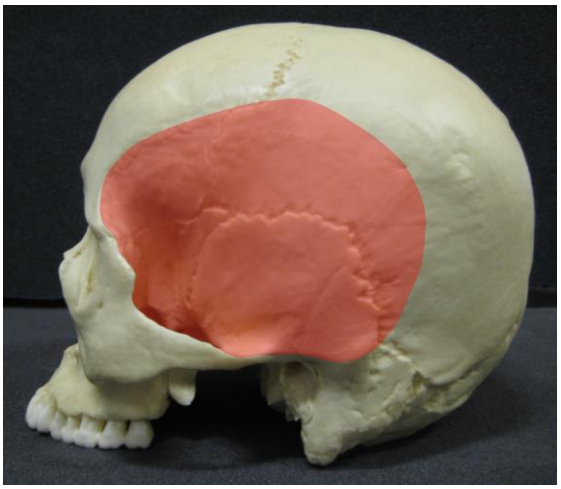

Figure 28: Lateral view of cranium with the region of the temporalis muscle attachment highlighted in red. Photo by the author.

Table 12: Landmarks from (Paschetta *et al.*, 2010) used to generate masticatory shape parameters. Numbering is from this study, not the original article.

Number of landmark	Name of landmark	Definition
1	Zygomaxillare	Lower border of the zygomatic synchondrosis
2	Stephanion	The point where the coronal suture crosses the temporal line
3	Enthomion	Parietal notch
4	Posterior infratemporal fossa	Most posterior point in the infratemporal fossa
5	MW1	Most inferior point on the sphenotemporal crest on the greater wing of the sphenoid
6	MW2	Most inferior internal point on the zygomatic arch (orthogonal to sagittal plane) at the level of MW1

GMM methods as described for the identification of SVSPs in Section 2.III.c.i. were used to define shape variables that separated DOM from Foragers. These differences were modelled to check their interpretation as shape differences in temporalis muscle shape related to differences in diet (Section 5.I.).

Error test for masticatory landmark set

The method described in Section 2.III.c.i. for estimating error in digitising landmarks was used. As for the full landmark set, a single recent *H. sapiens* was digitised with the masticatory landmark set (Table 12) five times with at least a day separating each data collection. The Mahalanobis distances between error test repetitions were significantly smaller than distances between different sample configurations ($Z = -3.43$, $p = 0.001$).

2.IV.b.iii. Method of testing differences in sinus variables between subsistence classifications

The differences in sinus volume and SVSP PC scores between Forager and DOM groups were tested using t-tests.

2.IV.b.iv. Method for relating sinus variables to masticatory shape parameters and dietary differences

Relationship between masticatory strain shape parameters and sinus volume

Reduced major axis regression analysis in PAST was used to test for a relationship between MSPs and sinus volume in each sinus in turn

Relationship between masticatory strain shape parameters and sinus shape parameters

Reduced major axis regression analysis in PAST was used to test for a relationships between MSPs and SVSP as above. Regression was used, rather than partial least squares, which would enable the comparison of multiple SVSPs from different landmark sets simultaneously (for example, full landmark set frontal SVSP PC3 and frontal landmark set PC6), to maximise the sample size (as the samples for each landmark set differ) for each analysis, and because partial least squares lacks the predictive power of regression and it was of interest whether differences in craniofacial morphology associated with masticatory strain predict differences in sinus volume.

2.IV.c. RQ3: Relating sinus variables to climate variables

There are long-standing theories relating sinus volume to climate via a thermoregulatory sinus function. Extreme cold is also one of the few selective pressures consistently shown to have an effect on craniofacial morphology in recent *H. sapiens* populations (see Introduction). The methods described below were used to calculate climate variables for the sample and to investigate the effect of climate variables on sinus variables.

2.IV.c.i. Calculation of climate variables

Measures of temperature and precipitation were chosen for investigation because both these variables have been shown to affect craniofacial shape in recent *H. sapiens* (Weiner, 1954; Steegmann & Platner, 1968; Beals, 1972; Beals *et al.*, 1984; Franciscus & Long, 1991; Harvati & Weaver, 2006b; Rae *et al.*, 2006; Hubbe *et al.*, 2009; Betti *et al.*, 2010; Noback, 2011; Nowaczewska *et al.*, 2011). The precision of palaeoclimatic reconstructions is not good for the time and geographic location of many of the fossils. Therefore, continuous temperature and precipitation variables were calculated for the recent *H. sapiens* populations and broader temperature/precipitation categories were calculated for the entire sample.

Continuous climate variables

A mean latitude and longitude was calculated for each recent *H. sapiens* population using the latitude and longitude of known locations (found using the Google Maps latitude and longitude finder: http://www.doogal.co.uk/LatLong.php) for each specimen, substituted with the approximate centre of the country for each specimen

where a more precise location was unknown (see Section 2.I.b.i.). Weather data for each population were then compiled from the KNMI Climate Explorer (http://climexp.knmi.nl) website. The nearest weather station to the population's mean latitude and longitude was chosen and monthly temperature and precipitation records were exported (for weather station details and periods covered by data, see Appendix 3). From these data, the following variables were calculated: MAT (mean annual temperature); maxTemp (maximum monthly temperature); minTemp (minimum monthly temperature); MAP (mean annual precipitation); maxPrecip (maximum monthly precipitation); and minPrecip (minimum monthly precipitation).

Categorical climate variables for full sample

Recent climate data may not be representative for fossil samples, given the amount of climate variation over the Pleistocene (e.g., Schmit & Hertzberg, 2011; Blome *et al.*, 2012). Accurate palaeoclimatic reconstructions detailing mean and maximum/minimum temperature and precipitation variables, however, are not available for the geographical and chronological spread of the fossil sample in this study. Good records exist for arctic regions due to ice-core records, and in some instances sea surface temperatures are available, but these are not applicable to tropical, inland regions (see for example, National Oceanic and Atmospheric Administration palaeoclimatic database: www.ncdc.noaa.gov/paleo/datalist.html). Furthermore, dates are not well-defined for many of the fossils, and some are currently in the process of being re-dated (e.g., Kabwe – C. Stringer, pers. comm.). Since the climate has been extremely variable over time and space in the Pleistocene (Schmit & Hertzberg, 2011; Blome *et al.*, 2012), inaccuracies in dating or distance

between sites with good palaeoclimate records and fossil sites may lead to poor estimations of continuous climatic variables for fossil samples. For this reason, in an attempt to obtain a level of palaeoclimatic validity whilst avoiding making too many assumptions, fossil specimens were only classified according to climate category (e.g., Beals, 1972; Butaric *et al.*, 2010). The recent *H. sapiens* sample was also categorised in this way in addition to the calculation of continuous climatic variables. The widely used Köppen-Geiger climate classification system, up-dated by Kottek *et al.* (2006), was used to assign specimens to climate groups. This system divides global ecosystems into vegetation-based regions structured by temperature and precipitation. Since the full Köppen-Geiger climate classification requires variables not available for fossil specimens, a simplified version (following Butaric *et al.*, 2010) was used here. The temperature and precipitation values used to define categories are given below in Table 13. Justification for placing populations of recent *H. sapiens* and individual fossil specimens in climate categories is given in Sections 2.I.b.i. and 2.I.b.ii.

Table 13: Definition of climate categories. MAP: mean annual temperature; MAP: mean annual precipitation.

Climate category	Definition
Hot/Wet	MAP > 15.5°C & MAP > 550mm/yr
Hot/Dry	MAT > 15.5°C & MAP < 550mm/yr
Temperate	MAT = 5 – 15.5°C
Cold/Wet	MAT < 5°C & MAP > 275mm/yr
Cold/Dry	MAT <5°C & MAP < 275mm/yr

The categories shown in Table 13 were further sub-divided by into temperature categories (Cold/Temperate/Hot) and precipitation categories (Wet/Dry) to unpick the separate effects of temperature and precipitation differences on sinus variables. Specimens classified as Temperate were not included in the precipitation group

analyses to simplify grouping and avoid over-lap between categories (see also Butaric *et al.*, 2010).

2.IV.c.ii. Methods for testing relationships between climatic variables and sinus variables

Continuous climate variables

Reduced major axis (RMA) regression in PAST was used to analyse the relationship between each of the climatic variables for each of the sinus volumes and each SVSP in turn. Individual regression analyses with Bonferroni correction (see Section 2.II.), rather than multiple regression, was chosen, as it allowed the use of RMA regression, which is preferable due to the likelihood of error in both independent and dependent variables (see also Butaric *et al.*, 2010). Regression was chosen over partial least squares in order to test if the climatic variables could predict sinus variables.

Climate categories

To test for differences in sinus volumes and PC scores on SVSPs in different climate categories and temperature categories, ANOVAs were performed in SPSS 19.0. Games-Howell and Hochberg's GT2 post-hoc tests were run (in SPSS 19.0) and, to be conservative, differences between categories were only accepted as significant if they were significant using both tests. This was because Hochberg's GT2 works well with unequal sample sizes, but Games-Howell is more resistant to unequal variances (Field, 2009), and it is possible that both of these problems may occur with the current sample. As there were only two groups (Wet/Dry), t-tests were performed to test for differences in volumes and SVSP PC scores in the precipitation categories.

Chapter 3: Results – Identification of sinus volume shape parameters

To investigate hypotheses that differences in sinus volume are adaptive and affect craniofacial form (see Introduction), it must be established whether there are relationships between the size of the different sinuses and craniofacial shape. In this chapter, geometric morphometric methods (GMM) are used to decompose total craniofacial shape differences in the sample to obtain variables of shape related to sinus volume. These variables are designated sinus volume shape parameters (SVSPs) and are used in the subsequent chapters to analyse relationships between sinus-related shape and taxonomic/population, dietary, and climatic variables. Fragmentary remains are a perennial problem in palaeoanthropological studies; one must balance the opposing needs of data quality and sample size. To attempt to achieve this balance in the current study, the analyses were repeated, favouring first one consideration and then the other. In Section 3.I. the GMM analyses were conducted on a small sample composed of all the individuals on which it was possible to collect the full set of 46 landmarks (see Methods) to get the best possible shape data. In Section 3.II, the number of specimens was favoured over the number of landmarks in a series of sinus-specific subsets of the full landmark set designed to focus in on a particular sinus with fewer landmarks, and so allow the inclusion of

more fragmentary specimens. First the frontal sinus-specific, then the maxillary sinus-specific, and then the sphenoidal sinus-specific results are presented.

3.I. Full landmark set

In this section, full landmark set SVSPs are indentified and then the shape change they represent is modelled. The full landmark set containing all 46 landmarks (see Table 9) reduces the sample to only 43 specimens, all of which are recent *Homo sapiens*. This is 38% of the recent *H. sapiens* sample and 32% of the entire sample. See below (Table 14) for a breakdown of these specimens by population (two populations in the recent *H. sapiens* sample, Tasmania and North Africa, have no specimens with all landmarks present, and so are not included in this analysis).

Table 14: Table showing number of specimens with all landmarks preserved and their geographic origin.

(*Homo sapiens)* Population	**Number of specimens in population sample**	**Number with all 46 landmarks preserved**
China	9	3
Greenland	7	6
Hawaii	10	4
India	10	1
Lithuania	10	3
Mexico	9	4
Peru	10	9
Russia	4	1
Torres Straits	10	5
Western Africa	10	2
Western Europe	10	5
Total		**43**

The eigenvalues and a scree-plot of this PCA were scrutinised to determine how many PCs contained valuable information about the variation in shape between crania (see Figure 26, Section 2.III.c.ii).

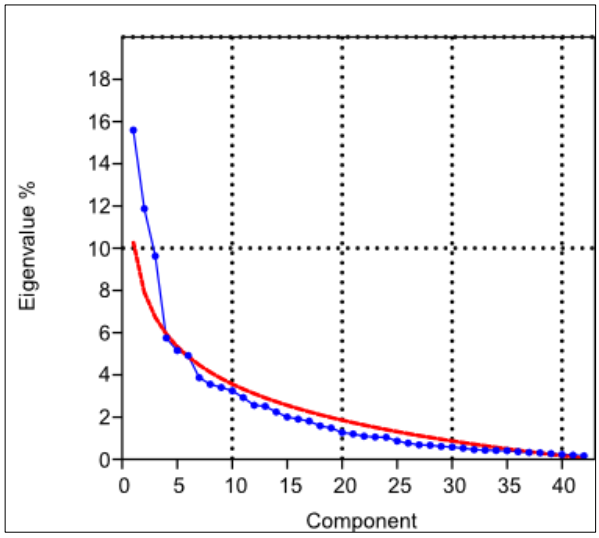

Figure 29**:** Scree-plot of PC eigenvalues for full landmark set. This is used to visualise which principal components contain substantial information.

Table 15: Eigenvalues from principal components analysis of shape in crania with full landmark set. The first seven PCs account for nearly 60% of the variation in the sample.

Principal component	Eigenvalue	Proportion of variance explained	Cumulative variance explained (%)
1	0.00124	0.16	0.16
2	0.00095	0.12	0.28
3	0.00077	0.10	0.37
4	0.00046	0.06	0.43
5	0.00041	0.05	0.48
6	0.00039	0.05	0.53
7	0.00031	0.04	0.57

The scree-plot and eigenvalues suggest that PCs higher than six or seven are unlikely to describe any meaningful amount of variation; therefore, for each PC 1-7, a Pearson's test for correlation was performed between the PC scores and the relative sinus volumes.

3.I.a. Full landmark set frontal sinus volume shape parameters

The wireframes (see Figure 30) below are intended to help visualise shape change in the full landmark set.

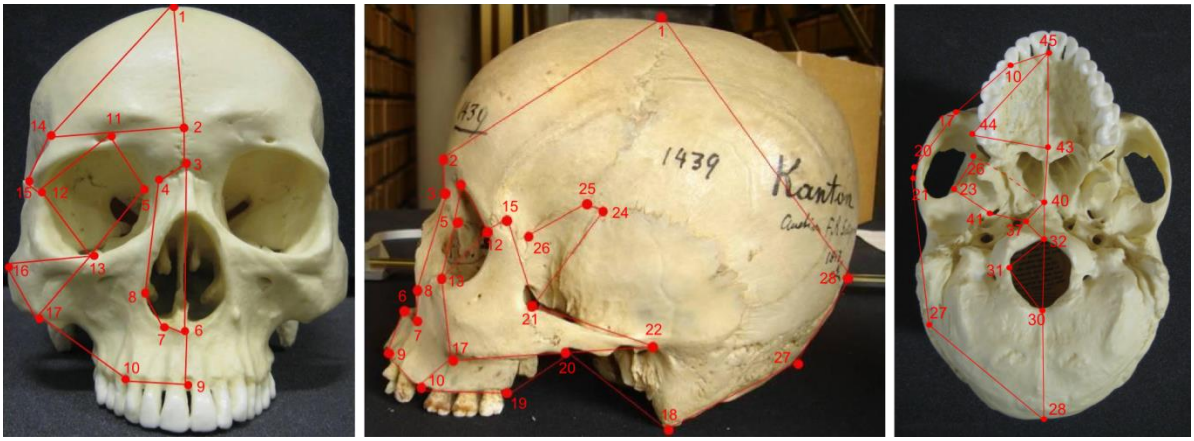

Figure 30: From left to right top: norma frontalis, norma lateralis; bottom: norma basalis wireframes and landmarks for full landmark set. For numbering and landmark definitions see Section 2.III.c.i., Table 9. For clarity, not all landmarks are shown. Photos by the author here and henceforth.

Only one PC showed a moderate, negative, and significant (remaining so if a Bonferroni correction is applied) relationship with relative frontal sinus volume (see Figure 30) and was thus identified as a sinus volume-related shape variable, a frontal SVSP:

- **Full landmark set frontal SVSP PC3**: Full landmark set PC3 x relative frontal sinus volume: r= -0.46, r^2 = -0.21, $p < 0.005$, 2-tailed.

The correlation between full landmark set frontal SVSP PC3 and relative frontal sinus volume is negative, meaning that a lower score on the SVSP is associated with a relatively larger frontal sinus volume.

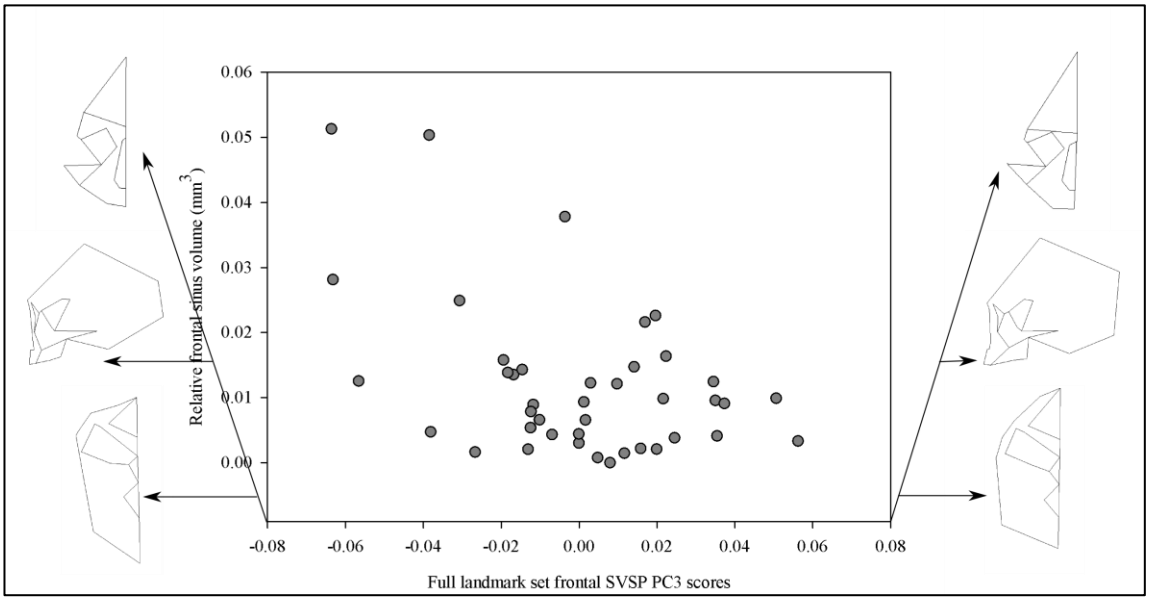

Figure 31**:** The significant, negative relationship between full landmark set PC3 and relative frontal sinus volume. Illustrated wireframes (in norma frontalis, norma lateralis and norma basalis respectively from top to bottom) show the landmark configurations at the extremes of SVSP.

There is no significant correlation between ln centroid size and full landmark set frontal SVSP PC3 scores; this is not an allometric relationship.

3.I.a.i. Shape change along full landmark set frontal SVSP PC3

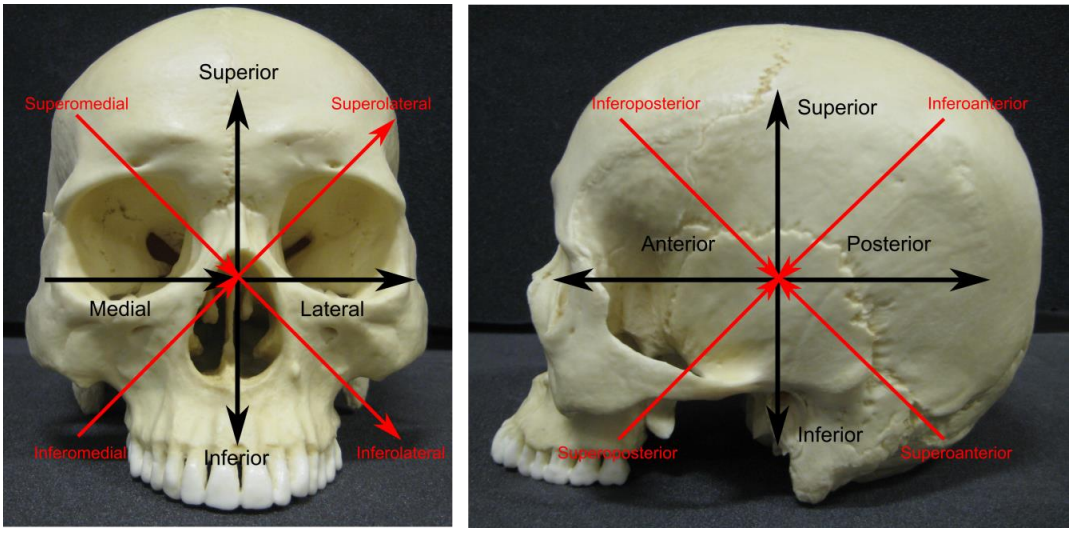

Figure 32: Definition of anatomical directions as they relate to the hominin cranium. These terms are used to describe landmark movement in the text below.

For greater detail of landmark movements for each SVSP, see Appendix 6. There are four main shape changes in the recent *H. sapiens* along full landmark set frontal SVSP PC3. The neurocranium shows a change from more dolichocephalic at the lowest end to more brachiocephalic at the highest end (Figure 33). Configurations at the lower end also have smaller (anterior-posterior), flatter faces, and smaller palates (Figure 34). Interestingly, with reference to frontal sinus size, shapes at the lower end of the PC show a larger supraorbital region (Figure 35).

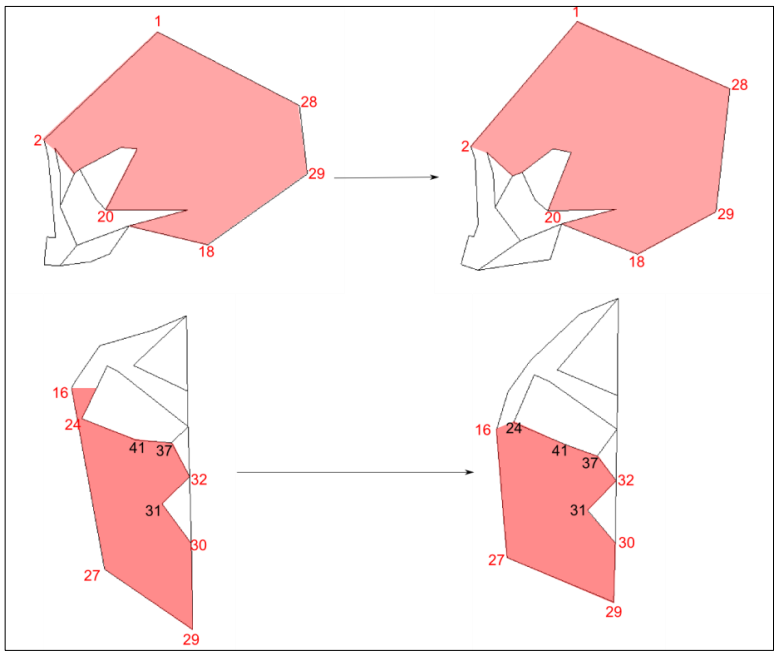

Figure 33**:** Neurocranial shape change along full landmark set frontal SVSP PC3 (significant negative relationship with relative frontal sinus volume). Wireframes in norma lateralis (top) and basalis (bottom) show change from low (left) to high (right) scores. Landmarks are numbered and neurocranium is highlighted in red. Glabella: 2, bregma: 1, lambda: 28, inion: 29, mastoidale: 18, zygotemporale inf.: 20, 16: zygion, 24: krotaphion, 27: asterion, 29: inion, 30: opisthion, 31: foramen magnum lat., 32: basion, 37: sphenobasion lat., 41: foramen ovale lat.

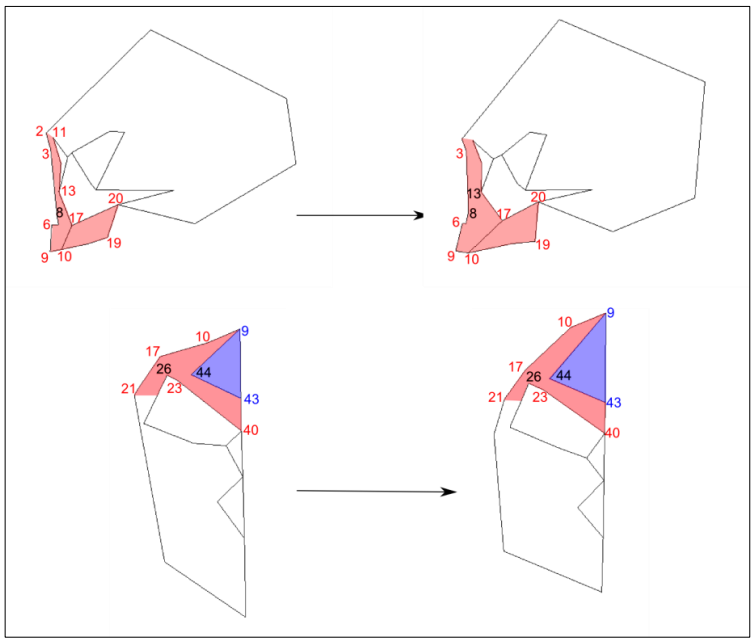

Figure 34**:** Facial and palatal shape change along full landmark set frontal SVSP PC3 (significant negative relationship with relative frontal sinus volume). Wireframes in norma lateralis (top) and basalis (bottom) show change from low (left) to high (right) scores. Face is highlighted in red, palate is highlighted in blue. Glabella (2), nasion (3), nasiospinale (6), prosthion (9), nariale (7), alare (8), supraorbital notch (11), zygoorbitale (13), zygomaxillare (17), C/P3 (10), molars pos. (10), and zygotemporale inf. (20), alveolon (43), ectomolare (44), hormion (40), sphenozygomatic pos. (23), FRED (26), zygotemporale sup. (21).

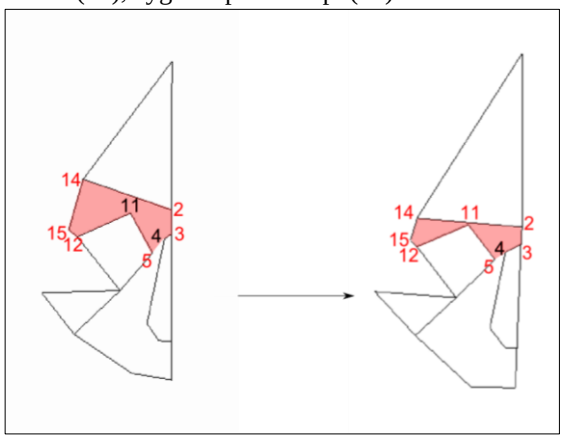

Figure 35**:** Supraorbital shape change along full landmark set frontal SVSP PC3 (significant negative relationship with relative frontal sinus volume). Wireframes in norma frontalis show change from low (left) to high (right) scores. Supraorbital region is highlighted in red, and glabella (2), nasion (3), infranasion (4), supraorbital notch (11), frontomalare orbitale (12), frontomalare temporal (15), and frontotemporale (15) are labelled.

3.I.b. Full landmark set maxillary/sphenoidal sinus volume shape parameters

The first seven PCs of the full landmark set analysis were tested for correlations with relative maxillary sinus volume and relative sphenoidal sinus volume. No significant relationship was found between the volume of either sinus type and any of the PCs.

3.II. Sinus-specific landmark sets

In the second part of this chapter the number of individuals in the sample is prioritised over the number of landmarks preserved. Each sinus is treated individually and landmarks in the region of that sinus are chosen to maximise the number of specimens from each taxonomic group. Fossil specimens are included to elucidate craniofacial shape associated with sinus volumes in Pleistocene hominins in general, not just in recent *H. sapiens*. This necessarily means that the numbers of landmarks used are low, but all sinus-specific landmark sets include fossil taxa. Sinus-by-sinus, the landmark set is explained, SVSPs are identified, and shape changes represented by SVSPs described.

3.II.a. Frontal sinus-specific landmark set

The frontal sinus-specific landmark set consists of ten landmarks (Table 16), mainly in the supraorbital region. In the text that follows below, landmarks will be referred to by their number in the frontal landmark set, rather than the full landmark set; e.g., C/P3 will be referred to as landmark 4, and so on. The frontal landmark set allows the inclusion of 110 specimens (see Table 17 for a breakdown of the sample by

group). This is 81% of the entire sample and includes 26% of the fossil specimens. All taxa are represented except *H. erectus.*

Table 16: Landmarks used in frontal sinus volume vs. frontal sinus-specific landmark set analyses.

Landmark	Number in full landmark set	Number in frontal landmark set
Bregma	1	1
Glabella	2	2
Nasion	3	3
C/P3	10	4
Frontomalare orbitale	12	5
Zygoorbitale	13	6
Frontotemporale	14	7
Frontomalare temporale	15	8
Porion	22	9
Lambda	28	10

Table 17: Table showing number of specimens with the frontal sinus-specific landmark set preserved and their geographic origin/taxonomic group.

Group	Number of specimens in sample	Name/number of specimens in frontal sinus-specific set
China	9	9
Greenland	7	7
Hawaii	10	10
India	10	10
Lithuania	10	10
Mexico	9	8
North Africa	6	3
Peru	10	10
Russia	4	4
Tasmania	7	5
Torres Straits	10	10
Western Africa	10	8
Western Europe	10	10
Fossil *H. sapiens*	6	1 Cro-Magnon 2
H. neanderthalensis	9	2 La Chapelle La Ferassie
H. heidelbergensis	5	3 Kabwe Petralona Steinheim
H. erectus	4	0
Total		**110**

After GPA and PCA analyses of landmark coordinates, the eigenvalues and a scree-plot were scrutinised to determine how many PCs contained valuable information about the variation in shape between crania (see Table 18, Figure 36). It was decided that the first six PCs (accounting for over 70% of variance) should be investigated.

Table 18: Eigenvalues from principal components analysis of shape in crania with frontal sinus-specific landmark set. The first six PCs account for over 70% of the variance in the sample.

Principal component	Eigenvalue	Proportion of variance explained	Cumulative variance explained
1	0.00120	0.23	0.23
2	0.00075	0.14	0.37
3	0.00066	0.12	0.49
4	0.00057	0.11	0.59
5	0.00043	0.08	0.67
6	0.00036	0.07	0.74

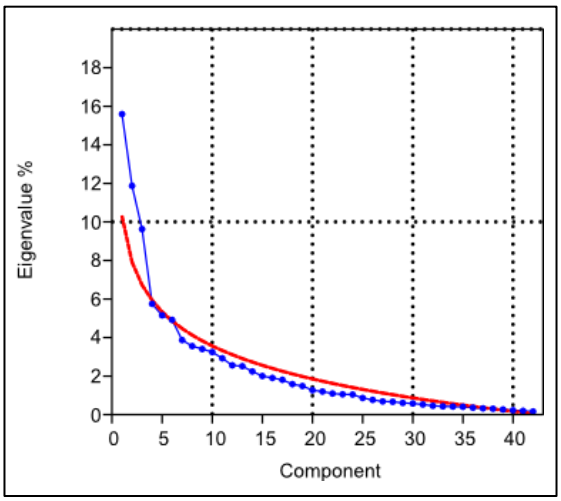

Figure 36**:** Scree plot used to visualise which principal components contain substantial information in frontal sinus-specific landmark analyses. The scree plot suggests that about the first 6 PCs should be investigated.

For each PC1-6, a Pearson's test for correlation was performed between the PC score and the relative frontal sinus volume. One SVSP was identified; PC6 showed a negative, significant correlation (remains so with Bonferroni correction):

- **Frontal SVSP PC6**: Frontal sinus-specific landmark set PC6 x relative frontal sinus volume: r= -0.35, r^2 = -0.12, p= < 0.001, 2-tailed.

The correlation between frontal SVSP PC6 and frontal sinus volume is negative (see Figure 37), meaning that a lower score on PC6 is associated with a larger relative frontal sinus volume.

The relationship is clearly greatly affected by one individual with a very large relative frontal sinus volume (Figure 37). This is Petralona (*H. heidelbergensis*). This is of particular interest because it has been suggested that frontal hyperpneumatisation could explain craniofacial shape in *H. heidelbergensis* (Seidler *et al.*, 1997).

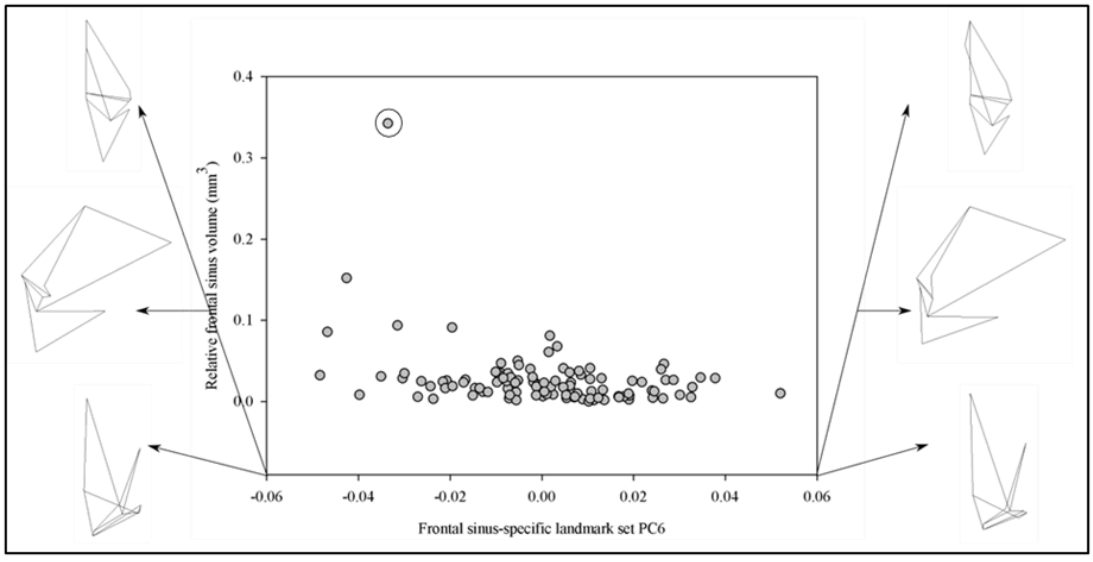

Figure 37**:** The significant, negative relationship between relative frontal sinus volume and frontal sinus-specific landmark set PC6 scores. Illustrated wireframes in norma frontalis (top), norma lateralis (middle), and norma basalis (bottom) show the landmark configurations at the extremes of SVSP. Petralona is circled to show extremely high frontal sinus volume, which renders it an outlier.

Effect of size on frontal SVSP PC6

A regression of ln frontal SVSP PC6 scores (lnPC6s) on ln frontal sinus-specific landmark set centroid size (lnFCS) shows a small, but significant, negative relationship:

- lnPC6s = 1.80 + -0.33 x lnFCS, r = -0.19, r^2 = 0.04, $p < 0.05$.

If the G-FMT measurement is successful in standardising frontal sinus volume for craniofacial size, this result indicates that the relationship between frontal SVSP PC6 and relative frontal sinus volume is one of positive allometry; larger crania are more likely to have lower scores on this PC, and also more likely to have relatively larger frontal sinuses. This may, in part, be due to some of the *H. heidelbergensis* sample; Petralona in particular, and, to a lesser extent Bodo have very large frontal sinuses (see Chapter 4) and also large faces. The residuals of the regression between ln frontal SVSP PC6 and ln frontal sinus-specific landmark set centroid size were correlated against relative frontal sinus volume and there was no longer a significant relationship, showing that a substantive part of the relationship between this craniofacial shape variable and frontal sinus volume is due to their shared relationship with size. It does not account for the entire relationship, however, since the r^2 value of the regression analysis between frontal SVSP PC6 and centroid size is smaller than that between frontal SVSP PC6 and relative frontal sinus volume.

3.II.a.ii. Shape change along frontal SVSP PC6

The wireframes used to visualise shape change on frontal SVSP PC6 are shown in Figure 38.

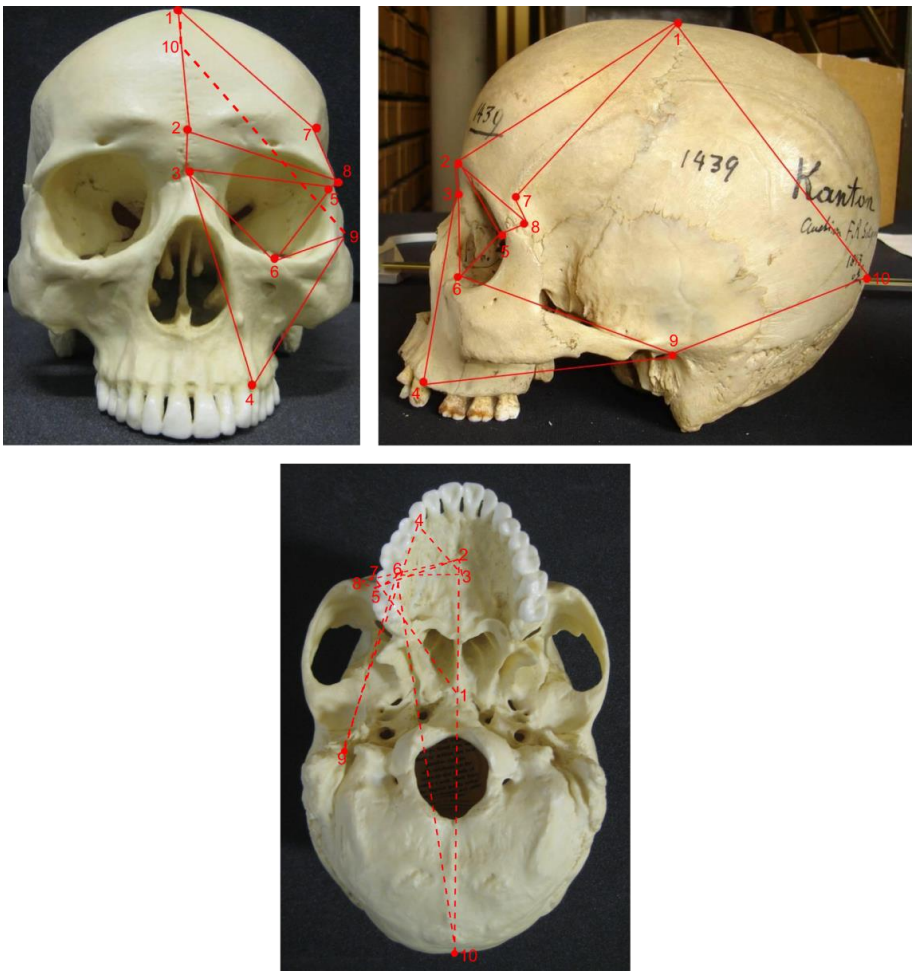

Figure 38: Top, from left to right: norma frontalis and norma lateralis, bottom: norma basalis wireframes of the frontal sinus-specific landmark set with landmarks numbered as in Table 16. Dashed lines connect landmarks not visible when cranium is shown.

The main difference along frontal SVSP PC6 is that shapes at the lower end of the SVSP (larger frontal sinuses) have a relatively larger frontal regions, both mediolaterally and anteroposteriorly, than those at the upper end (Figure 39). There are also differences in the lower face: the maxillary region is taller superoinferiorly in shapes associated with larger frontal sinuses (the low end of frontal SVSP PC6).

The shape of the supraorbital region may be particularly relevant for the frontal sinus; configurations at the lower end of the SVSP also show anteroposteriorly, but not superoinferiorly, deeper supraorbital regions than those at the higher end (Figure 40), but the orbit is shorter superoinferiorly (Figure 40).

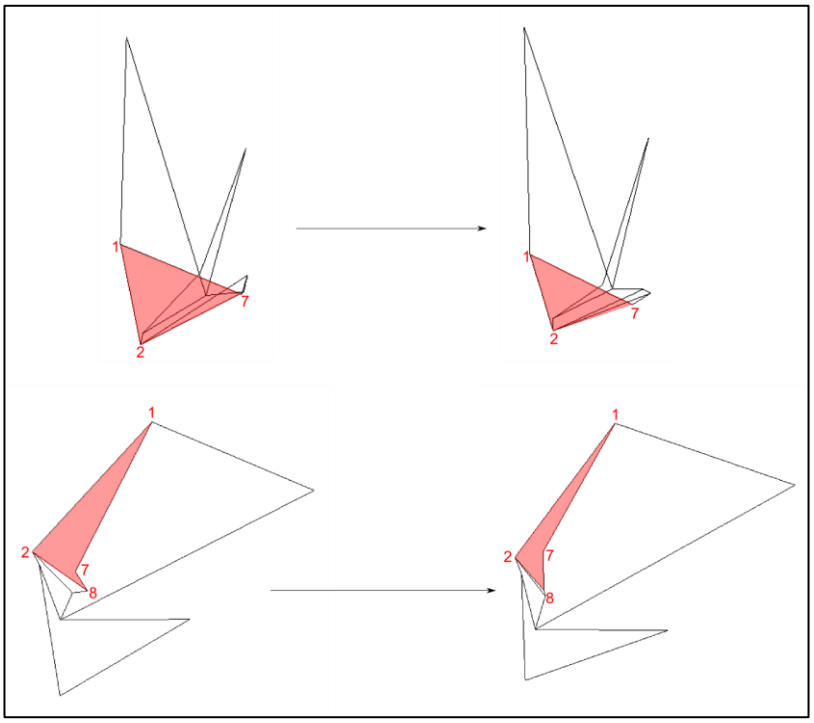

Figure 39: Frontal bone shape change along frontal SVSP PC6 (significant, negative relationship with relative frotnal sinus volume). Wireframes in norma basalis (top) and norma lateralis (bottom) show shape configurations at the lowest (left) and highest (right) extremes of the SVSP. The frontal region is highlighted in red. Bregma (1), glabella (2), frontotemporale (7), frontomalare temporale (8).

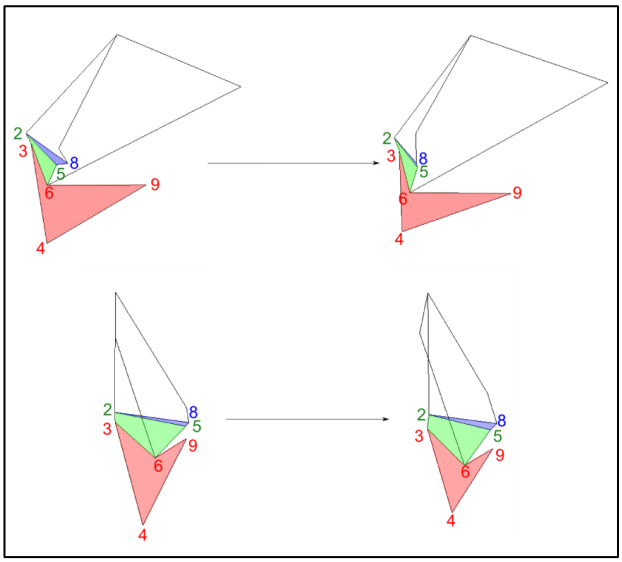

Figure 40: Supraorbital, orbital, and maxillary shape change along frontal SVSP PC6 (significant, negative relationship with relative frontal sinus volume). Wireframes in norma lateralis (top) and frontalis (bottom) show shape configurations at the lowest (left) and highest (right) extremes of frontal SVSP PC6. The maxillary region is highlighted in red, the orbit is highlighted in green, and the supraorbital region is highlighted in blue. Glabella (2), nasion (3), frontomalare temporale (8), frontomalare orbitale (5), zygoorbitale (6), C/P3 (4), and porion (9).

3.II.b. Maxillary sinus-specific landmark set

The maxillary sinus landmark set consists of 13 landmarks (Table 19), concentrating on the maxillary region. The maxillary sinus-specific landmark set allowed the inclusion of 88 specimens (Table 20). This is 65% of the entire sample and includes 21% of the fossil specimens. All taxa are represented except *H. erectus.* In the text that follows below, landmarks will be referred to by their number in the maxillary landmark set, rather than the full landmark set (e.g., C/P3 will be referred to as landmark 5, and so on).

Table 19: Landmarks used in maxillary sinus-specific landmark set.

Landmark	Number in full landmark set	Number in frontal landmark set
Bregma	1	1
Glabella	2	2
Nasion	3	3
Alare	8	4
C/P3	10	5
Zygoorbitale	13	6
Zygion	16	7
Zygomaxillare	17	8
Molars pos	19	9
Porion	22	10
Lambda	28	11
Ectomolare	44	12
Orale	45	13

Table 20: Number of specimens with the maxillary sinus-specific landmark set preserved and their geographic origin/taxonomic group.

Group	Number of specimens in sample	Name/number of specimens with maxillary landmarks preserved
China	9	8
Greenland	7	7
Hawaii	10	8
India	10	5
Lithuania	10	8
Mexico	9	5
North Africa	6	1
Peru	10	10
Russia	4	2
Tasmania	7	3
Torres Straits	10	8
Western Africa	10	8
Western Europe	10	10
Fossil *H. sapiens*	6	1 Mladeč
H. neanderthalensis	9	2 La Chapelle La Ferrassie
H. heidelbergensis	5	2 Kabwe Petralona
H. erectus	4	0
Total	**136**	**88**

The landmark data were processed and analysed using GMM, as above. The cumulative variance explained by successive PCs, as shown by the eigenvalues, was scrutinised (Table 21) and a scree-plot consulted (Figure 41). These suggested only the first 6-8 PCs will be informative, therefore the first 7 PCs (accounting for about 70% of variance) were analysed.

Table 21: Eigenvalues from principal components analysis of shape in crania with maxillary sinus-specific landmark set. The first 7 PCs account for over 70% of the variance in the sample.

Principal Component	Eigenvalue	Proportion of variance explained	Cumulative variance explained
1	0.0012	0.2060	0.2060
2	0.0008	0.1350	0.3410
3	0.0006	0.1060	0.4470
4	0.0005	0.0908	0.5380
5	0.0004	0.0737	0.6120
6	0.0003	0.0616	0.6730
7	0.0003	0.0461	0.7190

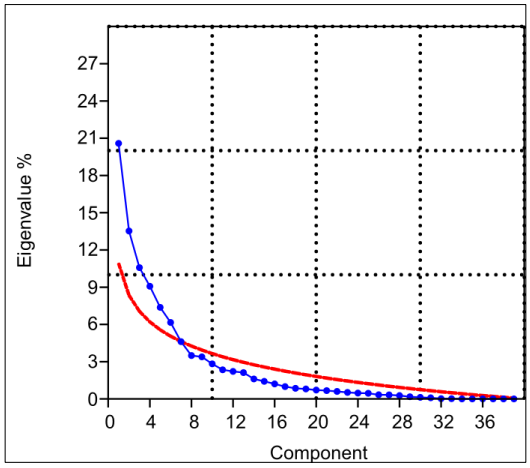

Figure 41**:** Scree plot used to visualise which principal components contain substantial information in the maxillary sinus-specific landmark set. The scree plot suggests that about the 7 PCs should be investigated.

For PC1-7, a Pearson's test for correlation was performed to test for significant relationships between the PC score and the relative maxillary sinus volume. Two significant (with the application of a Bonferroni correction) results were obtained, the first much stronger than the second. These two significant relationships were used to identify two maxillary SVSPs:

- **Maxillary SVSP PC3**: PC3 x relative maxillary sinus volume: $r = 0.64$, $r^2 = 0.41$, $p < 0.001$, 2-tailed.

- **Maxillary SVSP PC7**: PC7 x relative maxillary sinus volume: r = 0.28, r^2 = 0.07, p = < 0.005, 2-tailed.

The correlation between both PCs and relative maxillary sinus volume is positive (see Figure 42 and 43), meaning that a higher score is associated with a larger maxillary sinus volume.

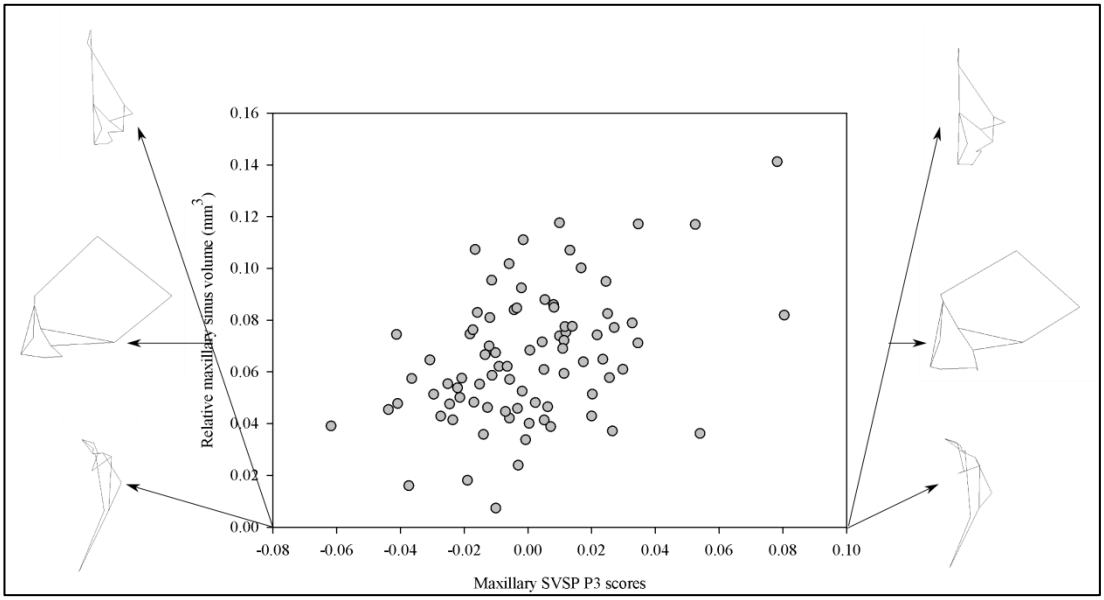

Figure 42: The significant, positive relationship between relative maxillary sinus volume and maxillary sinus-specific landmark set PC3 scores. Wireframes show norma frontalis (top), norma lateralis (middle), and norma basalis (bottom) wireframes of the lowest (left), and highest (right) extremes of maxillary SVSP PC3.

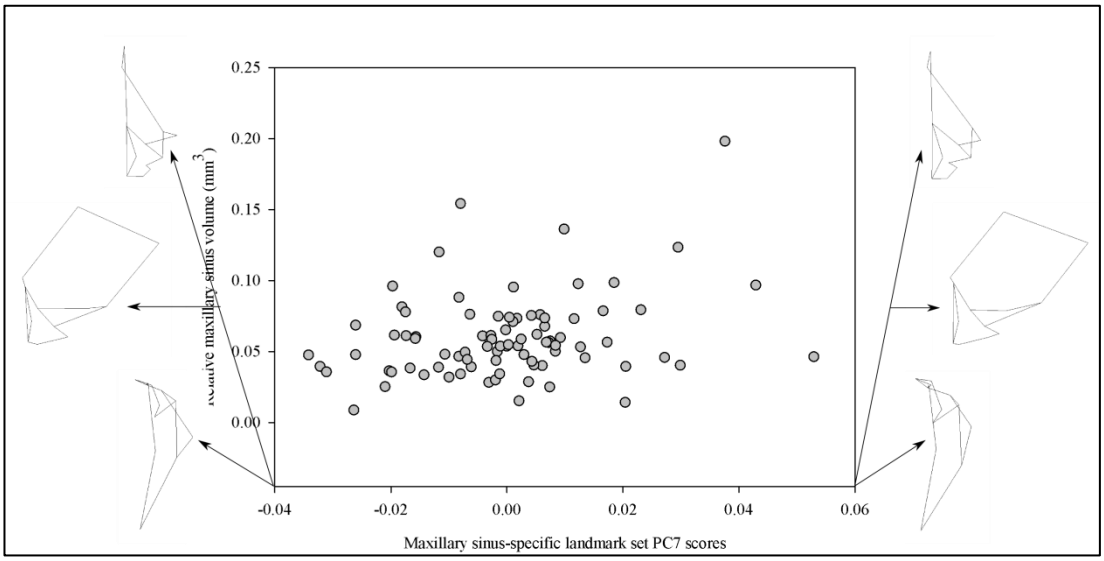

Figure 43**:** The significant, positive relationship between relative maxillary sinus volume and maxillary specific landmark set PC7 scores. Wireframes are norma frontalis (top), lateralis (middle), and basalis (bottom) views of the lowest (left) and highest (right) extremes of maxillary SVSP PC7.

Effect of size on maxillary SVSPs PC3 and PC7

There is no significant correlation between PC scores on maxillary SVSP PC3 or PC7 and ln maxillary sinus-specific landmark set centroid size.

3.II.b.i. Shape changes along maxillary SVSP PC3

The wireframes used to visualise shape change along both maxillary SVSPs are shown below (Figure 44).

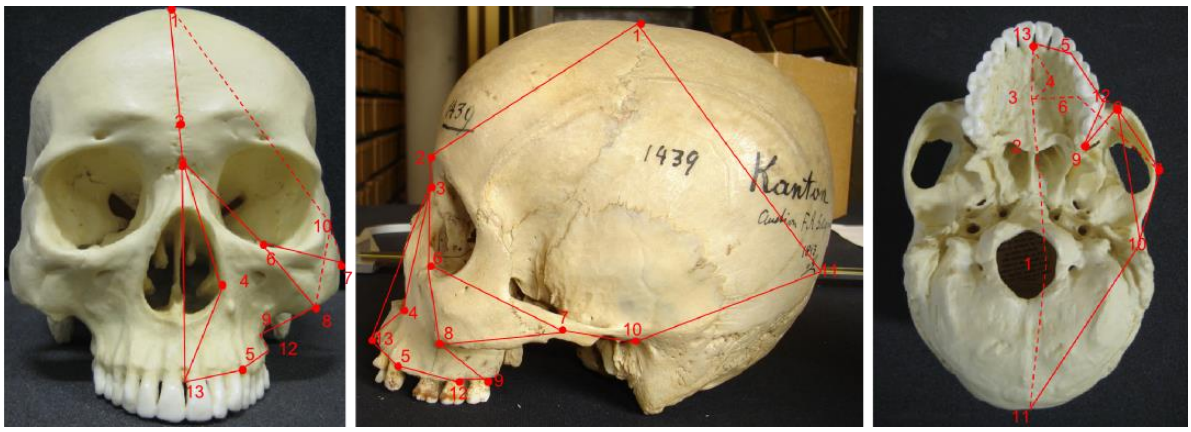

Figure 44: Left to right: norma frontalis, norma lateralis, and norma basalis wireframes of the maxillary sinus-specific landmark set with landmarks numbered as in Table 19. Dashed lines show where wireframes appear when cranium is not shown.

The facial changes along maxillary SVSP PC3, which are associated with a change from small maxillary sinuses at the lower end to large ones at the upper end, are visually striking. Moving from low to high values on maxillary SVPS PC3, there is a shape change towards a configuration with a larger, longer, more anteriorly projecting face relative to the neurocranium (Figure 45).

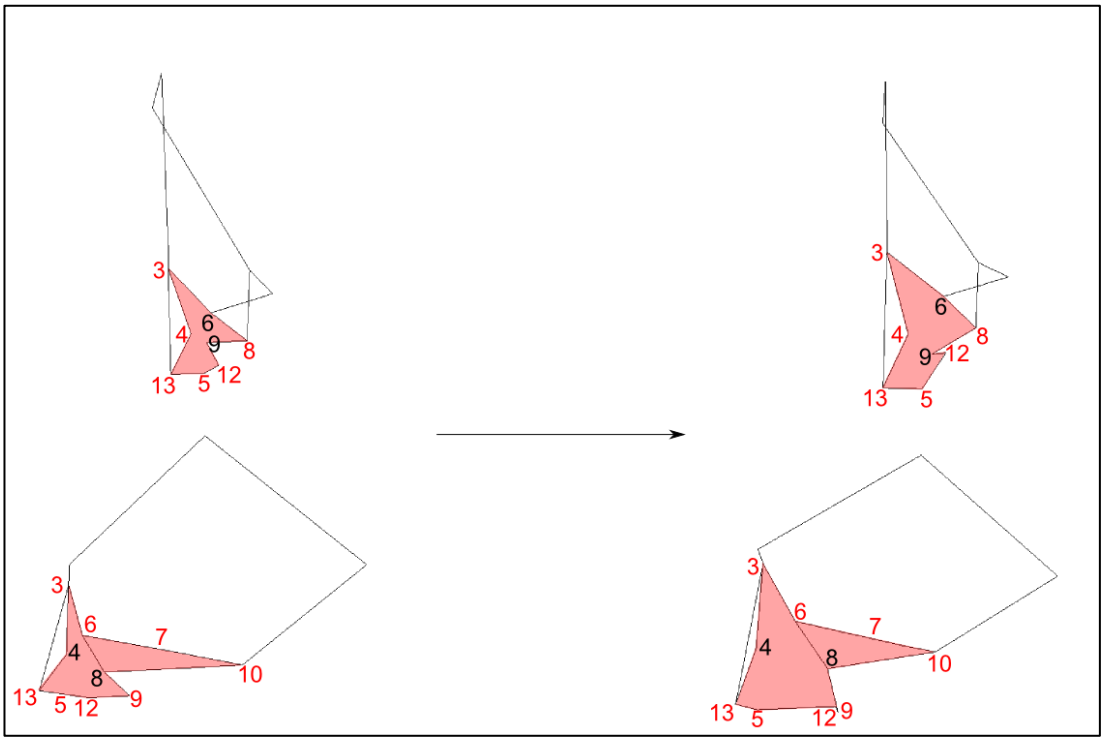

Figure 45**:** Maxillary and malar shape changes on maxillary SVSP PC3 (significant positive relationship with relative maxillary sinus volume). Wireframes in norma frontalis (top) and norma lateralis (bottom) show shape changes in the lower face (highlighted in red) from lowest (left) to highest (right) extremes on PC3. Nasion (3), alare (4), C/P3 (5), zygoorbitale (6), molars pos. (9), ectomolare (12), zygomaxillare (8), zygion (7), and porion (10).

The malar region also appears superoinferiorly taller (see Figure 45) in high scoring configurations and, in norma basalis (Figure 46), the zygomatic arch appears more swept back in configurations at the higher end of maxillary SVSP PC3. The arch is more posteriorly sloping across the front of the face, and the widest point moves posteriorly, giving a longer and less protruding shape.

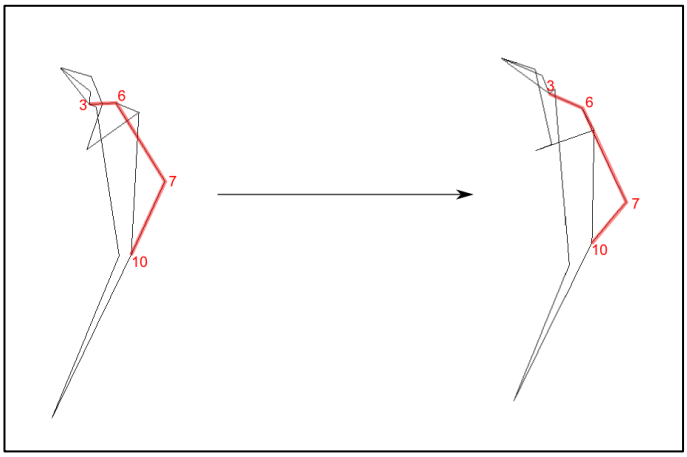

Figure 46: Zygomatic shape change on maxillary SVSP PC3 (significant positive relationship with relative maxillary sinus volume). Wireframes (in norma basalis) show shape changes along the zygomatic arch, which is highlighted in red, from lowest (left) to highest (right) extremes on PC3. Nasion (3), zygoorbitale (6), zygion (7), and porion (10).

As seen in the frontal SVSPs, the neurocranium is more dolichocephalic in configurations associated with larger maxillary sinuses on maxillary SVSP PC3. The neurocrania in configurations towards the upper end of the SVSP are shorter superoinferiorly, with an acute angle at glabella, and a more acutely angled occipital region (Figure 47). There are also differences in the shape of the dental arcade as one moves along maxillary SVSP PC3, with the widest point moving to a more posterior position towards the higher end of the SVSP (Figure 48).

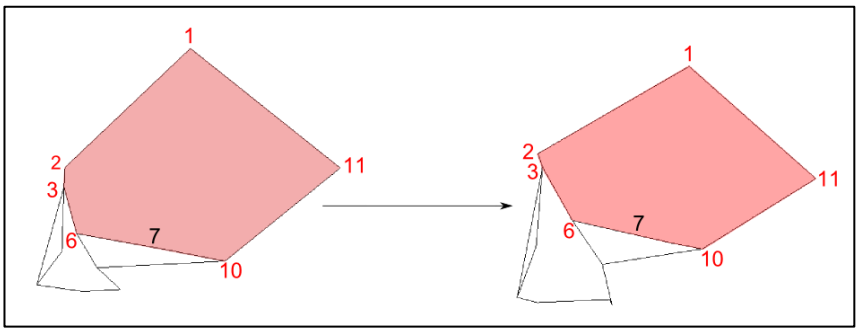

Figure 47**:** Neurocranial shape change on maxillary SVSP PC3 (significant positive relationship with relative maxillary sinus volume). Wireframes (in norma lateralis) show shape changes in the neurocranium, which is highlighted in red, from lowest (left) to highest (right) extremes on PC3. Bregma (1), glabella (2), nasion (3), zygoorbitale (6), zygion (7), porion (10), and lambda (11).

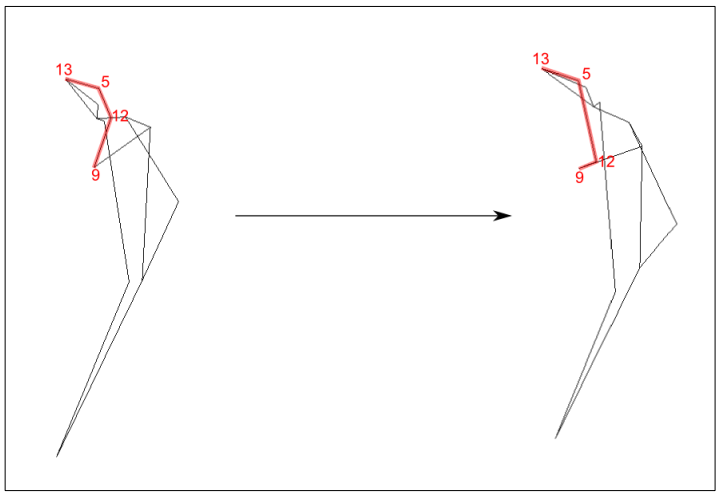

Figure 48**:** Palatal shape change on maxillary SVSP PC3 (significant positive relationship with relative maxillary sinus volume). Wireframes (in norma basalis) show shape changes in the dental arcade, which is highlighted in red, from lowest extreme (left) and highest extreme (right) of PC3. Orale (13), C/P3 (5), ectomolare (12), and molars pos (9).

3.II.b.ii. Shape change along maxillary SVSP PC7

The most obvious shape change between configurations at the low end of maxillary SVSP PC7 (associated with relatively small maxillary sinuses) and the high end (associated with relatively large maxillary sinuses) is that the face is longer anteroposteriorly, with greater lower-face prognathism at the top end of the SVSP. Shapes scoring high on maxillary SVSP PC7 also have a more pronounced glabella region than those at the bottom end of the SVSP (see Figure 49). The shape changes in the zygomatic arch along maxillary SVSP PC7 can be seen best in norma basalis (Figure 50). At the top end of the SVSP, the arch is less projecting; the shape is longer anteroposteriorly, but narrower, and smoother (i.e., the angle at zygion is less acute and zygion, landmark 7, is further anterior). There is also a difference in the dental arcade, which appears flatter across the front, and longer anteroposteriorly in high scoring configurations (Figure 51).

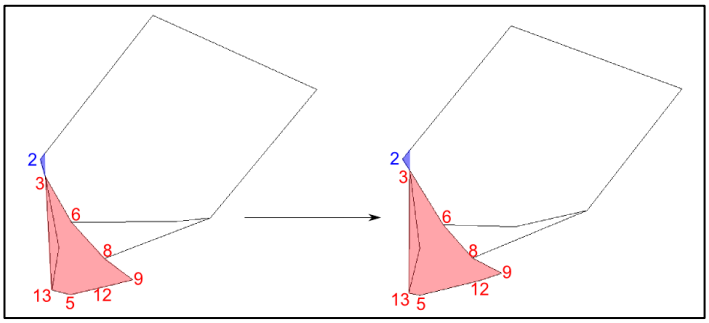

Figure 49**:** Facial and glabella region shape changes along maxillary SVSP PC7 (significant positive relationship with relative maxillary sinus volume). Wireframes (in norma lateralis) show shape change from lowest extreme on maxillary SVSP PC7 (left) to highest extreme (right). Glabella region is highlighted in blue, lower face is highlighted in red. Glabella (2), nasion (3), orale (13), C/P3 (5), ectomolare (12), molars pos. (9), zygomaxillare (8), and zygoorbitale (6) are numbered.

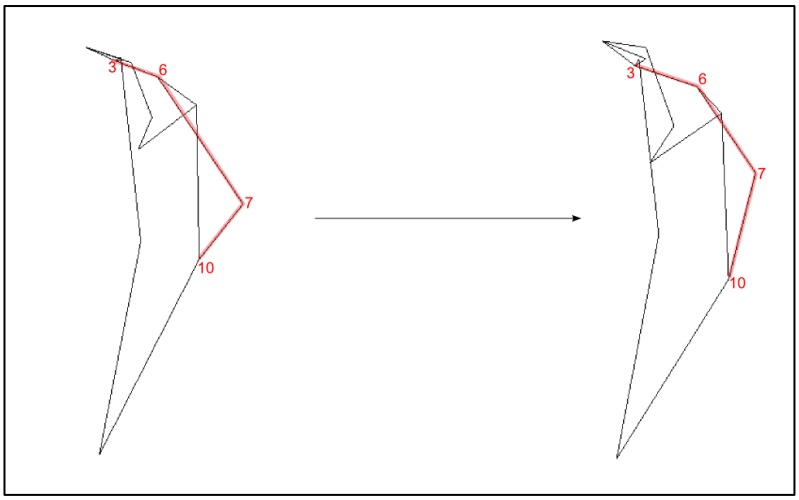

Figure 50**:** Zygomatic shape change along maxillary SVSP PC7 (significant positive relationship with relative maxillary sinus volume). Wireframes (in norma basalis) show shape change from lowest extreme on maxillary PC7 (left) to highest extreme (right). The zygomatic arch is highlighted in red. Nasion (3), zygoorbitale (6), zygion (7), and porion (10).

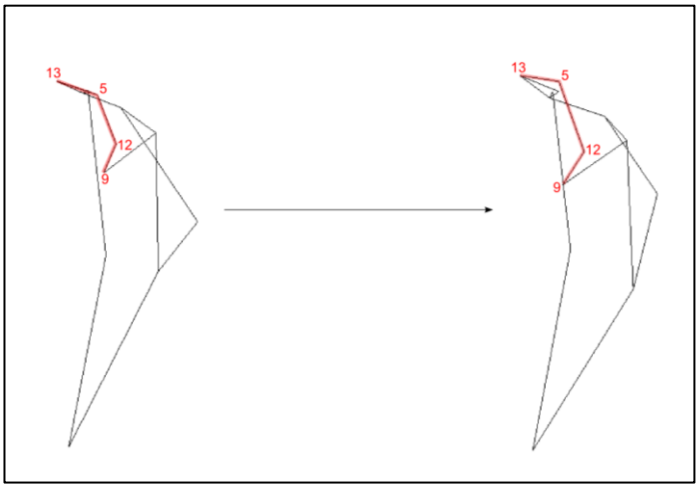

Figure 51**:** Palatal shape change along maxillary SVSP PC7 (significant positive relationship with relative maxillary sinus volume). Wireframes (in norma basalis) show shape change from lowest extreme on maxillary SVSP PC7 (left) to highest extreme (right). The dental arcade is highlighted in red. Orale (13), C/P3 (5), ectomolare (12), and molars pos. (9).

3.II.c. Sphenoidal sinus-specific landmark set

The sphenoidal sinus-specific landmark set consists of eleven landmarks, mainly in the anterior part of the neurocranium (see Table 22). This landmark set allowed the inclusion of 97 specimens (Table 23). This is 71% of the entire sample, but includes just 13% of the fossil specimens due to insufficient preservation; however, all taxa are represented except *H. erectus.* In the text that follows below, to avoid confusion, landmarks will be referred to by their number in the sphenoidal landmark set, rather than the full landmark set (e.g., porion will be referred to as landmark 3, and so on).

Table 22: Landmarks used in sphenoidal sinus-specific landmark set.

Landmark	Number in full landmark set	Number in sphenoidal sinus-specific landmark set
Bregma	1	1
Glabella	2	2
Porion	22	3
Sphenozygomatic pos.	23	4
Krotaphion	24	5
Coronosphenoidale	25	6
FRED	26	7
Lambda	28	8
Sphenobasion lat.	37	9
Foramen ovale pos.	41	10
Foramen ovale ant.	42	11

Table 23: Number of specimens with the sphenoidal sinus-specific landmark set preserved and their geographic origin/taxonomic group.

Group	Number of specimens in sample	Name/number of specimens with sphenoidal sinus-specific preserved
China	9	9
Greenland	7	7
Hawaii	10	9
India	10	10
Lithuania	10	7
Mexico	9	8
North Africa	6	3
Peru	10	10
Russia	4	3
Tasmania	7	1
Torres Straits	10	9
Western Africa	10	8
Western Europe	10	10
Early *H. sapiens*	6	1 Cro-Magnon 1
H. neanderthalensis	9	1 Guattari
H. heidelbergensis	5	1 Kabwe
H. erectus	4	0
Total	**136**	**97**

The landmark data were processed and analysed using GMM as above. The cumulative variance explained by successive PCs, as showed by the eigenvalues, was scrutinised (Table 24) and a scree-plot was consulted (Figure 52), based on this information, the first seven PCs were analysed, accounting for over 70% of the variance in shape in the sample.

Table 24: Eigenvalues from principal components analysis of shape in crania with sphenoidal sinus-specific landmark set. The first seven PCs account for over 70% of the variance in the sample.

Principal Component	Eigenvalue	Proportion of variance explained	Cumulative variance explained
1	0.0018	0.23	0.23
2	0.0010	0.14	0.36
3	0.0008	0.11	0.47
4	0.0007	0.09	0.57
5	0.0005	0.06	0.63
6	0.0004	0.06	0.69
7	0.0004	0.05	0.74

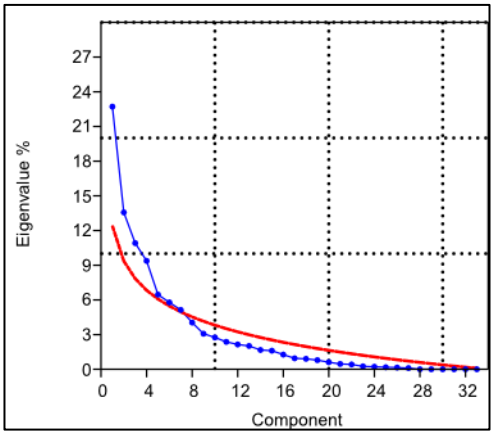

Figure 51**:** Scree plot used to visualise which principal components contain substantial information in the sphenoidal sinus-specific landmark set analyses. The scree plot suggests that about the first 7 PCs should be investigated.

For PC1-7, a Pearson's test for correlation was performed between the PC score and relative sphenoidal sinus volume. Two PCs showed (very small) significant, correlations and so were identified as sphenoidal SVSPs:

- **Sphenoidal SVSP PC3**: PC3 x relative sphenoidal sinus volume: r= 0.25, r^2 = 0.06, p < 0.05, 2-tailed. Not significant (NS) with a Bonferroni correction.
- **Sphenoidal SVSP PC6**: PC6 x relative sphenoidal sinus volume: r = 0.21, r^2 = 0.04 p = < 0.05, 2-tailed. NS with Bonferroni correction.

The correlation between both SVSPs and relative sphenoidal sinus volume is positive, meaning that a higher score is associated with a larger sphenoidal sinus (see Figures 53 and 54).

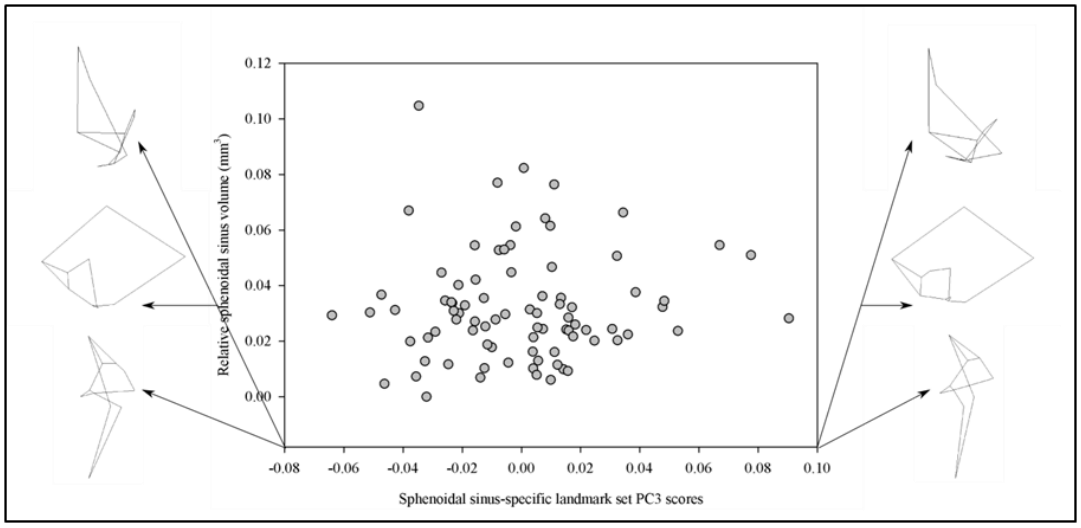

Figure 53**:** The significant, positive relationship (with small effect size) between relative sphenoidal sinus volume and sphenoidal sinus-specific landmark set PC3 scores. Wireframes model the extreme points of sphenoidal SVSP PC3 in norma frontalis (top), lateralis (middle), and basalis (bottom).

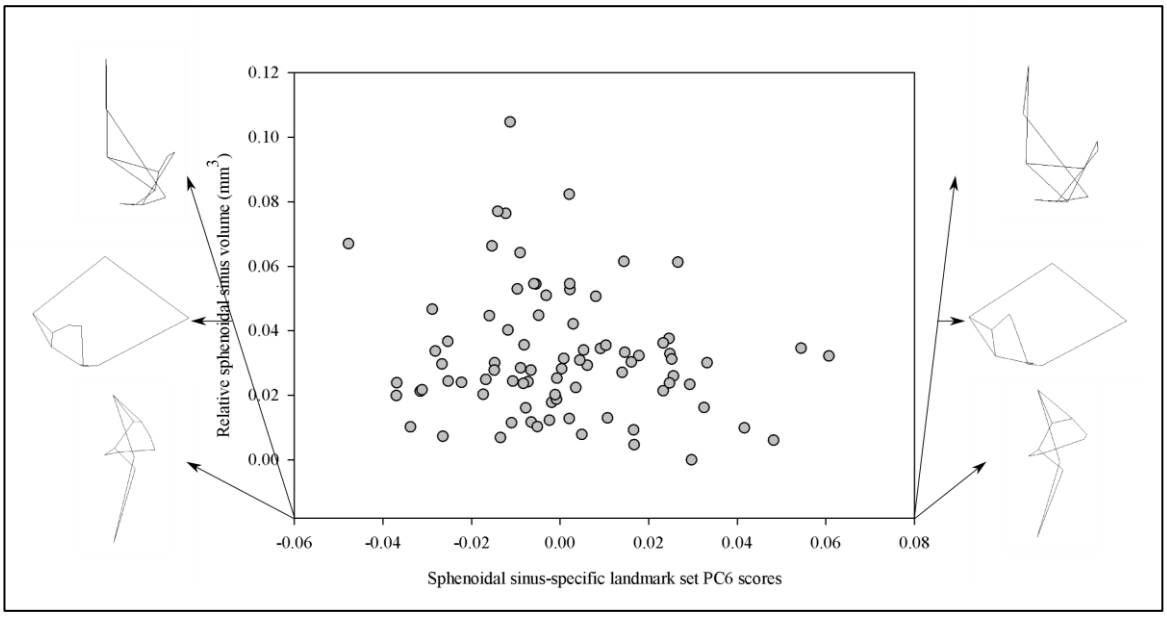

Figure 54: The significant, positive relationship (with very small effect size) between relative sphenoidal sinus volume and sphenoidal-sinus specific landmark set PC6. Wireframes models the extreme points of sphenoidal SVSP PC6 in norma frontalis (top), lateralis (middle), and basalis (bottom).

Effect of size on sphenoidal SVSP PC3 and PC6

There is no significant relationship between ln sphenoidal sinus-specific landmark set centroid size and PC scores on either sphenoidal SVSP PC3 or PC6.

3.II.c.i. Shape change along sphenoidal SVSP PC3

The wireframes used to visualise shape change along both sphenoidal SVSPs are illustrated in Figure 55.

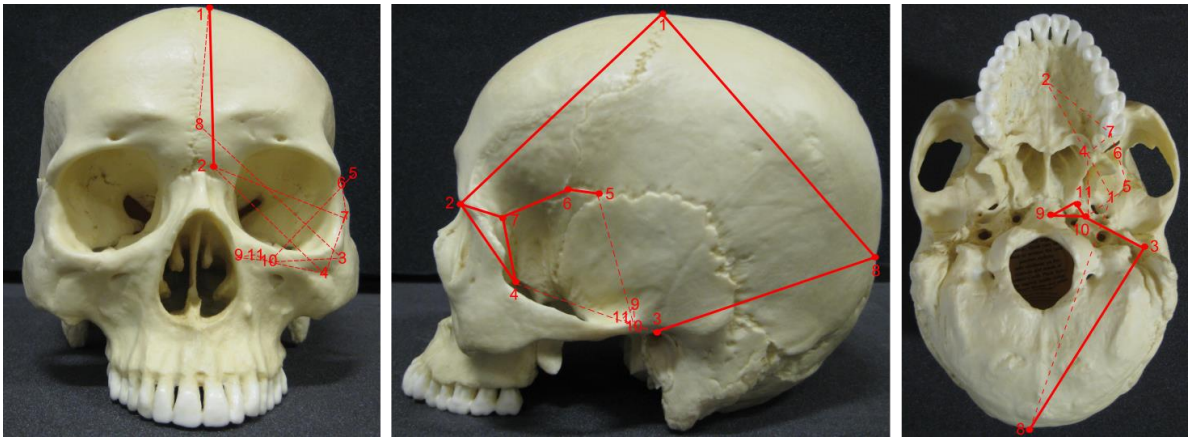

Figure 55: Top from left to right: wireframes in norma frontalis , norma lateralis, and norma basalis of the sphenoidal sinus-specific landmark set with landmarks numbered as in Table 22. Dashed lines show where wireframes appear when cranium is not shown.

To include the landmarks that would be most informative about shape changes in the sphenoidal region (and thus most likely to relate to sphenoidal sinus volume), this landmark set includes less information than the preceding ones regarding the overall shape of the cranium; there is little information about the middle and lower face. Therefore, most of the shape changes seen are in the mid-cranial region, not necessarily because there are no changes in the rest of the cranium, but because there are fewer landmarks there.

The major shape changes on sphenoidal SVSP PC3 is a broadening of the neurocranium, both in the region of the greater wing of the sphenoid and more posteriorly at the level of the external auditory meatus, at the high end of the SVSP (Figure 56). There is also a superoinferior shortening of the cranium, with the basicranium moving superiorly (Figure 57). Thus, crania at the lower end of sphenoidal SVSP PC3 are taller and narrower than crania at the top of the SVSP (which have relatively larger sphenoidal sinuses).

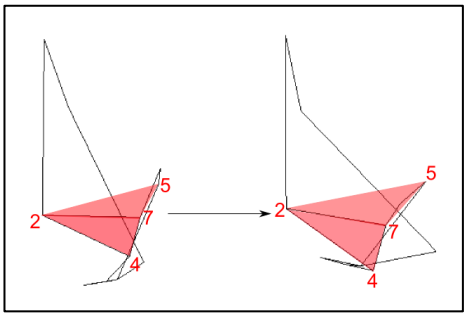

Figure 56**:** Sphenoidal region shape change on sphenoidal SVSP PC3 (significant positive relationship with relative sphenoidal sinus volume). Wireframes (norma frontalis) model the lowest (left), and the highest (right) ends of PC3. Landmarks are indicated by number and changes in the breadth of the sphenoid are highlighted in red. Glabella (2), sphenozygomatic (4), and FRED (7). The filled red area highlights the changing relationship between glabella and krotaphion (5).

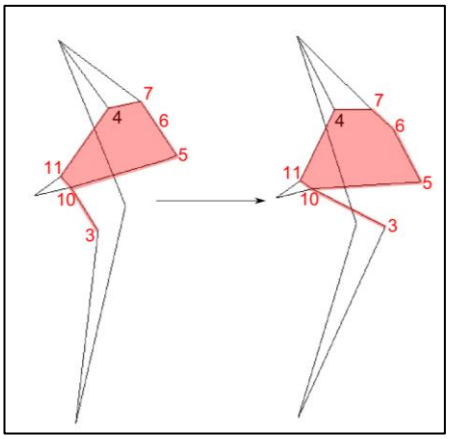

Figure 57**:** Sphenoidal region shape change on sphenoidal SVSP PC3 (significant positive relationship with relative sphenoidal sinus volume). Wireframes (norma basalis) model the lowest (left), and the highest (right) ends of sphenoidal SVSP PC3. Landmarks are indicated by number and changes in the greater sphenoidal wing region shape are highlighted in red. FRED (7), coronosphenoidale (6), krotaphion (5), foramen ovale pos. (10), foramen ovale ant. (11), and sphenozygomatic pos. (4), porion (3).

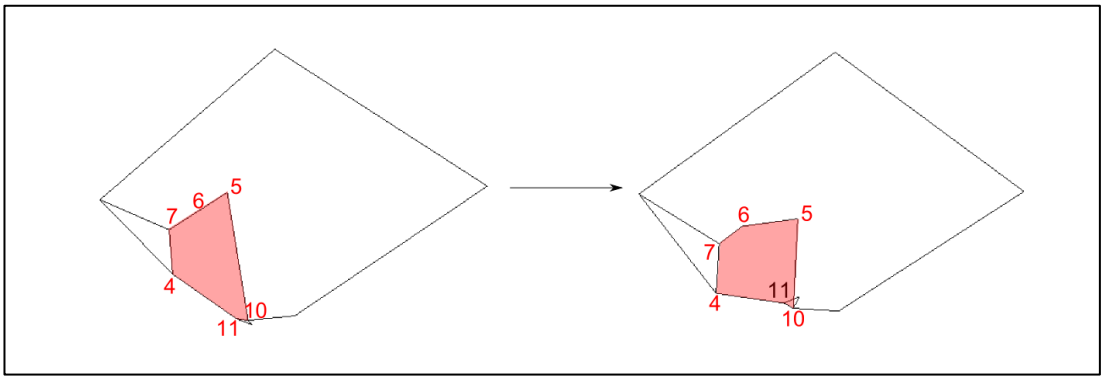

Figure 58**:** Sphenoidal regions shape change on sphenoidal SVSP PC3 (significant positive relationship with relative sphenoidal sinus volume). Wireframes (norma lateralis) model the lowest (left), and the highest (right) ends of sphenoidal SVSP PC3. Landmarks are indicated by number and changes in the greater sphenoidal wing region shape are highlighted in red. FRED (7), coronosphenoidale (6), krotaphion (5), foramen ovale pos. (10), and sphenozygomatic pos. (4).

3.II.c.ii. Shape change along sphenoidal SVSP PC6

There are several neurocranial shape changes shown by sphenoidal SVSP PC6. At the higher end of sphenoidal SVSP PC6 (relatively large sphenoidal sinuses), shape configurations show a lower neurocranial vault, due to the relative superior movement of the cranial base, compared to configurations at the lower end of the SVSP (see Figure 59).

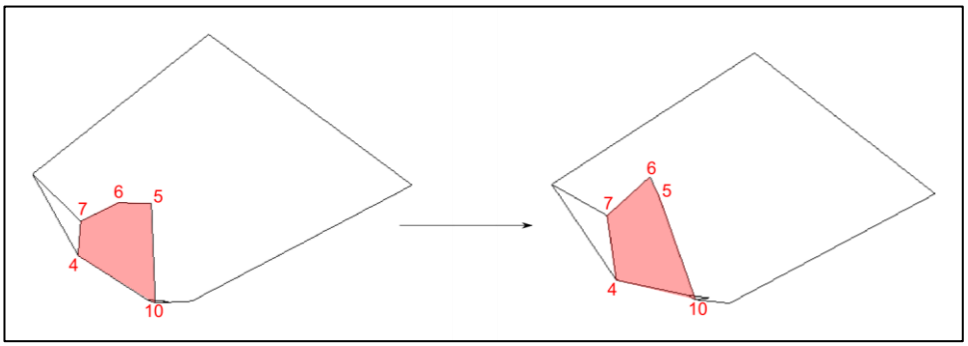

Figure 59**:** Sphenoidal region shape change on sphenoidal SVSP PC6 (significant relationship with relative sphenoidal volume). Wireframes modelled from the lowest (left), and the highest (right) ends of sphenoidal SVSP PC6 (norma lateralis). Landmarks are indicated by number and changes in the breadth of the sphenoidal region are highlighted in red. Sphenozygomatic pos. (4), foramen ovale pos. (10), krotaphion (5), coronosphenoidale (6), and FRED (7) are numbered.

There is also a change in the proportions of the anterior and posterior portions of the neurocranium, such that there is a relative increase (anteroposteriorly and mediolaterally) in the anterior portion of the vault (compared to the posterior portion) in configurations scoring highly on sphenoidal SVSP PC6 (see Figure 59). This is due to a relative increase in the distance between the sphenoidal wing region and the external auditory meatus, which increases the length of the midcranium anteroposteriorly (Figure 60).

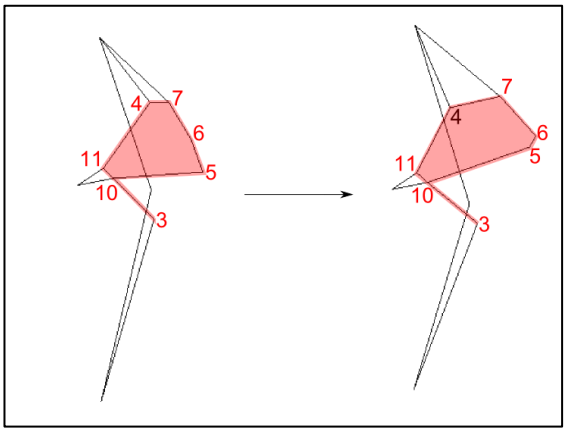

Figure 60**:** Sphenoidal region shape change on sphenoidal SVSP PC6 (significant relationship with relative sphenoidal volume). Wireframes modelled from the lowest (left), and the highest (right) ends of sphenoidal SVSP PC6 (norma basalis). Landmarks are indicated by number and changes in the breadth of the sphenoidal region are highlighted in red. FRED (7), coronosphenoidale (6), krotaphion (5), foramen ovale pos (10), foramen ovale ant. (11), and sphenozygomatic pos. (4), porion (3).

As with sphenoidal SVSP PC3, higher scoring configurations on sphenoidal SVSP PC6 have mediolaterally broader, superoinferiorly taller crania in the region of the greater sphenoidal wing (see Figure 61).

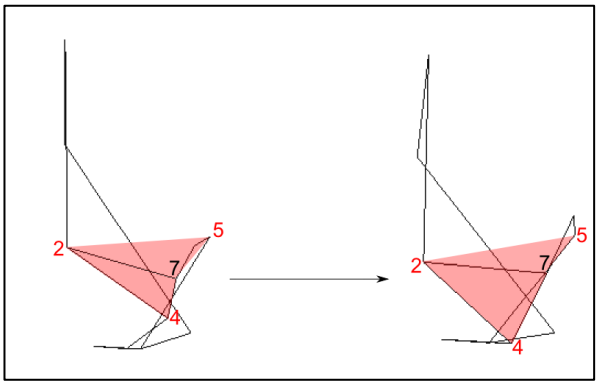

Figure 61**:** Sphenoidal region shape change on sphenoidal SVSP PC6 (significant relationship with relative sphenoidal volume). Wireframes modelled from the lowest (left), and the highest (right) ends of sphenoidal SVSP PC6 (norma frontalis). Landmarks are indicated by number and changes in the breadth of the sphenoidal region are highlighted in red. Glabella (2), sphenozygomatic (4), and FRED (7), krotaphion (5).

3.III. Summary

Shape variables representing significant relationships with sinus volumes have been identified and modelled in this chapter. Of the SVSPs identified, some are less robust and not all are of equal strength (see Table 25). The two maxillary SVSPs together describe ~50% of the variation in maxillary sinus volume in the sample, whereas the two sphenoidal SVSPs together only describe ~10% of variation in sphenoidal sinus volume and are not significantly correlated with relative sphenoidal sinus volume when a Bonferroni correction is applied.. The differences in relationship strength may, in part, be connected to the number and distribution of landmarks in each set. However, the full landmark set is not successful in capturing shape related to the maxillary and sphenoidal sinuses, suggesting that fewer landmarks are not necessarily less informative, and that sample number and breadth contribute substantively. Each sinus type and each taxon is represented by more than one variable, so, in combination, they should provide a useful picture of the interactions between this one particular facet of craniofacial shape (shape associated with paranasal pneumatisation) and outside factors that influence it. They will be used in

subsequent analyses in conjunction with taxonomic/population, dietary, and climatic variables to ascertain the relationship, if any, these factors have on the craniofacial form associated with sinus volume.

3.III.a. Frontal sinus volume shape parameters

Full landmark set frontal SVSP PC3 and frontal SVSP PC6 show that crania with relatively larger frontal sinus volumes are more likely to have dolichocephalic neurocrania, large frontal regions, and large supraorbital regions when compared to crania with relatively small frontal sinus volumes. Facial shape seems to tell a slightly different story, depending on whether fossil taxa are included in the sample (frontal SVSP PC6) or not (full landmark set frontal SVSP PC3). The former analysis links larger faces with larger sinuses, whilst the latter links smaller, flatter faces with larger sinuses. However, not only are these different sample and landmark sets, but the full landmark set frontal SVSP PC3 shows a far stronger relationship with frontal sinus volume than frontal SVSP PC6.

3.III.b. Maxillary sinus volume shape parameters

Maxillary SVSP PC3 and PC7 show that crania with relatively larger maxillary sinuses tend to have more dolichocephalic neurocrania, larger, more prognathic faces, more pronounced glabella regions, flatter, more swept-back zygomatic arches, and dental arcades that are flatter along the front, compared to crania with relatively small maxillary sinuses.

3.III.c. Sphenoidal sinus volume shape parameters

The relationships between sphenoidal sinus-specific PC3 and PC6 (sphenoidal SVSP PC3 and 6) and relative sphenoidal sinus volumes have very small effect sizes, but they are significant. They show that crania with relatively large sphenoidal sinus volumes are likely to have broader, shorter neurocrania with a relative expansion of the anterior portion of the vault, when compared to specimens with relatively small sphenoidal sinus volumes.

Table 25: Summary of SVSPs.

Sinus	SVSP	Variance explained	r^2 value	Robust to a Bonferroni correction?	Direction of relationship	Allometry?
Frontal	Full landmark set frontal SVSP PC3	10%	-0.21	Yes	Negative	No
	Frontal SVSP PC6	7%	-0.07	No	Negative	Yes
Maxillary	Maxillary SVSP PC3	11%	0.41	Yes	Positive	No
	Maxillary SVSP PC7	5%	0.08	Yes	Positive	No
Sphenoidal	Sphenoidal SVSP PC3	11%	0.06	No	Positive	No
	Sphenoidal SVSP PC6	6%	0.04	No	Positive	No

Chapter 4: Results – Population/taxonomic differences in sinus variables

---

In this chapter, research question 1 is addressed. Differences in sinus variables (sinus volumes and sinus volume shape parameters – SVSPs – see Chapter 3) between populations of recent *H. sapiens*, and between Pleistocene hominin taxa, are investigated. Paranasal sinuses are said to be variable between populations of recent *H. sapiens* (Brothwell *et al.*, 1968; Buckland-Wright, 1970; Fernandez, 2004a, b; Holton *et al.* 2013), yet this assertion has not, until now, been tested on a large, world-wide sample of recent *H. sapiens*. It has also been argued that both Neanderthals and *H. heidelbergensis* are hyperpneumatised (Coon, 1962; Seidler *et al.*, 1997; Wolpoff, 1999; Zollikofer *et al.*; 2008, Stringer, 2012c) and that *H. neanderthalensis* facial morphology is shaped by this characteristic (Blake, 1864; Coon, 1962). These long-standing ideas are tested by measuring relative sinus volumes, and the relationships between sinus volumes and craniofacial morphology, between taxa. One hypothesis for the success of *H. sapiens* in dispersing from Africa to populate the entire earth is that, despite our relative genetic homogeneity, we are peculiarly able to adapt plastically to changing environments, using morphological, physiological, life history and cultural mechanisms (Wells & Stock, 2007; Stock,

2008). One outcome of this is hypothesised to be the high level of intraspecific variation in skeletal morphology between *H. sapiens* individuals when compared to other catarrhine taxa (Stock & Buck, 2010). This assertion is tested by quantifying intraspecific levels of sinus volume variation in recent *H. sapiens* and closely related hominins. Finally, many studies of sinus function fail to address the question of whether the sinus types are homologous, or are subject to local pressures in their respective craniofacial modules. This question is addressed here by comparing levels of intra-group variation in each sinus type and determining whether volumes within each sinus type covary within individuals. If the sinuses are homologous, they would be expected to have similar levels of variation and they should covary. Descriptive statistics of sinus volumes are presented in Appendix 7, details of coefficients of variation for individual groups are presented in Appendix 8.

4.I. RQ1.a: Are there population differences in sinus variables in recent *H. sapiens*

In this section the results of investigations into the differences in sinus variables between populations of recent *H. sapiens* are presented by sinus type (frontal, then maxillary, and sphenoidal sinus). It was ascertained whether there are significant differences between populations first in sinus volume, and then SVSPs, then the possibility that these differences are due to population history was considered. For each sinus, volume intra-population variation was also investigated.

4.I.a. Population differences in frontal sinus variables

For descriptive statistics from sinus volume analyses, see Appendix 7.

Table 26: Relative frontal sinus volume sample for populations of recent *H. sapiens.*

Population	n
China	9
Greenland	7
Hawaii	11
India	11
Lithuania	11
Mexico	10
North Africa	7
Peru	10
Russia	4
Tasmania	8
Torres Straits	12
Western Africa	13
Western European	11
Total:	**124**

4.I.a.i. Differences in frontal sinus volume between populations of recent H. sapiens

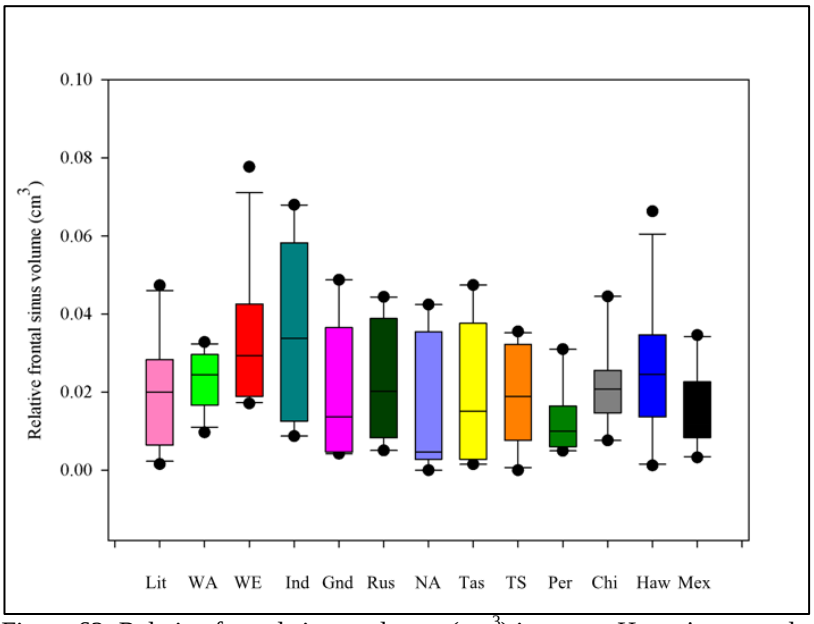

Figure 62: Relative frontal sinus volumes (cm^3) in recent *H. sapiens* populations. Lit: Lithuania; WA: Western Africa; WE: Western Europe; Ind: India; Gnd: Greenland; Rus: Russia; NA: North Africa; Tas: Tasmania; TS: Torres Straits; Per: Peru; Chi: China; Haw: Hawaii; Mex: Mexico. There are significant differences between some of the populations – see Table 27.

Despite a fairly wide spread of measurements for most populations (see Figure 62), and a great degree of overlap, there are extremely small, significant differences in relative frontal sinus volume between populations of recent *H. sapiens*:

- **Relative frontal sinus volume by population:** ANOSIM: R = 0.06, r^2 = 0.004, $p < 0.05$. Non significant (NS) with a Bonferroni correction.

The sizes of individual differences between populations are shown in Table 27. The populations showing the highest number of differences to others are Western Europe and Western Africa. The greatest difference is between Western Africa and North

Africa. The similarities and differences between groups are summarised by a cluster diagram (Figure 63).

Allometry in relative frontal sinus volume differences among populations of recent *H. sapiens*

There is no significant relationship between ln relative frontal sinus volume in recent *H. sapiens* and ln frontal sinus-specific centroid size.

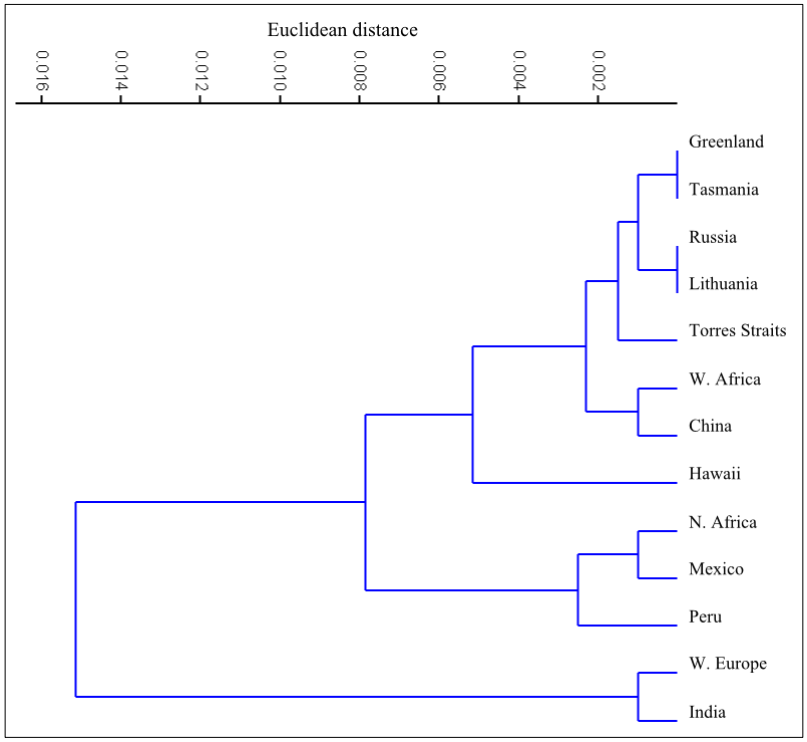

Figure 63: Cluster diagram showing differences in population means of relative frontal sinus volumes between populations of recent *H. sapiens*.

Table 27: Results from an ANOSIM comparing relative frontal sinus volumes between recent *H. sapiens* populations. The matrix is symmetrical, numbers below the trace are p values. Significant values are highlighted red. Above the trace are R values highlighted from red (lowest/least different) to green (highest/most different). No differences remain significant if a Bonferroni correction is applied. Lit: Lithuania; WA: Western Africa; WE: Western Europe; Ind: India; Gre: Greenland; Rus: Russia; NA: North Africa; Tas: Tasmania; TS: Torres Straits; Per: Peru; Chi: China; Haw: Hawaii; Mex: Mexico.

	Lit	**WA**	**WE**	**Ind**	**Gre**	**Rus**	**NA**	**Tas**	**TS**	**Per**	**Chi**	**Haw**	**Mex**
Lit		0.034	0.011	0.040	-0.018	-0.093	0.060	-0.029	-0.061	0.069	-0.080	-0.059	0.002
WA	0.218		0.030	0.167	0.339	0.230	0.493	0.275	0.028	0.338	0.008	0.013	0.185
WE	0.321	0.211		0.002	0.186	-0.001	0.279	0.104	0.057	0.371	0.003	-0.033	0.222
Ind	0.215	0.016	0.366		0.028	-0.087	0.104	-0.007	0.079	0.213	0.058	-0.011	0.114
Gre	0.452	0.006	0.047	0.275		-0.109	-0.090	-0.108	0.004	0.045	0.132	0.009	0.001
Rus	0.719	0.088	0.425	0.742	0.768		0.032	-0.134	-0.024	0.243	-0.002	-0.096	0.124
NA	0.202	0.001	0.014	0.121	0.954	0.290		-0.063	0.061	0.098	0.282	0.060	0.092
Tas	0.537	0.010	0.104	0.390	0.964	0.889	0.746		-0.002	0.092	0.090	-0.027	0.029
TS	0.900	0.242	0.139	0.103	0.390	0.489	0.181	0.397		0.044	-0.044	-0.044	-0.043
Per	0.133	0.004	0.001	0.011	0.215	0.091	0.119	0.104	0.201		0.207	0.166	-0.037
Chi	0.960	0.360	0.382	0.179	0.091	0.398	0.019	0.137	0.679	0.026		-0.052	0.076
Haw	0.916	0.299	0.730	0.453	0.365	0.626	0.208	0.545	0.760	0.031	0.796		0.050
Mex	0.374	0.029	0.014	0.058	0.378	0.194	0.134	0.243	0.672	0.623	0.132	0.170	

Effect of population history on differences in relative frontal sinus volume between populations of recent *H. sapiens*

A Mantel test comparing differences in relative frontal sinus volumes between populations with geographic distance between populations was not significant, showing that the differences in frontal sinus volume are not compatible with an explanation of population history.

Intra-population variation in relative frontal sinus volume between populations of recent *H. sapiens*

For tables of coefficients of variation in each population, see Appendix 8.

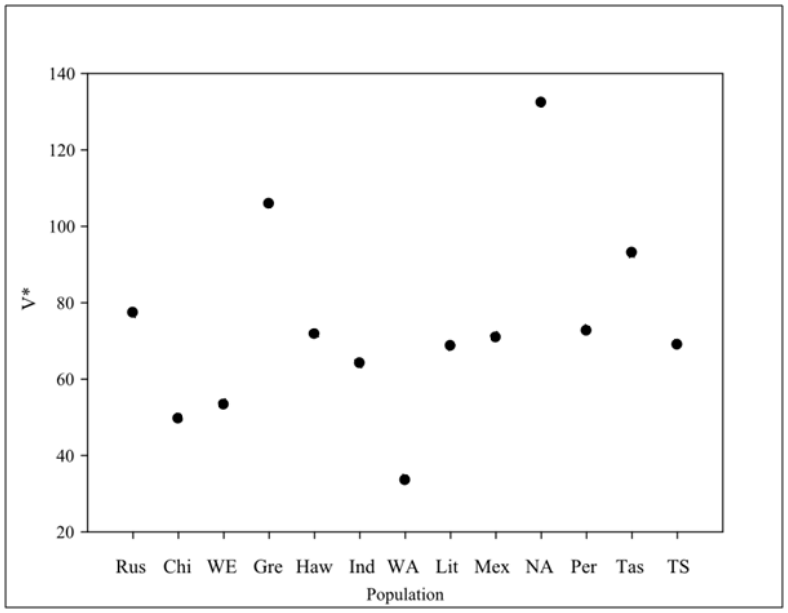

Figure 64: Differences in intra-population coefficients of variation (V*) in relative frontal sinus volumes between recent *H. sapiens* populations. Rus: Russia, Chi: China, WE: Western European; Gre: Greenland, Haw: Hawaii, Ind: India, WA: Western Africa, Lit: Lithuania, Mex: Mexico, NA: North Africa, Per: Peru, Tas: Tasmania, TS: Torres Straits.

Two populations are particularly variable: North Africans (by far the highest) and Greenland Inuit. The Western African population has very low levels of variation.

Potentially problematic populations (Chinese, Russian, Western European, and Western African populations - see Section 2.IV.a.iii.) do not demonstrate significantly more variation than other populations, nor is variation related to differences in precision between specimens with microCT scans and medical CT scans (see Section 2.I.a.), since there is no significant difference between these groups.

There is a significant negative relationship with sample size. Smaller sample sizes are associated with more intra-population variation, such that approximately 40% of the difference in coefficients of variation (V*) in relative frontal sinus volume is due to sample size:

- **Intra-population variation x sample size:** $V^* = 171.39 + -10.21 \times n$. $r = -0.63$, $r^2 = 0.40$, $p < 0.05$).

4.I.a.ii. Differences in frontal SVSPs between populations of recent H. sapiens

For samples for SVSP analyses, see Chapter 3.

Full landmark set frontal SVSP PC3

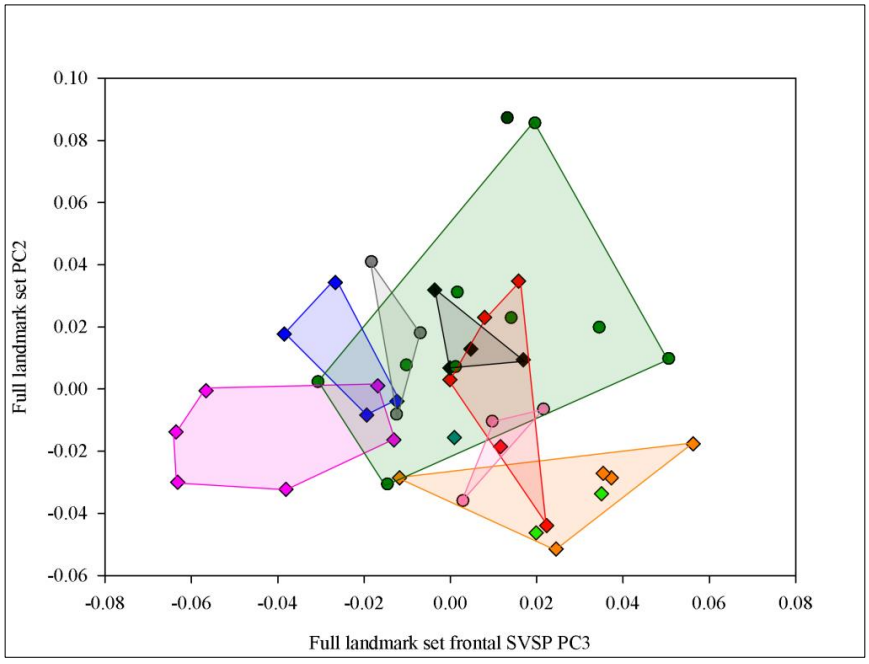

Figure 65: PCA showing full landmark set frontal SVSP against PC2 by population of recent *H. sapiens*. Dark green circles: Russia; mid green circles: Peru; light green diamonds: Western Africa; orange diamonds: Torres Straits; red diamonds: Western European; teal diamonds: India; grey circles: China; blue diamonds: Hawaii; pink circles: Lithuania; magenta diamonds: Greenland; black diamonds: Mexico. Convex hulls added post-hoc for ease of visualisation. There are significant differences between some of the populations – see Table 28.

There is some separation visible between populations of recent *H. sapiens* along full landmark set frontal SVSP PC3. In particular, the Greenland Inuit (Figure 65) mostly fall noticeably lower on the SVSP than other groups. An ANOSIM shows small but significant differences between populations:

- **Full landmark set frontal SVSP PC3 by population:** ANOSIM: R = 0.20, $r^2 = 0.04$, $p < 0.05$.

Differences between individual populations are detailed in Table 28. None of the individual differences remain significant when a Bonferroni correction is applied. The other differences between groups are more easily visualised using a cluster analysis of the mean scores for each population (see Figure 65).

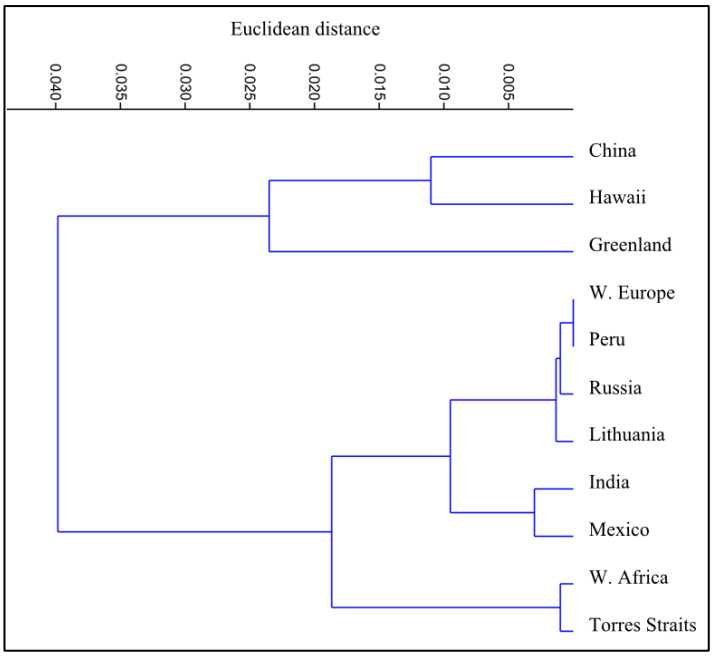

Figure 66: Cluster analysis of differences in mean population positions (group mean PC scores) on full landmark set frontal SVSP PC3.

Table 28: Results from ANOSIM comparing recent *H. sapiens* populations' scores on full landmark set frontal SVSP PC3. The matrix is symmetrical, numbers above the trace show R values, cells coloured on a scale to from green (from highest/most different) to red (lowest/most similar). Numbers below the trace are p values with light red highlighting indicating a significant result. No results remain significant if a Bonferroni correction is applied. Lit: Lithuania; WA: Western Africa; WE: Western Europe; Ind: India; Gre: Greenland; Rus: Russia; NA: North Africa; Tas: Tasmania; TS: Torres Straits; Per: Peru; Chi: China; Haw: Hawaii; Mex: Mexico.

	Lit	**Gre**	**WE**	**WA**	**Ind**	**TS**	**Rus**	**Chi**	**Mex**	**Per**	**Haw**
Lit		0.654	-0.231	0.167	-0.11	0.139	-0.556	0.815	-0.139	-0.23	0.907
Gre	0.023		0.741	0.854	0.378	0.755	0.733	0.173	0.429	0.548	0.02
WE	1	0.007		0.327	0	0.36	-0.44	0.836	0.012	-0.12	0.931
WA	0.389	0.037	0.189		1	-0.291	0	1	0.327	-0.04	1
Ind	0.498	0.149	0.504	0.331		0.16	2	0.778	-0.44	-0.3	0.667
TS	0.254	0.002	0.03	0.806	0.495		-0.04	0.405	0.314	0.064	0.638
Rus	1	0.138	1	0.658	1	0.51		1	-0.2	-0.3	0.917
Chi	0.1	0.14	0.018	0.101	0.254	0.09	0.249		0.108	-0.02	-0.019
Mex	0.666	0.035	0.359	0.197	1	0.059	0.662	0.286		-0.1	0.306
Per	0.926	0.002	0.838	0.513	0.779	0.239	1	0.445	0.778		0.307
Haw	0.03	0.376	0.008	0.066	0.199	0.016	0.208	0.373	0.084	0.066	

The greatest number of significant differences is between Greenland and the other populations. The greatest number of 'large' distances is between Hawaii and other groups, and there are also several high scores in the comparisons between China and other populations. These three form a group somewhat separate from the rest (see Figure 66). The largest difference of all is between Russia and India, but these two are single individuals, and so more likely to be outliers with unrepresentative SVSP scores than samples of larger sizes.

Effect of population history

A Mantel test comparing geographic distances between individuals with distances between them on full landmark set frontal SVSP PC3 shows a low, but highly significant correlation:

- **Geographic distance x full landmark set frontal SVSP PC3:** Mantel test: $R = 0.15$, $r^2 = 0.02$, $p < 0.001$.

This shows that a small part of the differences in sample distribution on the SVSP are likely to be partly due to population history.

Frontal SVSP PC6

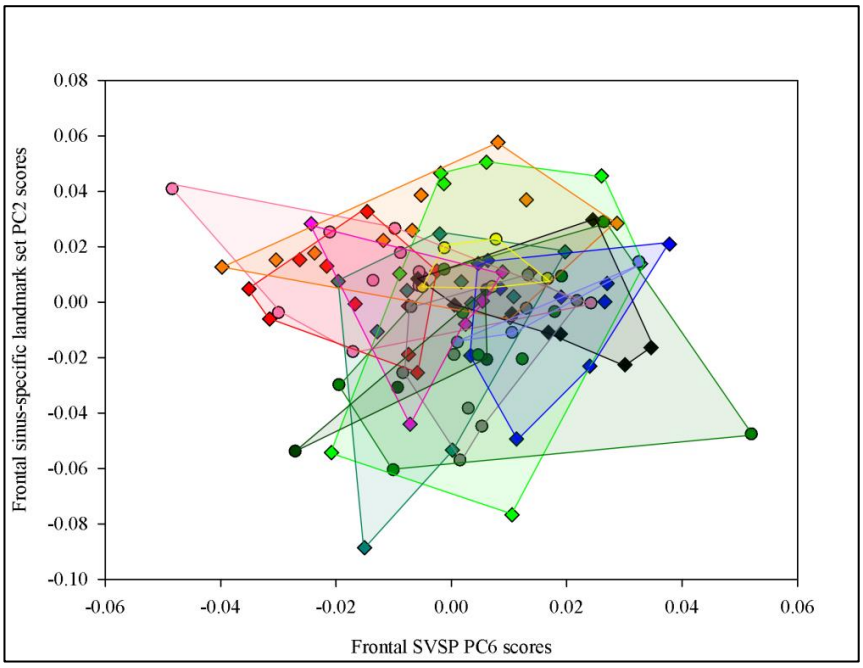

Figure 67: PCA of frontal SVSP PC6 and frontal sinus-specific landmark set PC2 by population of recent *H. sapiens*. Dark green circles: Russia; mid green circles: Peru; light green diamonds: Western Africa; orange diamonds: Torres Straits; red diamonds: Western Europe; teal diamonds: India; grey circles: China; blue diamonds: Hawaii; pink circles: Lithuania; magenta diamonds: Greenland; black diamonds: Mexico; mauve circles: North Africa; yellow circles: Tasmania. Convex hulls added post-hoc for ease of visualisation. There are some significant differences between populations – see Table 29.

There is a great deal of overlap between populations and no obvious difference between populations, in Figure 67. An ANOSIM, however, shows there are significant differences, albeit extremely small ones, between the groups overall:

- **Frontal SVSP PC6 by population:** ANOSIM: R = 0.09, $r^2 = 0.01$, $p < 0.005$.

Table 29 shows the results for each population, which are also summarised by the cluster diagram in Figure 68.

The population showing the most differences from other populations is Western Europe; Hawaii is also quite distinct from other populations. Some of these differences are the same/similar to those in full landmark set frontal SVSP PC3 and may be picking up on the same shape differences (see Chapter 3). If a Bonferroni correction is applied the differences between Western Europe and Hawaii, China, and Mexico, and the difference between Hawaii and Lithuania remain significant (see Table 29).

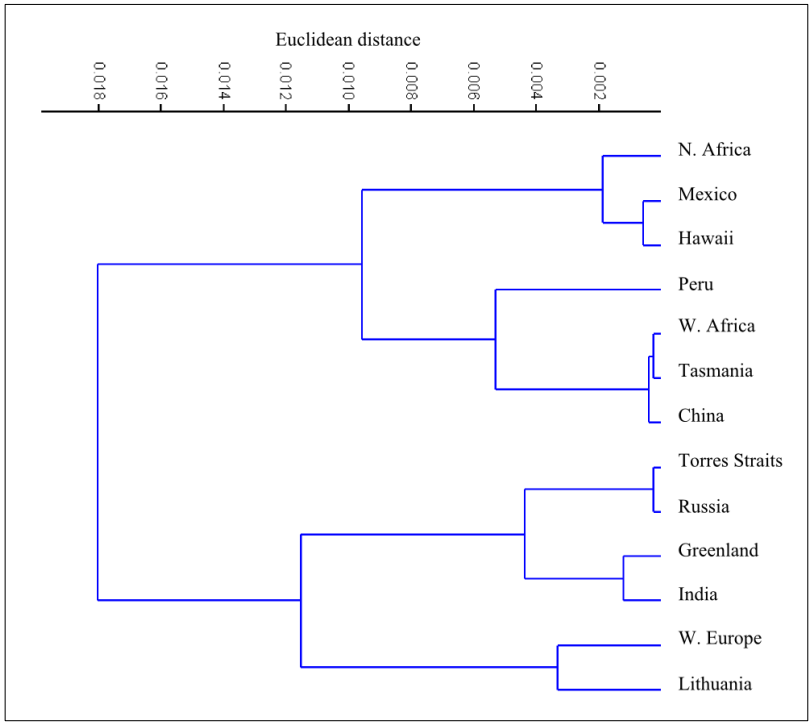

Figure 68: Cluster analysis of recent *H. sapiens* population means of PC scores on frontal SVSP PC6.

Effect of population history on recent *H. sapiens* population positions on frontal SVSP PC6

A Mantel test comparing a matrix of geographic distances between populations with their positions on frontal SVSP PC6 showed a very low, but highly significant correlation:

- **Geographic distance x frontal SVSP PC6:** Mantel test: $R = 0.12$, $r^2 = 0.01$, $p < 0.001$.

This suggests a very small component of the differences between individuals on frontal SVSP PC6, a very small amount of craniofacial shape associated with relative frontal sinus volume, is due to population history.

Table 29: The results of an ANOSIM comparing frontal SVSP PC6 scores of recent *H. sapiens* populations. The matrix is symmetrical, numbers above the trace show R values, with cells coloured from on a scale from green (highest/most different) to red (lowest/most similar). Numbers below the trace are p values of between group comparisons with light red highlighting indicating a significant result when no Bonferroni correction is applied. *: differences that remain significant when a Bonferroni correction is applied. Lit: Lithuania; WA: Western Africa; WE: Western Europe; Ind: India; Gre: Greenland; Rus: Russia; NA: North Africa; Tas: Tasmania; TS: Torres Straits; Per: Peru; Chi: China; Haw: Hawaii; Mex: Mexico.

	Haw	**Gre**	**WA**	**WE**	**Ind**	**TS**	**Rus**	**Lit**	**Tas**	**NA**	**Per**	**Chi**	**Mex**
Haw		0.1619	0.0863	0.7296	0.2756	0.1837	0.2868	0.5101	0.0306	-0.0014	-0.0002	0.0988	-0.0520
Gre	0.0581		-0.0915	0.2320	-0.0697	-0.1069	-0.0979	0.0857	-0.1373	0.0298	-0.0766	-0.0769	0.1552
WA	0.1413	0.8884		0.2421	-0.0171	-0.0646	-0.1066	0.1113	-0.1533	-0.1465	-0.0880	-0.0109	0.0050
WE	0.0001*	0.0290	0.0130		0.1276	0.0563	0.1412	-0.0620	0.4196	0.5958	0.3114	0.3962	0.6380
Ind	0.0064	0.7626	0.4859	0.0536		-0.0106	-0.0196	0.0512	-0.0626	0.1500	0.0054	-0.0250	0.2418
TS	0.0212	0.9682	0.7908	0.1701	0.4437		-0.1745	-0.0139	-0.1178	-0.0167	-0.0027	0.0276	0.1187
Rus	0.0689	0.6879	0.7095	0.1552	0.4804	0.9534		0.0049	0	0.0370	-0.0667	0.0661	0.2261
Lit	0.0002*	0.1554	0.0861	0.9588	0.1569	0.4888	0.4497		0.1924	0.3361	0.1742	0.2450	0.3978
Tas	0.3224	0.9246	0.9756	0.0098	0.6057	0.8128	0.4004	0.1019		-0.0256	-0.1836	-0.1304	0.0211
NA	0.4422	0.4298	0.7913	0.0111	0.1997	0.4233	0.4018	0.0856	0.5353		-0.1583	0.0693	-0.1089
Per	0.3857	0.8004	0.9425	0.0022	0.3462	0.3960	0.5693	0.0220	0.9857	0.7457		-0.0447	-0.0551
Chi	0.0951	0.8215	0.4509	0.0003*	0.5297	0.2691	0.2962	0.0074	0.8989	0.3095	0.7139		0.1170
Mex	0.6724	0.0762	0.3444	0.0001*	0.0225	0.0909	0.0926	0.0041	0.3290	0.7347	0.7314	0.0986	

4.I.b. Population differences in maxillary sinus variables

4.I.b.i. Differences in relative maxillary sinus volumes between recent H. sapiens *populations*

Table 30: Recent *H. sapiens* population sample for relative maxillary sinus volumes.

Country	n
China	10
Greenland	7
Hawaii	10
India	10
Lithuania	11
Mexico	9
North Africa	2
Peru	10
Russia	4
Tasmania	8
Torres Straits	12
Western Africa	12
Western Europe	10
Total	**115**

There is no significant difference in relative maxillary sinus volume between populations of recent *H. sapiens*.

Intra-population variation in recent *H. sapiens* populations' relative maxillary sinus volume

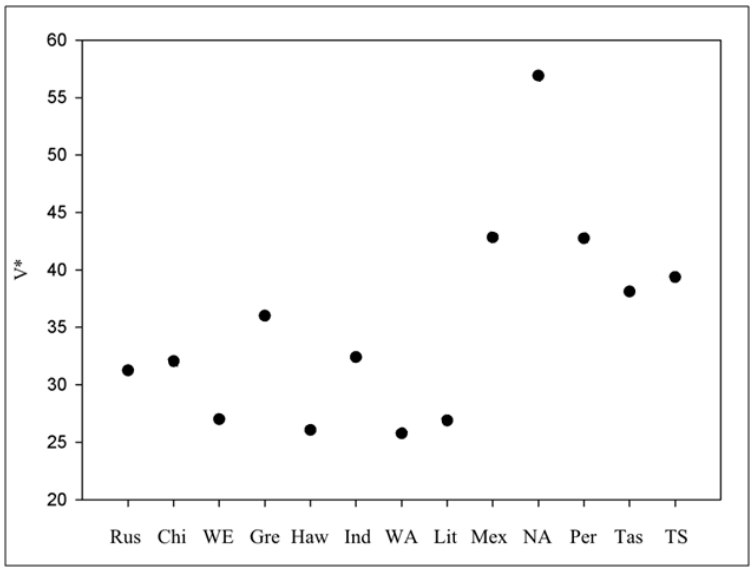

Figure 69: Plot showing intra-population coefficients of variation (V*) in relative maxillary sinus volume between populations of recent *H. sapiens*. . Rus: Russia; Chi: China; WE: Western Europe; Gre: Greenland; Haw: Hawaii; Ind: Indian; WA: Western Africa; Lit: Lithuania; Mex: Mexico; N A: North Africa; Per: Peru; Tas: Tasmania; TS: Torres Straits.

There is considerably more variation in relative maxillary sinus volume, as shown by the coefficients of variation, within North Africans than within any other population. That this is probably due, at least in part, to the small sample size can be seen from the moderately strong and significant result in the regression analysis below::

- **Coefficient of variation x sample size:** RMA regression **:** V* = 20.55 + -0.33 x n, $r^2 = 0.34$, $p < 0.05$.

However, this is likely to be due to the outlier status of the North African population, since, if this population is removed, there is no significant relationship between V* and sample size.

Neither the potentially problematic population designations (see Section 2.IV.a.iii.), nor type of CT data (microCT or medical CT – see Section 2.I.a.), had any effect on intra-population variation in relative maxillary sinus volume; there are no significant differences between groups in either case.

4.I.b.ii. Differences in maxillary SVSPs between populations of recent H. sapiens

Maxillary SVSP PC3

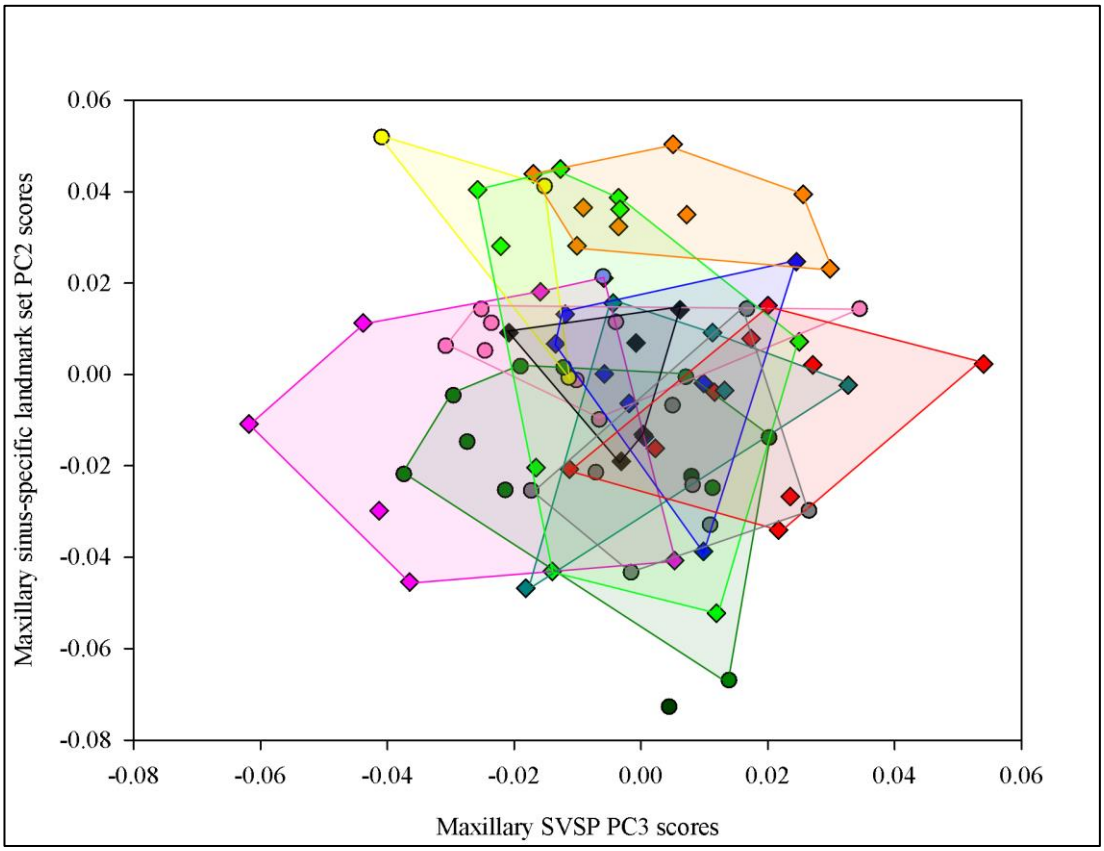

Figure 70: PCA of maxillary SVSP PC3 and maxillary sinus-specific landmark set PC2 by population of recent *H. sapiens*. Dark green circles: Russia; mid green circles: Peru; light green diamonds: Western Africa; orange diamonds: Torres Straits; red diamonds: Western Europe; teal diamonds: India; grey circles: China; blue diamonds: Hawaii; pink circles: Lithuania; magenta diamonds: Greenland; black diamonds: Mexico; mauve circles: North Africa; yellow circles: Tasmania. Convex hulls added post-hoc for ease of visualisation. There are significant differences between some of the populations – see Table 31.

Despite substantial overlap in Figure 70, there is some population separation, particularly between Greenland and Western European populations. An ANOSIM shows that there are some minor significant differences between groups, although they are very small:

- **Maxillary SVSP PC3 by population:** ANOSIM: R = 0.069, r^2 = 0.01, p < 0.05.

The differences between groups are shown in Table 31 and summarised in Figure 71. The only difference that remains significant when a Bonferroni correction is applied is between Greenland and Western Europe. These two groups also show the most differences from other populations (see Table 61).

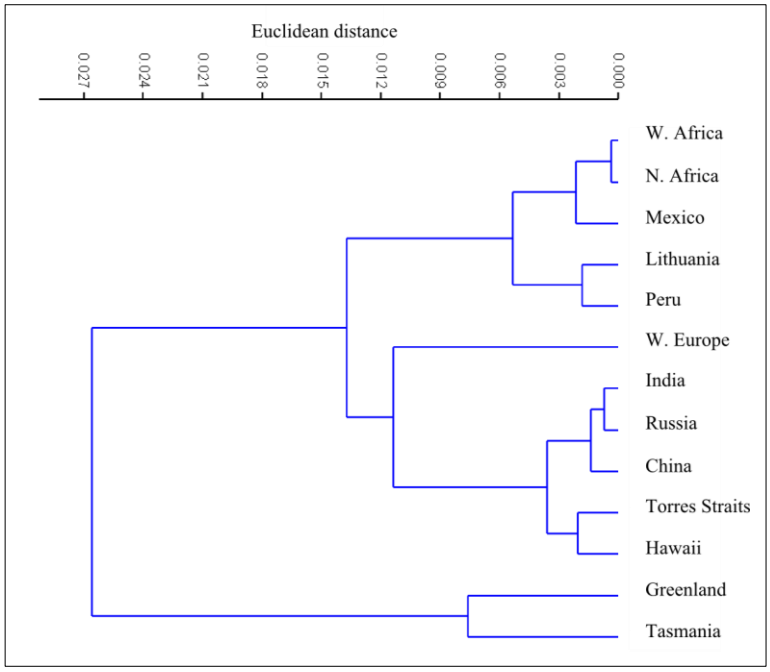

Figure 71: Cluster analysis of differences between mean recent *H. sapiens* population PC scores on maxillary SVSP PC3.

Effect of population history

A Mantel test comparing geographic distances between populations with differences in position on maxillary SVSP PC3 was not significant.

Table 31: Results from an ANOSIM comparing maxillary SVSP PC3 scores in different populations of recent *H. sapiens*. The table is symmetrical. Numbers below the trace are p values, with significant differences highlighted in red. Numbers above the trace are R values coloured red (lowest/most similar) to green (highest/most different). *: remains significant if a Bonferroni correction is applied. Haw: Hawaii; Gre: Greenland; WA: Western Africa; Western Europe; Ind: India; TS: Torres Straits; Rus: Russia; Lit: Lithuania; Tas: Tasmania; NA: North Africa; Per: Peru; Chi: China; Mex: Mexico.

	Haw	**Gre**	**WA**	**WE**	**Ind**	**TS**	**Rus**	**Lit**	**Tas**	**NA**	**Per**	**Chi**	**Mex**
Haw		0.389	-0.016	0.052	-0.003	-0.086	-0.194	0.170	0.263	-0.241	0.047	-0.074	-0.107
Gre	0.003		0.175	0.5567*	0.356	0.323	0.279	0.068	-0.151	0.048	0.070	0.428	0.209
WA	0.471	0.059		0.162	-0.005	-0.054	-0.043	-0.043	-0.046	-0.321	-0.065	0.039	-0.072
WE	0.197	0.0002*	0.054		-0.026	0.018	-0.133	0.349	0.501	0.049	0.188	-0.025	0.109
Ind	0.383	0.027	0.420	0.503		-0.076	-0.291	0.147	0.210	-0.320	-0.007	-0.067	0.008
TS	0.902	0.011	0.656	0.297	0.671		-0.216	0.095	0.159	-0.304	0.022	-0.075	-0.088
Rus	0.757	0.113	0.537	0.628	0.813	0.758		0.246	0.333	1.000	-0.100	-0.328	0.018
Lit	0.049	0.175	0.639	0.008	0.129	0.131	0.226		-0.083	-0.170	-0.041	0.248	0.112
Tas	0.094	0.778	0.562	0.017	0.138	0.195	0.203	0.568		0.111	-0.088	0.384	0.333
NA	0.668	0.378	1.000	0.279	0.839	0.887	0.339	0.562	0.499		-0.173	-0.134	-0.160
Per	0.217	0.183	0.757	0.027	0.441	0.297	0.703	0.642	0.647	0.726		0.046	-0.050
Chi	0.786	0.006	0.256	0.537	0.621	0.798	1.000	0.021	0.050	0.555	0.210		-0.067
Mex	0.796	0.075	0.677	0.187	0.427	0.715	0.378	0.189	0.089	0.497	0.609	0.620	

Maxillary sinus-specific SVSP PC7

There are no significant differences between populations of recent *H. sapiens*, or between different taxa on maxillary SVSP PC7.

4.I.c. Population differences in sphenoidal sinus volumes

4.I.c.i. Recent H. sapiens *population differences in sphenoidal sinus volume*

Table 32: Recent *H. sapiens* sample for relative sphenoidal sinus volumes.

Country	n
China	10
Greenland	7
Hawaii	9
India	11
Lithuania	11
Mexico	9
North Africa	1
Peru	9
Russia	4
Tasmania	8
Torres Straits	13
Western Africa	14
Western Europe	11
Total	**117**

There are no significant differences in relative sphenoidal sinus volume between populations of recent *H. sapiens*.

Intra-population variation in relative sphenoidal sinus volume between populations of recent *H. sapiens*

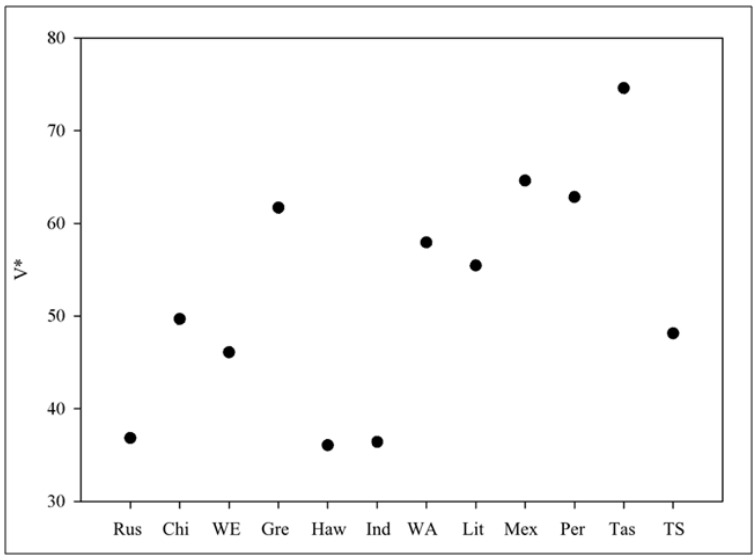

Figure 72: Scatter and line plot of intra-population coefficients of variation (V*) in relative sphenoidal sinus volume in recent *H. sapiens*. Rus: Russia; Chi: China; WE: Western Europe; Gre: Greenland; Haw: Hawaii; Ind: Indian; WA: Western Africa; Lit: Lithuania; Mex: Mexico; Per: Peru; Tas: Tasmania; TS: Torres Straits.

There is a high degree of dissimilarity between the coefficients of variation of different populations in the recent *H. sapiens* sample. The low coefficient of variation in the Russians could be due to low sample size. There is, however, no significant relationship between sample size and coefficient of variation in relative sphenoidal sinus volume across all populations.

Some of the highest levels of variation (Greenland and Tasmania) are in populations for which micro-CT data was used; however, there is no significant difference in level of variation (V*) between groups analysed using the two different types of CT data (microCT and medical CT – see Section 2.I.a.).

There is no significant difference in intra-population variation in relative sphenoidal sinus volume between potentially problematic populations (see Section 2.IV.a.iii.) and populations with specimens from relatively small geographical regions. None of the four groups with the highest intra-population variation is a potentially problematic population.

4.I.c.ii. Differences in sphenoidal SVSPs between populations of recent H. sapiens

There are no significant differences between populations of recent *H. sapiens* on either sphenoidal SVSP PC3 or PC6.

4.II. RQ1.b: Are there differences in sinus variables between Mid-Late Pleistocene taxa?

In this section, the results of investigations into the differences in sinus variables between different Pleistocene hominin taxa are presented by sinus type. It was ascertained whether there are significant differences between taxa first in sinus volume, and then SVSPs. Intra-taxon variation was also investigated for each sinus type.

4.II.a. Taxonomic differences in frontal sinus variables

4.II.a.i. Taxonomic differences in relative frontal sinus volumes

Table 33: Frontal sinus volume sample by taxon.

Group	Specimen	Country	n
Recent *H. sapiens*		China	9
		Greenland	7
		Hawaii	11
		India	11
		Lithuania	11
		Mexico	10
		North Africa	7
		Peru	10
		Russia	4
		Tasmania	8
		Torres Straits	12
		Western Africa	13
		Western Europe	11
		Total:	**124**
Early *H. sapiens*	Cro-Magnon 1	France	
	Cro-Magnon 2	France	
	Cro-Magnon 3	France	
	Mladeč	Czech Republic	
	Ngaloba	Tanzania	
	Singa	Sudan	
	Skhul 5	Israel	
		Total:	**7**
H. neanderthalensis	Forbes' Quarry	Gibraltar	
	Guattari 1	Italy	
	Krapina 3	Croatia	
	La Chapelle	France	
	La Ferrassie	France	
	La Quina	France	
	Neanderthal 1	Germany	
	Tabun 1	Israel	
		Total:	**8**
H. heidelbergensis	Bodo	Ethiopia	
	Ceprano	Italy	
	Kabwe	Zambia	
	Petralona	Greece	
		Total:	**4**
H. erectus	KNM-ER 3883	Kenya	**1**
		Total:	**144**

Sample composition

Since recent and early *H. sapiens* volumes relative frontal sinus volumes overlap nearly exactly, these groups are combined for subsequent analyses. The sole *H. erectus* is not included in statistical analyses due to insufficient sample size.

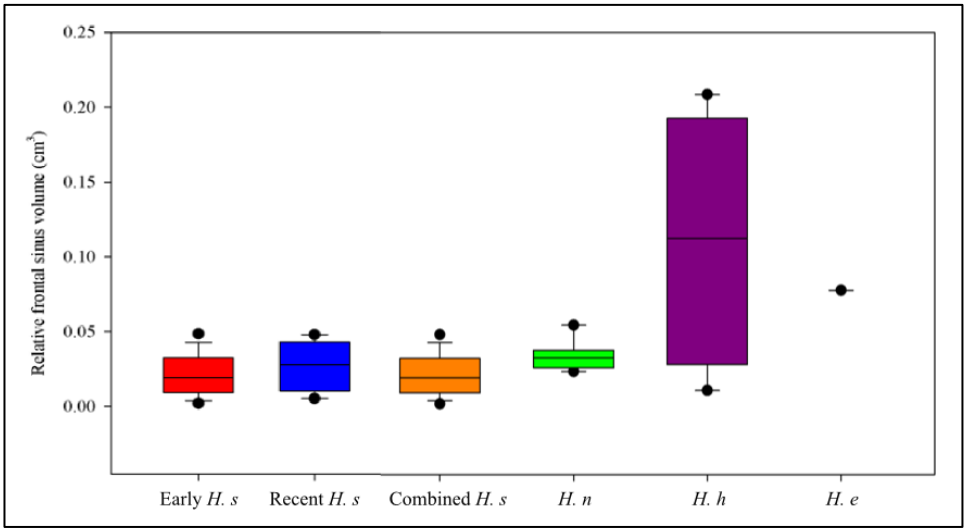

Figure 73: Relative frontal sinus volume by taxon. *H. heidelbergensis* has significantly larger relative frontal sinus volumes than any of the other taxa (with the exception of *H. erectus*, which was not included in statistical analyses due to a sample size of one).

There are moderate significant differences in relative frontal sinus volumes between taxa:

- **Relative frontal sinus volume by taxon:** ANOSIM: R = 0.33, $r^2 = 0.11$, $p < 0.001$.

The most important feature in this analysis is *H. heidelbergensis* variation, which is further addressed below. On average *H. heidelbergensis* has significantly larger relative frontal sinus volumes than either *H. sapiens* or *H. neanderthalensis*. These relationships remain significant if a Bonferroni correction is applied (see Table 34).

Table 34: Results from an ANOSIM comparing relative frontal sinus volumes between taxa. The matrix is symmetrical; numbers above the trace are R values, numbers below the trace are p values. Red highlighting indicates a significant result. *: remains significant if a Bonferroni correction is applied.

	H. sapiens	***H. neanderthalensis***	***H. heidelbergensis***
H. sapiens		0.05848	0.6914*
H. neanderthalensis	1		0.0693*
H. heidelbergensis	0.0006*	0.0186*	

Allometry in relative frontal sinus volume differences between populations of recent *H. sapiens*

There is no significant relationship between relative frontal sinus volumes and ln frontal sinus-specific centroid size.

Intra-taxon variation in relative frontal sinus volume

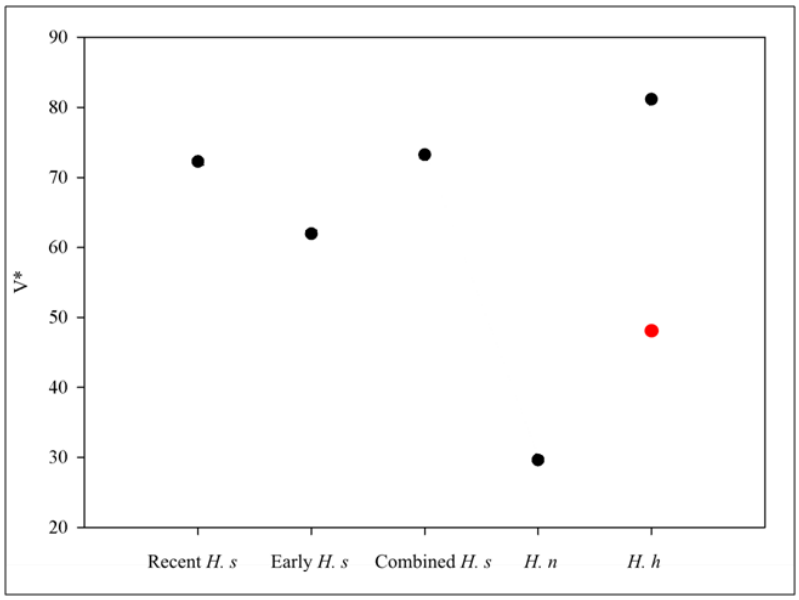

Figure 74: Scatter and line plot showing differences in coefficient of intra-taxon variation (V*) in relative frontal sinus volumes. *H. s*: *H. sapiens*, *H. n*: *H. neanderthalensis*, *H. h*: *H. heidelbergensis*. Red circle indicates approximate V* of *H. heidelbergensis* without Ceprano. See text for details.

Homo heidelbergensis

Relative frontal sinus volumes are significantly larger in *H. heidelbergensis* than in *H. sapiens/neanderthalensis* on average, but there is a very high level of variation in this taxon. Ceprano is very different in frontal sinus size and shape to the other members of the *H. heidelbergensis* sample (see Table 35). Figure 75 of *H. heidelbergensis* crania with their frontal sinuses highlighted shows how large the sinuses of Kabwe, Bodo, and Petralona appear, and the qualitative difference between these three and Ceprano. In fact, Ceprano's relative frontal sinus is small even compared to mean Neanderthal and *H. sapiens* (recent and early). The shape of the frontal sinus(es) is also very different in Ceprano (See Figure 123), being composed of a small right and a small left sinus which are entirely separate and do not extend superiorly past the supraorbital torus. The other members of the *H. heidelbergensis* sample all have a single continuous frontal sinus, which pneumatises the frontal squama (as seen in Kabwe, see Figure 122). This type and size of sinus is occasionally present in recent *H. sapiens* specimens, but it is very rare. If Ceprano is removed from the *H. heidelbergensis* sample, the differences between this taxon and both *H. sapiens* and *H. neanderthalensis* increases. The coefficient of variation for the *H. heidelbergensis* without Ceprano, however, would be much reduced (see Figure 74).

Table 35: Relative frontal sinus volumes in the *H. heidelbergensis* sample in order of size from smallest to largest.

Specimen	Relative frontal sinus volume (cm^3)
Ceprano	0.01
Kabwe	0.08
Bodo	0.14
Petralona	0.21

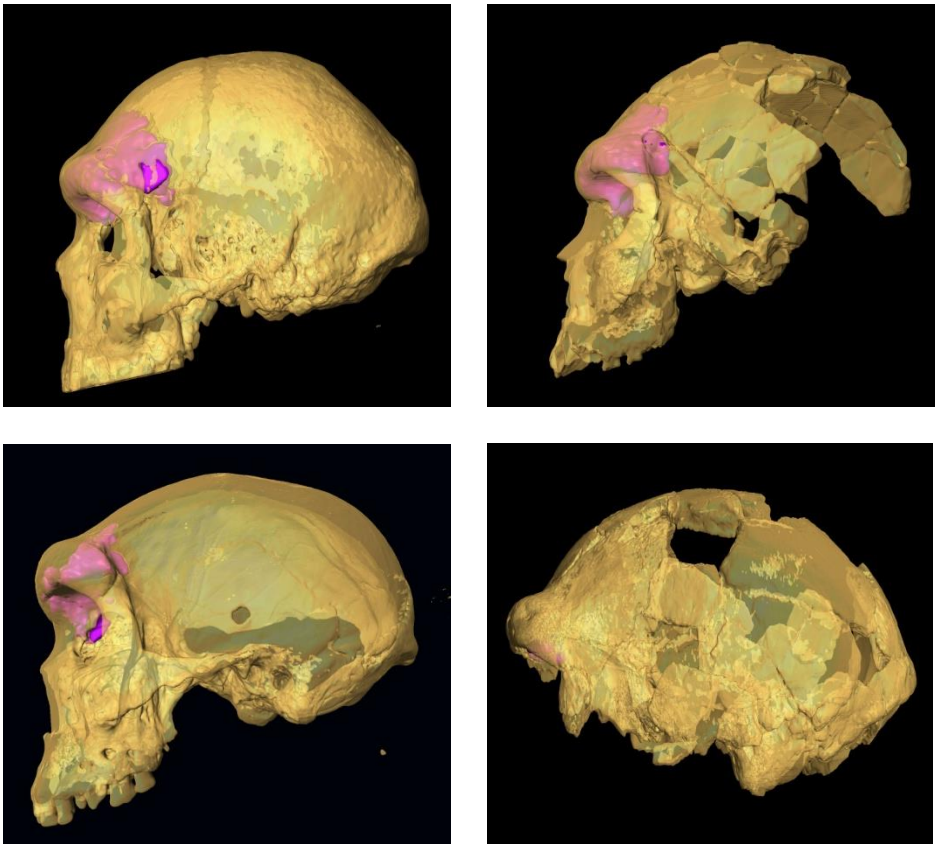

Figure 75: Images of the virtually reconstructed crania of (top left to bottom right) Petralona, Bodo, Kabwe, and Ceprano. Frontal sinuses are sectioned out in magenta (see Section 2.II.a.i). The images are not to scale.

H. neanderthalensis

The intra-taxon variation in the *H. neanderthalensis* sample is very low compared to other taxa.

4.II.a.ii Taxonomic differences in Frontal SVSPs

Since the sample for full landmark set frontal SVSP PC3 was exclusively recent *H. sapiens*, that SVSP is not included in this section.

Frontal SVSP PC6

Sample composition

The sole representative of the early *H. sapiens* group (Cro-Magnon 2) falls close to the centre of the recent *H. sapiens* cluster, so these latter two groups were combined for ANOSIM analysis.

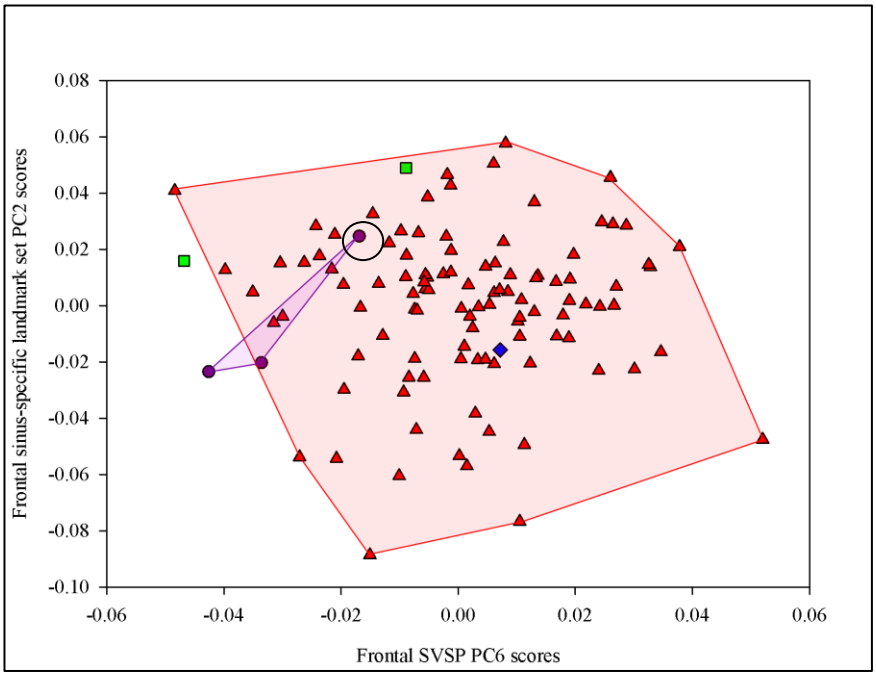

Figure 76: PCA showing frontal SVSP PC6 against frontal sinus-specific landmark set PC2 by taxon. Convex hulls to show taxonomic groups are added post-hoc for ease of visualisation. Red triangles: recent *H. sapiens*; blue diamond: early *H. sapiens*; green squares: *H. neanderthalensis*; purple circles: *H. heidelbergensis*. Circled *H. heidelbergensis* is Steinheim. *H. sapiens* scores significantly higher on frontal SVSP PC6 than *H. neanderthalensis* or *H. heidelbergensis*.

Despite the fact that all taxa fall within the range of *H. sapiens* variation, there is a small, significant difference between the mean scores of taxonomic groups on frontal SVSP PC6:

- **Frontal SVSP PC6 by taxon:** ANOSIM: $R = 0.28$, $r^2 = 0.08$, $p < 0.005$.

H. sapiens has a significantly (remains so with a Bonferroni correction) higher score on frontal SVSP PC6 than *H. heidelbergensis*:

- ***H. heidelbergensis* x *H. sapiens* on frontal SVSP PC6:** ANOSIM: R = 0.42, $r^2 = 0.18$, $p < 0.05$.

Taxonomic position of Steinheim

Steinheim is taxonomically uncertain, being classified as either *H. heidelbergensis* or *H. neanderthalensis* (see Section 2.I.b.ii). In order to ascertain the effect of this potentially confounding fossil, the analysis of frontal SVSP PC6 was repeated both with Steinheim reclassified as a Neanderthal and with it removed from the sample. Neither reanalysis changes the results in any substantial way. If Steinheim is reclassified there is still a significant difference between *H. heidelbergensis* and *H. sapiens*, but the differentiation is slightly improved. This shows that the difference in frontal sinus-related morphology between *H. heidelbergensis* and *H. sapiens* is robust to the taxonomic ambiguity of Steinheim.

4.II.b. Taxonomic differences in maxillary sinus variables

4.II.b.i. Taxonomic differences in relative maxillary sinus volumes

Table 36: Sample for relative maxillary sinus volumes by taxon.

Group	Specimen	Country	n
Recent *H. sapiens*		China	10
		Greenland	7
		Hawaii	10
		India	10
		Lithuania	11
		Mexico	9
		North Africa	2
		Peru	10
		Russia	4
		Tasmania	8
		Torres Straits	12
		Western Africa	12
		Western Europe	10
Early *H. sapiens*	Mladeč	Czech Republic	2
	Cro-Magnon 1	France	
H. neanderthalensis	La Chapelle-aux-Saints	France	3
	Forbes' Quarry	Gibraltar	
	Guattari 1	Italy	
	La Ferrassie 1	France	
H. heidelbergensis	Kabwe	Zambia	2
	Petralona	Greece	
		Total	**122**

Sample composition

Although early *H. sapiens* seems to have larger volumes than the majority of recent *H. sapiens*, the former is still within the range of variation of the latter and there is no significant difference between them; thus, they are combined for subsequent analyses.

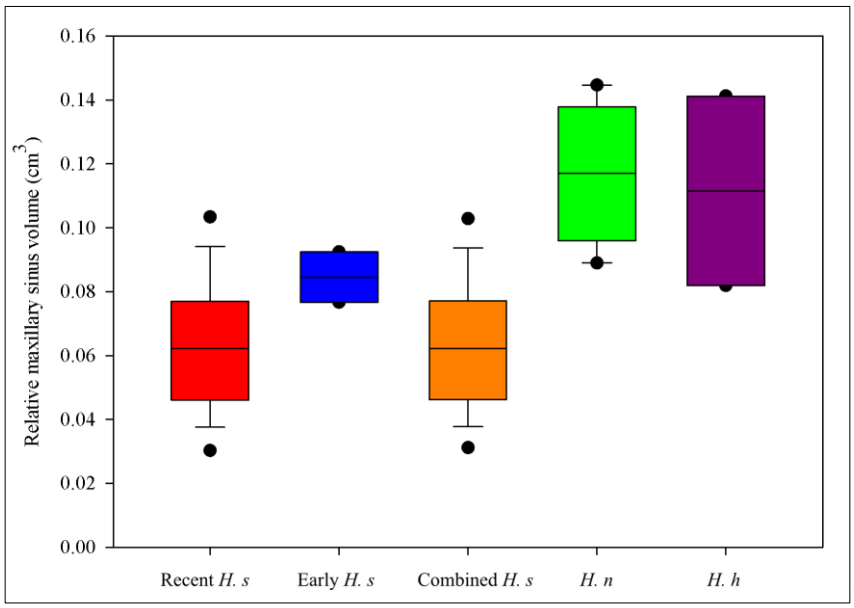

Figure 77: Relative maxillary sinus volume in taxonomic groups. *H. s*: *H. sapiens*; *H. n*: *H. neanderthalensis*; *H. h*: *H. heidelbergensis*. *H. sapiens* has significantly smaller relative maxillary sinus volumes than *H. neanderthalensis* or *H. heidelbergensis*.

Despite some overlap, there are large, significant differences between relative maxillary sinus volumes in different taxonomic groups:

- **Relative maxillary sinus volumes by taxon:** ANOSIM: $R = 0.55$, $r^2 = 0.30$, $p < 0.001$.

H. sapiens has significantly smaller relative maxillary sinus volumes than both *H. neanderthalensis* and *H. heidelbergensis* (Table 37); these results remain significant if a Bonferroni correction is applied.

Table 37: Results from ANOSIM of relative maxillary sinus volume differences between groups. The matrix is symmetrical. Above the trace are R values, below the trace are p values; significant p values are highlighted in red, *: remains significant if a Bonferroni correction is applied.

	H. sapiens	***H. neanderthalensis***	***H. heidelbergensis***
H. sapiens		0.6059*	0.4542*
H. neanderthalensis	0.0001*		-0.0714
H. heidelbergensis	0.0147*	0.5275	

Allometry in relative maxillary sinus volume

Figure 77 shows that maxillary sinus volume increases with craniofacial size, despite the relative maxillary sinus volumes being standardised for size using G-FMT^3. This suggests that larger hominins have relatively, as well as absolutely, larger maxillary sinus volumes. It may also indicate that the simple measurement used to standardise for size is failing to some extent to capture cranial size sufficiently (see Section 2.II.a.ii). A regression analysis was carried out to assess the relationship between the natural log of maxillary sinus-specific centroid size (lnMCS) and the natural log of relative maxillary sinus volumes (lnRMV). There was a small, but significant relationship:

- **Relative maxillary sinus volumes x maxillary sinus-specific landmark set centroid size:** Reduced major axis regression: lnRMV = -45.08 + 7.68 x lnMCS, $r^2 = 0.06$, $p < 0.05$

This shows that larger crania do indeed have relatively larger maxillary sinus volumes, but this is a relationship with a small effect size. Since the slope is greater than 1, this is an example of positive allometry (see Section 2.II.a.ii). If the fossil species are removed there is no longer a significant relationship between lnRMV and lnMSC, suggesting that this relationship may differ between taxa. Unfortunately, with so few fossil specimens available (and not all of those well preserved enough to measure the maxillary sinus volume were well enough preserved to include in the maxillary sinus specific landmark set; e.g., Guattari and Cro-Magnon 1, Chapter 3), it is not possible to investigate the relationship in individual taxa.

Intra-taxon variation in maxillary sinus volume

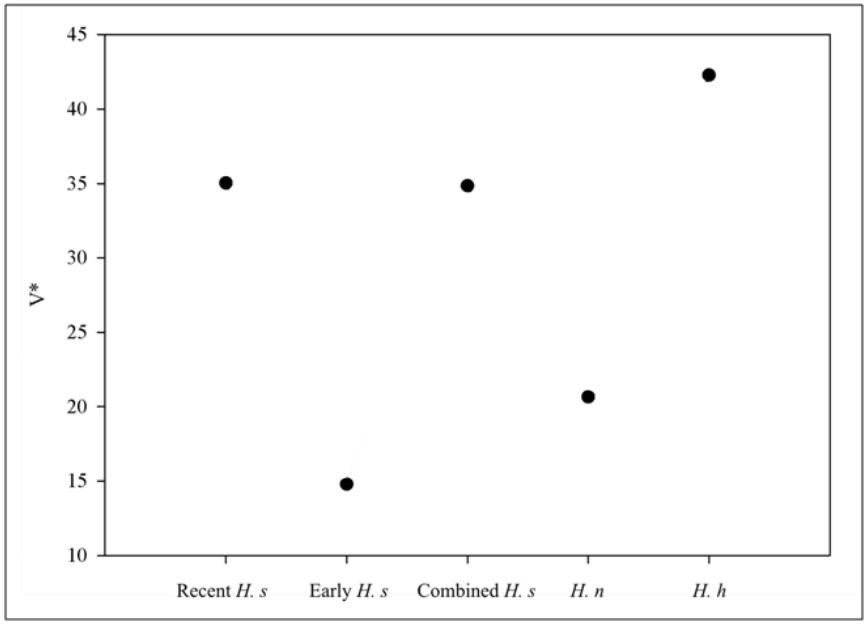

Figure 78: Scatter and line plot showing intra-taxon coefficient of variation (V*) in relative maxillary sinus volumes. *H.s*: *H. sapiens*; *H. n*: *H. neanderthalensis*; *H. h*: *H. heidelbergensis*.

H. sapiens and *H. heidelbergensis* (note that Ceprano is not present in the sample for these analyses as the lower face is not preserved) show far higher levels of intra-specific variation than *H. neanderthalensis*. When early and recent *H. sapiens* are considered separately, early *H. sapiens* have the lowest V* of all. The small fossil sample sizes may be responsible for these results.

4.II.b.ii. Taxonomic differences on maxillary volume shape parameters

Maxillary SVSP PC3

Sample composition

The only early *H. sapiens* individual it was possible to include in this analysis (Mladeč) falls well within the range of recent *H. sapiens* variation, so these groups were combined for subsequent analyses of maxillary SVSP PC3.

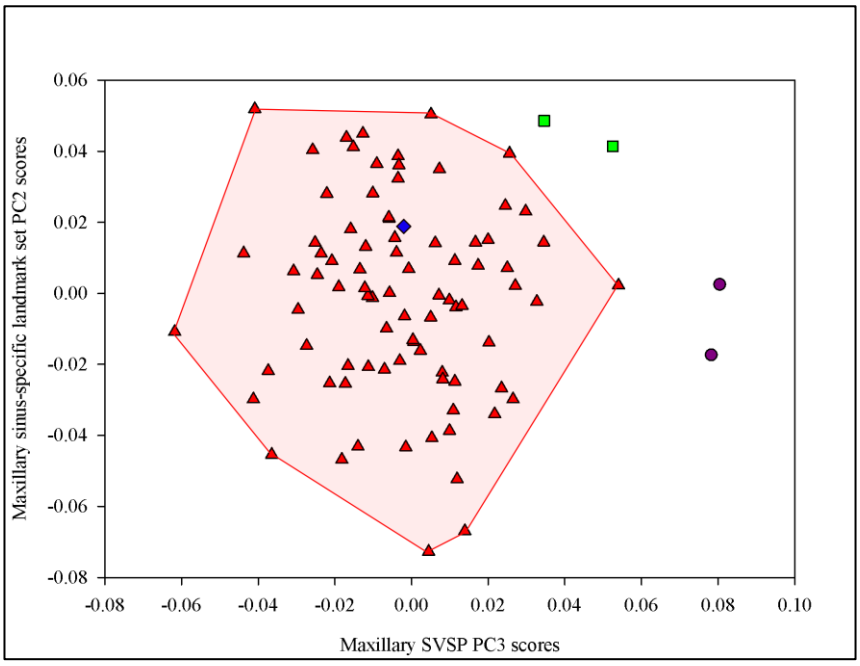

Figure 79: PCA of maxillary SVSP PC3 against maxillary sinus-specific landmark set PC2 by taxon. Red triangles: recent *H. sapiens*; blue diamond: early *H. sapiens*; green squares: *H. neanderthalensis*; purple circle: *H. heidelbergensis*. Convex hull added post-hoc for ease of visualisation. *H. sapiens* scores significantly lower on maxillary SVSP PC3 than either of the other taxa.

There seems to be some taxonomic differentiation along maxillary SVSP PC3. Indeed, *H. heidelbergensis* falls outside the range of variation for other hominins. Neanderthals fall within the *H. sapiens* range of variation, but at the higher end of

maxillary SVSP PC3. An ANOSIM shows that there is a very strong significant difference between taxonomic groups on maxillary SVSP PC3:

- **Maxillary SVSP PC3 by taxon:** ANOSIM: R = 0.78, r^2 = 0.61 p < 0.001.

H. sapiens scores significantly lower on maxillary SVSP PC3 than either *H. neanderthalensis* or *H. heidelbergensis* (see Table 38). These differences persist whether or not a Bonferroni correction is applied.

Table 38: Results from ANOSIM of taxonomic position on maxillary SVSP PC3 with Bonferroni correction applied. Matrix is symmetrical, numbers above trace are R values, and numbers below trace are p values. Significant p values are highlighted in red. *: remains significant with a Bonferroni correction.

	H. sapiens	***H. neanderthalensis***	***H. heidelbergensis***
H. sapiens		0.9599*	0.6119*
H. neanderthalensis	0.0001*		1
H. heidelbergensis	0.0062*	0.3447	

4.II.c. Taxonomic differences in sphenoidal sinus variables

4.II.c.i. Taxonomic differences in relative sphenoidal sinus volumes

Table 39: Sample for relative sphenoidal sinus volumes by taxon.

Population/taxon	Specimen	Country	n
Recent *H. sapiens*		China	10
		Greenland	7
		Hawaii	9
		India	11
		Lithuania	11
		Mexico	9
		North Africa	1
		Peru	9
		Russia	4
		Tasmania	8
		Torres Straits	13
		Western Africa	14
		Western Europe	11
Early *H. sapiens*	Mladeč	Czech Republic	1
H. neanderthalensis	Guattari 1	Italy	1
H. heidelbergensis	Kabwe	Zambia	1
		Total	**120**

There are no significant differences between relative sphenoidal sinus volumes in different taxonomic groups; this is unsurprising given the small sample sizes.

4.II.c.ii. Taxonomic differences in sphenoidal sinus shape parameters

Sphenoidal SVSP PC3

Sample composition

The sole early *H. sapiens* falls within the range of recent *H. sapiens* variation in sphenoidal SVSP PC3 scores; therefore, these samples are combined in the following analyses.

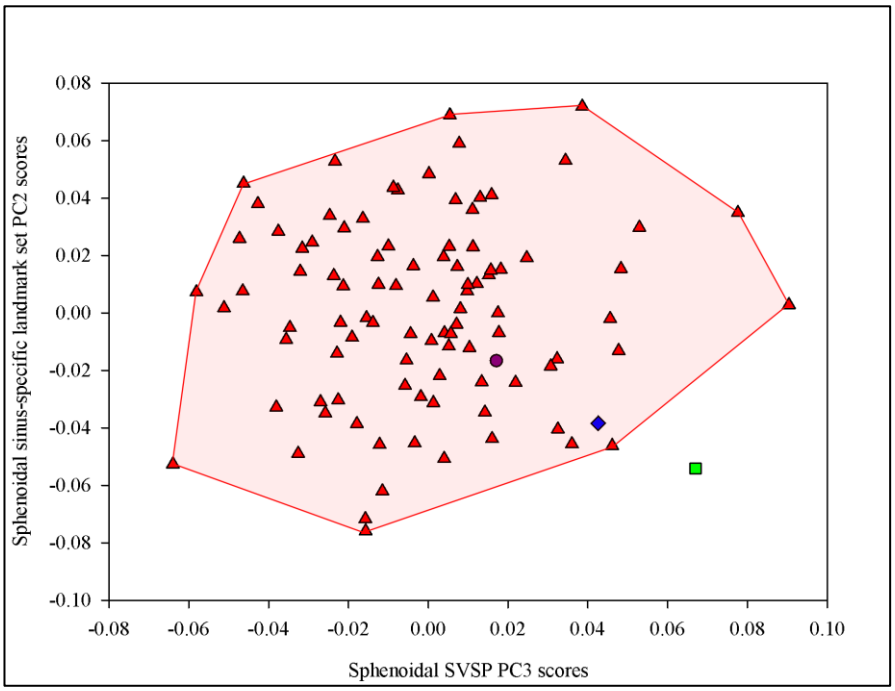

Table 80: PCA of sphenoidal SVSP PC3 scores by sphenoidal sinus-specific landmark set PC2 by taxon. Red triangles: recent *H. sapiens*, green square: *H. neanderthalensis*, purple circle: *H. heidelbergensis*. Convex hull added post-hoc for ease of visualisation. On average, *H. sapiens* scores lower on sphenoidal SVSP PC3 than *H. neanderthalensis*, but this result should be interpreted with caution, as there is only one Neanderthal in this sample.

With such small fossil sample sizes, it is difficult to draw conclusions about differences between the placements of taxonomic groups on sphenoidal SVSP PC3; all three fossil specimens fall within the range of *H. sapiens* variation on this SVSP.

Despite the overlap, there are significant differences between taxonomic groups, but these should be treated with caution:

- **Sphenoidal SVSP PC3 by taxon:** $R = 0.31$, $r^2 = 0.10$, $p < 0.05$. NS with Bonferroni correction.

This is due to a large (but not robust) significant difference between *H. neanderthalensis* and *H. sapiens*, with *H. sapiens* on average scoring lower on sphenoidal SVSP PC3 than *H. neanderthalensis*:

- ***H. neanderthalensis* x *H. sapiens* on sphenoidal SVSP PC3:** $R = 0.6$, $r^2 = 0.36$, $p < 0.05$. NS with a Bonferroni correction.

Taxonomic differences on sphenoidal SVSP PC6

There are no significant taxonomic differences on sphenoidal SVSP PC6.

4.III. RQ1.c: Are the sinuses homologous across type?

Most theories for sinus function assume the sinus types are homologous, but, in her thesis, Tillier (1975) argued that this was unlikely to be the case, as some were much more variable than others, and she found no correlation between volumes of different types within the same individual, suggesting some degree of modularity. The question of homology was investigated here by examining intra-group variation and covariation between sinus types in the current sample, which is larger and more

geographically representative than that of Tillier, whilst still including many important fossil specimens.

4.III.a. Intra-group variation between sinus types

When coefficients of variation within taxa are compared, the frontal sinus displays much more variation than the maxillary sinus for all taxa (Figure 82). Where it is possible to examine the sphenoidal sinus (only in the recent *H. sapiens* sample), it is intermediately variable between these two (Figure 82). This pattern extends to intra-population variation in recent *H. sapiens* (Figure 81). The order of most to least variable sinus runs from frontal to sphenoidal to maxillary for all but the West African population, where the coefficient of variation for the sphenoidal sinus is the most variable, and the Chinese population, where the frontal and sphenoidal sinuses are the same. The maxillary sinus has the lowest variation in every population. The intra-population coefficients of variation are also more similar for the maxillary sinuses than in other sinuses; they vary most in the frontal sinus. Figure 82 also shows that *H. sapiens* is not the most variable taxon in terms of sinus volumes. *H. neanderthalensis* seem to display little within-taxon pneumatic variation. These results should be interpreted with caution due to the small fossil sample sizes.

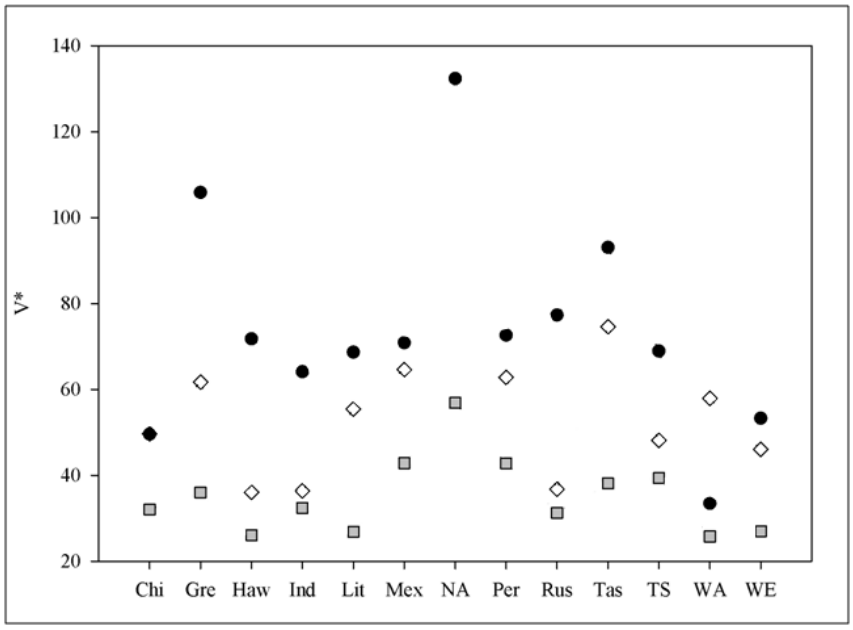

Figure 81: Scatter and line plot showing intra-population variation (V*) in different sinus types. Black circles: frontal sinus; white diamonds: sphenoidal sinus; grey squares: maxillary sinus. It was not possible to calculate V* for the sphenoidal sinuses of the North African sample as they were insufficiently well preserved to measure the sphenoidal sinus. Chi: Chinese; Gre: Greenland; Haw: Hawaii; Ind: India; Lit: Lithuania; Mex: Mexico; NA: North Africa; Per: Peru; Rus: Russia; Tas: Tasmania; TS: Torres Straits; WA: Western Africa; WE: Western Europe.

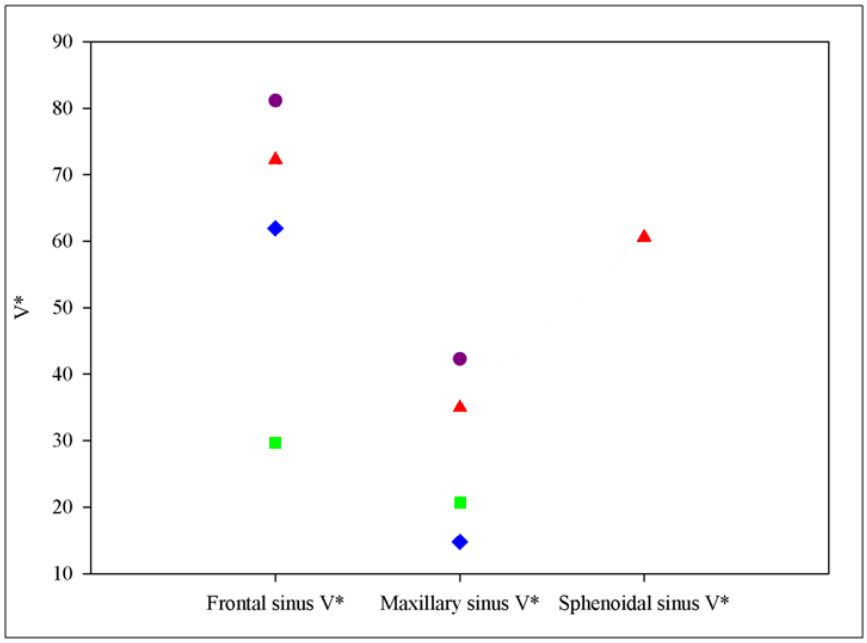

Figure 82: Scatter and line plot showing intra-taxon coefficient of variation (V*) in different sinus types. Purple circles: *H. heidelbergensis*; red triangles: recent *H. sapiens*; blue diamonds: early *H. sapiens*; green squares: *H. neanderthalensis*. It was not possible to calculate V* for the sphenoidal sinuses of the fossil taxa due to only one specimen of each taxon being sufficiently well preserved to measure the sphenoidal sinus.

4.III.b. Covariation between sinus types

The current results show significant, but not particularly large, positive correlations between all three types of sinus (see also Figure 81); if one sinus is large, then the others also tend to be large. The relationship with the largest effect size is between the relative sphenoidal and maxillary sinus volumes and the smallest between the frontal and maxillary sinuses. This pattern is true for both recent *H. sapiens* (Table 40) and all taxa (Table 41). This may be because, even in the mixed taxa sample, the great majority of specimens are recent *H. sapiens*.

Table 40: Non-parametric (Spearman's Rho) correlation tests between relative sinus volumes in recent *H. sapiens*. Significant p values are highlighted in red. *: significant with a Bonferroni correction. n = 102 for all analyses.

Sinuses	r_s	r_s^2	p
Frontal & maxillary	0.24	0.06	0.0001*
Frontal & sphenoidal	0.39	0.15	0.0001*
Sphenoidal & maxillary	0.45	0.21	0.0001*

Table 41: Results from non-parametric (Spearman's Rho) correlation tests between relative sinus volumes including all taxa. Significant p values are highlighted in red. *: significant with a Bonferroni correction. *H. s*: *H. sapiens*; *H. n*: *H. neanderthalensis*; *H. h*: *H. heidelbergensis*.

Sinuses	n	Recent *H. s*	Early *H. s*	*H. n*	*H. h*	r_s	r_s^2	p
Frontal & maxillary	118	111	2	3	2	0.33	0.11	0.0002*
Frontal & sphenoidal	111	108	1	1	1	0.35	0.12	0.0001*
Sphenoidal & maxillary	106	104	1	0	1	0.55	0.30	0.000003*

4.IV. Summary

4.IV.a. RQ1.a: Are there differences in sinus variables between populations of recent *H. sapiens*?

4.IV.a.i. Population differences in relative sinus volumes

The existence of between-population differences in sinus volume seems to depend on sinus type, but, where they exist, they are slight. There are some significant differences in relative frontal sinus volume among populations of recent *H. sapiens*, but these are not robust, as they do not remain significant when a Bonferroni correction is applied. The differences are not due to population history. There are no appreciable differences in maxillary or sphenoidal sinus volumes between populations of recent *H. sapiens*.

Intra-population variation (as measured by coefficients of variation) also differs between the sinus types; this appears to be a real difference, and not one driven by sample inadequacy. There is a substantial amount of intra-population variation in relative frontal sinus volumes between different recent *H. sapiens* populations. These differences do not seem to be due to problematic population combination, or differences in type of CT data, but they do show some relationship with sample size. In their relative maxillary sinus volumes, the North African population is highly variable, which may be due to the small sample size for this group. In general, however, sample size does not seem to affect within-population variation in recent *H. sapiens* relative maxillary sinus volumes and the same is true for the type of CT data and the grouping of specimens in populations. As with the other types of sinus,

the levels of intra-population variation in sphenoidal sinus volume differ widely between geographic populations of recent *H. sapiens*, but this does not appear to be related to the type of CT data, to sample size in individual populations, nor to potential problems in combining specimens in population groups. Therefore, it can be concluded that the recent *H. sapiens* sinus volume results are not substantially affected by potential error in data type, group composition, or sample size.

4.IV.a.ii. Population differences in SVSPs

There are differences in sinus volume-related craniofacial shape among populations of recent *H. sapiens*. There are small population differences on full landmark set frontal SVSP PC3 between populations, but they do not remain statistically significant when a Bonferroni correction is applied, despite a visible separation along this SVSP, supporting the idea that the correction is over-conservative. Greenland, Hawaii, and China are quite distinct from the other populations. All three of these populations fall on the lower end of the SVSP, which is associated with relatively large frontal sinuses and more dolichocephalic neurocrania, smaller face, and larger supraorbital region when compared to higher scoring shapes. A small, but significant correlation between geographic and full landmark set frontal SVSP PC3 distances supports the hypothesis that some of the placement of specimens on this SVSP is due to a weak population history effect. There are some recent *H. sapiens* population differences on frontal SVSP PC6 but they are extremely small. The most robust difference is between Western Europe and Lithuania at the low end of the PC (larger sinuses), China in the middle, and Hawaii and Mexico at the high end of the PC (smaller sinuses). The lower end of frontal SVSP PC6 is associated with large

frontal regions, deep supraorbital regions and taller maxillary regions. A significant correlation between geographic distance and distance on frontal SVSP PC6 (although small) shows a minor effect of population history on this aspect of frontal sinus-related morphology. There is some limited separation between populations on maxillary SVSP PC3, the most robust of which is between Greenland Inuit (low scoring) and Western Europeans (high scoring). Large sinuses on this SVSP are associated with high scores and with a larger, more projecting faces, less angled malar regions, and more dolichocephalic neurocrania. The pattern of differences between populations does not correspond to population history. There were no population differences between recent *H. sapiens* populations for any of the sphenoidal sinus shape parameters.

4.IV.b. RQ1.b: Are there differences in sinus variables between Mid-Late Pleistocene taxa?

4.IV.b.i. Taxonomic differences in relative sinus volumes

There is a moderate, robust significant difference between frontal sinus volumes in *H. heidelbergensis* and *H. sapiens/H. neanderthalensis*, with *H. heidelbergensis* showing much larger relative volumes. Relative maxillary sinus volumes are significantly smaller in *H. sapiens* than both *H. neanderthalensis* and *H. heidelbergensis*; this appears to be due in part to weak positive allometry between cranial size and relative maxillary sinus volume across all taxa. This size relationship is not seen within *H. sapiens*, and the samples are too small to test for such a relationship within the fossil taxa. The sphenoidal sinus volumes of all the

measureable fossil specimens fall within the range of variation seen in recent *H. sapiens* relative sphenoidal sinus volumes; therefore, based on this sample, it cannot be shown that there are taxonomic difference in relative sphenoidal sinus volumes.

Investigation of intra-taxon variation shows some of the differences in volumes may be due to sample composition. There is high variation in frontal sinus volume in the putative *H. heidelbergensis* group due to the inclusion of (the taxonomically disputed) Ceprano, which seems to have an anomalously small frontal sinus for that taxon. Recent *H. sapiens* is also very variable in relative frontal sinus volume, whilst *H. neanderthalensis* shows very low levels of variation. If divided along species lines, the highest levels of intra-group variation in relative maxillary sinus volume are in *H. heidelbergensis*, followed by recent *H. sapiens*. This is the same as for the frontal sinus, but is contrary to expectations if *H. sapiens* is a particularly plastic species. As with frontal sinus volumes, the maxillary sinus is not highly variable in the *H. neanderthalensis* sample. Variation in relative maxillary sinus volume is lowest in early *H. sapiens*, but this (and the *H. heidelbergensis* result) may be due to sample size. It was not possible to investigate taxonomic differences in intra-taxon variation in relative sphenoidal sinus volume because of sample size.

4.IV.b.ii. Taxonomic differences in SVSPs

There are taxonomic differences in sinus-related craniofacial shape for all sinus types. *H. sapiens* scores moderately significantly higher on frontal SVSP PC6 than *H. heidelbergensis* and the low scores of the latter are associated with relatively larger frontal sinuses, larger frontal regions, including taller supraorbital regions, and

taller faces. There is also marked taxonomic differentiation along maxillary SVSP PC3. *H. sapiens* scores significantly lower than both *H. neanderthalensis* and *H. heidelbergensis* on this SVSP. At the upper end of maxillary SVSP PC3 (larger maxillary sinuses) configurations have larger, more projecting faces relative to their neurocrania, which are more dolichocephalic than those at the lower end. Frontal bones in crania with shapes associated with relatively larger maxillary sinuses on maxillary SVSP PC3 are more posteriorly sloping and their zygomatic arches are more swept back. *H. neanderthalensis* scores strongly significantly higher on sphenoidal SVSP PC3 than *H. sapiens*, which denotes relatively larger sphenoidal sinuses and a broader, (superoinferiorly) shorter neurocranium, in which the anterior portion is relatively expanded compared to low scoring configurations. Despite the size of the difference, it is not robust to a Bonferroni correction and it rests on a single individual; given the overlap visible in the data, the result may well be due to chance.

4.IV.c. RQ1.c: Are the sinuses homologous across types?

The sinus types do not show the same amount of intra-group variation: the frontal sinus is much more variable than the maxillary sinus for all taxa and the sphenoidal sinus appears to be intermediate. The same pattern extends to intra-population variation in recent *H. sapiens*. This result suggests that the sinus types vary due to different stimuli and are not homologous. However, there are significant, positive correlations between the sizes of all three types of sinus. The relationship with the largest effect size is between the relative sphenoidal and maxillary sinus volumes and the smallest is between the frontal and maxillary sinuses; this appears to be the

case for all taxa. This suggests there is some shaping force common to all the sinus types. In combination, these two conflicting results suggest that the sinus types are affected by some of the same stimuli, but that they are also free to respond to local, individual stimuli.

Chapter 5: Results – Interactions between masticatory stress/strain and sinus variables

Chapter 5 is concerned with research question 2: are there interactions between masticatory stress/strain and sinus variables? Biomechanical stresses and strains resulting from mastication are one of the key factors determining primate craniofacial morphology (Antón, 1996; Larsen, 1997; Viguier, 2004; Pucciarelli *et al.*, 2006; von Cramon-Taubadel, 2009b) and dissipation of masticatory strains is also proposed as a function for paranasal sinuses (Greene & Scott, 1973; Bookstein *et al.*, 1999; Prossinger *et al.*, 2000; Rae & Koppe, 2004; Fitton *et al.*, 2013). In the current thesis, the relationships between masticatory stress/strain and sinus variables (sinus volumes and sinus volume shape parameters, SVSPs – see Chapter 3) are examined in a large group of hominins with a range of subsistence strategies. In Section 5.I, shape variables found to be significantly different between subsistence groups are identified and designated masticatory shape parameters (MSPs). In Section 5.II and 5.III sinus variables are tested for relationships with MSPs. Differences between subsistence groups are also examined as an additional means of testing for differences in sinus variables in groups assumed to have had contrasting masticatory stress/strain regimes.

5.I. Generating shape proxies for masticatory stress/strain

To establish differences in temporalis region shape between subsistence groups assumed to have experienced different levels of masticatory stresses/strains, a masticatory landmark set previously validated by Paschetta *et al*. (2010), was used (Table 42, Section 2.IV.b.ii.) on all specimens in the sample for which these six landmarks were preserved. As discussed in Section 2.IV.b., this landmark set was used because it had been shown to capture shape differences between members of the (presumed) same population with different diets, thus avoiding some of the possible confounding genetic/dietary contributions to shape differences between different populations with different diets. Given that dietary data of sufficient detail was unavailable for the sample, it was judged that Paschett *et al*.'s shape differences were a reasonable proxy.

Table 42: Masticatory sample: specimens used in masticatory landmark set analyses.

Group	Number of specimens in sample	Name/number of specimens in masticatory landmark set
China	10	10
Greenland	7	7
Hawaii	10	10
India	10	10
Lithuania	10	10
Mexico	10	9
North Africa	6	3
Peru	10	10
Russia	4	3
Tasmania	8	8
Torres Straits	10	9
Western Africa	10	10
Western Europe	10	10
Fossil *H. sapiens*	6	Skhul 5 Mladeč
H. neanderthalensis	9	La Chapelle La Ferrassie
H. heidelbergensis	5	Kabwe Petralona
H. erectus	4	KNM-ER 3733
Total		**116**

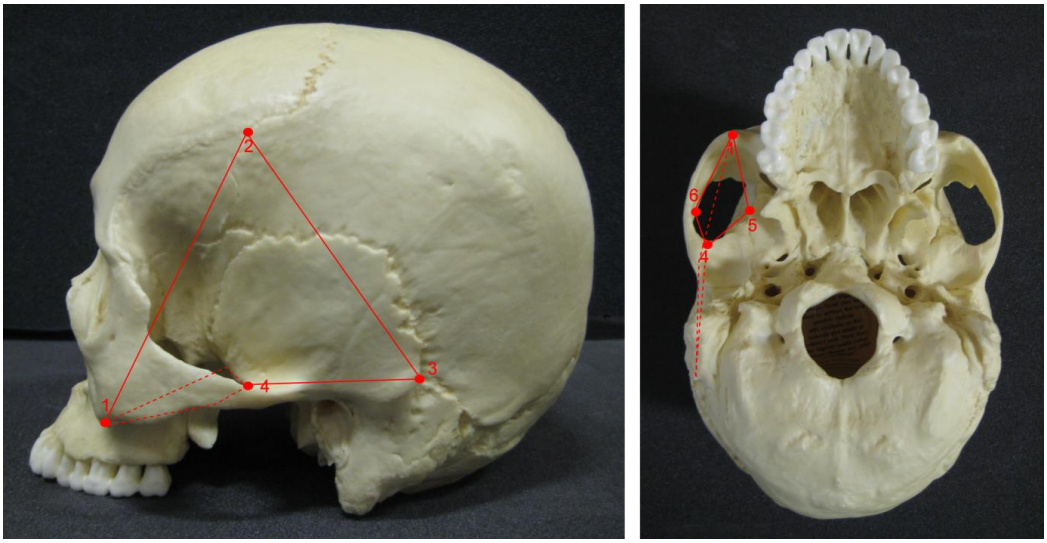

Figure 83: Landmarks and wireframe for masticatory landmark set, following Paschetta *et al.*, 2010. Dotted lines show parts of wireframe not visible when cranium is shown. 1: zygomaxillare, 2: stephanion, 3: enthomion, 4: posterior infratemporal fossa, 5: MW1, 6: MW2 (for definitions, see Table 12). The landmark set approximates the size and shape of the temporalis. Numbering refers to this study, not the original. Photos by the author.

Masticatory landmark data were tested for error and then analysed using geometric morphometric methods as previously described (see Section 2.III.c.ii.). Following screeplot and eigenvalue inspection (see Figure 84 and Table 43), the first three principal components from the analysis of the masticatory landmark set (accounting for >70% variance, as for the majority of geometric morphometric analyses in this study) were analysed further.

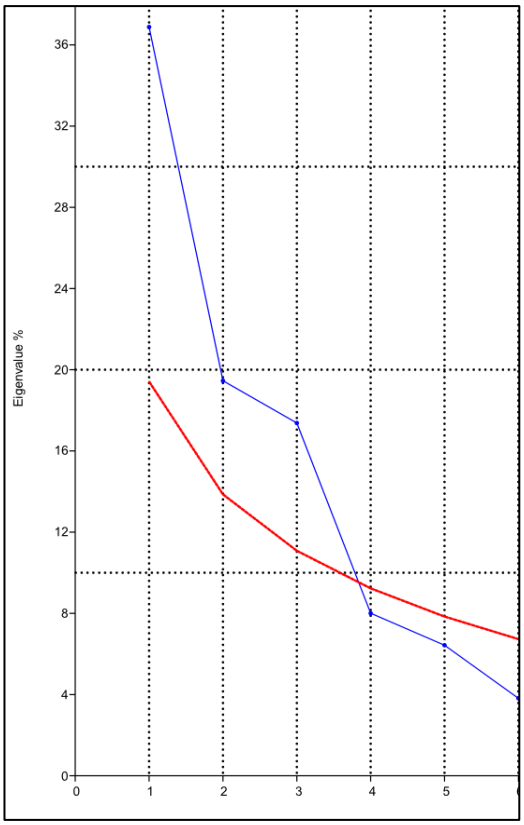

Figure 84: Scree plot of masticatory landmark set PCA showing that first 3 PCs are likely to be of interest.

Table 43: Table of eigenvalues and variance explained for first three principal components of masticatory landmark set analysis. The first three PCs account for > 70% of variance, so these are used in subsequent analyses (see Methods).

Principal component	Eigenvalue	Proportion of variance explained	Cumulative variance explained
1	0.004	0.37	0.37
2	0.002	0.20	0.56
3	0.002	0.17	0.74

For PC1-3, t-tests were performed to test for significant differences in PC scores between subsistence groups. No significant difference was found on PC1. A small, significant difference was found between subsistence groups on PC2, and a slightly larger one on PC3 (see Figure 85):

- **Masticatory landmark set PC2 by subsistence group:** T test: $t(115) = -2.98$, $r^2 = 0.08$, $p < 0.005$.
- **Masticatory landmark set PC3 by subsistence group:** T test: $t(62.62) = 2.68$, $r^2 = 0.10$, $p < 0.01$.

Notwithstanding a considerable degree of overlap on both PCs, on PC2 the domestic species consumers (DOM) group have, on average, significantly higher scores than the Forager group and, along PC3, the DOM group have significantly lower scores than the Forager group. Differences on both PCs remain significant if Bonferroni correction is applied.

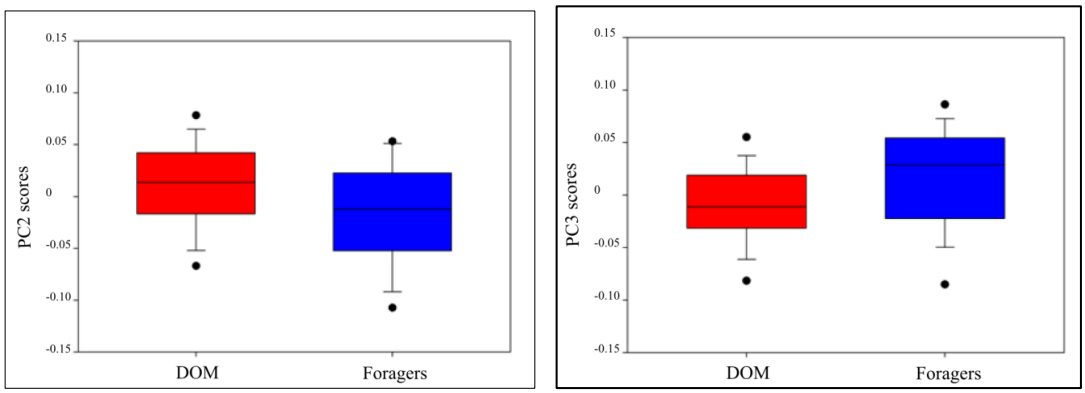

Figure 85: Differences between subsistence groups on PCs from masticatory landmark analysis. Left: PCs scores on PC2, DOM score significantly higher than Foragers. Right: PC scores for both groups on PC3, Foragers scores significantly higher than DOM.

Since they showed significant differences between subsistence groups, and the landmark set was designed to show differences in temporalis shape, PC2 and PC3 were held to show differences in temporalis region shape associated with levels of masticatory strain as shown by Paschetta *et al*., 2010, see Section 2.IV.b.ii. The shape differences represented by these PCs were modelled and are described in Section 5.I.a and 5.I.b (PC2 and PC3 respectively). These two PCs were designated masticatory shape parameters (MSPs), and were used as shape variables showing differences in masticatory strain in subsequent analyses.

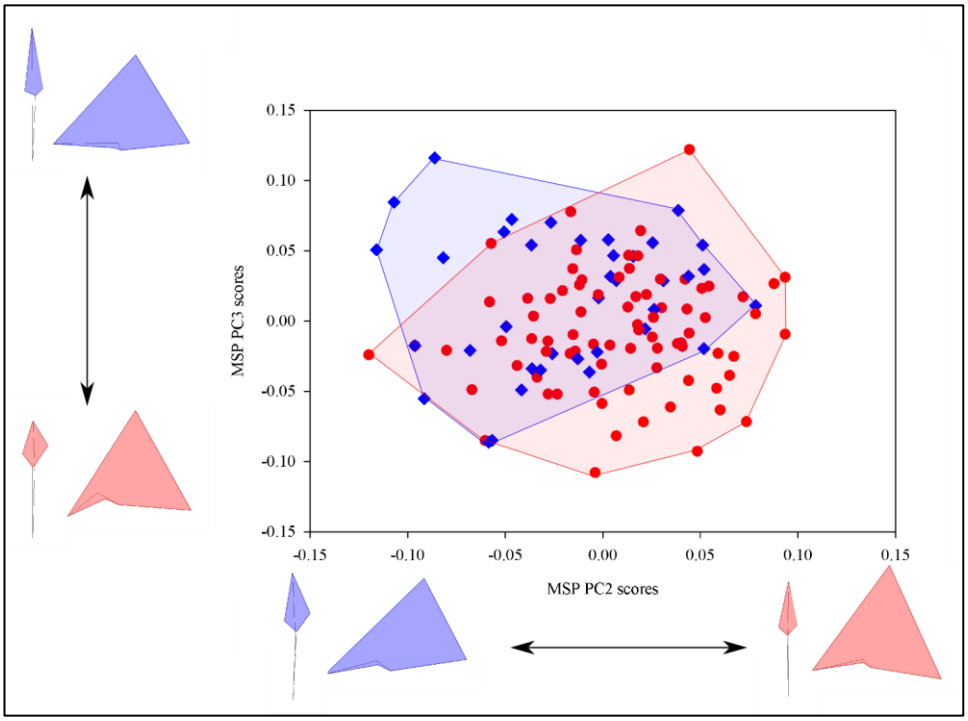

Figure 86: Shape differences as represented by MSPs from masticatory landmark analysis. X axis is MSP PC2, y axis is MSP PC3. Wireframes represent landmark configuration reconstructions at extremes of axes in norma basalis and norma lateralis. Red circles: DOM, blue diamonds: Foragers. Colour of wireframes indicates the significant differences found between subsistence groups on the two MSPs: red wireframes show the DOM group, blue wireframes show the Forager group. Convex hulls added post-hoc for ease of visualisation.

5.I.a. Shape differences described by MSP PC2

On PC2, in norma lateralis (Figure 87), the wireframe shows that the temporalis region is shorter anteroposteriorly and taller superoinferiorly in shapes with higher scores (more likely to be DOM). This produces a temporalis shape that appears more like an equilateral triangle, rather than a scalene triangle (lower scores: Foragers). Relative to other landmarks, at higher scores, zygomaxillare (1) is further posterior and stephanion (2) is more anteriorly placed. This decreases the distance between the furthest point anterior and the furthest point superior in the masticatory landmark set. In higher scoring configurations, enthomion (3) is more inferior, which increases the distance between the most superior and most posterior points in the masticatory landmark set (Figure 87). These differences illustrate a superoinferiorly taller, anteroposteriorly shorter temporalis in DOM (as described by this PC alone).

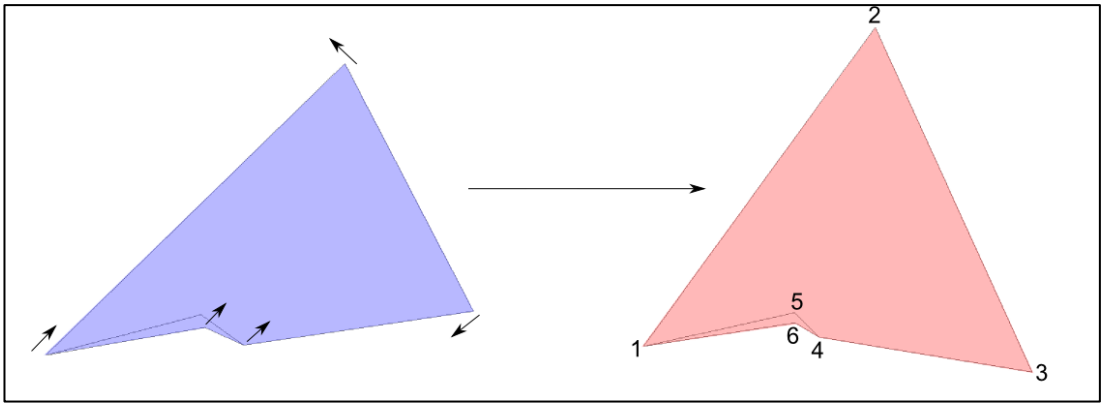

Figure 87: Wireframes of shape differences on PC2 of the masticatory landmark set analysis in norma lateralis. Left shows lowest extreme on PC2, right shows highest extreme. Numbers indicate landmark numbers (see Figure 81 for landmark numbers). Arrows on left hand diagram show directions landmarks move relative to one another to achieve the configuration in the right hand diagram. Foragers (blue wireframe) are more likely to have low scores on PC2, DOM (red wireframe) are more likely to have high scores on PC2.

In norma basalis (Figure 88), the diamond formed by the wireframe lines connecting zygomaxillare (1), posterior infratemporal fossa (hereafter referred to as PIF) (4),

MW1 (5), and MW2 (6) becomes mediolaterally narrower in configurations with higher scores on PC2 (more likely to be DOM). Relative to other landmarks MW1 and MW2 move posteriorly and closer to one another (that is, MW1 moves medially, and MW2 moves laterally). This PC demonstrates a mediolaterally narrower temporalis at high scores (more likely to be DOM).

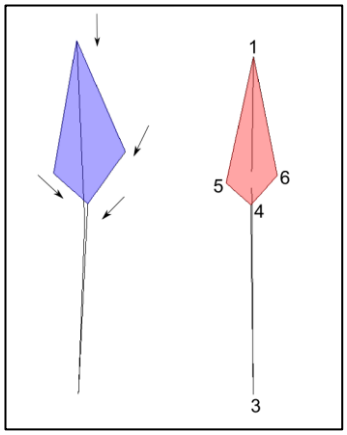

Figure 88: Wireframes of shape differences on PC2 of the masticatory landmark set analysis in norma basalis. Left shows lowest extreme on PC2, right shows highest extreme in norma basalis. Numbers indicate landmark numbers. Arrows on left-hand diagram show directions landmarks move relative to one another to achieve the configuration in the right hand diagram. Foragers (blue wireframe) are more likely to have low scores on PC2, DOM (red wireframe) are more likely to have high scores on PC2.

5.I.b. Shape differences described by MSP PC3

In norma lateralis (Figure 89), configurations at the low end of PC3 (more likely to be DOM) are shorter anteroposteriorly than those at the higher end as with PC2, but the greatest difference between the two extremes of this component are in the relative relationship between the landmarks at the base of the wireframes. In individuals scoring low on PC3 (more likely to be DOM), MW1 (5), MW2 (6), and PIF (4) are superiorly placed relative to zygomaxillare (1) and enthomion (3); in individuals at the higher end of PC3 (more likely to be Foragers), MW1, MW2, and PIF are much more inferiorly placed, relative to zygomaxillare and enthomion. This

means that the zygomatic arch moves inferiorly relative to the zygomaxillare and the most posterior point on the temporal fossa. From this viewpoint, shapes at the lower end of the PC have a superoinferiorly taller anterior temporalis, with a relatively much lower anterior attachment and more superiorly placed temporal fossa.

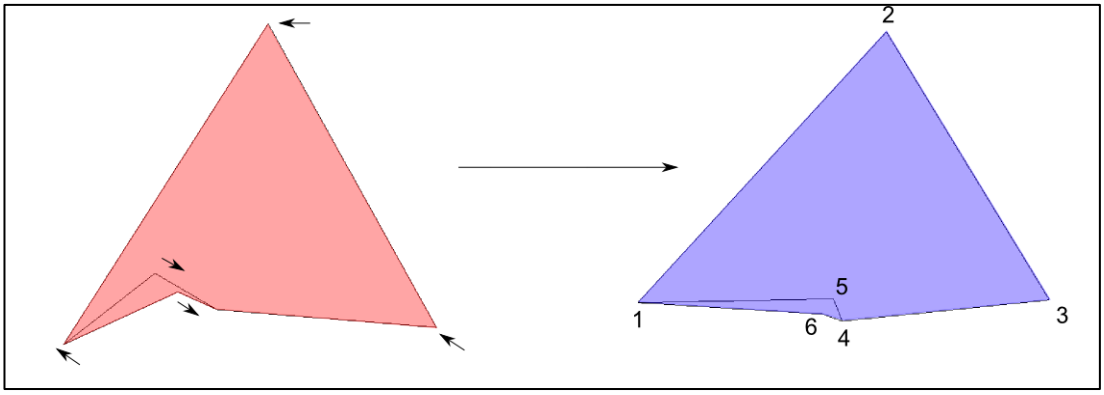

Figure 89: Wireframes of shape differences on PC3 of the masticatory landmark set analysis in norma lateralis. Left shows highest extreme on PC3, right shows lowest extreme in norma lateralis. Numbers indicate landmark numbers. Arrows on left hand diagram show directions landmarks move relative to one another to achieve the configuration in the right hand diagram. Foragers (blue wireframe) are more likely to have low scores on PC2, DOM (red wireframe) are more likely to have high scores on PC2.

In norma basalis wireframes, individuals at the lower end of PC3 (more likely to be DOM) show a much squatter diamond shape formed by the wireframe connecting zygomaxillare (1), PIF (4), MW1 (5) and MW2 (6), than configurations at the upper end. This is partly the effect of the viewpoint, however, since the inferoanterior projection of the temporal fossa seen in norma lateralis (Figure 90) is not visible from beneath. The temporal fossa is broader mediolaterally in low-scoring specimens on this PC. Relative to other landmarks, the change from low to high scores in PC3 describes a superoanterior movement in zygomaxillare and a posteromedial movement in MW1 and MW2, particularly MW2. This demonstrates an anteroposteriorly shorter, mediolaterally thicker temporalis muscle at lower PCs (more likely to be DOM) as represented solely by this PC.

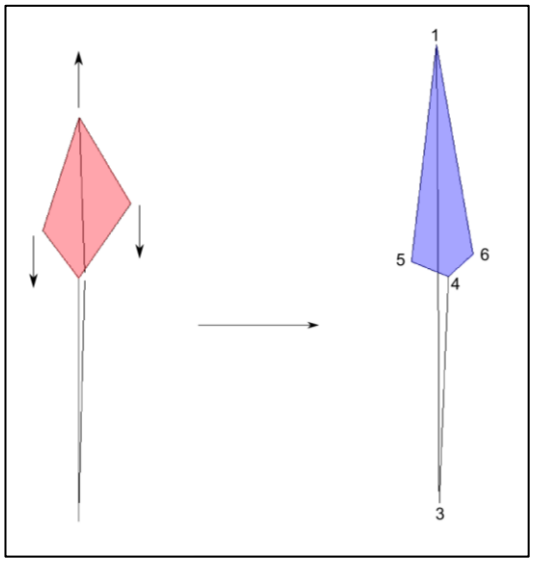

Figure 90: Wireframes of shape differences on PC3 of the masticatory landmark set analysis in norma basalis. Left shows highest extreme on PC3, right shows lowest extreme in norma basalis. Numbers indicate landmark numbers. Arrows on left hand diagram show directions landmarks move relative to one another to achieve the configuration in the right hand diagram. Foragers (blue wireframe) are more likely to have low scores on PC2, DOM (red wireframe) are more likely to have high scores on PC2.

5.I.c. Summary – shape differences in the temporalis related to dietary differences in masticatory strain

There is a moderately small but robust difference between DOM (assumed to experience relatively lower masticatory stress/strain) and Foragers (assumed to experience relatively high masticatory stress/strain) on two PCs: PC2 and PC3. DOM have, on average, significantly lower scores on the former and higher on the latter, the reverse is true for Foragers. Together, these PCs account for 37% of variance in masticatory landmark configurations in the sample. Between a half and a third of the variation in temporalis shape, as described by this landmark set, shows significant differences between subsistence groups. These shape variables were taken to represent shape differences in the temporalis muscle corresponding to differing levels of masticatory strain and were used in subsequent analyses as such.

From the combination of PC2 and PC3 of the masticatory landmark set (MSPs), it is possible to show that the Foragers have, in general, an anteroposteriorly longer and superoinferiorly shorter temporalis muscles in norma lateralis. The most anterior point of the temporalis (as measured by MSP2 and 3) is relatively superiorly placed, and the temporal fossa relatively inferiorly placed in the masticatory landmark set. From the base of the cranium, one can see that the temporal fossa in Foragers also appears to be longer anteroposteriorly when compared to that of DOM, but this is partly due to the fact it bends further inferiorly in DOM when compared with foragers (Figure 89).

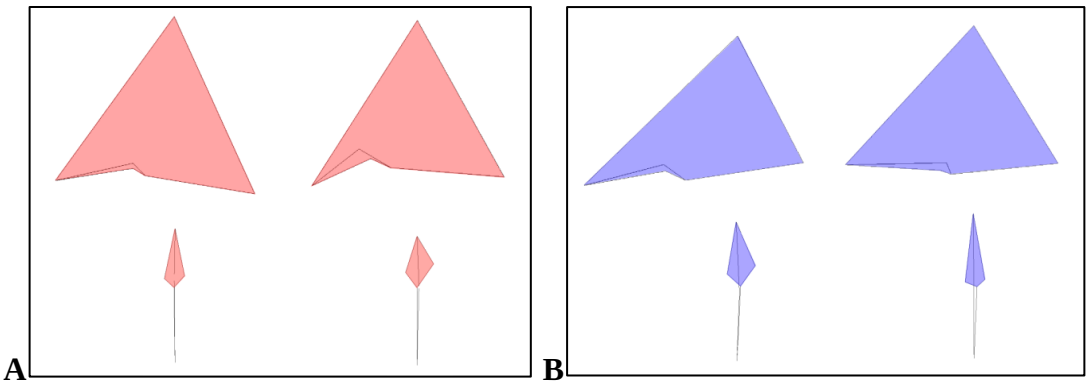

Figure 91: Wireframes of PC2 and PC3 of masticatory landmark set combined to show temporalis region shape (as described by these two PCs) of DOM and Foragers. A: DOM wireframes. DOM group is at high end of masticatory landmark set PC2 and low end of masticatory landmark set PC3. B: Forager wireframes. Forager group is at low end of masticatory landmark set PC2, high end of masticatory landmark set PC3. For both A & B: Left: PC2, right: PC3. Top: norma lateralis, bottom: norma basalis.

5.II. RQ2: Are there interactions between masticatory stress/strain and sinus volume shape parameters?

PC2 and PC3 of the masticatory landmark set, which were found to significantly differentiate between DOM and Foragers in 5.I, were used as masticatory shape parameters in analyses with sinus variables in 5.II and 5.III. This was to ascertain

whether shape differences associated with masticatory strain showed relationships with sinus volume, either directly, or indirectly via craniofacial morphology previously shown to be linked to sinus volume (SVSPs). Differences in sinus variables between subsistence groups were also investigated for comparison with relationships with MSPs.

5.II.a. Differences in relative sinus volume between subsistence groups

For sinus volume analyses sample composition, see Chapter 4.

There is no significant difference between DOM and Forager groups in relative frontal sinus volume or maxillary sinus volume.

Despite considerable overlap (see Figure 92), there is a small significant difference in relative sphenoidal sinus volume between Foragers and DOM, with foragers having significantly smaller sphenoidal sinuses:

- **Relative sphenoidal sinus volume by subsistence group:** $t(112) = -2.70$, $r^2 = 0.07$, $p < 0.05$. Not significant (NS) with a Bonferroni correction.

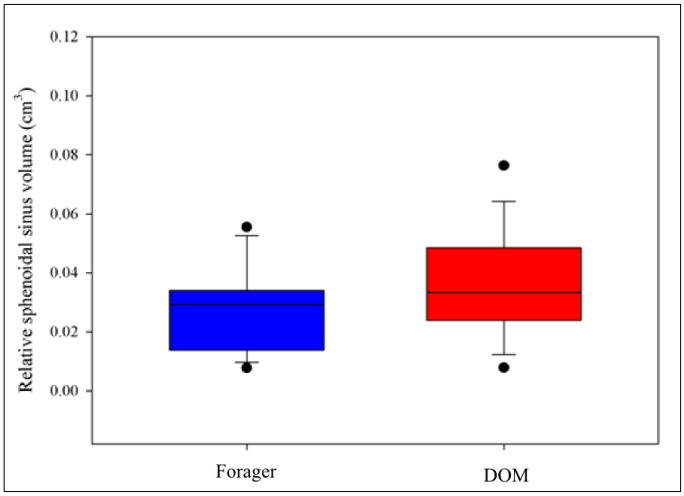

Figure 92: The significant difference in relative sphenoidal sinus volumes between Forager and DOM groups.

5.II.b. Relationships between relative sinus volume and masticatory shape parameters

There is no significant relationship between relative frontal sinus volume, relative maxillary sinus volume, or relative sphenoidal sinus volume and MSP PC2 or PC3.

5.III. RQ2: Are there interactions between masticatory stress/strain and sinus volume shape parameters?

In this section, analyses test whether there is a relationship between PC score on MSPs, which reflects temporalis muscle shape (a proxy for masticatory stress/strain), and sinus volume-related craniofacial morphology, as shown by SVSPs. For sample composition of each SVSP, see Chapter 3.

5.III.a. Differences in sinus volume shape parameters between subsistence groups

There is no significant difference in SVSP PC score between subsistence groups for any of the frontal, maxillary, or sphenoidal SVSPs.

5.III.b. Relationships between sinus volume shape parameters and masticatory shape parameters

5.III.b.i. Relationships between frontal SVSPs and MSPs

Neither full landmark set frontal SVSP PC3, nor frontal SVSP PC6 (frontal specific landmark set) showed a significant relationship with MSP PC2 or PC3.

5.III.b.ii. Relationships between maxillary SVSPs and MSPs

Maxillary SVSP PC3

There is no significant relationship between maxillary SVSP PC3 and MSP PC2.

Maxillary SVSP PC3 showed a small but significant negative relationship with MSP PC3:

- **Maxillary SVSP PC3 x MSP PC3:** Maxillary SVSP PC3 = -0.003 + -1.935 x MSP PC3, $r^2 = 0.06$, $p < 0.05$. NS with Bonferroni correction

This means that the higher end of the MSP (associated with high masticatory strain/Foragers) is associated with the lower end of maxillary SVSP PC3, where

specimens with craniofacial morphology associated with smaller maxillary sinuses tend to fall (Figure 93).

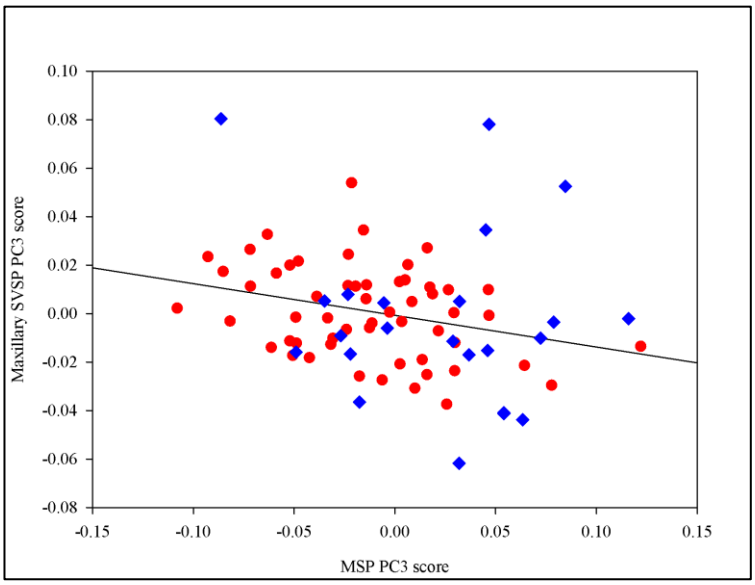

Figure 93: The small, significant, negative relationship between maxillary SVSP PC3 and MSP PC3 scores. Red circles: DOM; blue diamonds: Foragers

The maxillary sinus-related craniofacial morphology associated with the Forager group (the lower end of maxillary SVSP PC3, associated with smaller maxillary sinuses) shows shorter, flatter faces relative to their neurocrania. The neurocrania are rounder and taller superoinferiorly than those at the upper end. Frontal regions are less posteriorly sloping and the maxillary regions are shorter, narrower and less projecting, with a flatter zygomatic arch when seen in norma frontalis. There are also differences in the shape of the dental arcade, with the widest point moving to a more anterior position towards the lower end of the SVSP. These subsistence-related SVSP differences are illustrated in Figure 92, as are the associated temporalis shapes shown by MSP PC3.

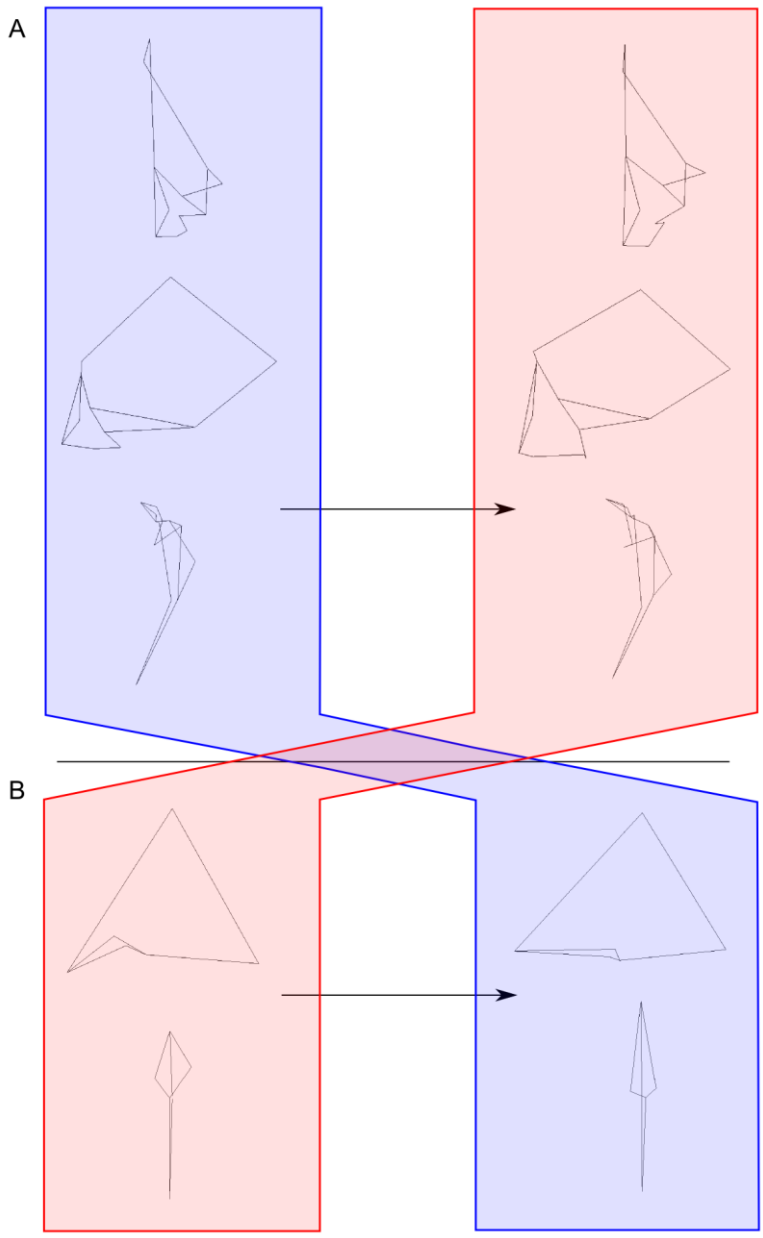

Figure 94: Figure showing wireframes for associated shapes on maxillary SVSP PC3 and MSP PC3. A: Maxillary SVSP PC3, left: lowest extreme of PC, right: highest extent of PC. Top: norma frontalis, middle: norma lateralis, bottom: norma basalis. B: MSP PC3 showing temporalis shape differences between DOM and Foragers. Left: lowest extreme of PC, right: highest extreme of PC. Top: norma lateralis, bottom: norma basalis. Red highlighting: relationship between shapes associated with DOM subsistence (low dietary stress/strain) and small maxillary sinus-related craniofacial morphology. Blue highlighting: relationship between shapes associated with Forager subsistence (high dietary stress/strain) and large maxillary sinuses-related craniofacial morphology.

The potentially confounding effects of shared landmarks

The landmark zygomaxillare is in both the maxillary sinus-specific landmark set (landmark 8, Table 12) and the masticatory landmark set (landmark 1, Table 12). This could have resulted in an inflated relationship between MSP PC3 and maxillary SVSP PC3. The eigenvector loadings of zygomaxillare in the two landmark sets are not similar in any of the three dimensions (x, y, or z) (see Appendix 5), suggesting that the landmark contributes to shapes in the two analyses in different ways and that it does not account for the relationship between the two shape parameters. Its lack of importance is also highlighted by the lack of a significant relationship between MSP PC2 and maxillary SVSP PC3, between full landmark set frontal SVSP PC3, and between maxillary SVSP PC7 and either of the MSPs, despite zygomaxillare also being included in both variables in all these analyses. Zygomaxillare is not in the frontal sinus-specific, or the sphenoidal sinus-specific landmark set. Zygomaxillare was not removed from either landmark set when analysing the relationships between them, as it contains substantial information for both shape variables, and because both comprise relatively few landmarks, increasing the relative value of each.

Maxillary SVSP PC7

This SVSP showed no significant relationship with MSP PC2 or PC3.

5.III.b.iii. Relationships between sphenoidal SVSPs and MSPs

Sphenoidal SVSP PC3

There is no significant relationship between sphenoidal SVSP PC3 and MSP PC2.

Sphenoidal SVSP PC3 shows a small, significant negative relationship with MSP PC3:

- **Sphenoidal SVSP PC3 x MSP PC3:** Sphenoidal SVSP PC3 = -0.005 + -1.563 x MSP PC3, $r^2 = 0.06$, $p < 0.05$. NS with Bonferroni correction.

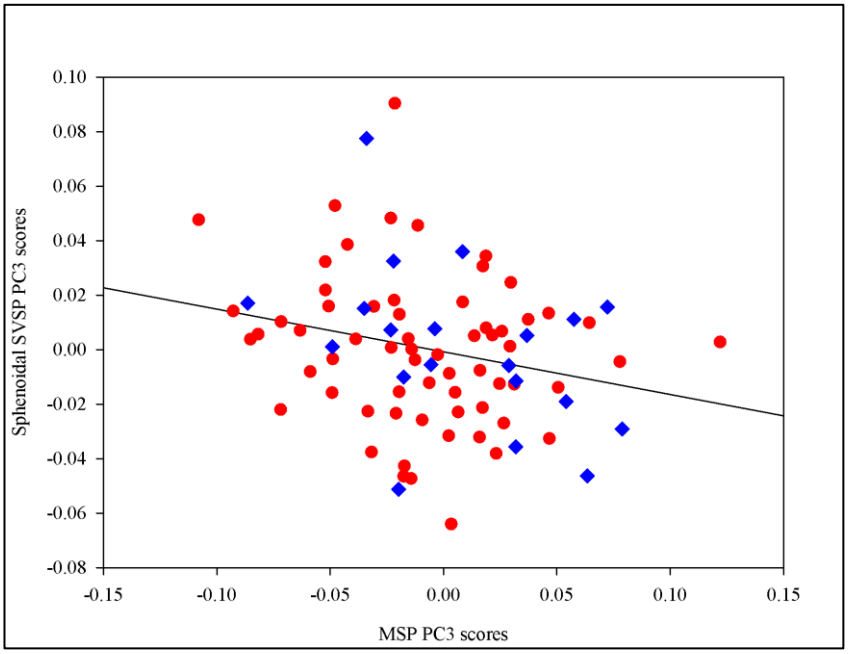

Figure 95: The small, significant, negative relationship between sphenoidal SVSP PC3 and MSP PC3. Red circles: DOM; blue diamonds: Foragers.

Individuals with low scores (linked to with relatively small sphenoidal sinuses) on sphenoidal SVSP PC3 are associated with temporalis shapes linked to high masticatory strains. Crania at the bottom end of sphenoidal SVSP PC3 have mediolaterally narrower and superoinferiorly taller neurocrania, basicrania of shapes at the lower end are also placed inferiorly compared to shapes scoring higher on sphenoidal SVSP PC3. The sphenoidal region itself is both narrower mediolaterally and shallower anteroposteriorly in configurations at the lower end of PC3. There is therefore a weak association between the craniofacial morphology described, which

is linked to smaller sphenoidal sinuses, and higher masticatory strains as shown by the association with MSP PC3.

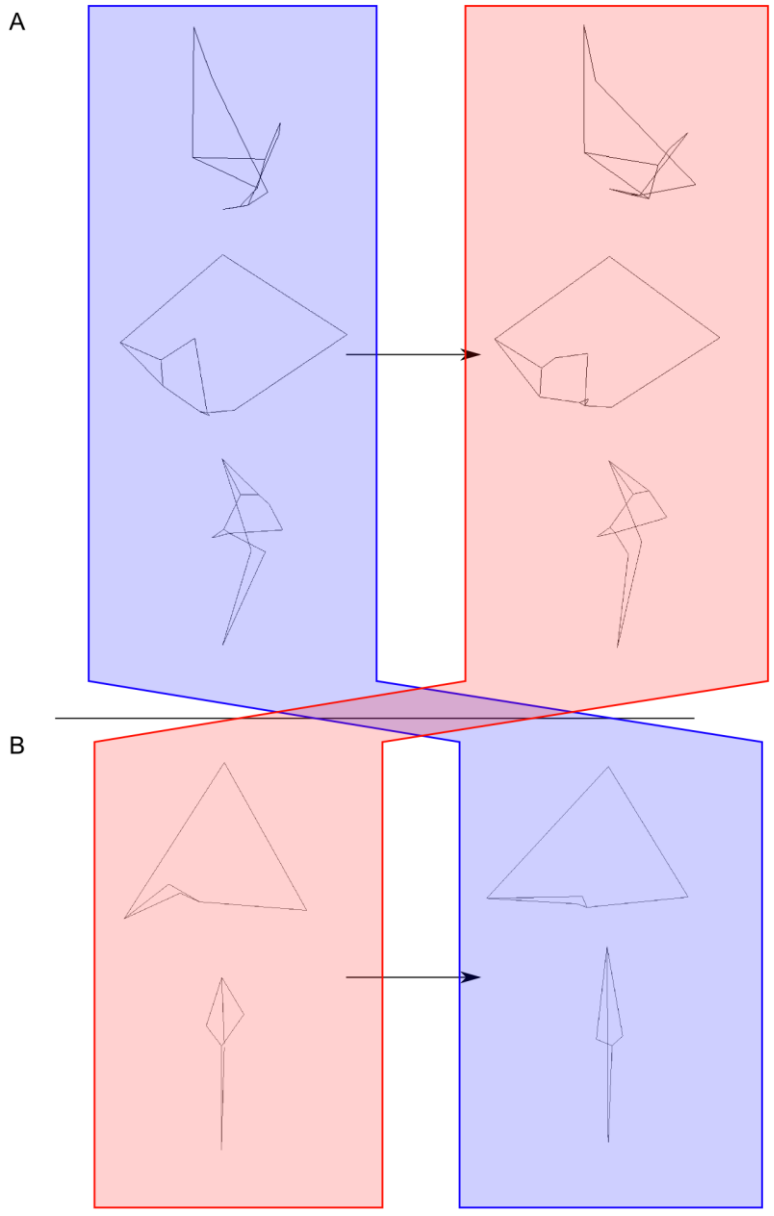

Figure 96: Schematic of relationship between sphenoidal SVSP PC3 and MSP PC3. A: Sphenoidal SVSP PC3, left: lowest extreme of PC, right: highest extent of PC. Top: norma frontalis, Middle: norma lateralis, bottom: norma basalis. B: MSP showing temporalis shape. Left: lowest extreme of PC, right: highest extreme of PC. Top: norma lateralis, bottom: norma basalis. Red highlighting: relationship between shapes associated with DOM subsistence (low dietary stress/strain) and small maxillary sinus-related craniofacial morphology. Blue highlighting: relationship between shapes associated with Foragers (high dietary stress/strain) and large maxillary sinuses-related craniofacial morphology.

Sphenoidal SVSP PC6

There is no significant relationship between sphenoidal SVSP PC6 and either MSP PC2 or PC3.

5.IV. Summary

5.IV.a. RQ2: Relationships between relative sinus volume and masticatory stress/strain

There is no significant difference in relative frontal or maxillary sinus volume between subsistence groups; nevertheless, there is a small, but significant difference (if no Bonferroni correction is applied) in relative sphenoidal sinus volumes, with foragers having significantly smaller relative sphenoidal sinus volumes than DOM.

There is no direct relationship between MSPs and relative sinus volumes. This suggests that there is not a direct relationship between degree of masticatory strain and relative sinus size for any type of sinus.

5.IV.b. Relationships between sinus volume shape parameters and masticatory stress/strain

There is no significant difference in PC scores between subsistence groups for any of the SVSPs.

MSPs show small, but significant, relationships with some aspects of shape reflecting relative maxillary and sphenoidal (but not frontal) sinus volumes. For both

maxillary SVSP PC3 and sphenoidal SVSP PC3, sinus-specific landmark set PCs denoting shapes related to smaller sinus volumes show significant relationships with temporalis shape linked to Forager groups, who are assumed to have a harder diet, and greater masticatory stresses/strains. None of the relationships between SVSPs and MSPs are significant if a Bonferroni correction is applied; this may suggest that the results are merely due to chance. However, the consistency of the relationship between the craniofacial morphology linked to small sinuses and high masticatory strains (or the morphology linked to them) in the maxillary SVSP, the sphenoidal SVSP, and in the sphenoidal sinuses themselves suggests this is not the case.

Chapter 6: Results – interactions between climate and sinus variables

Chapter 6 addresses research question 3: are there interactions between climate and sinus variables? Both high and low temperatures have been invoked as selective pressures resulting in large sinuses (e.g., Koertvelyessy, 1972; Tillier, 1977; Fernandez, 2004b; Irmak *et al.*, 2004). Yet, the geographic scope of samples, and/or the size of samples, in published analyses to date have been low. In the current thesis, these hypotheses are tested by analysing differences in sinus variables (sinus volumes and sinus volume shape parameters, SVSPs – see Chapter 3) in populations of recent *H. sapiens* from a wide range of different climates and a large sample of Mid-Late Pleistocene fossil hominins. Palaeoclimatic modelling was used to reconstruct likely climate categories for the fossil sample, but since it is possible to make far more accurate inferences about the climate experienced by recent *H. sapiens* than the fossil component of the sample, the former group was examined separately and in more detail than the fossils (see Section 2.I.c.i.). In Section 6.I. the relationships between continuous climatic variables and sinus variables are examined in recent *H. sapiens*. In section 6.II. differences in sinus variables between climate categories were investigated in the full sample.

6.I: RQ3.a: Are there differences in sinus variables between populations of recent *H. sapiens* experiencing different climates?

In this section, continuous climate variables are used, the climate variables are (for details, see Section 2.I.c.i.):

- mean annual temperature (MAT)
- maximum monthly temperature (maxTemp)
- minimum monthly temperature (minTemp)
- mean annual precipitation (MAP)
- maximum monthly precipitation (maxPrecip)
- minimum monthly precipitation (minPrecip)

First, the results of analyses on relative sinus volumes, and then SVSPs are presented. The effect of the results of potentially problematic populations (China-cool, Russia, Western Africa and Western Europe - those that combine relatively geographically disparate individuals, see Section 2.IV.a.iii.) are discussed where appropriate in each section.

6.I.a. Relationships between relative sinus volumes and continuous climatic variables in recent *H. sapiens*.

There is no significant relationship between relative frontal sinus volume, or relative maxillary sinus volume, and any continuous climate variable

6.I.a.i. Relationships between relative sphenoidal sinus volume and continuous climatic variables

Temperature

There is a very small, yet significant, positive relationship between relative sphenoidal sinus volume and maxTemp (Figure 97):

- **Relative sphenoidal sinus volume x maxTemp:** reduced major axis regression: Relative sphenoidal sinus volume = -0.0318 + 0.0030 x maxTemp, $p < 0.05$, $r^2 = 0.04$). Not significant (NS) with a Bonferroni correction.

There is no significant relationship with either MAT or minTemp.

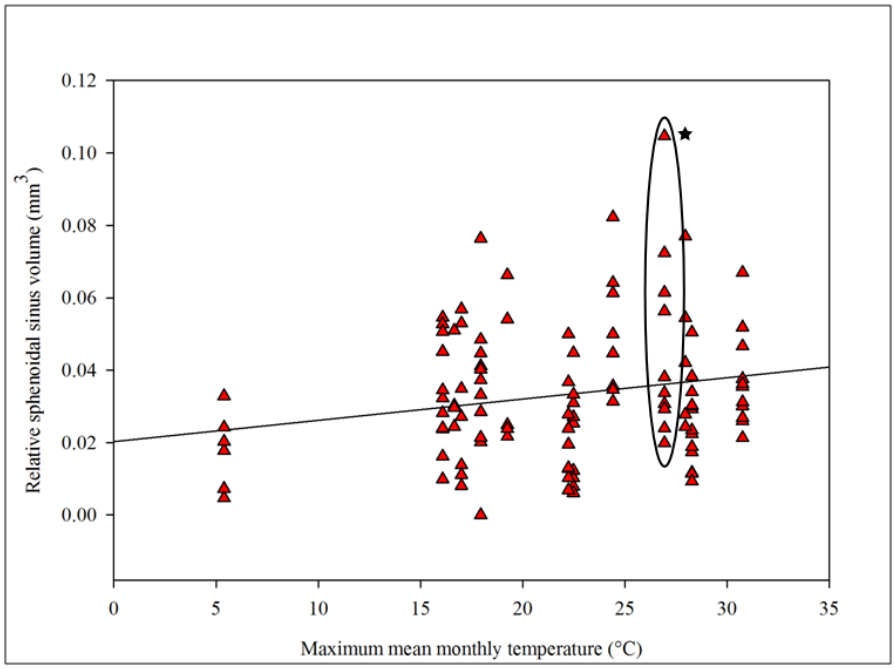

Figure 97: The significant, positive relationship between relative sphenoidal sinus volume and maxTemp. Western African populations is circled; star shows approximate location of Morton 1094 if individual maxTemp value is used. See text for explanation.

The potentially problematic Western African population includes a high-scoring outlier (Morton 1094, Figure 97). This individual has a relative sphenoidal sinus volume of 0.1cm^3, the largest relative sphenoidal volume of the entire sample (including all taxa). Mean maxTemp for Western Africa is 26.94 °C (see Table 1); maxTemp calculated for the outlier would be 27.73 °C. This is not a large difference, however. Indeed, if the individual's maxTemp is substituted for the group mean, neither the r^2 value, nor the p value of the relationship change. Therefore it seems reasonable therefore to conclude that this result is not driven by problems in the grouping of the sample. The other potentially problematic populations all appear to fit well within the general pattern of the data.

Precipitation

There is a small significant positive relationship between relative sphenoidal sinus volume and maxPrecip:

- **Relative sphenoidal sinus volume x maxPrecip:** reduced major axis regression: Relative sphenoidal sinus volume = 0.0136 + 0.0001 x maxPrecip, $r^2 = 0.04$, $p < 0.05$). NS with Bonferroni correction.

There was no significant relationship between relative sphenoidal sinus volume and MAP or minPrecip.

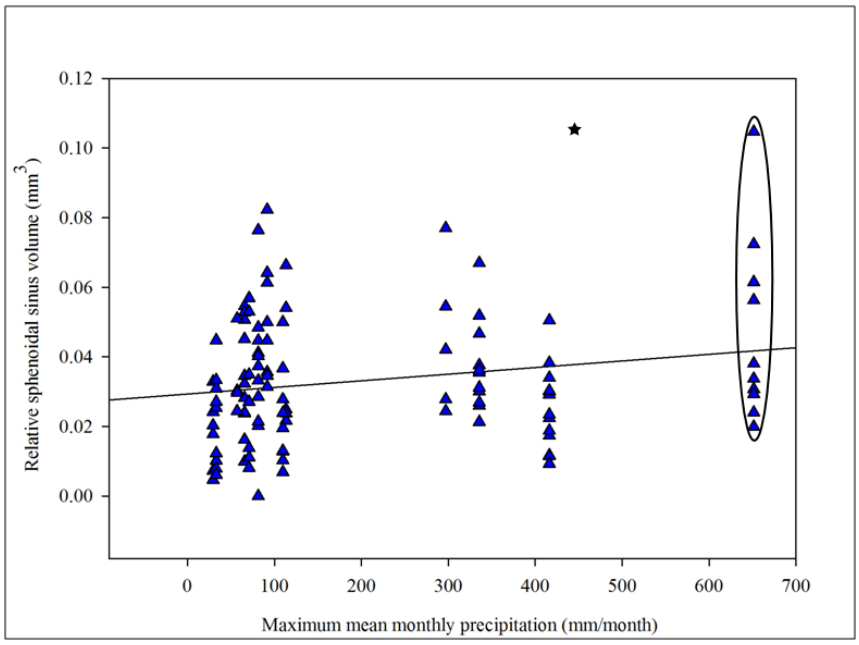

Figure 98: The small, significant, positive relationship between relative sphenoidal sinus volume and maxPrecip. Western African is circled; star indicates approximate position of the Western African outlier if individual maxPrecip, rather than group mean is used. See text for explanation.

As with temperature, the very large sphenoidal sinus of the same Western African individual results in its position as an outlier from the rest of its population in the

relationship between maxPrecip and relative sphenoidal sinus volume. The maxPrecip for the Western African sample as a whole is 651.38mm/month. If the outlier is treated individually, its maxPrecip would be 445.58mm/month. This adjusted maxPrecip would make this individual much more of an outlier compared to the rest of the Western African population. It would also make the relationship between maxPrecip and relative sphenoidal sinus volume much smaller. Indeed, if the outlier's individual maxPrecip is used, the relationship between maxPrecip and relative sphenoidal sinus volume is no longer significant. In conclusion, this relationship is not very robust, due to possible issues with population combination in the Western African sample. None of the other potentially problematic populations (China – cool, Russia, and Western Europe) appear to influence the relationship unduly.

6.I.b. Relationships between continuous climatic variables and sinus volume shape parameters in populations of recent *H. sapiens*

6.I.b.i. Relationships between frontal SVSPs and continuous climate variables in recent *H. sapiens*

Full landmark set frontal SVSP PC3

Temperature

There are strong, significant (remaining significant if a Bonferroni correction is applied) positive relationships between full landmark set frontal SVSP PC3 scores and all three temperature variables:

- **Full landmark set frontal SVSP PC3 x MAT:** reduced major axis regression: Full landmark set frontal SVSP PC3 = -0.0334 + 0.0024 x MAT, $p < 0.0005$, $r^2 = 0.2$.
- **Full landmark set frontal SVSP PC3 x maxTemp:** reduced major axis regression: Full landmark set frontal SVSP PC3 = -0.0778 + 0.0039 x maxTemp, $p < 0.0005$, $r^2 = 0.3$.
- **Full landmark set frontal SVSP PC3 x minTemp:** reduced major axis regression: Full landmark set frontal SVSP PC3 = -0.0125 + 0.0017 x minTemp, $p < 0.005$, $r^2 = 0.2$.

The full landmark set SVSP PC3 is negatively correlated with frontal sinus volume, thus, higher mean, maximum, and minimum temperatures are linked to craniofacial morphology that is associated with relatively smaller frontal sinuses.

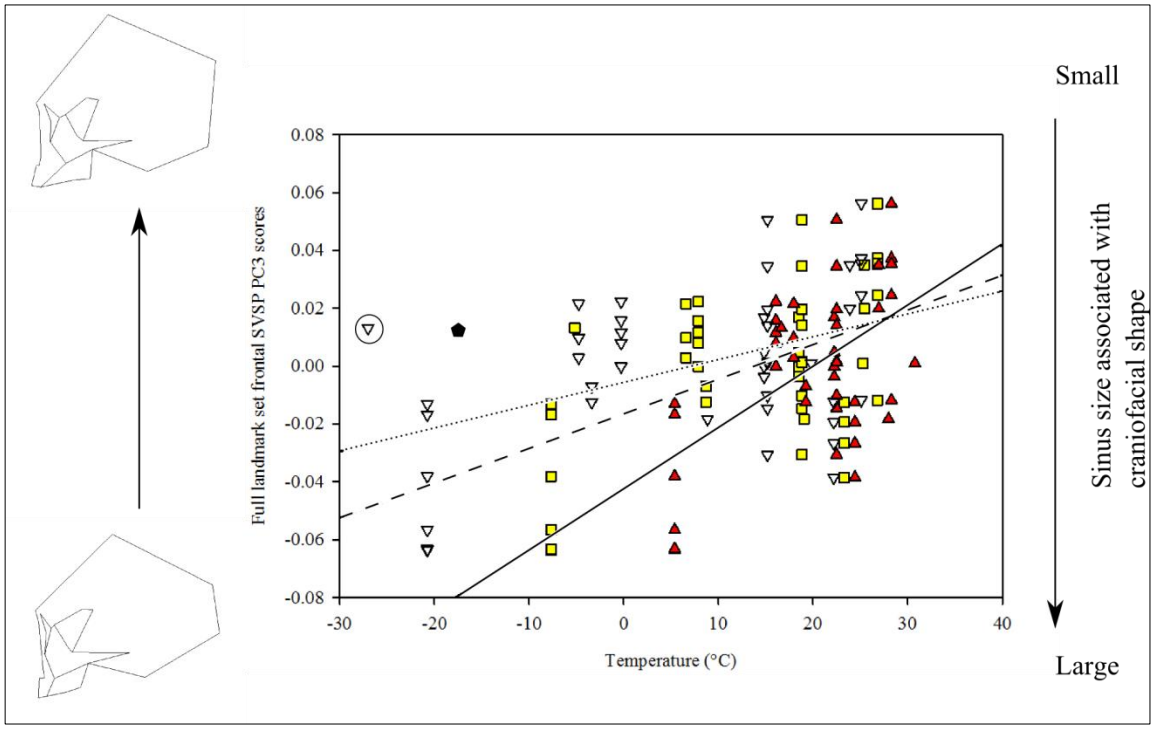

Figure 99: The relatively large, significant, positive relationships between full landmark set frontal SVSP PC3 and minTemp (unfilled downwards triangles, dotted line), MAT (yellow squares, dashed line), and maxTemp (red upwards triangles, unbroken line). Russian outlier is circled; see explanation in text. Wireframe diagrams on the left-hand y axis show the shape change described by full landmark set frontal SVSP PC3, right hand y axis shows the direction of the relationship between the frontal SVSP and relative frontal sinus volume.

The individual with the lowest minTemp (circled on Figure 99) appears to be an outlier. It is part of the Russian sample, which is a potentially problematic sample, as it combines Chuckchi from the far east of Russia with Kalmyks from the west of Russia. This specimen is a Chuckchi; as such, on its own it would have an estimated minTemp of -22.05 °C (see pentagon, Figure 99). At this slightly higher temperature, this individual would not appear as such an outlier, and would strengthen the relationship between minTemp and full landmark set frontal SVSP PC3. Indeed, if

this individual's minTemp is replaced with the Chuckchi value, the r^2 value does not change, but the level of significance is slightly improved ($p < 0.001$). The other potentially problematic populations (China – cool, Western Africa, and Western Europe) do not appear to affect these relationships.

Precipitation

There are significant, positive relationships between full landmark set frontal SVSP PC3 scores and all three precipitation variables:

- **Full landmark set frontal SVSP PC3 x MAP:** reduced major axis regression: Full landmark set PC3 = -0.0205 + 0.00002 x MAP, $p < 0.005$, $r^2 = 0.21$.
- **Full landmark set frontal SVSP PC3 x maxPrecip:** reduced major axis regression: Full landmark set PC3 = -0.0234 + 0.0002 x maxPrecip, $p < 0.005$, $r^2 = 0.2$.
- **Full landmark set frontal SVSP PC3 x minPrecip:** reduced major axis regression: Full landmark set PC3 = -0.0266 + 0.0023 x minPrecip, $p = 0.05$, $r^2 = 0.009$.

The first two relationships remain significant if a Bonferroni correction is applied, the last does not.

The positive relationship between precipitation and full landmark set PC3 PC scores shows increased precipitation is linked to craniofacial morphology associated with smaller frontal sinuses.

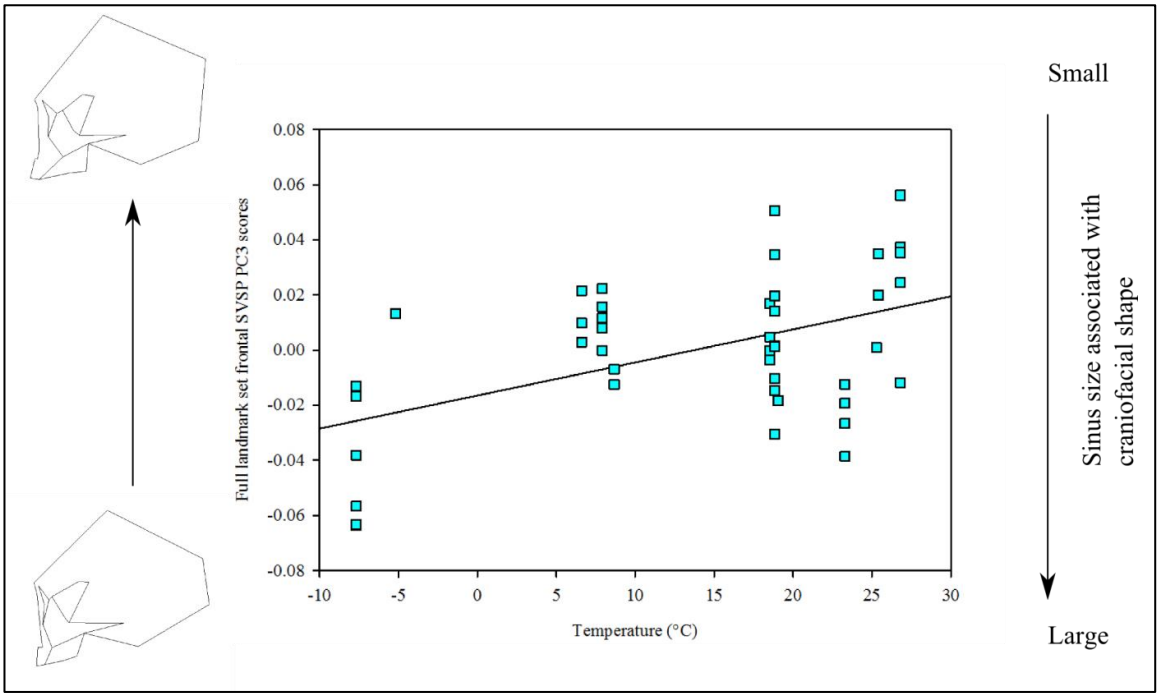

Figure 100: The relatively large, significant, positive relationship between full landmark set frontal SVSP PC3 and MAP. Wireframe diagrams on the left-hand y axis show the shape change described by full landmark set frontal SVSP PC3, right hand y axis shows the direction of the relationship between the frontal SVSP and relative frontal sinus volume.

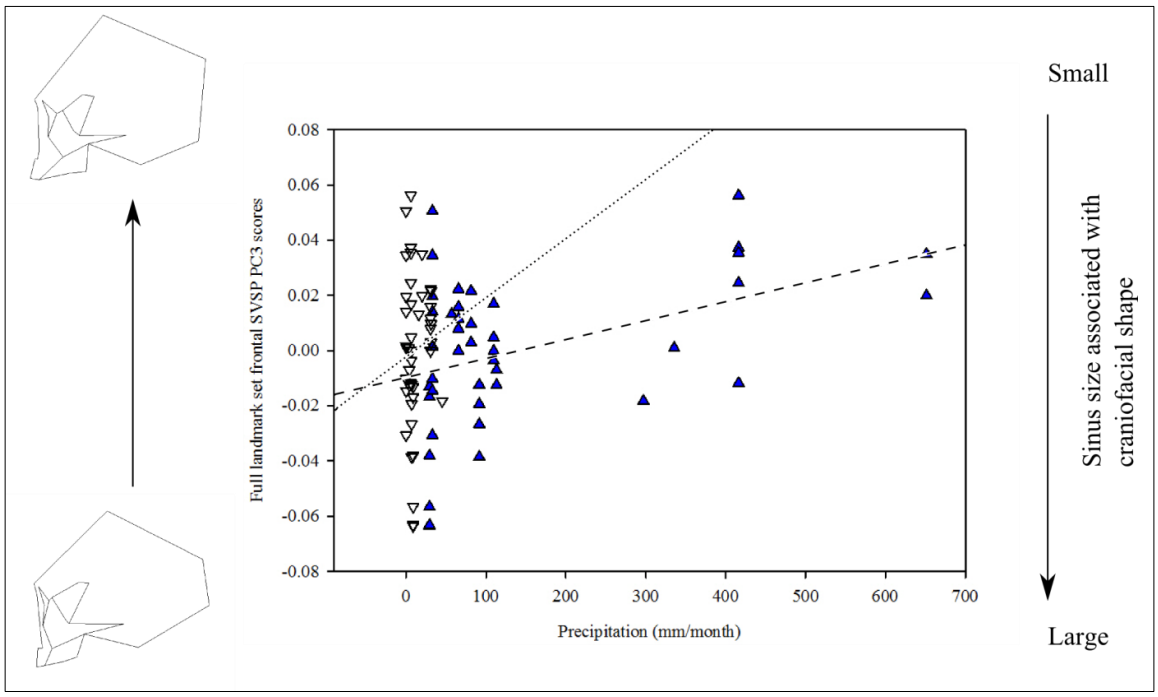

Figure 101: The relatively large, positive, significant relationship between full landmark set frontal SVSP PC3 and maxPrecip (blue upwards triangles, dashed line) and the extremely small, border-line significant, positive relationship with minPrecip (unfilled downwards triangles, dotted line). Wireframe diagrams on the left-hand y axis show the shape change described by frontal SVSP PC3, right hand y axis shows the direction of the relationship between the frontal SVSP and relative frontal sinus volume.

Frontal SVSP PC6

Temperature

There are small, significant (remaining so if a Bonferroni correction is applied), positive relationships between frontal SVSP PC6 scores and both MAT and minTemp:

- **Frontal SVSP PC6 x MAT:** reduced major axis regression: Frontal SVSP PC6 = -0.0257 + 0.0017 x MAT, $p < 0.01$, $r^2 = 0.07$).
- **Frontal SVSP PC6 x minTemp:** reduced major axis regression: Frontal SVSP PC6 = -0.0098 + 0.0012 x minTemp, $p < 0.005$, $r^2 = 0.08$).

The relationship between frontal SVSP PC6 and frontal sinus volume is negative. Therefore, as in the case of full landmark set SVSP PC3, higher temperatures are associated with craniofacial morphology linked to smaller frontal sinuses.

There is no significant relationship between frontal SVSP PC6 and maxTemp.

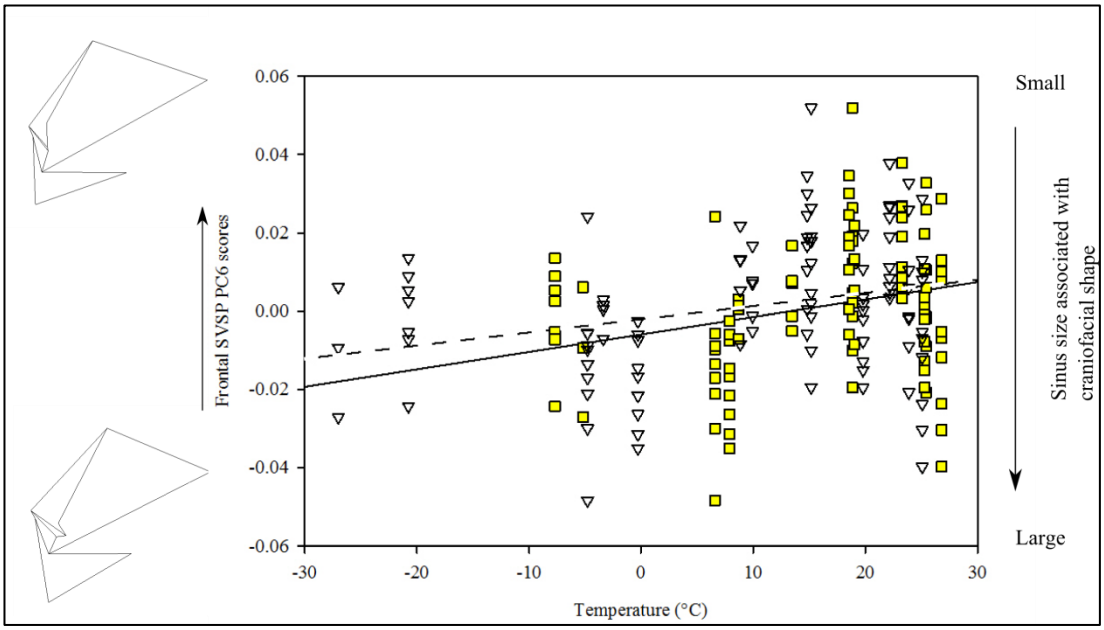

Figure 102: The significant, positive relationships between frontal SVSP PC6 and MAT (yellow squares, dashed line) and minTemp (unfilled downwards triangles, dashed line). Wireframe diagrams on the left-hand y axis show the shape change described by frontal SVSP PC6, right hand y axis shows the direction of the relationship between the frontal SVSP and relative frontal sinus volume.

Precipitation

There is a very small, significant, negative relationship between frontal SVSP PC6 scores and minPrecip:

- **Frontal SVSP PC6 x minPrecip:** reduced major axis regression: Frontal SVSP PC6 = 0.0208 + -0.0013 x minPrecip, $p < 0.05$, $r^2 = 0.05$. NS with Bonferroni correction.

The relationship between frontal SVSP PC6 and frontal sinus volume is negative. Therefore, higher minimum levels of precipitation are associated with craniofacial morphology linked to larger frontal sinuses.

There is no significant relationship between frontal SVSP PC6 and MAP or maxPrecip.

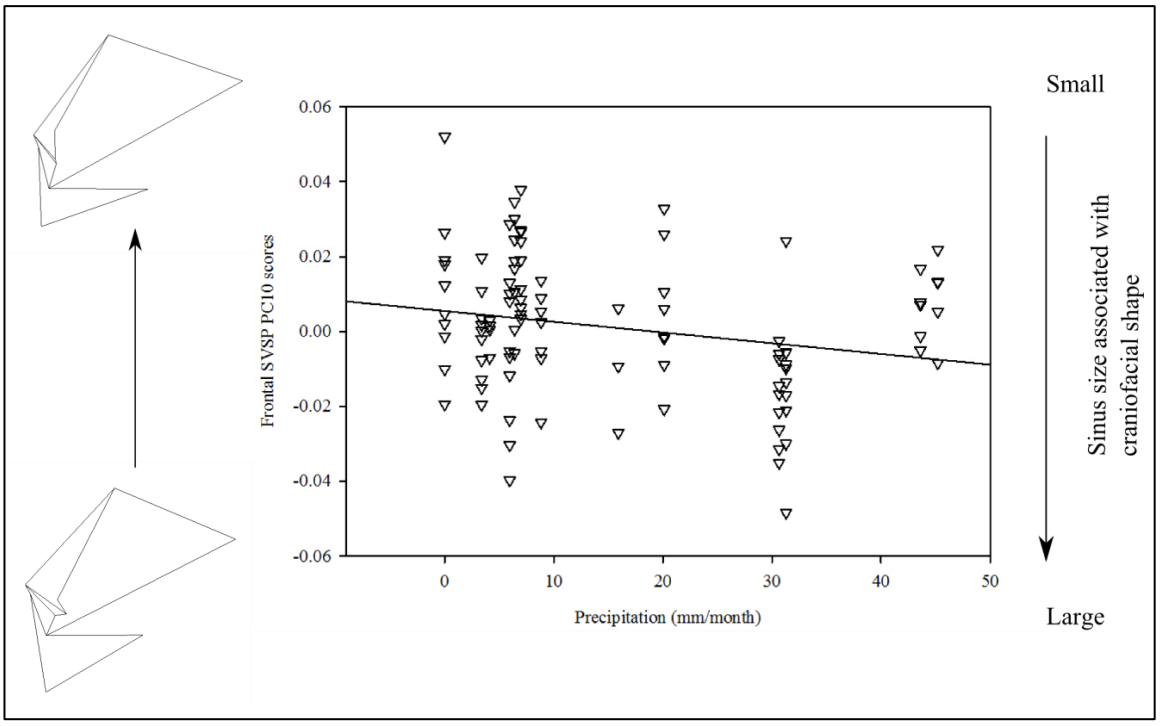

Figure 103: The significant, negative relationship between frontal SVSP PC6 and minPrecip. Wireframe diagrams on the left-hand y axis show the shape change described by full landmark set frontal SVSP PC6, right hand y axis shows the direction of the relationship between the frontal SVSP and relative frontal sinus volume. Wireframe diagrams on the left-hand y axis show the shape change described by maxillary SVSP PC6, right hand y axis shows the direction of the relationship between the frontal SVSP and relative maxillary sinus volume.

6.I.b.ii. Relationships between maxillary SVSPs and continuous climate variables in recent *H. sapiens*

Maxillary SVSP PC3

Temperature

There is a small significant, positive relationship between maxillary SVSP PC3 scores and MAT, and a stronger, significant, positive relationship with maxTemp:

- **Maxillary SVSP PC3 x MAT:** reduced major axis regression: Maxillary SVSP PC3 = -0.0323 + 0.0020 x MAT, $p < 0.05$, $r^2 = 0.06$. NS with Bonferroni correction.
- **Maxillary SVSP PC3 x maxTemp:** reduced major axis regression: Maxillary SVSP PC3 = -0.0687 + 0.0031 x maxTemp, $p < 0.005$, $r^2 = 0.10$). NS with Bonferroni correction.

Maxillary SVSP PC3 is positively correlated with maxillary sinus volume, thus warmer temperatures are associated with craniofacial morphology linked to larger maxillary sinuses.

There is no significant relationship between maxillary SVSP PC3 and minTemp.

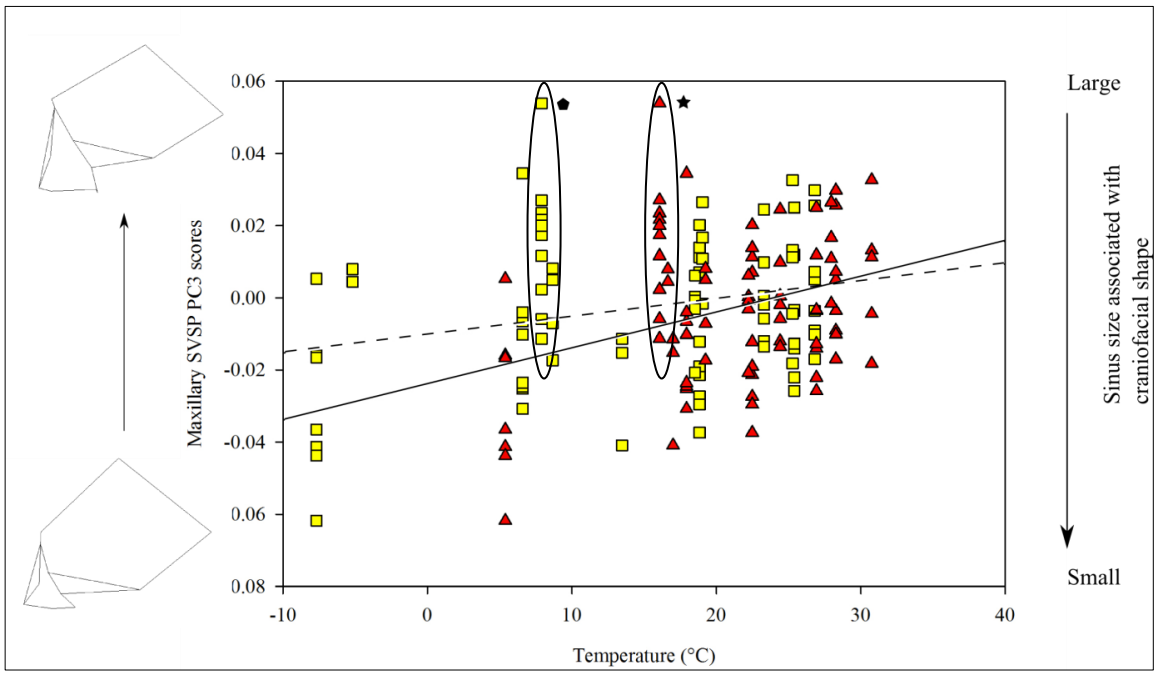

Figure 104: The small, significant, positive relationships between maxillary SVSP PC3 and MAT (yellow squares, dashed line) and the stronger one with maxTemp (red upwards triangles, unbroken line). Wireframe diagrams on the left-hand y axis show the shape change described by maxillary SVSP PC3, right hand y axis shows the direction of the relationship between the maxillary SVSP and relative maxillary sinus volume. Western European MAP and maxTemp circled, pentagon shows approximate position of outlier's MAT, star shows approximate position of outlier's maxTemp; see explanation in text.

The Western European sample is one of the potentially problematic populations and in this analysis seems to show a high-scoring outlier, which is an individual from the Netherlands. The MAT for the Netherlands alone would be 9.49 °C (shown as black pentagon on Figure 104) and the maxTemp would be 17.47 °C (shown as black star on Figure 104). These temperatures are slightly higher than the Western European means (see Table 1). Although this individual remains an outlier if Netherland-specific temperatures are used, its position is not causing the significant relationship, which would in fact be stronger if the Netherlands-specific temperatures were used. None of the other potentially problematic populations (Western Africa, China – cool, or Russia) seem to stand out from the pattern of the other data.

Precipitation

There is no significant relationship between maxillary SVSP PC3 and any of the measures of precipitation.

Maxillary SVSP PC7

There is no significant relationship between maxillary SVSP PC3 and any of the continuous climatic variables.

6.I.b.iii. Relationships between sphenoidal SVSPs and continuous climate variables in recent *H. sapiens*

Sphenoidal SVSP PC3

Temperature

There are significant (remaining so if a Bonferroni correction is applied), negative relationships between sphenoidal SVSP PC3 scores and all three temperature variables:

- **Sphenoidal SVSP PC3 x MAT:** reduced major axis regression: Sphenoidal SVSP PC3 = 0.0424 + -0.0027 x MAT, $p < 0.005$, $r^2 = 0.09$.
- **Sphenoidal SVSP PC3 x maxTemp:** reduced major axis regression: Sphenoidal SVSP PC3 = 0.0904 + -0.0041 x maxTemp, $p < 0.05$, $r^2 = 0.05$.
- **Sphenoidal SVSP PC3 x minTemp:** reduced major axis regression: Sphenoidal SVSP PC3 = 0.0179 + -0.0019 x minTemp, $p < 0.005$, $r^2 = 0.10$.

Sphenoidal SVSP PC3 is positively correlated with relative sphenoidal sinus volume. Thus warmer temperatures are associated with craniofacial morphology linked to smaller sphenoidal sinuses.

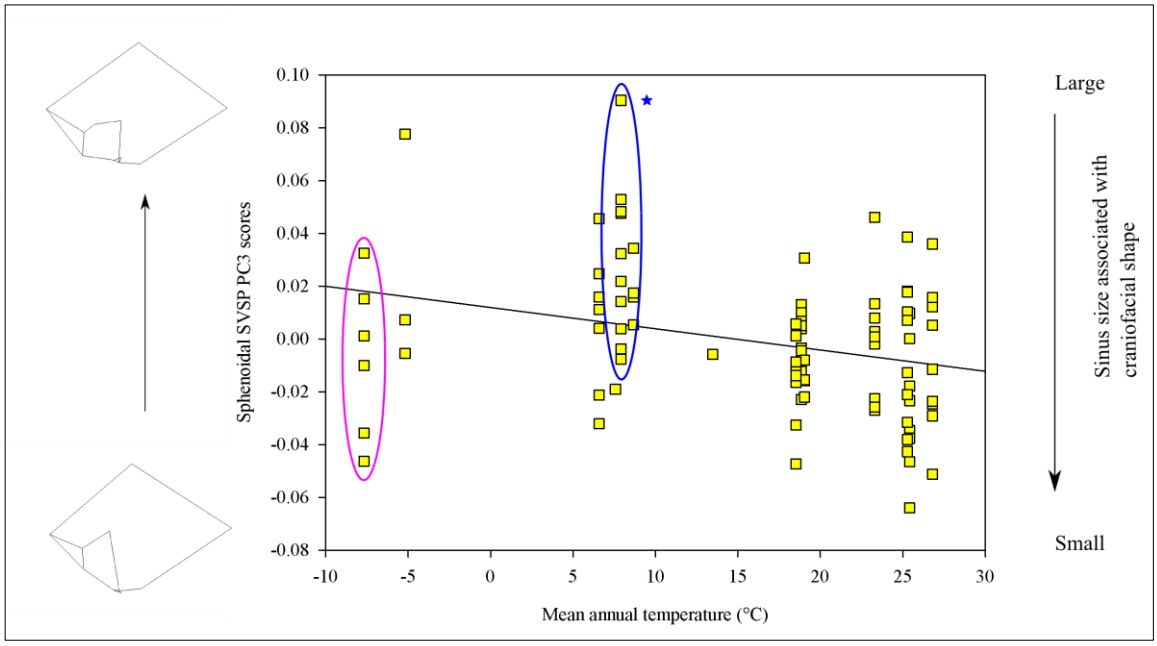

Figure 105: The small, significant, negative relationship between sphenoidal SVSP PC3 and MAT. Wireframe diagrams on the left-hand y axis show the shape change described by sphenoidal SVSP PC3, right hand y axis shows the direction of the relationship between the sphenoidal SVSP and relative sphenoidal sinus volume. Magenta circle highlights Greenland population. Blue circle highlights Western European population, blue star indicates approximate position of Western European outlier if the individual's, not the group mean, mean temperature is used. See text for details.

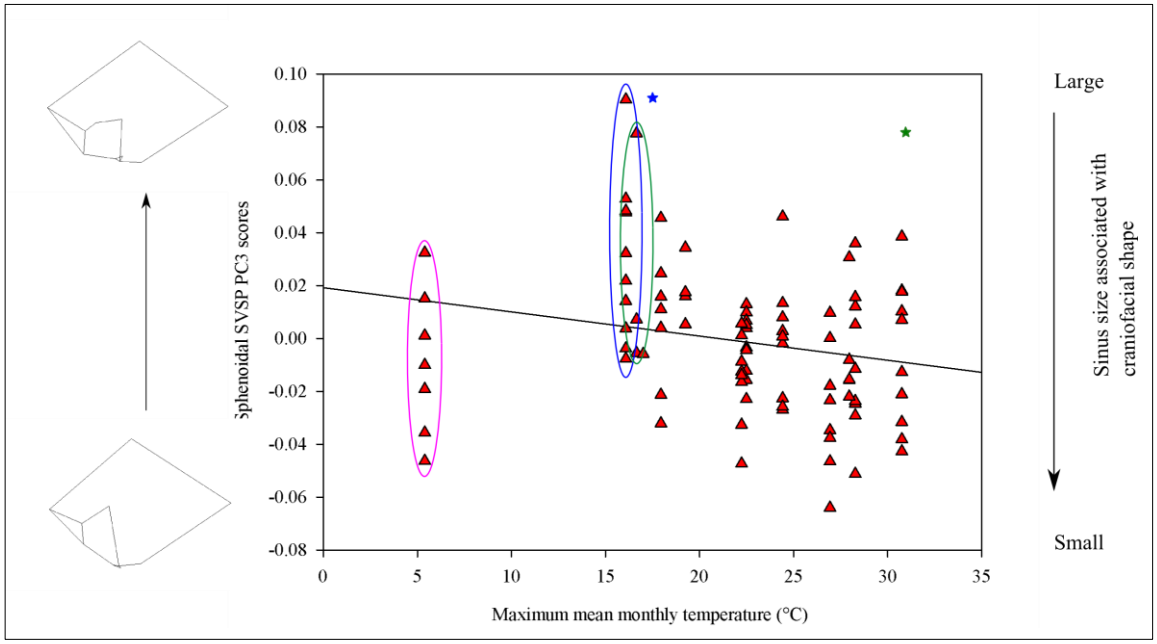

Figure 106: The relatively large, significant, negative relationships between sphenoidal SVSP PC3 and maximum mean monthly. Wireframe diagrams on the left-hand y axis show the shape change described by sphenoidal SVSP PC3, right hand y axis shows the direction of the relationship between the sphenoidal SVSP and relative sphenoidal sinus volume. Magenta circle highlights Greenland sample. Blue circle highlights Western European population; blue star indicates approximate position of W. European outlier if the individual's, not the group maxTemp is used; dark green circle highlights Russian population; dark green start star indicates approximate position of Russian outlier if the individual's, not the group maxTemp is used. See text for details.

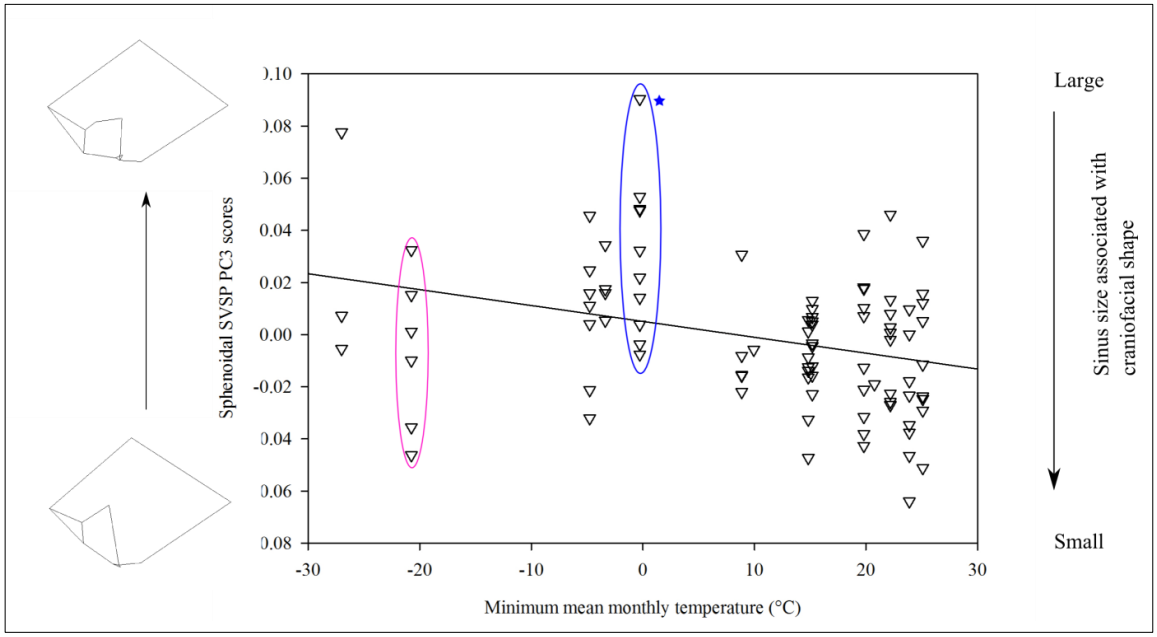

Figure 107: The significant, negative relationship between sphenoidal SVSP PC3 and minTemp. Wireframe diagrams on the left-hand y axis show the shape change described by sphenoidal SVSP PC3, right hand y axis shows the direction of the relationship between the sphenoidal SVSP and relative sphenoidal sinus volume. Magenta circle highlights Greenland sample. Blue circle highlights W. European population, blue star indicates approximate position of W. European outlier if individual, and not the group minTemp is used. See text for details.

The Greenland population (circled in magenta in Figure 105 to 107) seems to have a different relationship with temperature than any of the other populations; it falls lower on the sphenoidal SVSP PC3 scores than would be expected (based on the positions of the other populations) for all three temperature variables. Greenland is the population experiencing the lowest maxTemp and MAT in the sample, but the Russian population experiences lower minTemp. Despite this fact, the Russian sample does not fall similarly low on the sphenoidal SVSP PC3 axis, showing that the two populations are not similar in this aspect of craniofacial shape.

In all three graphs (Figures 105-107) of temperature variables versus sphenoidal SVSP PC3, there is a Western European outlier (from the Netherlands) that falls very high on the SVSP, quite isolated from other members of that sample (circled in blue, Figures 105 to 107). As Western Europe is a potentially problematic population, the outlier specimen's position was plotted with Netherlands, rather than Western European temperature values (see blue stars, Figure 105 to 107). If Netherlands temperature values are used, the minTemp, MAT, and maxTemp are 1.5 °C, 9.5 °C, and 17.5 °C respectively. Using these individual values, instead of group means, the outlier's positions change very little, showing that it is unlikely that the geographic spread of the sample is responsible for the outlying position of this individual in term of the craniofacial shape as described by sphenoidal SVSP PC3. In fact, the removal of this individual from the analysis changes neither the r^2, nor the p value for any of the three analyses. This is the same outlier as discussed in relation to maxillary SVSP PC3 in Section 6.I.b.ii, which suggests this individual's morphology may generally be distinctive in shape within the sample.

In the Figure 106, which displays the relationship between maxTemp and sphenoidal SVSP PC3, one of the Russian sample (a Kalmyk) appears to be an outlier to the rest of the group (circled in dark green, Figure 106). Similar to the Western European population, the Russian population is potentially problematic. If the approximate location of the Kalmyk is used to estimate its maxTemp, the value is 30.8 °C, far higher than the group mean of 16.7°C. A dark green star in Figure 106 shows the approximate location of the Kalmyk outlier using maxTemp of 30.8 °C. This position would clearly weaken the relationship and so the analysis was re-run with this individual's local maxTemp value. The result was no longer significant, showing that the relationship is sensitive to this one individual and that an unrepresentative temperature for this population may have biased the result. This is not to say, however, that there is no maxTemp signal in the data. If the Greenland population, which appears to show an anomalous relationship between temperature and craniofacial shape as described by sphenoidal SVSP PC3 (see above), is removed, the relationship is far stronger, even if the individual value is used for the Kalmyk outlier (sphenoidal SVSP PC3 = 0.134 + -0.006 x maxTemp, $r^2 = 0.2$, $p < 0.005$).

Precipitation

There are significant, negative relationships between sphenoidal SVSP PC3 and MAP and maxPrecip:

- **Sphenoidal SVSP PC3 x MAP:** reduced major axis regression: Sphenoidal SVSP PC3 = 0.0251 + -0.00002 x MAP, $p < 0.05$, $r^2 = 0.07$. NS with Bonferroni correction.

- **Sphenoidal SVSP PC3 x maxPrecip:** reduced major axis regression: Sphenoidal SVSP PC3 = 0.0277 + -0.0001 x maxPrecip, $p < 0.005$, $r^2 = 0.11$). Remains significant if a Bonferroni correction is applied.

Since the relationship between sphenoidal SVSP is positive, greater precipitation is linked to craniofacial morphology associated with smaller sphenoidal sinuses.

There is no significant relationship between sphenoidal SVSP PC3 and minPrecip.

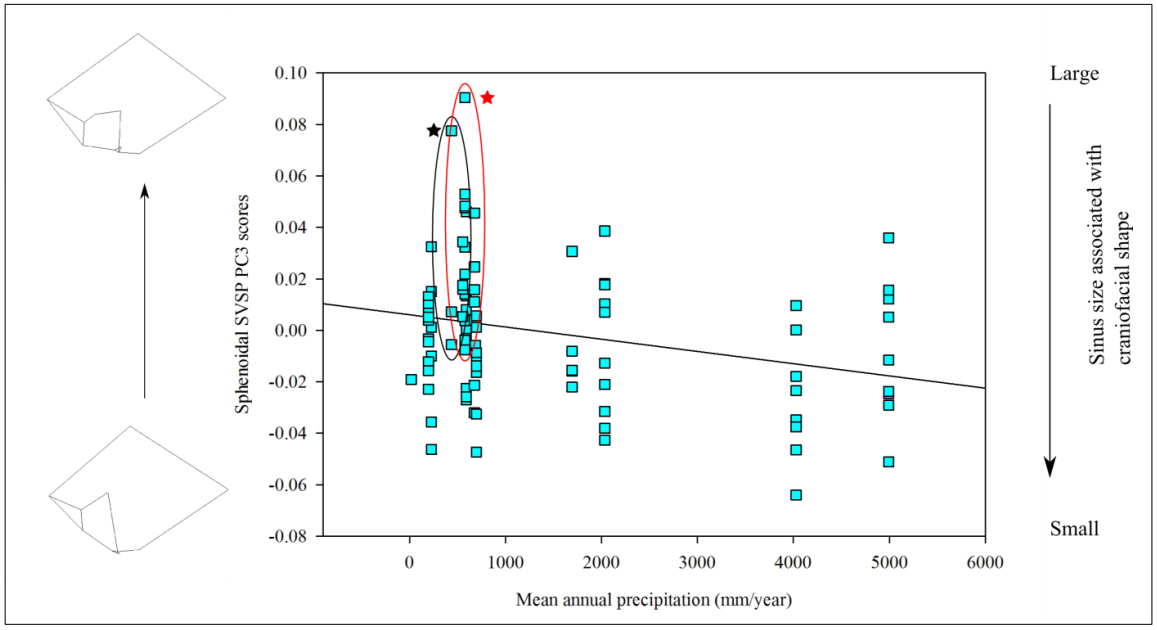

Figure 108: The negative, significant relationship between sphenoidal SVSP PC3 and MAP. Wireframe diagrams on the left-hand y axis show the shape change described by sphenoidal SVSP PC3, right hand y axis shows the direction of the relationship between the sphenoidal SVSP and relative sphenoidal sinus volume. Red circle shows Western European population, red star shows approximate location of outlier if individual MAP is used. Black circle shows Russian population and black star shows approximate location of outlier if individual MAP is used. See text for details.

The Russian (circled in black on Figure 108) and Western European (circled in red on Figure 108) samples are potentially problematic population groupings, and, as for temperature, individuals from both populations appear as high-scoring outliers that

may bias the relationship seen between sphenoidal SVSP PC3 and MAP. If the individual location is used, the Russian (Kalmyk) has a MAP of 249.61 mm/yr, somewhat drier than the Russian mean; this would make no difference to the relationship. The Western European (Dutch) outlier has an individual MAP of 766.30 mm/year, slightly wetter than the Western European mean, this could weaken the relationship, albeit only slightly. To test this possibility, the analysis was run again with the Dutch outlier's MAP value instead of the Western European mean. The r^2 value remains unchanged, whilst the p value is then < 0.01, showing that this one individual is not biasing the results and the relationship is robust.

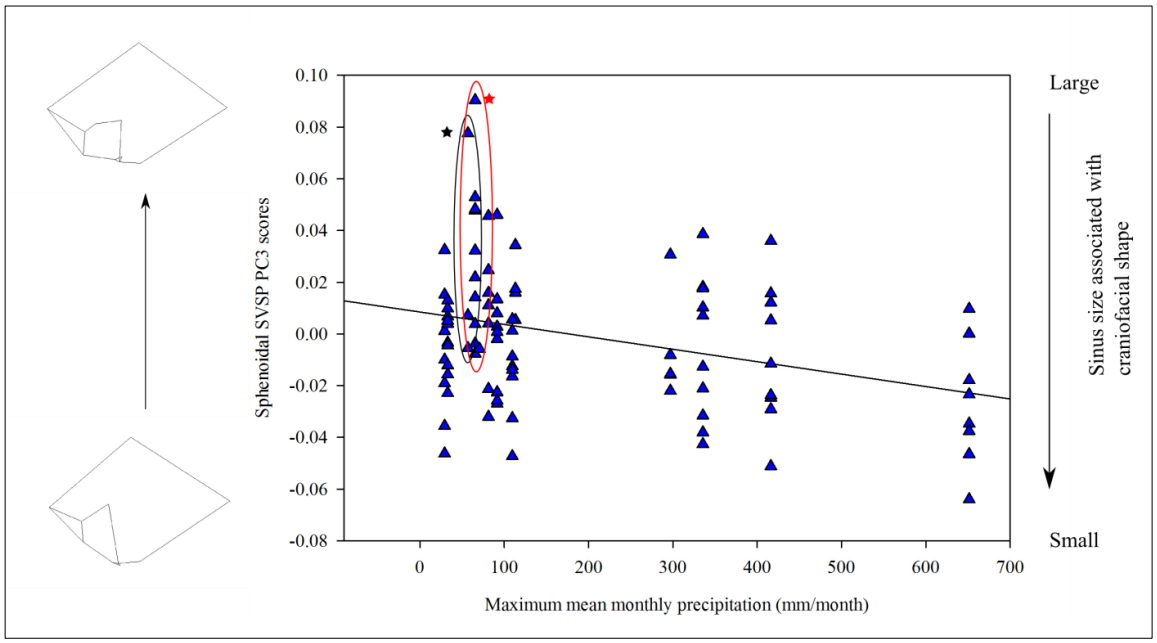

Figure 109: The significant relationships between sphenoidal SVSP PC3 and maxPrecip. Wireframe diagrams on the left-hand y axis show the shape change described by sphenoidal SVSP PC3, right hand y axis shows the direction of the relationship between the sphenoidal SVSP and relative sphenoidal sinus volume. Black circle: Russian sample, black star shows approximate location if individual location is used for Russian outlier. Red circle: Western European sample, red star shows the approximate location W. European outlier, if individual location is used to calculate maxPrecip. See text for details.

The same two individuals stand out in the maxPrecip analysis as the MAP (Figure 109). If their individual locations are used, the Kalmyk has a maxPrecip of 30.79 mm/month, and the Dutch outlier has a mean monthly precipitation of 82.26

mm/month. These values are shown in Figure 109 as black and red stars, respectively. Both individuals' locations are very close to their population means, and the difference is very unlikely to affect the relationship. The Dutch individual is an outlier from its population on all sphenoidal SVSP PC3 analyses with continuous climate variables, and the results of comparisons between the individual's position using group means and using individual values suggest that this is due to an unusual craniofacial form (as described by this PC) not associated with climate; indeed, the sphenoidal SVSP PC3 scores are so high for both the Dutch and Kalmyk outliers that they would appear separate from their groups at any precipitation value.

Sphenoidal SVSP PC6

Temperature and precipitation

There is no significant relationship between sphenoidal SVSP PC6 and any of the continuous climatic variables.

6.II. RQ3.b.: Are there differences in sinus variables between groups (across taxa) experiencing different climates?

In this section, the sample is divided into climate categories based on current temperature and precipitation data for the recent *H. sapiens* sample and palaeoreconstructions of temperature and precipitation data for the fossil sample. See Table 44 for the climate, temperature, and precipitation categories for the populations of recent *H. sapiens* and fossil specimens; for the definition of (and rationale behind) categorisation, see Sections 2.IV.c.i. and 2.II.b.ii.

Fossil dates always incorporate a certain margin of error, but the dates for some of the fossils in the sample are particularly open to question and/or encompass an especially large amount of variability. This could lead to error in the climate categorisation of fossils. In cases where there was uncertainty regarding the validity of the climate category due to dating (see Section 2.II.b.ii), the position of the individual in each analysis was studied to ascertain if it had any effect on the result. The fossils considered in this way are shown below in Table 45. The positions of these fossils are reported and discussed in each section where appropriate.

Table 44: Classification of fossils and populations of recent humans in climatic categories (rationale as described in Chapter 2). Temperature categories: Hot/Wet + Hot/Dry = Hot; Cold/Wet + Cold/Dry = Cold; Temperate. Precipitation categories: Hot/Wet + Cold/Wet = Wet; Hot/Dry + Cold/Dry = Dry; Temperate not included.

Hot/Dry	Hot/Wet	Temperate	Cold/Wet	Cold/Dry
KNM-ER 3883	Bodo	China (cool)	Cro-Magnon	Greenland
KNM-ER 3733	Ceprano	Guattari	La Ferrassie	
Kabwe	China (warm)	Krapina	Neanderthal	
North Africa	Forbes' Quarry	La Chapelle	Russia	
Peru	Hawaii	La Quina		
Singa	India	Lithuania		
Skhul	Mexico	Mladeč		
Tabun	Ngaloba	Steinheim		
	Petralona	Tasmania		
	Torres Straits	Western Europe		
	Western Africa			

Table 45: Fossils with potentially problematic climate category attributions due to uncertain dates. See Section 2.II.b.ii. and Table 2 for dates and climate categories.

Specimen	Taxonomic group
Kabwe	*H. heidelbergensis*
Petralona	*H. heidelbergensis*
Forbes' Quarry	*H. neanderthalensis*
La Quina	*H. neanderthalensis*
La Ferrassie	*H. neanderthalensis*
Neanderthal	*H. neanderthalensis*
Tabun	*H. neanderthalensis*
Skhul 5	Early *H. sapiens*
Ngaloba	Early *H. sapiens*

6.II.a. Differences in relative sinus volume between categorical climate categories

6.II.a.i. Differences in relative frontal sinus volumes between climate categories

Temperature

There is no significant difference in relative frontal sinus volumes between temperature categories.

Precipitation

Individuals in the Wet category have significantly larger frontal sinus volumes than the Dry category:

- **Relative frontal sinus volume by precipitation category:** t-test: $Z = -1.993$, $r^2 = 0.04$, $p < 0.05$, 2-tailed. NS with Bonferroni correction.

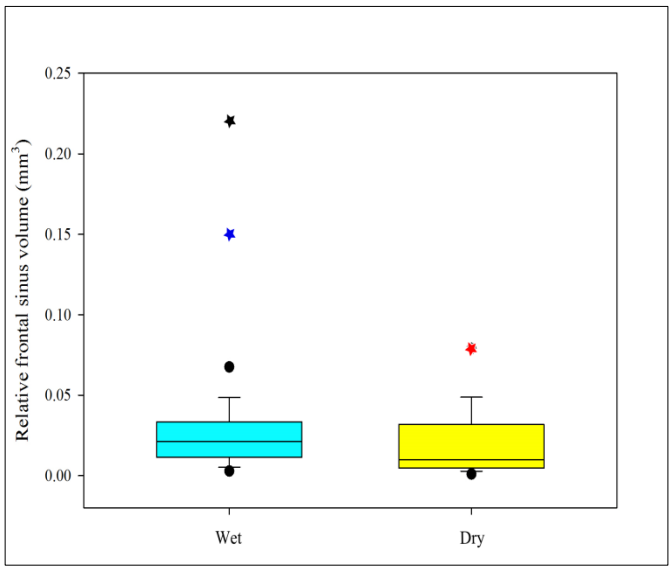

Figure 110: The significant difference between relative frontal sinus volume in Wet and Dry precipitation categories. Black star: Petralona, blue star: Bodo, red star: Kabwe. For details, see text.

Given the placement of Bodo and Petralona in the Wet category (see stars in Figure 110) and the merely border-line significance ($p = 0.046$) of the result, it seems likely that the difference is driven purely by these two individuals, who have very large frontal sinuses and happen to be in the Wet category. If Bodo and Petralona are removed from the sample: there is no longer a significant difference between precipitation categories. This is also the case if all *H. heidelbergensis* individuals are removed. The difference between *H. heidelbergensis* with very large frontal sinuses (Bodo and Petralona: Hot/Wet) and fairly large frontal sinus (Kabwe: Hot/Dry) (see Chapter 4) may be of interest, but it is not possible to investigate this further with such a small sample.

Full climate categories

There is no significant difference in relative frontal sinus volumes between any of the climate categories.

6.II.a.ii. Differences in relative maxillary sinus volumes between climate categories

There is no significant difference in relative maxillary sinus volume between any of the temperature, precipitation, or climate categories.

6.II.a.iii. Differences in relative sphenoidal sinus volumes between climate categories

Temperature

There is no significant difference in relative sphenoidal sinus volume between different temperature categories.

Precipitation

Specimens in the Wet category have significantly (remaining so if a Bonferroni correction is applied) larger relative sinus volumes than those in the Dry category:

- **Relative sphenoidal sinus volume by precipitation category:** t-test: $t(75) = 3.101$, $r^2 = 0.11$, $p < 0.005$)

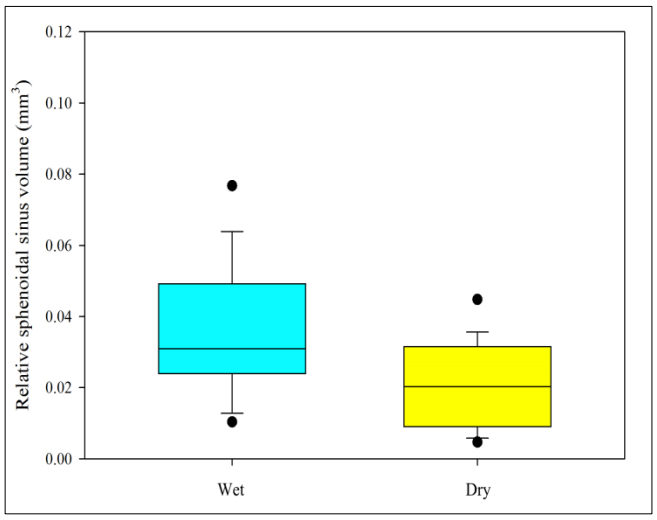

Figure 111: The significant difference between relative sphenoidal sinus volumes in the Wet category and the Dry category.

Full climate categories

There is a significant difference in relative sphenoidal sinus volume between some of the climate categories:

- **Relative sphenoidal sinus volume by climate category:** ANOVA: $F(113) = 2.505$, $\omega^2 = 0.08$, $p < 0.05$. NS with Bonferroni correction

This result, however, is only border-line significant ($p = 0.046$). There is no consistent significant difference between categories in the post-hoc tests (Games Howell and Hochberg's GT2, see Section 2.IV.c.ii.).

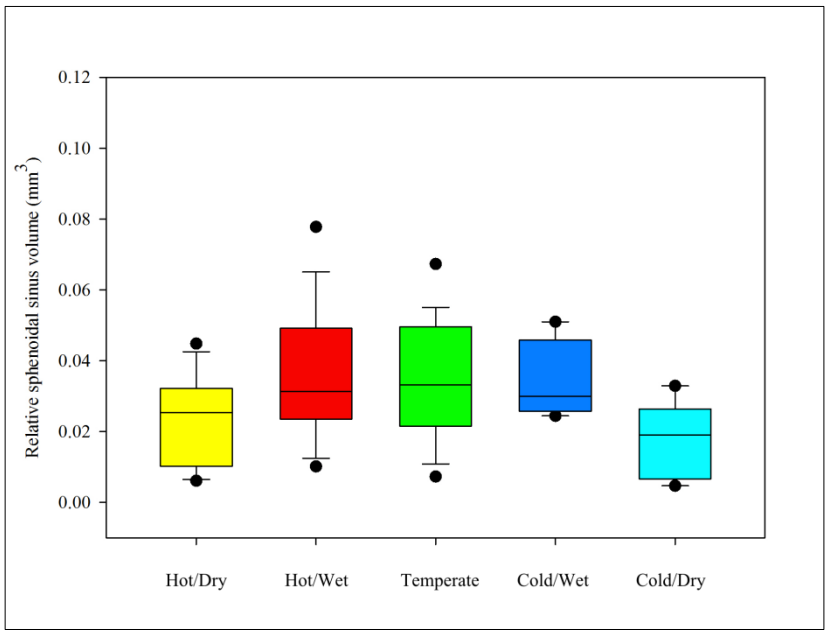

Figure 112: The border-line significant difference in relative sphenoidal sinus volume between climate categories shown by an ANOSIM. Post-hoc tests show no consistent individual differences between categories (see Section 2.IV.c.ii).

6.II.b. Differences in sinus volume shape parameters between climate categories

6.II.b.i. Differences in frontal SVSPs between climate categories

Full landmark set Frontal SVSP PC3

Temperature

There is a large, significant difference in full landmark set frontal SVSP PC3 scores between the Cold category and both the Temperate and the Hot category (Figure 113):

- **Full landmark set frontal SVSP PC3 by temperature category:** ANOVA: $F(42) = 8.61$, $\omega^2 = 0.24$, $p < 0.001$.

The PC scores are lower in the Cold category than in the Temperate and Hot categories (see details in Table 46 below).

As full landmark set frontal SVSP is negatively correlated with relative frontal sinus volume, the specimens in the cold category have craniofacial morphology associated with larger frontal sinuses than the other two categories.

Table 46: Differences in full landmark set frontal SVSP PC3 scores between temperature categories, results from post-hoc tests following ANOVA. The matrix is symmetrical, above the trace mean differences are shown; below the trace p values are shown. NS = not significant. Red highlight = significant.

	Cold	**Temperate**	**Hot**
Cold		-0.04	-0.04
Temperate	0.003		NS
Hot	0.001	NS	

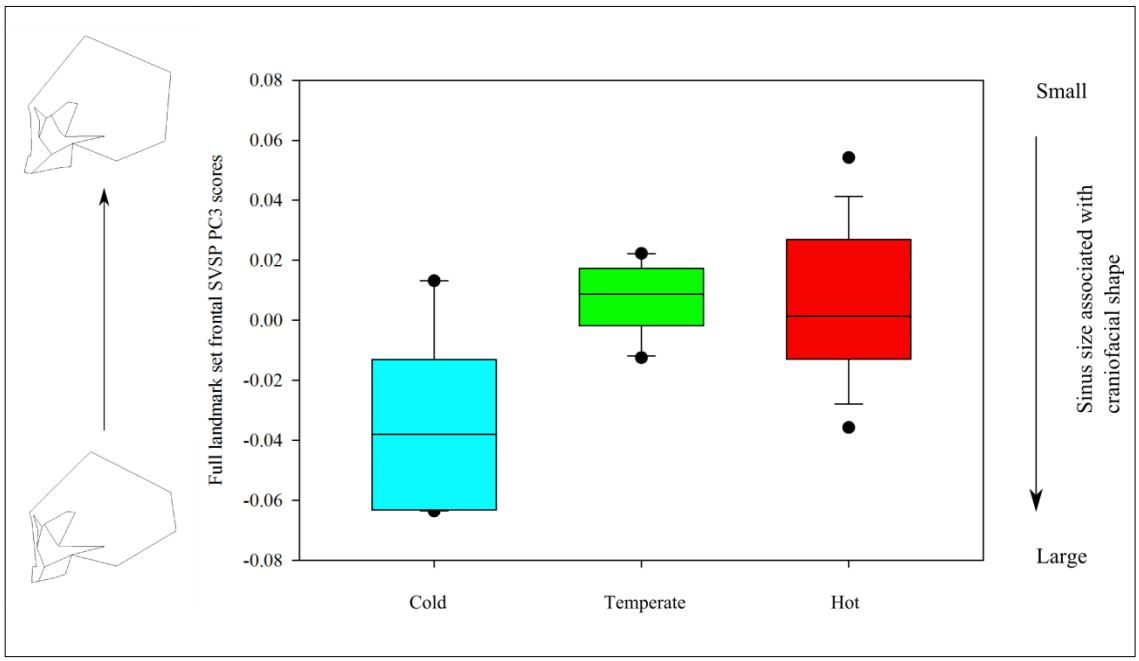

Figure 113: The significant differences between temperature categories in full landmark set SVSP frontal PC3 scores. Specimens in the Cold category score significantly lower on full landmark set frontal SVSP than specimens in the Temperate or Hot categories. Wireframes on the right show shape change along the PC. Wireframe diagrams on the left-hand y axis show the shape change described by full landmark set frontal SVSP PC3, right hand y axis shows the direction of the relationship between the full landmark set frontal SVSP PC3 and relative frontal sinus volume.

Precipitation

There is no significant difference in full landmark set frontal SVSP PC3 scores between precipitation categories.

Full climate categories

There is a large, significant difference between some of the climate categories in full landmark set frontal SVSP PC3 scores (see Figure 114):

- **Full landmark set SVSP PC3 by climate category:** ANOVA: $F(42) = 5.879$, $\omega^2 = 0.24$, $p < 0.001$.

Post hoc tests (see Table 47) show that Cold/Dry category scores lower on frontal SVSP PC6 than the Temperate, Hot/Wet and Hot/Dry categories.

The lower scores in the Cold/Dry category show that the specimens have craniofacial morphology more likely to be associated with large frontal sinuses than the other categories.

Table 47: Results of post-hoc tests following ANOVA comparing full landmark set frontal SVSP PC3 scores between climate categories. The matrix is symmetrical, above the trace mean differences are shown; below the trace p values are shown. NS = not significant. Red highlight = significant.

	Cold/Wet	**Cold/Dry**	**Temperate**	**Hot/Wet**	**Hot/Dry**
Cold/Wet		NS	NS	NS	NS
Cold/Dry	NS		0.05	-0.05	0.05
Temperate	NS	0.001		NS	NS
Hot/Wet	NS	0.001	NS		NS
Hot/Dry	NS	0.001	NS	NS	

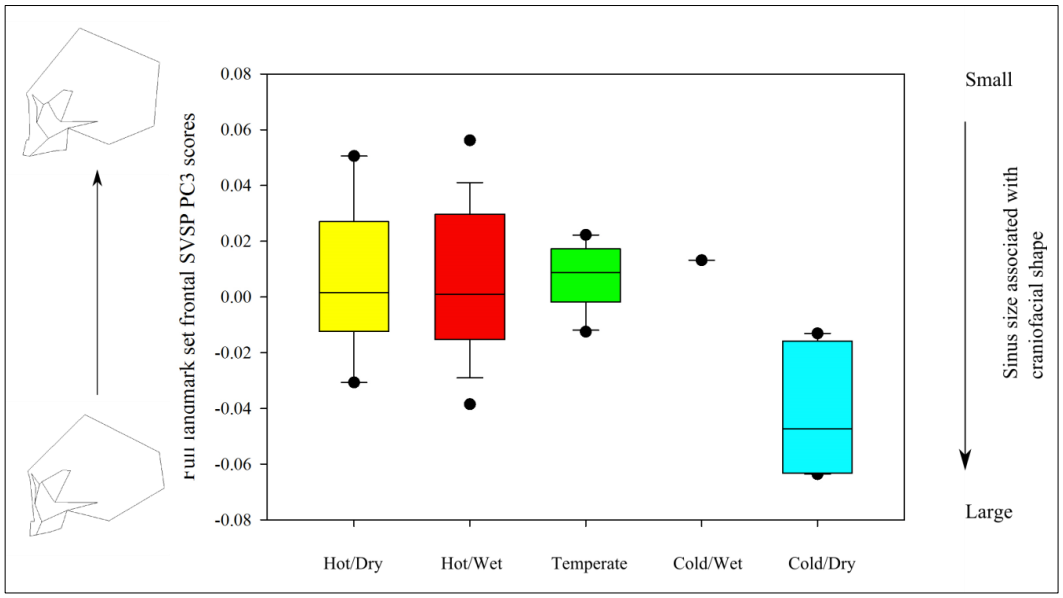

Figure 114: The significant differences between climatic categories in full landmark set SVSP frontal PC3 scores. Individuals in the Cold/Dry category score significantly lower on frontal SVSP PC6 than individuals in the other categories. Wireframes on the right show shape change along the PC. Wireframes on the right show shape change along the PC. Wireframe diagrams on the left-hand y axis show the shape change described by full landmark set frontal SVSP PC3, right hand y axis shows the direction of the relationship between the full landmark set frontal SVSP PC3 and relative frontal sinus volume.

Frontal SVSP PC6

Temperature

There is a medium-sized, significant difference in frontal SVSP PC6 scores in temperature categories (see Figure 115):

- **Frontal SVSP PC6 by temperature category:** ANOVA: $F(109) = 8.831$, $\omega^2 = 0.15$, $p < 0.001$.

Post-hoc tests show that this difference is higher scores in the Hot category than the temperate category:

- **Hot x Temperate category:** Mean difference = 0.0157, $p < 0.001$.

As frontal SVSP PC6 has a negative relationship with relative frontal sinus volume, this shows that the Hot category exhibits craniofacial morphology associated with smaller sinuses than the Temperate category.

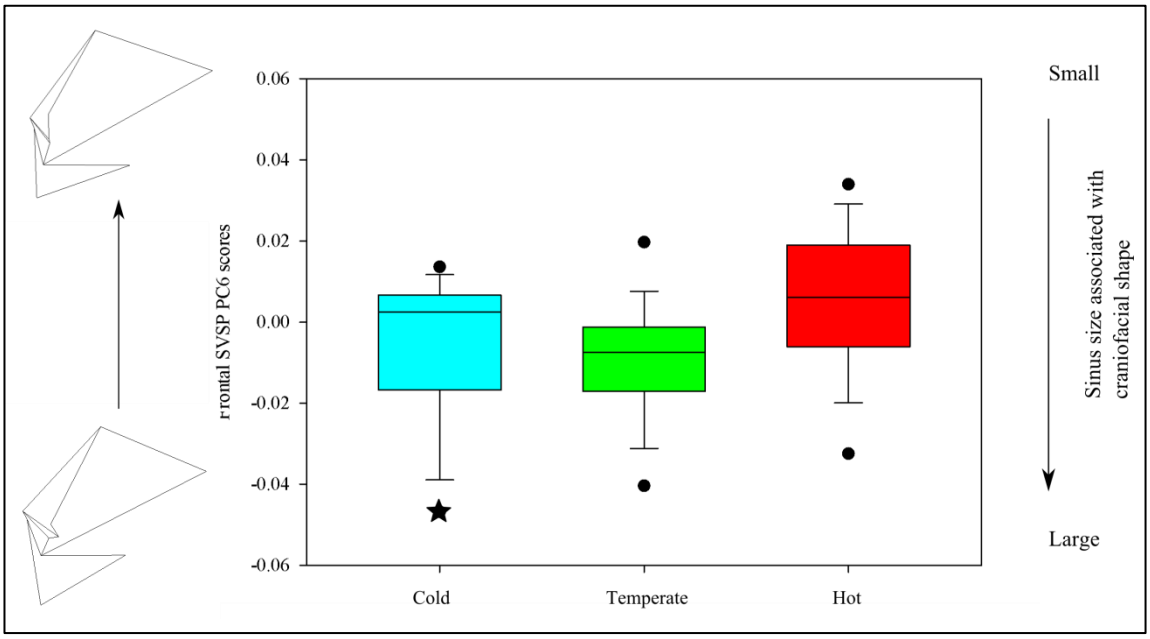

Figure 115: Boxplot showing significant difference in frontal SVSP PC6 scores between temperature categories. Wireframes on the right show shape change along the PC. Wireframe diagrams on the left-hand y axis show the shape change described by frontal SVSP PC6, right hand y axis shows the direction of the relationship between the frontal SVSP PC6 and relative frontal sinus volume. Star indicates approximate position of La Ferrassie (see text).

La Ferrassie (one of the possibly problematic fossils) scores low on frontal SVSP PC6 compared to the rest of the Cold category (see black star in Figure 115) and pulls the PC scores of the Cold category towards the negative end of the SVSP. However, if this specimen is removed there is still no significant difference between the Cold category and the other temperature categories.

Precipitation

There is no significant difference in frontal SVSP PC6 scores between precipitation categories.

Full climate categories

There are significant differences in frontal SVSP PC6 scores between climate categories (see Figure 116):

- **Frontal SVSP PC6 by climate category:** ANOVA: $F(109) = 4.67$, $\omega^2 = 0.18$, $p < 0.005$.

Post-hoc tests show this is due to the Hot/Wet category scoring higher on frontal SVSP PC6 than the Temperate category:

- **Hot/Wet x Temperate category:** Mean difference = -0.016, $p < 0.05$.

Lower scores on frontal SVSP PC6 imply that the Temperate category have craniofacial morphology associated with larger frontal sinuses than the Hot/Wet category.

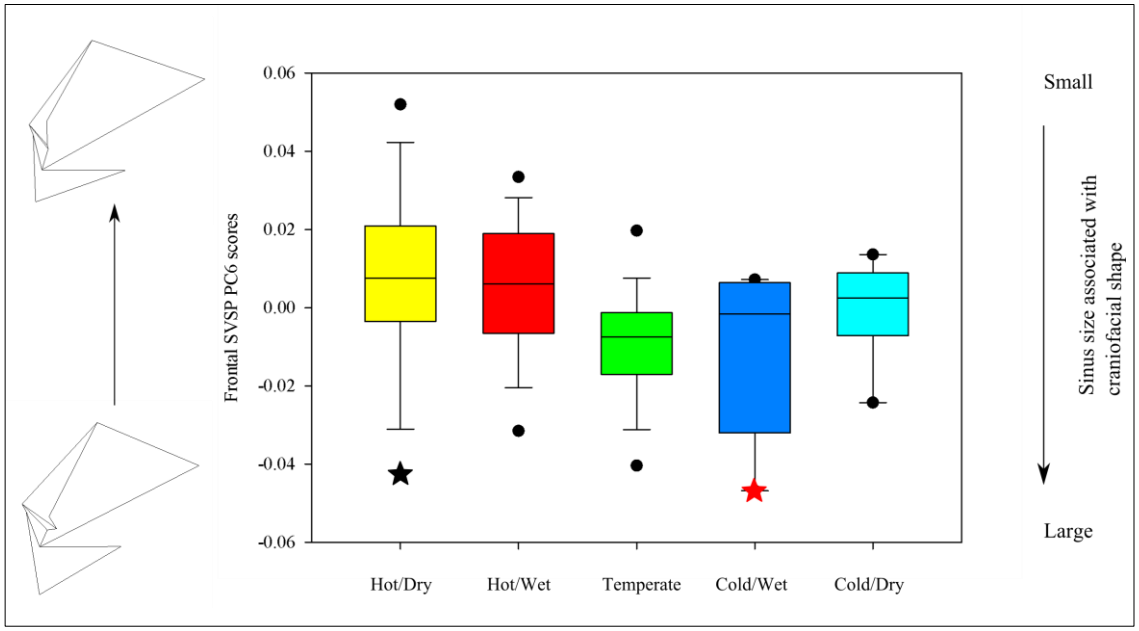

Figure 116: The significant differences between climatic categories in frontal SVSP PC6 scores. Wireframes on the right show shape change along the PC. The Hot/Wet category scores significantly higher on frontal SVSP PC6 than the Temperate category. Wireframe diagrams on the left-hand y axis show the shape change described by frontal SVSP PC6, right hand y axis shows the direction of the relationship between the frontal SVSP PC6 and relative frontal sinus volume. Black star indicates Kabwe; red star indicates La Ferrassie, see text for details.

In terms of fossils with possibly problematic climatic categorisation, La Ferrassie and Kabwe are the lowest scoring individuals in the Cold/Wet and Hot/Dry categories respectively (see Figure 116). If La Ferrassie is removed there is no difference in which categories are significantly different, or the strength of the difference between them. If Kabwe is removed, however, there is a greater difference between categories ($F(108) = 5.75$, $\omega^2 = 0.18$, $p < 0.0001$) and the difference between Temperate and Hot/Dry categories becomes significantly different (mean difference = -0.021, $p < 0.05$) in addition to the difference between Temperate and Hot/Wet categories. Thus, Kabwe's category uncertainty does not affect the differences reported above, but may mask other significant differences, such as a potential difference between the Temperate and Hot/Dry categories.

6.II.b.ii. Differences in maxillary SVSPs between climate categories

Maxillary SVSP PC3

Temperature

There is no significant difference in maxillary SVSP PC3 scores between temperature categories.

Precipitation

Maxillary SVSP PC3 scores are on average significantly higher in the Wet category than in the Dry category (see Figure 117):

- **Maxillary SVSP PC3 by precipitation category:** t-test: t(59) = 2.550, r^2 = 0.10, $p < 0.05$, 2-tailed.

The Wet category shows craniofacial morphology indicative of larger maxillary sinuses than the Dry category.

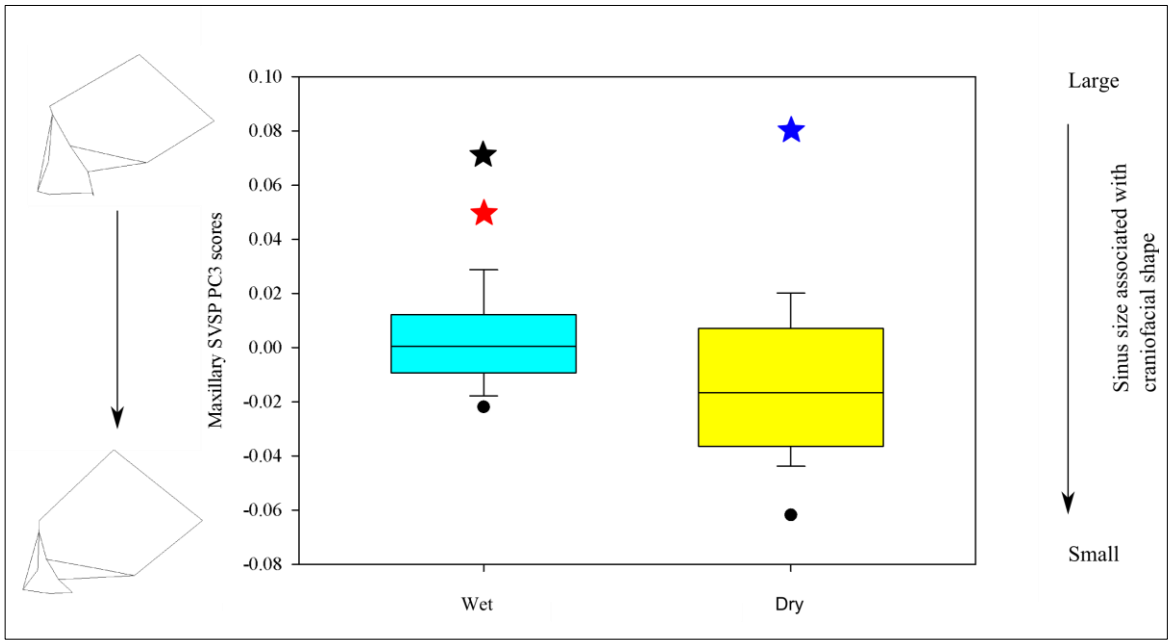

Figure 117: The significant difference between precipitation categories in maxillary SVSP PC3 scores. Maxillary SVSP PC3 scores are on average significantly higher in the Wet category than in the Dry category. Wireframes on the right show shape change along the PC. Wireframe diagrams on the left-hand y axis show the shape change described by maxillary SVSP PC3, right hand y axis shows the direction of the relationship between the maxillary SVSP PC3 and relative maxillary sinus volume. Black, red, and blue stars indicate Petralona, La Ferrassie, and Kabwe respectively. See text for details.

Petralona and La Ferrassie are the highest scoring individuals in the Wet category and Kabwe is the highest scoring in the Dry category (see Figure 117), which means that their uncertain climate categorisation could affect the results. If Kabwe or La Ferrassie are removed from the sample, the difference remains statistically significant, but if Petralona is removed the difference between the Wet and Dry categories is no longer significant. Thus, the difference detected is to some extent

dependent on an individual with a relatively uncertain categorisation. The relationship is considered in Chapter 7 in the context of this uncertainty and the other results.

Full climate categories

There are significant differences in maxillary SVSP PC3 scores between some of the climate categories (see Figure 118):

- **Maxillary SVSP PC3 by climate category:** ANOVA: $F(87) = 3.960$, $\omega^2 = 0.08$, $p = 0.005$.

Post-hoc tests show the difference to due to lower scores in the Cold/Dry category than the Hot/Wet category:

- **Cold/Dry x Hot/Wet category:** Mean difference = -0.0337, $p < 0.01$.

The Cold/Dry category shows craniofacial morphology associated with smaller maxillary sinuses that the Hot/Wet category.

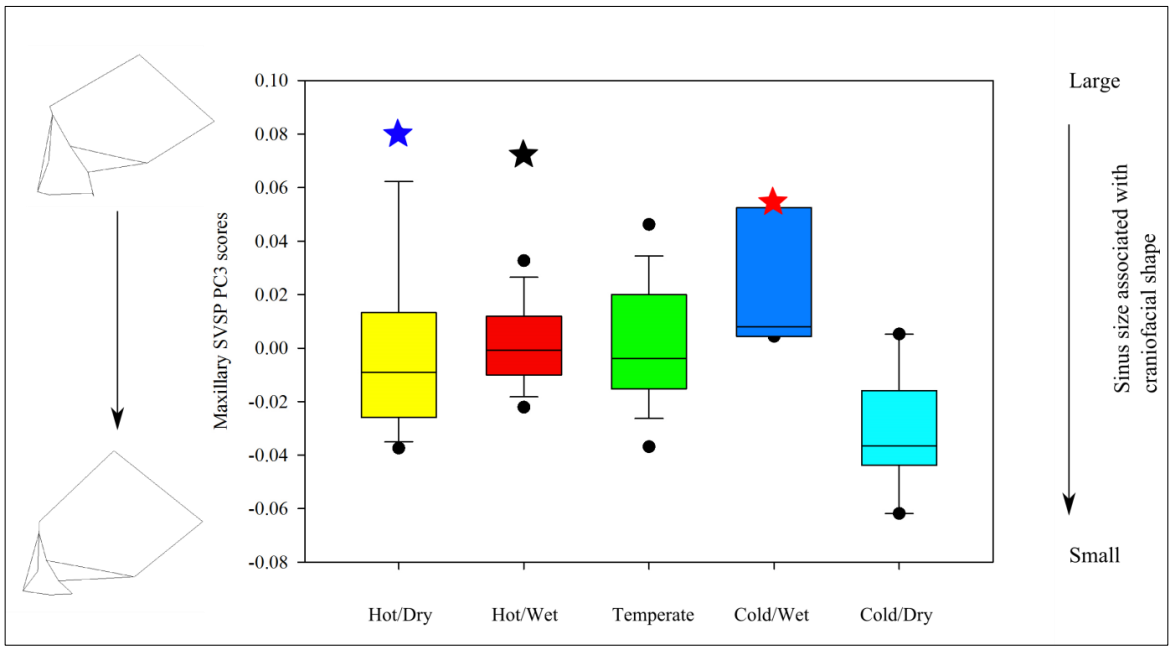

Figure 118: The significant differences between climatic categories in maxillary SVSP PC3 scores. Wireframes on the right show shape change along the PC. Scores in the Cold/Dry category are significantly lower than in the Hot/Wet category. Wireframe diagrams on the left-hand y axis show the shape change described by maxillary SVSP PC3, right hand y axis shows the direction of the relationship between the maxillary SVSP PC3 and relative maxillary sinus volume. Blue, black, and red stars indicate approximate location of Kabwe, Petralona, and La Ferrassie, respectively. See text for details.

Again, the potentially problematic fossils Petralona, Kabwe, and La Ferrassie stand out as outliers on maxillary SVSP PC3, (see Figure 118). Each in turn was removed from the analyses, but no difference was found in which climate categories showed significant differences to one another. The removal of Petralona and Kabwe (separately) strengthened the significance of the difference between categories ($p < 0.005$ and $p = 0.001$, respectively), but when La Ferrassie is removed, the p value rises to $p < 0.05$ (still significant, but a higher chance of type I error). Based on these tests, it seems that the differences found in maxillary sinus-associated craniofacial morphology in different climates are not unduly affected by specimens that may have inaccuracies in their climate categorisation, despite the sensitivity of the precipitation result to the position of La Ferrassie as noted above.

Maxillary SVSP PC7

There is no significant difference in maxillary SVSP PC7 scores between temperature, precipitation, or climate categories.

6.II.b.iii. Differences in sphenoidal SVSPs between climate categories

Sphenoidal SVSP PC3

Temperature

There are significant differences between sphenoidal SVSP PC3 scores between the temperature categories (see Figure 119):

- **Sphenoidal SVSP PC3 by temperature category:** ANOVA: $F(96) = 10.911$, $\omega^2 = 0.16$, $p < 0.0001$.

Post-hoc tests show that the Hot category has significantly lower scores on sphenoidal SVSP PC3 than the Temperate category.

- **Hot x Temperate category:** Mean difference = 0.0296, $p < 0.0001$.

This result shows that specimens in the Hot category have craniofacial morphology linked to smaller sphenoidal sinuses than those in the Temperate category.

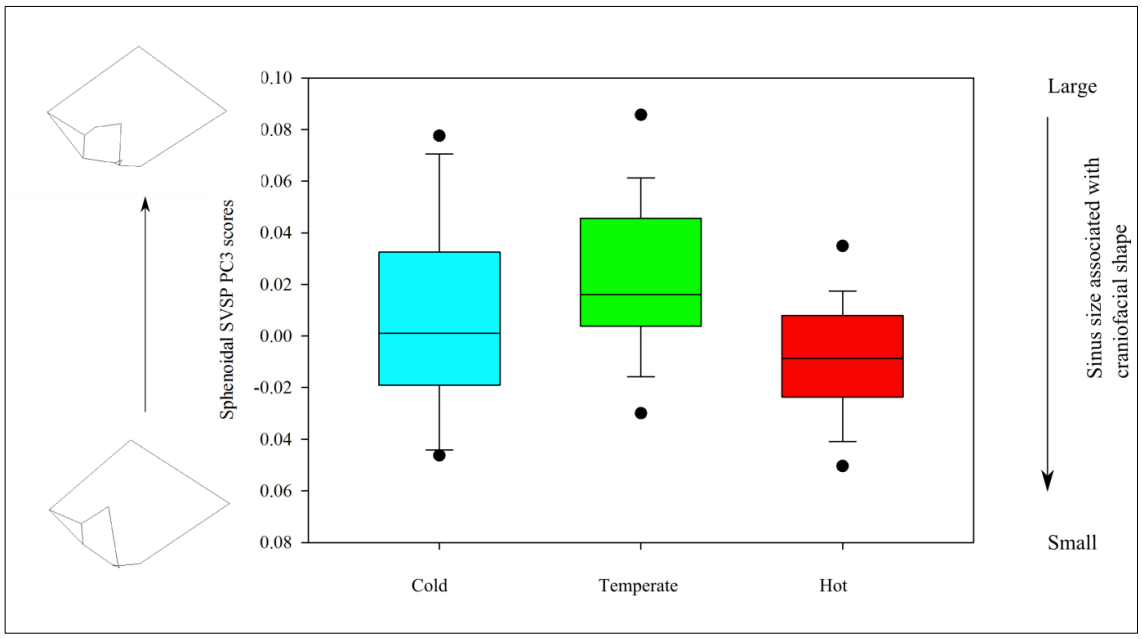

Figure 119: The significant differences between temperature categories in sphenoidal SVSP PC3 scores. The Hot category has significantly lower scores on sphenoidal SVSP PC3 than the Temperate category. Wireframes on the right show shape change along the PC. Wireframe diagrams on the left-hand y axis show the shape change described by sphenoidal SVSP PC3, right hand y axis shows the direction of the relationship between the sphenoidal SVSP PC3 and relative sphenoidal sinus volume.

Precipitation

There are no significant differences in sphenoidal SVSP PC3 scores between precipitation categories.

Full climate categories

There are large, significant differences in sphenoidal SVSP PC3 scores between some of the climate categories (see Figure 120):

- **Sphenoidal SVSP PC3 by climate categories:** ANOVA: $F(96) = 7.448$, $\omega^2 = 0.20$, $p < 0.0001$.

Post hoc tests show that this is due to significantly higher scores in the Temperate category compared to the Hot/Wet category:

- **Temperate x Hot/Wet category:** Mean difference = 0.0312, $p < 0.0001$.

The higher scores in the Temperate category show that individuals in the Temperate category have craniofacial form linked to relatively larger sphenoidal sinus volume than in the Hot/Wet category.

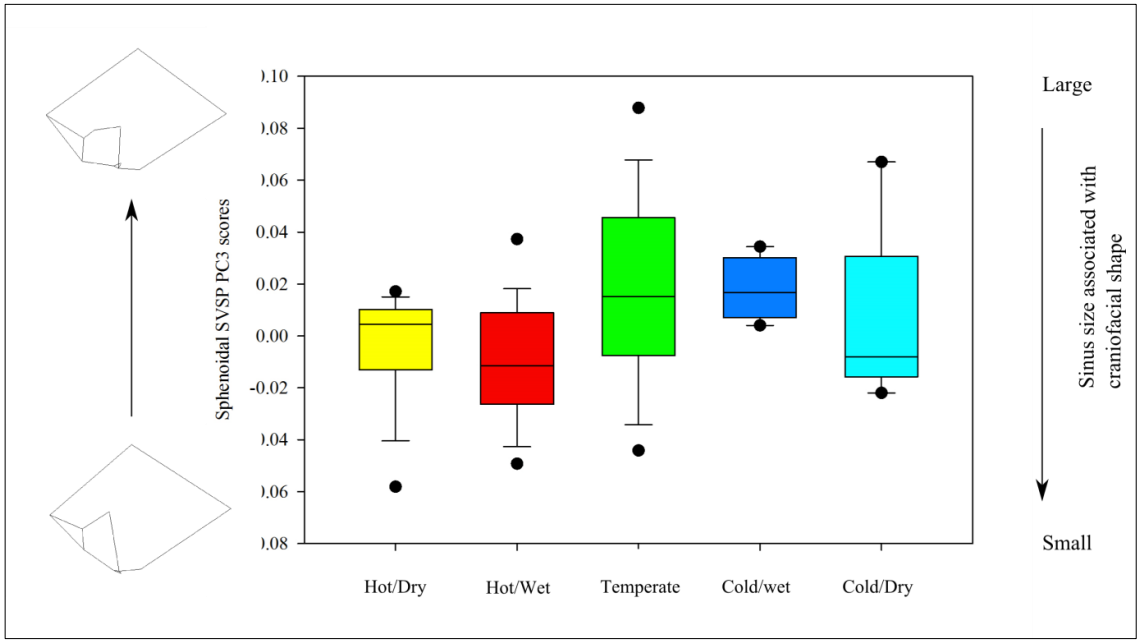

Figure 120: The significant differences in sphenoidal SVSP PC3 scores between climate categories. There are significantly higher scores on sphenoidal SVSP PC3 in the Temperate category compared to the Hot/Wet category. Wireframe diagrams on the left-hand y axis show the shape change described by sphenoidal SVSP PC3, right hand y axis shows the direction of the relationship between the sphenoidal SVSP PC3 and relative sphenoidal sinus volume.

Sphenoidal SVSP PC6

There is no significant difference in sphenoidal SVSP PC6 between temperature, precipitation, or climate categories.

6.III. Summary

RQ3: Are there interactions between climate and sinus variables?

Neither relative frontal, nor relative maxillary sinus volume shows any reliable relationship with any climatic variable. Relative frontal sinus volumes are significantly larger in the Wet category than the Dry category, but this may be affected by the outlier effects of the *H. heidelbergensis* (see Section 6.II.b.i). There are very small positive relationships between relative sphenoidal sinus volume and both maxTemp and maxPrecip, neither of which is significant if a Bonferroni correction is applied; hence it is possible that neither is reliable. The latter difference, however, is supported by the medium sized difference in sphenoidal sinus volumes found between the Wet and Dry categories. Sphenoidal sinus volumes are relatively larger in the Wet category, suggesting that this is the one relatively robust climatic interaction with any type of sinus volume directly.

In both continuous and categorical analyses, the results are broadly consistent; in frontal and sphenoidal SVSPs the craniofacial morphology associated with larger relative sinus volumes is linked to colder, wetter climates, whilst the reverse is true for the maxillary SVSPs. This shows the robusticity of the results, suggesting that the error inherent in the attribution of climates cannot obscure the relationships uncovered between climate and sinus-related craniofacial morphology. It also implies that different factors govern maxillary sinus-related shape compared to the other two sinus types. Furthermore, the patterns seen in the recent *H. sapiens*

populations seem to extend to the fossil groups. Some of the relationships between climate and SVSPs, both in recent *H. sapiens* and full samples, are relatively strong, in some cases explaining up to a third of the variation between specimens in sinus-related craniofacial shape.

Table 48: Summary of differences in relative sinus volume between climate categories. Red highlighting: significant difference, NS: non-significant, Sig.: ANOVA reaches significance, but post-hoc tests do not. * = $r^2/\omega^2 > 0.1$, ** = $r^2/\omega^2 > 0.2$.

Category	Relative frontal sinus volume	Relative maxillary sinus volume	Relative sphenoidal sinus volume
Temperature	NS	NS	NS
Precipitation	Dry < Wet	NS	Dry < Wet*
Climate	NS	NS	Sig.

Table 49: Summary of RMA regression results showing relationships between SVSPs and continuous climatic variables. +ve: significant positive relationship, -ve: significant negative relationship, NS: non-significant relationship. Light red: relationship non-significant if Bonferroni correction applied, dark red: relationship remains significant if Bonferroni correction applied. *: $r^2 \geq 0.05$, **: $r^2 \geq 0.1$.

	SVSPs					
SVSPs	**Frontal**		**Maxillary**			
Continuous climatic variables	**Full landmark set PC3**	**Frontal PC6**	**Maxillary PC3**	**Maxillary PC7**	**Sphenoidal PC3**	**Sphenoidal PC6**
MAT	+ve**	+ve*	+ve*	NS	-ve*	NS
MaxTemp	+ve**	NS	+ve**	NS	-ve*	NS
MinTemp	+ve**	+ve*	NS	NS	-ve**	NS
MAP	+ve**	NS	NS	NS	-ve*	NS
MaxPrecip	+ve**	NS	NS	NS	-ve**	NS
MinPrecip	+ve*	-ve*	NS	NS	NS	NS
Direction of relationship with relevant sinus volume	Negative	Negative	Positive	Positive	Positive	Positive

Table 50: Summary of differences (ANOVA/t-tests) in SVSP PC scores between climate categories. Direction: direction of relationship (positive or negative) between SVSP and relevant sinus volume. Red highlighting: significant result. NS: non-significant relationship. * = $r^2/\omega^2 \geq 0.10 < 0.20$, ** = $r^2/\omega^2 \geq 0.20$ (strength of effect in initial ANOVA, not post-hoc test).

			SVSPs			
	Frontal		**Maxillary**		**Sphenoidal**	
	Full LM set PC3	**Frontal PC6**	**Maxillary PC3**	**Maxillary PC7**	**Sphenoidal PC3**	**Sphenoidal PC6**
Temperature	Cold < Temperate** Cold < Hot**	Temperate < Hot*	NS	NS	Hot < Temperate*	NS
Precipitation	NS	NS	Dry < Wet*	NS	NS	NS
Climate	Cold/Dry < Temperate** Cold/Dry < Hot/Wet** Cold/Dry < Hot/Dry**	Temperate < Hot/Wet*	Cold/Dry < Hot/Wet	NS	Hot/Wet < Temperate**	NS
Direction	Negative	Negative	Positive	Positive	Positive	Positive

Chapter 7: Discussion

In this thesis, relative sinus volume and craniofacial shape related to relative sinus volume have been investigated to uncover their relationships with population/taxonomic affiliation, masticatory strain, and climate. The intention has been to identify which sinus variables show relationships with which taxonomic and ecological (masticatory strain/climate) variables, and to compare the strengths between these relationships in the hope of shedding light on taxonomic and functional questions about sinus morphology. Where there are significant differences in populations/taxa, these are evaluated in light of assertions about hyperpneumatisation in *H. heidelbergensis*/*H. neanderthalensis*, the validity of *H. heidelbergensis* as a taxon, pneumatic causes of diagnostic craniofacial morphology in *H. heidelbergensis* and *H. neanderthalensis*, and hyperplasticity in *H. sapiens*. Pneumatic differences identified are scrutinised through the lens of the ecological variables to ascertain whether a mechanical or climatic sinus function might be accountable for the differences determined. In analyses across taxa, where sinus volumes themselves show a direct relationship with an ecological variable that is stronger than the relationship between that variable and the relevant sinus-related craniofacial shape, this can support a functional role for the sinus. Where the reverse is true, and an ecological variable shows a stronger relationship with sinus-related craniofacial morphology than the sinus volume itself, this supports the theory that sinuses do not have a direct functional relationship with ecology.

7.I. RQ1: Taxonomic/population differences in paranasal pneumatisation

7.I.a. RQ1.a: Are there differences in sinus variables between populations of recent *H. sapiens*?

Sinus volume has been shown to differ between populations of recent *H. sapiens* (Brothwell *et al.*, 1968; Buckland-Wright, 1970; Fernandez, 2004a, b; Holton *et al.*, 2013), and it has even been suggested that it would be useful to make identifications to ethnic group in forensic cases (Fernandez, 2004a), yet most earlier studies on this subject have focused on comparisons of relatively few populations (Brothwell *et al.*, 1968; Buckland-Wright, 1970; Fernandez, 2004b; Holton *et al.*, 2013), or of only one type of sinus (Butaric *et al.*, 2010). To date, the reasons for population differences are not well understood, as the correlates of sinus morphology in hominins remain unclear. There is some evidence that differences between recent *H. sapiens* populations are related to climate (Koertvelyessy, 1972; Shea, 1977; Hanson & Owsley, 1980; Holton *et al.*, 2013) but the results are mixed when large-scale cross-population comparisons are made (Butaric *et al.*, 2010) (see Section 7.III.). Despite the knowledge that many of the craniofacial differences between populations of recent *H. sapiens* can be attributed to neutral mechanisms and population history rather than selective pressures (Roseman, 2004; Roseman & Weaver, 2004; Harvati & Weaver, 2006b; Betti *et al.*, 2010; Brewster *et al.*, 2014), the possibility that this is the reason for differences in sinus morphology between populations in recent *H. sapiens* has been little explored in previous research. The current thesis represents

the largest and most globally representative sample of recent *H. sapiens* to be analysed for sinus volumes and related craniofacial morphology to date. It expands on Zollikofer *et al.*'s (2008) pioneering work, which explicitly addresses sinus-related craniofacial shape by using geometric morphometrics, extending the analyses with a far larger sample and all three sinus types. In 13 populations of recent *H. sapiens* frontal, maxillary and sphenoidal sinus volumes, and the shape variables associated with them, have been compared and the plausibility of population history as an explanation for these differences has been explored.

The current thesis found small significant differences in frontal (but not maxillary or sphenoidal) sinus volumes between populations of recent *H. sapiens*. The differences in relative frontal sinus volumes are particularly between Western African (smaller) and Western European populations (larger). However, there is much overlap, the differences are extremely small, and they are not robust to Bonferroni correction. Both these populations combine individuals from a relatively wide geographical areas (see Section 2.IV.a.iii.), which may reduce their representativeness of their respective groups; these results must, therefore, be treated with caution. There is no relationship between population history and relative sinus volume for any of the sinus types.

The low level of population-level differentiation in craniofacial pneumatisation described in the current thesis is surprising, given the results of previous studies, as described above, although it echoes the maxillary sinus results of Holton *et al.* (2013) in the specific populations that show separation (see Section 7.III.). Given the

differences in samples between the current thesis and previous work, the dissimilarity in results could be due either to the relatively small sample sizes for each population in the current thesis failing to represent the true mean of relative sinus volume in each population, or to the few populations compared in the earlier studies, which could have failed to capture the true pneumatic variation in recent *H. sapiens*. Where multiple populations have been compared previously, the results have been similar to the current thesis, providing greater confidence in the results. For example, Butaric *et al.* (2010) found no difference in relative maxillary sinus volume between populations, the sample size in Butaric *et al.*'s study (per population), however, is very small. The possibility that the current study has failed to find true population differences due to insufficient sample sizes for each population could be explored with larger samples and perhaps improved global coverage, including, for example, Middle Eastern and North American material. Based on the results presented here, contrary to previous studies with less comprehensive samples, variation in sinus volume does not seem to be strongly patterned by population in recent *H. sapiens*. It does not seem, for example, that pneumatisation is a useful means of diagnosing ethnic group in a forensic context (as had been suggested for the maxillary sinuses by Fernandez, 2004a); though it is possible it could be of use in combination with other information.

In addition to the differences in relative frontal sinus volume found in the current thesis, there are small, but significant differences in craniofacial morphology associated with frontal sinus volume between populations of recent *H. sapiens*. These differences are mainly between Greenland/Hawaiian/Chinese populations and

the rest of the sample, and are much stronger than the direct differences between populations in relative frontal sinus volume. This suggests that, contrary to previous assumptions, population membership has an indirect relationship with relative frontal sinus volume, via population-patterned frontal sinus-related craniofacial morphology, and that the sinuses are spandrels, which vary in size according to craniofacial shape.

There are significant (albeit small) relationships between population history and frontal sinus-related craniofacial shape. The frontal sinus was the one sinus type that did show small significant population differences in sinus volume itself, but the strength of the differences in frontal sinus-related craniofacial morphology between recent *H. sapiens* populations is an order of magnitude greater than the differences in volume, and there is no direct relationship between population history and frontal sinus volumes (see above). This suggests that genetic drift has only an indirect relationship with frontal sinus volume. An indirect relationship between drift and frontal sinus volume is congruent with craniofacial morphology as a key influence on sinus volume and a small amount of this morphology being affected by population history. This finding augments the body of research that shows the great effect of population history and neutral accumulation of traits on population-level differences in craniofacial morphology in recent *H. sapiens* (e.g., Harvati & Weaver, 2006b; Betti *et al.*, 2009, 2010; von Cramon-Taubadel, 2009a; Brewster *et al*., 2014).

7.I.b RQ1.c: Are there differences in sinus variables between Mid-Late Pleistocene taxa?

Paranasal sinus size and morphology have been used to classify hominin specimens (e.g., Schwartz *et al.*, 2008) based on perceived differences in pneumatisation. Specific to later *Homo*, hyperpneumatisation has been frequently discussed as a characteristic trait of both *H. heidelbergensis* (Seidler *et al.*, 1997; Prossinger *et al.*, 2003; Zollikofer *et al.*, 2008; Stringer, 2012c) and *H. neanderthalensis* (Busk, 1861; Blake, 1864). It has also been used as an explanation for craniofacial morphology in both taxa (Coon, 1962; Seidler *et al.*, 1997; Wolpoff, 1999). Conversely, recent CT studies have suggested that *H. neanderthalensis* hyperpneumatisation is only relative, not absolute, when craniofacial size is taken into account (Zollikofer *et al.*, 2008; Rae *et al.*, 2011). Determining whether there really are taxonomic differences in sinus morphology between Pleistocene hominin taxa using the largest, most representative sample to date and a more objective, repeatable method than previously employed was a key aim of this study. The results presented here provide novel pneumatic support to the Euro-African hypodigm of *H. heidelbergensis*, and enable the assertion of hyperpneumatisation in Neanderthals to be refuted with greater confidence.

7.I.b.i. The case for hyperpneumatisation in H. heidelbergensis

The picture of *H. heidelbergensis* hyperpneumatisation garnered from the literature is complicated, in part due to the debate over which specimens should be included in the hypodigm (see Section 1.II.a.i.). Although Petralona, Bodo, and Kabwe are all known for their large frontal sinuses (Seidler *et al.*, 1997; Prossinger *et al.*, 2003;

Zollikofer *et al.*, 2008), and it has been claimed that other putative *H. heidelbergensis*, such as Steinheim, are similarly highly pneumatised (Prossinger *et al.*, 2003), specimens such as Ceprano (Bruner & Manzi, 2005) and Arago 21 (Tillier, 1975, 1977; Stringer, 1984; Balzeau, 2005), do not necessarily show the same pattern. Arago 21 is a key fossil in the *H. heidelbergensis* hypodigm, linking the mandibular (including the type specimen) and cranial material (Stringer, 1985b; Rightmire, 2008; Mounier *et al.*, 2009; Buck & Stringer, 2014). It was not possible to include Arago 21 in the current thesis, but there is evidence from other sources that its frontal sinuses are very small (Tillier, 1975, 1977; Stringer, 1984; Balzeau, 2005); they appear to be two widely separated cells that fail to pneumatise the frontal squama (Figure 121). Although Balzeau (2005) acknowledges the presence of some matrix within the sinuses on both sides, it is implausible that the matrix hides a frontal sinus like those of Kabwe/Bodo/Petralona. It was hoped that, by measuring a sample of key *H. heidelbergensis* fossils all using the same methodology, the results from the current thesis might clarify the hyperpneumatic status of *H. heidelbergensis*.

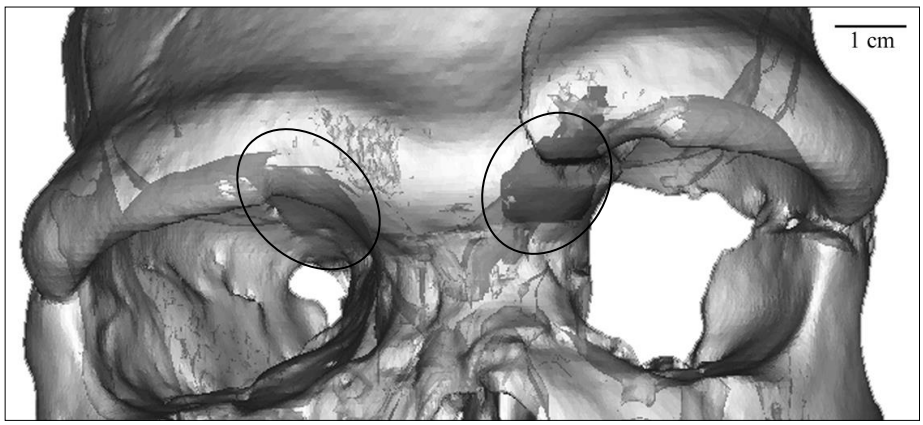

Figure 121: CT virtual reconstruction of Arago 21 rendered transparent and with frontal sinuses sectioned out. Taken from Balzeau (2005:144), circles added to mark sinuses.

The results of the current thesis corroborate those of previous studies (Seidler *et al.*, 1997; Prossinger *et al.*, 2003; Zollikofer *et al.*, 2008; Stringer, 2012c), that relative frontal sinus volumes are significantly greater on average in the *H. heidelbergensis* sample than in *H. sapiens* or *H. neanderthalensis* samples, strengthening the argument for the *H. heidelbergensis* hypodigm. Despite its significant difference from other taxa in the current thesis, however, the *H. heidelbergensis* sample investigated here is not homogeneous in frontal sinus morphology. There are differences in relative volume between Kabwe, Bodo, and Petralona, as discussed in Section 4.II.a.i, and Ceprano's frontal sinus volume is substantially smaller than that of all the other specimens. As discussed below, Ceprano may plausibly be excluded from the *H. heidelbergensis* hypodigm based on its morphology, an argument supported by the results from the current study regarding its frontal pneumatisation, which would be atypical for *H. heidelbergensis*. The shape and extension of the frontal sinuses of the remaining *H. heidelbergensis* in the current sample appear similar and seem qualitatively different from those of other taxa in the present study (see Figure 75). Given the amount of variation seen between recent *H. sapiens* sinuses (see below), we should expect at least some variation in *H. heidelbergensis*, particularly given the several hundred thousand years spread for the fossil specimens in the sample. The results from the current thesis suggests that, despite variation, on average *H. heidelbergensis* does indeed exhibit hyperpneumatised frontals compared to *H. sapiens* and *H. neanderthalensis* means and this is an important contribution to the discussion of this fraught, much debated topic.

As discussed in Section 1.II.a.i, the taxonomic status of *H. heidelbergensis* is still disputed and, as frontal hyperpneumatisation is a possible apomorphy of *H. heidelbergensis* (Seidler *et al.*, 1997; Stringer, 2012c), it was hoped that the data from the current thesis could contribute to this discussion. To evaluate whether the proposed frontal hyperpneumatisation in *H. heidelbergensis* is derived, it is necessary to consider the frontal pneumatisation of earlier *Homo*, as well as *H. sapiens* and *H. neanderthalensis*. The evidence for the apomorphic nature of large frontal sinuses in *H. heidelbergensis* compared to other taxa, given the nature of sinus volume in its presumed predecessor, *H. erectus,* is equivocal. The one *H. erectus* (KNM-ER 3883) in the current frontal sinus volume sample has a very similar relative frontal sinus volume to Kabwe in both size and morphology (i.e., similarity in continuity between sides and greatest superior extent; Figure 122). This would suggest that large frontal sinuses are the primitive condition (Sherwood *et al.*, 2002), yet it seems that this degree of pneumatisation may actually be very unusual for *H. erectus*, in both the Asian and African branches of the species (see Section 2.IV.a.i. for the definition of *H. erectus* employed here). The majority of *H. erectus* from Indonesia and China have small frontal sinuses that do not extend superiorly past the glabellar, or peri-glabellar, regions (Weidenreich, 1943, 1951; Tillier, 1975, 1977; Wu & Poirier, 1995; Balzeau, 2005; Vialet *et al.*, 2010). If regarded as *H. erectus*, the one exception to this may be the Maba specimen (China), where the frontal sinus is reported to protrude into the frontal squama (Wu & Poirier, 1995). However, the sinuses in this specimen are also said to be well-separated by a bony septum and to extend little further laterally than the centre of the orbit (Wu & Poirier, 1995). It seems unlikely that this is a description of anything resembling the

extreme pneumatisation seen in *H. heidelbergensis* (with the exception of Ceprano) in the current sample. Furthermore, most researchers do not regard Maba as *H. erectus*; for example, Stringer (2012c) considers it could be related to Neanderthals, or to *H. heidelbergensis*. CT data for Maba were not available for inclusion in the current sample, but would certainly be relevant to any further work on this topic. The African *H. erectus* sample, where it is sufficiently preserved, also suggests that small frontal sinuses are the norm for the taxon; the Daka calvaria from the Middle Awash has sinuses that (Gilbert *et al.*, 2008: 32):

> ...do not extend into the frontal squama toward bregma as they do in Petralona and Kabwe or Bodo, nor are they nearly as laterally extensive, expanding only to the approximate apices of the supraorbital torus arcs.

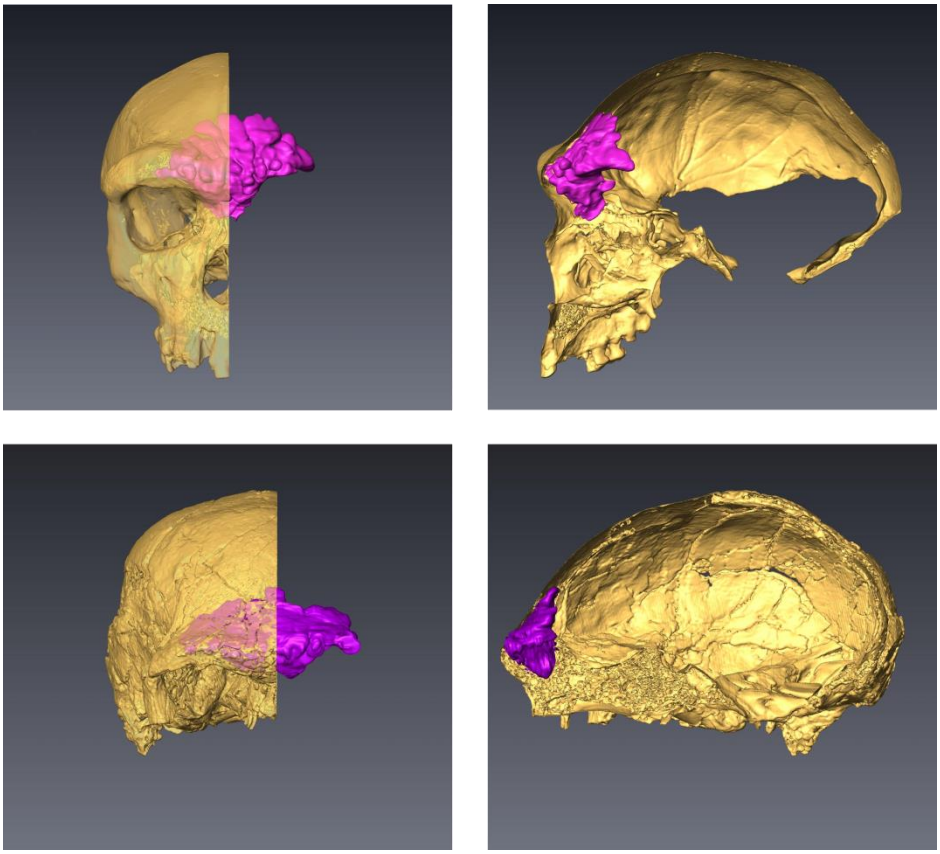

Figure 122: Virtual reconstructions of Kabwe (top) and KNM-ER 3883 (bottom) with frontal sinuses sectioned out and shown in magenta. Left: norma frontalis, Right: norma lateralis. Images not to scale.

Based on these reports, the general impression is of a small frontal sinus in *H. erectus*, with some exceptions, quite different to the morphology of at least some *H. heidelbergensis* specimens, as shown in this study. This supports the case for extreme frontal pneumatisation as an apomorphy in *H. heidelbergensis*, but further investigations are needed, preferably including key specimens, such as Arago 21 and Maba, and an increased *H. erectus* sample. If KNM-ER 3883 proves to be unusual for *H. erectus* in its frontal pneumatisation, it would be tempting to suggest a special link between this specimen and *H. heidelbergensis*, perhaps via Bodo, one of the oldest *H. heidelbergensis* in the hypodigm and, like KNM-ER 3883, from east Africa. Based on this character alone, anything more would be speculative, but it could be fruitful to study these crania in greater depth to ascertain if there is any further evidence for such a link.

If frontal hyperpneumatisation is a diagnostic feature of *H. heidelbergensis*, as seems plausible from the results presented here, does this shed any light on the two fossils in that sample that are of disputed taxonomic attribution; Ceprano and Steinheim, or on the plausibility of the Euro-African hypodigm itself (see Section 1.II.a.i.)? It has been suggested that Ceprano is more primitive than other members of the *H. heidelbergensis* hypodigm, and that it is more *H. erectus*-like in many aspects of its morphology (see Chapter 4). In fact, due to its more primitive features, Ceprano has been posited as the ancestral species for *H. heidelbergensis* by some authors (Manzi, *et al.*, 2001; Stringer, 2002b; Bruner & Manzi, 2005; Mounier *et al.*, 2011). The frontal sinuses in Ceprano are very different from the other *H. heidelbergensis* in the sample, as discussed above (Figure 123); although they may be more like those of

Arago 21 (Figure 121). Ceprano's frontal sinuses are relatively small, even compared to *H. neanderthalensis* and early *H. sapiens* (and most of recent *H. sapiens* sample). The results of this study therefore support the hypothesis that Ceprano is not most parsimoniously placed in the *H. heidelbergensis* hypodigm, but this only holds if large frontal sinus volume is a *H. heidelbergensis* apomorphy, which is not yet certain (see above). Given the range of variation in frontal sinus volume seen in *H. heidelbergensis*, both in this sample and with the addition of data from other sources such as Arago 21, it can at least be said that Ceprano's frontal pneumatisation supports the idea that it is not best placed in *H. heidelbergensis*.

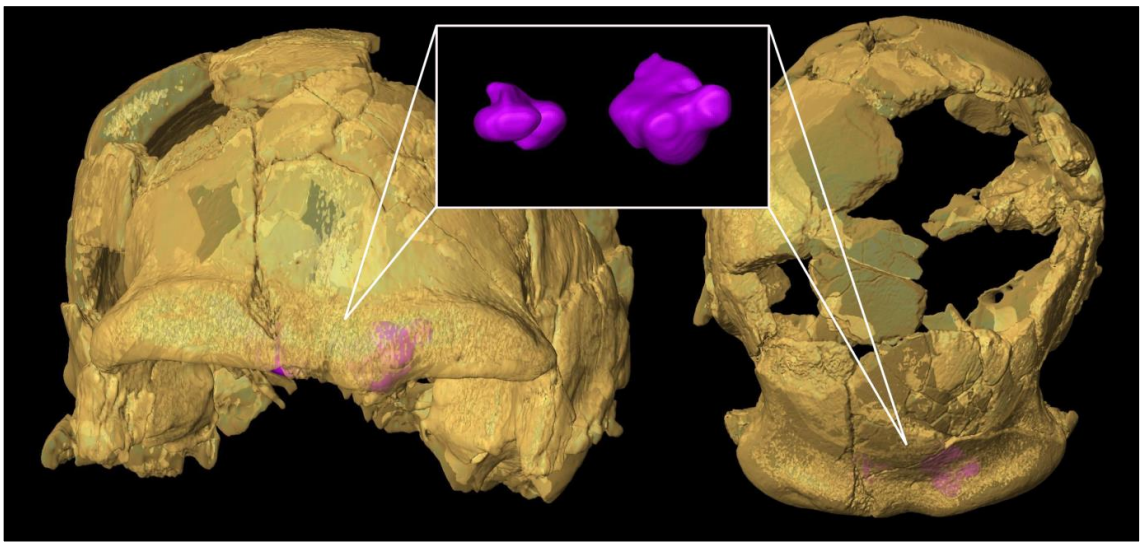

Figure 123: Frontal sinuses (magenta) of Ceprano *in situ* within virtual reconstructions of the calvaria, rendered transparent. Left: norma frontalis, right: aspectus superior. Highlighted box: frontal sinuses sectioned out (from aspectus superior). Compare with Figure 121 and 122 above.

The Steinheim fossil is variably placed in *H. heidelbergensis* (e.g., Friess, 2010a, b; Harvati *et al.*, 2010) or in *H. neanderthalensis* (e.g., Tattersall, 2007; Stringer, 2012c). In the current thesis, Steinheim was found to be closer to the *H. neanderthalensis* sample in its frontal sinus-specific morphology (the only analysis in which this fossil was included). As there was no significant difference between *H.*

heidelbergensis and *H. neanderthalensis* in this sinus-related morphology, however, and neither removing nor reclassifying Steinheim altered the results, this is not very informative in terms of its taxonomic affiliation. It had been reported that Steinheim has a very large frontal sinus "astonishingly similar" to that of Petralona (Prossinger *et al.*, 2003: 140). The figures in that publication, however, do not support the claim. Furthermore, examination of a stereolithgraphically printed reconstruction of the Steinheim cranium made by Christoph Zollikofer and his group at The University of Zurich, where the extent of the sinuses is visible through breaks, makes clear that the sinus was fairly small (right maximum width = 21.05mm, left maximum width = 31.4mm, maximum height = ~26mm), certainly far smaller than portrayed by Prossinger *et al.* (2003). A measurement of Steinheim's frontal sinus was not included in the present sample, as the extent of damage and matrix infill made a volume estimate imprudent. If Steinheim had a large frontal sinus, that might have supported *H. heidelbergensis* status for the fossil; its small frontal sinus does not preclude its inclusion, but it can be said that its pneumatisation would be atypical for that taxon, based on current evidence. This provides some small measure of support for the argument that Steinheim is better placed in *H. neanderthalensis* than *H. heidelbergensis*.

In the current study, some but not all, of the *H. heidelbergensis* individuals in the sample have exceptional frontal pneumatisation. Although one, seemingly unusual, *H. erectus* (KNM-ER 3883) has frontal pneumatisation comparable with Kabwe (see Figure 122). The current sample is the largest used for a comparable study to date, yet nothing in the entire sample (or in the literature) has frontal pneumatisation

comparable with Bodo or Petralona. This suggests that the taxonomic grouping of these European and African Mid Pleistocene hominins together is supported by their uniquely large frontal sinuses. There seems to be no geographic difference in pneumatisation; there is comparable difference between Petralona (Europe) and Bodo (Africa) and between Bodo and Kabwe (Africa) in terms of frontal sinus volume. Furthermore, the putative *H. heidelbergensis* with small frontal sinuses (Ceprano and Arago 21) are from Europe, as is Petralona, which has the largest frontal sinus of all. The pneumatic evidence from this study does not support a split between the African material (which might then be referred to as *H. rhodesiensis*; see Section 1.II.a.i.) and the European material, but shores up the Euro-African hypodigm. This problem can only be resolved with a larger sample of Mid Pleistocene fossils; in the meantime, it is most conservative to conclude from the data currently available that hyperpneumatised frontal sinuses are suggestive, but not definitive, of *H. heidelbergensis* membership.

In addition to the direct difference in relative frontal sinus volumes found between taxa presented here, inter-taxonomic differences were also found in frontal sinus-related craniofacial shape variables. It has been argued that hyperpneumatisation is a cause of *H. heidelbergensis* craniofacial morphology (Seidler *et al.*, 1997); conversely, if the sinuses are spandrels, the differences in craniofacial morphology between taxa presented here could explain the inter-taxon differences in the frontal sinus volumes, or the seeming intra-taxonomic variation between specimens such as Petralona and Arago 21. The morphology of the frontal bone (Balzeau, 2005), the orbital (Zollikofer *et al.*, 2008) and supraorbital regions (Vinyard & Smith, 1997)

have previously been suggested as candidate influences as on frontal sinus morphology.

In the current thesis, *H. heidelbergensis* specimens were found to have relatively larger frontal sinus volumes than both *H. sapiens* and *H. neanderthalensis*, and also to have significant differences in frontal sinus-related craniofacial shape from *H. sapiens* only. These shape differences show that *H. heidelbergensis* has taller supraorbital regions and deeper, taller faces, which may reflect greater prognathism compared to *H. sapiens* (see Chapter 4 for details). In common with earlier *Homo*, *H. heidelbergensis* has a larger face than either *H. sapiens* or *H. neanderthalensis*, both which show facial reduction (Rightmire, 2013). The particularly small, short, retracted face of *H. sapiens* is more derived compared to earlier *Homo* than the distinctive morphology of *H. neanderthalensis* (Trinkaus, 2003, 2006). It is likely that the shape analyses in the current thesis are picking up on these differences between *H. sapiens* and *H. heidelbergensis*. The difference between taxa in frontal sinus-related morphology is smaller than the direct relationship in frontal sinus volumes, however. This suggests that the reason the *H. heidelbergensis* crania have larger frontal sinuses is not just because of their difference in craniofacial form and presents the possibility that the differences in craniofacial shape between *H. heidelbergensis* and *H. sapiens* are to some extent affected by degree of frontal pneumatisation (cf. Seidler *et al.*, 1997; Bookstein *et al.*, 1999). The greater strength of the inter-taxon difference in sinus volume compared to sinus volume-related shape could also be evidence against the spandrel hypothesis, although it is not clear what selective pressure could lead to these enormous frontal sinuses. The relatively

few landmarks used in this study could affect the quality of the shape data captured by the sinus volume-related shape variables; therefore, it could be profitable to investigate the taxonomic differences in frontal sinus-related shape in greater detail if possible, given the state of preservation of much of the fossil material.

As an extension of the current project, it would be potentially useful to see if specimens that have atypical sinus sizes for their taxon differ in craniofacial shape from the mean shape for their taxon in similar ways. For example, a comparison of the shape differences between La Ferrassie (the *H. neanderthalensis* specimen with the largest relative frontal sinus volume) and the mean Neanderthal frontal sinus-related shape, the differences between the Western European ULAC 012 (the individual with the largest relative frontal sinus of all recent *H. sapiens*) and the mean shape for recent *H. sapiens* frontal sinus-related morphology, and the difference between Petralona and the *H. heidelbergensis* mean frontal sinus-related shape. These exceptionally pneumatised specimens could shed light on morphology specifically relevant to large frontal sinus size. The same is, of course, true for specimens with atypically small sinuses for their taxon.

7.I.b.ii. The case for hyperpneumatisation in H. neanderthalensis

Contrary to traditional theories on the cause of the supraorbital tori of this species (see above), but in accordance with the more recent findings of Rae *et al.* (2011) and Zollikofer *et al.* (2008), in the results presented here, *H. neanderthalensis* frontal sinuses are not relatively larger than those of *H. sapiens*. This is despite the much

greater size and geographic range of the *H. sapiens* sample in the current thesis compared to those of Rae *et al*. (2011) or Zollikofer *et al*. (2008). It is possible that this result could reflect the method used to standardise for size (see Section 2.II.a.ii.), but a different method was used by Zollikofer *et al.* (2008) and in the current thesis, the good correlation between sinus volumes standardised using G-FMT and using centroid size suggest this is not the case. Since several studies (including this one) have now shown that *H. neanderthalensis* does not have relatively larger frontal sinus volumes than *H. sapiens* and there is no evidence that differences in *H. sapiens* and *H. neanderthalensis* supraorbital morphology are shaped by large frontal sinuses (cf. Coon, 1962; Bookstein *et al.*, 1999; Wolpoff, 1999), it seems reasonable that this idea should now be abandoned. This is an important conclusion from the current study, given the longevity of the misinterpretation of Neanderthal frontal sinuses.

Supposed *H. neanderthalensis* maxillary hyperpneumatisation has been used to explain the characteristic mid-facial projection and lack of canine fossa in this species (Coon, 1962). In the current thesis, this belief is partially supported: relative maxillary sinus volumes in *H. neanderthalensis* are significantly larger than those of *H. sapiens*, but there is no significant difference between *H. neanderthalensis* and *H. heidelbergensis*; in fact, relative maxillary sinuses are significantly smaller in *H. sapiens* than in both the other taxa. The difference in relative volume between recent *H. sapiens* and *H. neanderthalensis* found in the current thesis are an interesting contrast with the results of Rae *et al.* (2011). Since they were looking at the difference in pneumatisation with reference to climatic adaptation, however, Rae *et al.* (2011) used a recent *H. sapiens* sample composed solely of Lithuanians and they

also had a smaller Neanderthal sample. These differences in sample composition are likely to be responsible for the difference in results between the two studies.

The results from the present study provide novel evidence that *H. sapiens* has *hypo*pneumatised maxillary sinuses, rather than *H. neanderthalensis* being *hyper*pneumatised, yet this is not the full story. Craniofacial size and maxillary sinus-related morphology, as well as taxonomic attribution, were substantive indicators of relative maxillary sinus volume in the results presented here. In the current thesis, the difference between relative maxillary sinus volume in *H. sapiens* is, in part, related to facial size.

The separation of shape from size is a perennial problem in studies of morphology, whether traditional methods, or GMM are employed (e.g., Adams *et al.*, 2004; Zelditch *et al.*, 2004). Isometric size components can be removed by standardising variables for size; allometric size, however, is more complex and is not removed by the standardisation of volume or shape variables. In the current thesis, an allometric size component was found in relative maxillary sinus volumes (standardised with the measurement G-FMT) and in the frontal sinus-related shape variable (standardised using GMM, where GPA uses centroid size to standardise landmark configurations). In both cases, non-isometric size differences were identified, showing that it is not always possible to compare shape, as opposed to form (shape plus size). Although the removal of size effects is not straightforward, they can be identified (see Section 2.II.a.ii.), and this is informative in its own right.

If it is accepted that the method used to standardise sinus volume for craniofacial size is successful, there is positive allometry between facial size and maxillary (and frontal) sinus volumes across taxa (see also Zollikofer *et al.*, 2008). This is plausible, since it is known that *H. sapiens* has smaller faces than other taxa, as described above. In addition to its size-mediated differences in relative maxillary sinus volume, the current thesis shows for the first time that *H. sapiens* is significantly different from the other two taxa in maxillary sinus-related craniofacial shape. The maxillary sinus shape parameters identified show that specimens with relatively smaller maxillary sinuses tend to have crania with more vertical frontal bones and smaller, shorter, flatter faces relative to their more brachycephalic neurocrania. The *H. sapiens* cranium is more derived compared to earlier hominins, than is *H. neanderthalensis* (Trinkaus, 2003, 2006); compared to its congeners, *H. sapiens* is characterised by a brachycephalic cranial vault and increased basicranial flexion, which results in the face being positioned more posteriorly under the braincase, leading to a flatter face with an anteroposteriorly short midface and a vertical forehead (e.g., Stringer *et al.*, 1984; Lieberman, 1998, 2008; Lieberman *et al.*, 2002; Stringer, 2002b, 2012d; Pearson, 2008; Stringer & Buck, 2014). These derived characteristics are reflected by the maxillary sinus shape parameters identified by the current thesis, despite the relatively few landmarks employed and the fact that these shape variables are not the vectors describing the greatest shape variation in the sample, showing the strength of the shape differences. The characteristic shape of *H. sapiens* (as described by the maxillary shape parameters) is associated with smaller maxillary sinuses. The indirect difference between *H. sapiens* and *H. neanderthalensis*/*H. heidelbergensis* in maxillary sinus-associated morphology is

much stronger than the direct difference in sinus volumes. This is congruent with the hypothesis that the maxillary sinuses are spandrels and offers important evidence that the derived smaller, flatter face and more brachycephalic neurocranium in *H. sapiens* lead to the relatively smaller maxillary sinuses seen in this species because in *H. sapiens* there is less maxillary space for potential opportunistic pneumatisation.

7.I.b.iii. Does H. sapiens *exhibit hyper-variable pneumatisation?*

It has been suggested that, amongst primates, *H. sapiens* is a uniquely plastic species, using this ability to adapt to a wide range of niches and colonise novel environments (Wells & Stock, 2007). As support for this theory there is evidence that recent *H. sapiens* exhibit greater intraspecific variation in some skeletal regions than other primates, suggesting that they are less canalised (Stock & Buck, 2010). Studies of hominin paranasal pneumatisation also refer to greater variation in *H. sapiens* sinuses compared to other taxa, albeit without quantification (e.g., Vlček, 1967; Zollikofer *et al.*, 2008). Thus, it was one of the aims of this thesis to ascertain whether *H. sapiens* is more variable in sinus volume than other taxa in a large, geographically and chronologically diverse sample. This was not found to be the case. Whilst in the current thesis *H. sapiens* is far more variable than *H. neanderthalensis* in both frontal and maxillary sinus volume, for both sinuses the most variable taxon is *H. heidelbergensis*, even when recent *H. sapiens* and early *H. sapiens* are combined. For the frontal sinuses, this may be because of the inclusion of the taxonomically uncertain Ceprano in the *H. heidelbergensis* sample. Indeed, if Ceprano is removed from the sample, the variation in *H. heidelbergensis* frontal

sinus volume is closer to that of the Neanderthal sample and much lower than the *H. sapiens* sample. Ceprano is not included in the maxillary sinus analysis, however, as it does not preserve this region, and yet *H. heidelbergensis* is still the most variable taxon. Small sample size, such as that for the *H. heidelbergensis* maxillary sinus volume sample, will exaggerate measures of intra-group variation if one specimen is an outlier, and in this case it may be that Petralona is hyperpneumatised for all its sinuses (Seidler *et al.*, 1997; Prossinger *et al.*, 2003; Zollikofer *et al.*, 2008). Studying the pneumatisation of other specimens in the *H. heidelbergensis* hypodigm, such as Arago 21, Dali, and Jinniushan, could help to clarify this point, but ultimately, until the alpha taxonomy of *H. heidelbergensis* is better understood, it cannot be determined what level of maxillary pneumatisation is characteristic of this taxon.

It may be that hyperplasticity is a *H. sapiens* trait, as suggested by Wells and Stock (2007), but that this flexibility is specific to certain regions of the skeleton. The cranium is known to be less variable than the postcranial skeleton across catarrhine primates, a pattern hypothesised to be due to the greater number of functional requirements of the cranium leading to stronger canalisation (Buck *et al.*, 2010). This may be the reason why *H. sapiens* is not particularly variable in sinus volume compared to *H. heidelbergensis*. For the moment, however, it must be concluded that the null hypothesis, that *H. sapiens* is not more variable in its paranasal pneumatisation than other hominin taxa, cannot be refuted and the pneumatic evidence can offer no support to the theory that *H. sapiens* is a particularly variable species due to its hyperplasticity.

7.II. RQ2: Are there interactions between masticatory stress/strain and sinus variables?

There is a long-standing theory that large sinuses are adapted to dissipate large masticatory strains, based on the idea that biomechanically advantageous properties of thin, curved-walled shells allow a stronger structure without the cost of heavy, metabolically expensive bone (e.g., Bookstein *et al.*, 1999; Koppe & Nagai, 1999; Ravosa *et al.*, 2000; Preuschoft *et al.*, 2002). The implication that large sinuses would be adaptive in reducing weight whilst maintaining strength was taken up by Bookstein *et al*. (1999), who linked large frontal sinuses to the presence of supraorbital tori in their study of changes in hominin frontal bone morphology across time. Ravosa *et al.* (2000) countered Bookstein *et al.*'s (1999) hypothesis by summarising the considerable evidence from *in vivo* strain gauge experiments that show only low strains in the supraorbital regions of non-human catarrhines, platyrrhines, and strepsirhines. This appears to be the case even early in ontogeny, before the supraorbital tori develop fully (Kupczik *et al.*, 2009), providing compelling evidence that neither large frontal sinuses, nor large supraorbital tori, are adapted to masticatory strain.

Contrary to the implication that large sinuses are adapted to high masticatory strains, Rae and Koppe (2004) have instead suggested a possible non-functional (but adaptive) link between reduced frontal sinuses and high levels of dental loading in recent *H. sapiens*. They point out that several populations with unusually high levels of frontal sinus agenesis are also characterised by high levels of masticatory or paramasticatory activity. This is an extension of the work of Greene and Scott

(1973), who suggested that the high frequency of sinus agenesis in their Wadi Halfa (Nubia) sample, in conjunction with large supraorbital tori (but see above), reflected a strengthening of the upper face in response to high local strains from dental loading; i.e., more bone is required for strength and so less sinus is desirable. This is in keeping with the normal biomechanical functional adaptation of bone to strain, whereby deposition occurs in response to local strain (Goodship & Cunningham, 2001; Pearson & Lieberman, 2004; Ruff *et al.* 2006; Gomez *et al.*, 2007; Shaw & Stock, 2009). In addition to the Wadi Halfa population, Rae and Koppe (2004) note that both Inuit and Australian populations have high rates of frontal sinus agenesis, combined with ethnographic accounts of extreme dental loading. However, given the evidence cited above that strains are low in the upper face it seems unlikely that mastication would cause sufficient strain to trigger bone functional adaptation in the supraorbital region and reduce frontal sinus size.

The distribution of masticatory strains in the face might suggest that a link between the maxillary sinus and masticatory strain is more likely than between masticatory strain and the frontal sinus, as strains are higher in the maxilla (e.g., Endo, 1965; Ross & Metzger, 2004). Yet, there is evidence from non-human primate species to suggest that there is no effect of masticatory strain on maxillary sinus volume; in a large study of maxillary sinuses across the order Primates, Lund (1988) found no correlation with diet, a result echoed by Swindler (1999) in his study of anthropoids. It is possible that relationships within taxa, or between closely related taxa, would be obscured by such a broad approach, but complementary results were found by others at lower taxonomic levels; Rae and Koppe (2008) compared the maxillary sinuses of

two species of *Cebus* (*C. apella* and *C. albifrons*) with different diets (hard object feeding and frugivorous, respectively) and found no significant difference in relative maxillary sinus volume, despite marked differences in craniofacial morphology linked to diet. In the current thesis, sinus variables were compared between subsistence groups in a large sample of Mid-Late Pleistocene hominins and tested for relationships with shape variables describing temporalis shape (shown to be a proxy for masticatory strain – see Section 5.I.) to explore the possibility of a relationship between dietary stress/strain and sinus morphology across Pleistocene taxa.

7.II.a. The possible effects of interactions between diet and climate

Although the impact of the two pressures are analysed separately here, there is an overlap between climate and diet for any organism: climate determines the types of food available in an ecosystem. In the case of hominins, reliance on domesticated species as defined in the current study (see Sections 2.I.b.i; 2.IV.b.i.) is not a subsistence strategy open to populations living at very cold temperatures without modern technology and trade (see also Noback, 2014). In the current study, there were no DOM in the Cold climate category because, whilst populations living in these regions may now depend on a modern Western (DOM) diet, this has only been the case for a short period of time (Fediuk, 2000, Kerttula, 2000, Mataskovna Gouchinova, 2006), and individuals are thus unlikely to show a clear signal of adaptation to this diet. There are two recent *H. sapiens* Forager populations in the Cold category, the Greenland Inuits and the Russian populations (to compare climate

parameters, see Table 1) and there are five fossils in the Cold category, all of which are classed as Foragers (see Sections 2.I.b.ii; 2.IV.b.i.).

The presence of cold-adapted individuals in the Forager group, but not the DOM group could affect the results of the shape analyses presented in Chapter 5. Adaptations to climatic pressures could be misinterpreted as dietary shape differences because they happen to be more frequent in the Forager group. Covariation between dietary and climatic influences (and, to perhaps a lesser extent, between both factors and population history) is difficult to unpick and a detailed study of the differences in the contributions of each factor is beyond the scope of this study. In accordance with Noback and Harvati (in revision), however, where a clear functional link can be made between diet and craniofacial shape, such as in the differences between temporalis shape and diet seen in this study (similar relationships were also seen by Noback and Harvati in the same region), it is reasonable to infer dietary influence. Furthermore, in the current study there is no significant relationship between latitude and shape change in the temporalis region as measured by the masticatory landmark set. This provides a certain confidence that at least a proportion of the shape differences presented as being diet-related are indeed such.

If, in future analyses, the different contributions of diet and climate could be untangled more precisely, since the actual diets of populations in different climates differ, there will still be an interaction between diet and climate. Possible climate-related dietary differences in craniofacial morphology may be due to two factors.

The absence of agriculture in at high latitudes may results in a harder diet because agriculture tends to lead to a diet with a predominance of processed foods (González-José *et al.*, 2005; Sardi *et al.*, 2006; Paschetta *et al.*, 2010) and also the greater proportion of animal foods in the diets of more northerly-living populations (Ströhle & Hahn, 2011) likely results in higher levels of masticatory stress because these foods are inherently harder to process, whether from wild or domesticated sources (Noback & Harvati, in revision). These two factors are, of course, not mutually exclusive. Therefore, although it is plausible to attribute temporalis shape differences described in this study largely to dietary factors, these factors themselves may, to some degree, be dependent on climate.

7.II.b. Are there differences in pneumatisation between groups with different levels of masticatory stress/strain?

In the current thesis, in support of previous non-human primate research, no direct relationship was detected between frontal or maxillary sinuses and masticatory stress/strain. It is possible that the shape data used as a proxy for masticatory stress/strain fails to capture this variation successfully, yet the co-occurring lack of difference in this variable between subsistence groups supports the interpretation that neither frontal, nor maxillary, sinus volume is directly related to masticatory stress/strain. Foragers do have significantly smaller relative sphenoidal sinus volumes compared to populations dependent on domestic species, although again no difference in the shape proxy for masticatory stress/strain is detected. This is a relationship with a small effect size and may merely be the result of chance, since it is not robust to a Bonferroni correction. That the direction of the relationship – the

group assumed to experience higher masticatory stresses/strains has smaller sinuses – is the same as that seen in the shape analyses (see below), however, provides some evidence against this conclusion. No other relationships with proxies for masticatory stress/strain were found with any type of sinus volume, leading to the conclusion that there is no direct mastication-related function in maxillary or frontal sinus size in Mid-Late Pleistocene hominins. The results are congruent, however, with a small, indirect effect of stress/strain from mastication resulting in a smaller sphenoidal sinus due to bone functional adaptation (*sensu* Ruff *et al*., 2006), as suggested by Rae and Koppe (2004) and Greene and Scott (1973) for the frontal sinus.

If relatively small sphenoidal sinuses in the Forager group are an indirect adaptation resulting from bone deposition, strengthening the sphenoid as a response to high masticatory strain, the sphenoid would have to be subject to high masticatory strain. Though the sphenoid is slightly removed from the lower face, where most masticatory strains are experienced (see above), it does articulate with the maxillae, palatines, and zygomas (Gray, 1997), where high masticatory strains are experienced (Endo, 1965; Ross & Metzger, 2004; Wang *et al.*, 2010); these regions may transmit strain to the sphenoid. The pterygoid muscles also originate from the sphenoid (Gray, 1997), and it is possible that differences in strain experienced by the sphenoid due to the activation of these muscles under different dental loading regimes would affect the amount of sphenoidal pneumatisation. Given that the maxillary sinus does not seem to reduce due to masticatory strain in the maxilla, and strains are presumably higher here, it seems unlikely that the sphenoidal sinus would do so. Yet it is possible that the maxillary sinus is responding preferentially to another factor,

since there is evidence, from their lack of covariation in size, to suggest that sinus types are not homologous (see Section 4.III.).

There is some evidence from the literature that sinuses may respond indirectly to masticatory strain via craniofacial adaptation, which comes from Fitton *et al.*'s (2010, 2013) finite element analysis (FEA) of masticatory strains in macaques (*Macacca fascicularis*) and mangabeys (*Cercocebus atys*/*torquatus*). The former species has a maxillary sinus, the latter external fossae in approximately the same anatomical location. Fitton *et al.* (2010, 2013) modelled the crania of both genera without pneumatisation/fossae and found that regions where sinuses/fossae would be in real crania experienced low strain under multiple biting scenarios. Following adaptive modelling (adding/removing bone according to peak strains), the models acquired hollows where there are sinuses/fossae in real animals. This suggests that maxillary pneumatisation in macaques (and the [potentially] functionally homologous external fossae in mangabeys) reflects differences in biomechanical loading such that, given a particular craniofacial morphology, differences in pneumatisation is one way of negotiating the opposing requirements of strength and efficiency. In this scenario, the direct relationship seems to be between dental loading and craniofacial morphology, whilst the sinuses secondarily develop during ontogeny as an indirect result of the craniofacial strains according the principles of bone functional adaptation (Fitton *et al.*, 2010, 2013).

In the context of the hominin species analysed in the current thesis, if Fitton *et al.*'s (2010, 2013) conclusions are correct, this would mean that the Forager group

experiences high strains from dental loading and, thus, has craniofacial morphology adapted to that diet. Therefore, less of the cranium experiences low enough strain to trigger bone loss via pneumatisation (to save energy due to reduced bone formation and weight). This would result in smaller sinuses in craniofacial shapes associated with higher strains, as seen in the current thesis. This mechanism seems quite plausible for the relationship seen between maxillary sinus-related shape and masticatory strain in the current thesis, given the evidence for high strains in this region (see above), but the effect cannot be strong, as no direct relationship with masticatory strain, nor subsistence group, is seen for the sinuses themselves. For this explanation to be relevant to the sphenoidal sinuses, high strains would need to be experienced locally as well as in the maxillary region. This is plausible, due to the position of the sphenoid and the attachment of the pterygoid muscles, and is a crucial avenue for future investigation (see below).

7.II.c. Could masticatory strain affect the sinuses indirectly, via sinus-related morphology?

In the current thesis, no relationship was detected between frontal sinus-related craniofacial form and proxies for masticatory strains or subsistence groups. This suggests that there is no influence of differential dietary strains on frontal sinus volume in Mid-Late Pleistocene hominins, either directly or indirectly (via craniofacial shape). This is in accordance with the research cited above that shows (in humans, non-human primates, and other taxa) that masticatory strains are negligible in the upper face, and so do not affect structures in that region (contra Bookstein *et al.*, 1999).

In the results presented here, however, craniofacial form associated with smaller relative sinus volumes in both maxillary and sphenoidal sinuses shows relationships with shape variables linked to higher masticatory strains. As with the direct relationship between subsistence strategy and sphenoidal sinus volume , these results must be treated with caution, due to the small size and weakness of the relationships and their lack of significance if a Bonferroni correction is applied. This could imply that the results are due to chance, but the fact that high strain is associated with the craniofacial morphology linked to relatively small sinuses in each case, and the fact that the same relationship is seen both in the sinus volumes themselves and in the sinus-related morphology, strengthens the evidence for a genuine relationship between relatively small volumes and high masticatory strain.

In the current thesis, maxillary sinus-related shape variables across taxa show that relatively small maxillary sinuses are associated with superoinferiorly taller neurocrania, smaller, more orthognathic faces, more upright frontal regions, and more coronally-orientated zygomatics. Configurations with these attributes are also associated with higher masticatory strain, as shown by temporalis morphology. As no direct relationship was found between maxillary sinus volume and masticatory strain (measured either by subsistence strategy or temporalis morphology), but there is a relationship with maxillary sinus-related morphology, it is possible that masticatory strain is indirectly affecting maxillary sinus volumes across taxa via craniofacial shape. Previous studies show diet-related shape changes in the same regions showing shape changes reflected by the maxillary sinus-related shape variables in the current thesis. The shape of the frontal bone and anterior

neurocranium is affected by the attachment of the temporalis, and its shape is informative regarding masticatory strain in recent *H. sapiens* populations (Paschetta *et al.*, 2010) and species of mangabeys (Singleton, 2005) with different diets. The shape of the zygomatic arch and, correspondingly, the shape of the temporal fossa, have been found to reflect masticatory strains in recent *H. sapiens* (von Cramon-Taubadel, 2009b; Paschetta, *et al.*, 2010), this is because the size of the temporal fossa reflects the size of the temporalis muscle (Hylander, 1975; Lieberman, 2011) and the medial side of the zygomatic arch and its inferior border are also attachment sites for the masseter (Gray, 1997). Non-human primate experiments using strain gauges show the anterior part of the zygomatic arch to be a site of high strain during dental loading (Ross & Metzger, 2004); muscle action causes strain in bones, which in turn is likely to shape the cranium as bone responds to strain by deposition (Goodship & Cunningham, 2001; Pearson & Lieberman, 2004; Ruff, *et al.* 2006; Gomez *et al.*, 2007; Shaw & Stock, 2009).

Of the shape differences in the lower face thought to reflect dietary adaptation, prognathism has received particular attention, due to the differences in this characteristic between the Inuit and Neanderthals, both groups who are thought to experience extreme dental loading (see Introduction). The Inuit are amongst the most orthognathic of recent *H. sapiens*, a state thought to be adaptive for the high masticatory and paramasticatory stresses/strains they are known to experience (Hylander, 1975), or at least to repetitive use of the anterior dentition (Wang *et al.*, 2010). The advantageous nature of reduced prognathism in managing high stresses/strains is also reported in non-human primate species; when scaled for size,

less prognathic faces in macaque species are associated with harder diets, which Antón (1996) argues shows their advantage in dissipating larger occlusal loads and reducing masticatory stresses/strains, whilst increasing muscle efficiency (see also Jolly, 1970, on *Theropithecus* dietary adaptations). The relationship found in the current thesis between wider, flatter faces with increased anterior temporalis attachment regions and higher strain reflects what has already been shown in both non-human primate studies and human comparisons to be more efficient under high loading conditions. In the current thesis, these shape differences are related to small maxillary sinuses, but stress/strain is not related to maxillary sinus volume itself. This suggests, contrary to traditional implications about the biomechanical utility of large sinuses, that craniofacial morphology shaped by masticatory strain may play a part in determining the size of the maxillary sinuses, which have no function of their own.

The relationship between sphenoidal sinus-related craniofacial morphology and the proxy for masticatory strain has almost the same strength as that between sphenoidal sinus volume and subsistence method, and seem to tell a similar story. The two masticatory strain variables (subsistence strategy and the shape variable representing temporalis muscle morphology) are not exactly equivalent, however, which makes the two results hard to compare. The difference between Foragers and DOMs may also include differences in climate, culture, or genes between the two groups; the shape variable describes only the difference in the temporalis muscle shape, but that too will reflect factors other than degree of masticatory strain. Further studies are necessary to unpick this relationship. It would be profitable to repeat the study on

Paschetta *et al.*'s (2010) sample, which consisted of a population that changed its diet over time (see Section 2.IV.b.). This would limit the effect of possible non-masticatory contributions to sphenoidal volume change and enable a more fruitful comparison between differences in volume and volume-related shape between dietary groups. It could also be profitable to use additional proxies for masticatory strain, if such data are available.

In the current thesis, sphenoidal sinus-related shape variables show that crania with relatively small sphenoidal sinus volumes tend to have narrower, taller neurocrania with a relative reduction of the anterior portion of the vault, which is associated with higher masticatory strain, as shown by temporalis muscle morphology. As described above, the pterygoid muscles (lateral and medial) both partially originate from the lateral pterygoid plates, and the lateral pterygoid muscle also partially originates from the greater wing of the sphenoid (Gray, 1997). Thus, the shape of the sphenoidal region, as described by sphenoidal sinus-related shape variables in the current thesis, may be related to changes in the action of the pterygoids, which are key masticatory muscles. The differences in craniofacial height described by the sphenoidal sinus-related shape variables in the current thesis may also be detecting differences related to the shape of the temporalis muscle, as discussed above. The correspondence between regions of shape change shown in the here to be related to differences in sinus volume, and the regions of the cranium shown by others to be substantially affected by masticatory strain supports the hypothesis that diet may, in part, affect the shape of the cranium, which in turn has consequences for sphenoidal sinus volume. There is some evidence that the mechanism by which small sinuses

are achieved could be bone functional adaptation to regional, variable strains, as discussed above. The current results extend and augment this work from the frontal sinuses to include both the maxillary and sphenoidal sinusesEvidence for a relationship between relative sphenoidal sinus volumes and masticatory strain from both the volumes themselves, and the craniofacial shape related to volumes, are in agreement in supporting this hypothesis. Neither relationship is strong enough to account for all the variation in sphenoidal sinus volume across taxa, and therefore it is likely that this is not the only influence; the relatively low detail shape information from the small landmark set in the current thesis may also play a part. These are noteworthy results, since few studies to date have quantified differences in sphenoidal sinus volume and very little is known about its correlates. It would be profitable to investigate this relationship further using a combination of CT analysis, GMM, and FEA to measure and compare sphenoidal sinus volume, sphenoidal shape, and strains experienced by the sphenoid.

7.III. RQ3: Are there interactions between climate and sinus variables?

Climatic theories are some of the most long-standing explanations for sinus morphology (for reviews see Blaney, 1990; Marquez, 2008). Large frontal sinuses have been hypothesised to be an adaptation to cold stress, serving to condition cold air (e.g., Coon, 1962). This hypothesis has been particularly influential in discussions about Neanderthal sinuses (see Section 1.II.a.ii.). Conversely, it has been suggested (e.g., Irmak *et al.*, 2004) that larger frontal sinuses are an adaptation to warmer

climates because they help to prevent the brain from overheating by extending the mucus membrane surface area available for evaporation, thus cooling by convection and cooling by conduction via the thin bone that separates the sinuses from the brain. Unlike some of the more outlandish theories (see Introduction) for sinus function, there is some quantitative evidence that sinus sizes differ with temperatures, although the mechanism behind this is unclear. Precipitation is not mentioned explicitly in most climatic theories of sinus function; although, since the mechanism suggested for blood cooling is evaporation from the mucous membrane, the humidity of the air would be important to the cooling ability of the sinuses (Dean, 1988). Presumably, if large sinuses serve to condition (heat and moisten) air, they would also be larger in drier climates. Thus, if the sinuses have either a thermoregulatory or conditioning function, one would expect to see larger sinuses in hot, dry climates where this adaptation would be effective.

Cold-adapted Inuit populations have been shown to have higher rates of aplasia and smaller frontal sinuses than recent *H. sapiens* populations living in warmer temperatures (Koertvelyessy, 1972; Tillier, 1977; Hanson & Owsley, 1980). Within Inuit populations, a temperature cline has also been found, with those living at colder temperatures possessing smaller frontal sinuses (Koertvelyessy, 1972; Hanson & Owsley, 1980). These results perhaps support the idea that larger frontal sinuses are beneficial at warmer temperatures, due to a thermoregulatory function as suggested by Irmak *et al*. (2004). This has widely been taken to mean that there is a general effect of climate on frontal sinuses, such that they will be smaller at colder temperatures (e.g., Irmak *et al.*, 2004), despite the geographically limited samples to

which the Inuit were compared in previous studies. Koertvelyessy (1972) compared his Inuit sample to 45 Zuni and Arikara (North American Indians), Tillier (1975) compared her Inuit sample to a French sample of 40 and an Australian sample of 15, and Hanson and Owsley (1980) state that their Inuit sample has smaller frontal sinuses than a Pueblo Indian comparative sample, but the details of the comparative samples are not given.

A similar relationship between maxillary sinus volume and temperature to that seen in the frontal sinus has been reported; Shea (1977) found that Inuit populations at higher latitudes have smaller relative maxillary sinus volumes. Contra to the thermoregulatory theory for sinus function, however, Shea (1977) concluded that reduction in sinus size is a passive secondary effect resulting from the primary association of larger nasal cavities with colder climates. Larger nasal cavities enable enhanced warming and humidifying of inspired air and regulation of heat loss from expired air. The same pattern between maxillary sinus size and temperature has also been found in non-human primates; Rae *et al.* (2003) report that relative maxillary sinus volumes in Japanese macaque populations are negatively correlated with latitude, and like Shea, they hypothesise that the true relationship is between climate and nasal cavity volume, since the relationship between maxillary sinus volume and latitude is no longer significant if the relationship between sinus volume and nasal cavity volume is taken into account. Similar results were found by Marquez and Laitman (2008) in a comparison of two species of macaques from different climates. This picture of a link between maxillary sinus volume and temperature was further strengthened by Rae *et al.*'s (2006) study on experimentally cold-adapted rats, which

showed that trial animals had smaller maxillary sinuses than control animals. Furthermore, this study suggests that at least a component of the mechanism by which maxillary sinuses are smaller in cold climates, whether due to integration with the nasal apparatus or adaptation in their own right, is due to phenotypic plasticity.

In contrast to the evidence described above, which suggests that smaller maxillary sinuses are associated with cold climates, Holton *et al.* (2013) compared maxillary sinus volumes in Americans of European descent to a mixed sample composed of African Americans and native South Africans, and reported that the former had significantly larger relative maxillary sinus volumes than the latter. They interpreted this result as a climatic adaptation linked to nasal cavity shape. In common with the authors cited above, Holton *et al.* (2013) hypothesise that the maxillary sinuses are non-functional and, thus, are free to vary with adjacent regions that are under selection. However, they focus on adaptive change in nasal cavity breadth, rather than nasal cavity volume. This leads them to hypothesise that the smaller maxillary sinuses in their proposed warm-adapted group are due to the requirement for a wider nasal cavity to facilitate heat loss (Holton *et al.*, 2013). The larger sinuses in a sample supposedly adapted to colder climates would also fit in with the conditioning theory proposed by Coon (1962), but this runs counter to the evidence described above that sinuses are generally smaller in colder climates. It was hoped that the current study could clarify these seemingly contradictory results.

Unlike the (comparatively) geographically limited studies of the frontal sinus described above, there is a recent study examining the relationship between maxillary

sinus volumes and climate in a geographically diverse sample of recent *H. sapiens*, albeit one with small overall sample size (Butaric *et al.*, 2010). Butaric *et al.* (2010) found no relationship between relative maxillary sinus volume and latitude across seven geographically diverse recent *H. sapiens* populations. They recorded that the populations assigned to cold groups did tend to have smaller relative maxillary sinus volumes than the warm groups, but there was no significant separation between the groups.

To date, few researchers have addressed the relationship between the sphenoidal sinus and climate directly, but Tillier (1975, 1977) suggested that the Inuit were distinctive in having high levels of sphenoidal sinus aplasia and hypoplasia. Tillier (1975, 1977) suggested, following the work of Koertvelyessy (1972), that the concurrent small size of the frontal and sphenoidal sinuses in her Inuit sample might suggest they (the frontal and sphenoidal sinuses) are both cold-adapted. Given this mix of results from previous studies, in the current thesis employs a large, globally distributed sample of recent *H. sapiens*, and (separately) a combined sample of recent *H. sapiens* and climatically diverse fossil hominins, to investigate whether intra-*H. sapiens* or intra-*Homo* relationships between climate and sinus volume exist for any of the three sinus types.

7.III.a. Are there differences in pneumatisation between groups with different climates?

In opposition to long-standing ideas inferred from small-scale (in terms of global coverage) studies on cold-adapted groups, the suggestion of a climate-mediating

function in recent *H. sapiens* frontal sinus volumes is not supported by the results of this study. Neither the thermoregulatory nor the insulating theories for sinus volume are supported in for this species by the results presented here. There is no significant relationship between relative frontal sinus volumes in recent *H. sapiens* and any of the continuous climatic variables examined above. Previous studies reporting differences in frontal sinus volumes between populations due to climate (Koertvelyessy, 1972; Tillier, 1975, 1977; Hanson & Owsley, 1980) have compared relatively few climatically different populations and assumed that the differences they found were due to sinus adaptation to climate, based on climate-correlated differences within Inuit populations. The current thesis suggests that instead, when a more geographically representative sample is used, these conclusions are not supported; there are small differences between some populations of recent *H. sapiens* (see Section 7.I.a.), but they are not correlated with climate.

The Inuit sample in the current thesis was too small and geographically homogenous (see Section 2.I.b.i.) to test for relationships with climate within the population. Therefore, given the previous results showing smaller frontal sinuses within Inuit populations (Koertvelyessy, 1972; Hanson & Owsley, 1980), it is not possible to discount the possibility that extreme cold-adapted groups show distinct relationships between frontal sinus morphology and climate compared to other populations, or that there are climate-patterned relationships between frontal sinus volume and temperature within populations (see also Butaric *et al.*, 2010).

In the full, multi-taxon sample of the present thesis, relative frontal sinus volumes are significantly larger in specimens from wet environments than those from dry environments, but this is a small difference and seems to have been biased by the extremely large frontal sinuses of two of the specimens in the Wet category: Bodo and Petralona (*H. heidelbergensis*). Given the small size effect of the relationship, and the fact that Petralona is one of the fossils for which dating (and thus palaeoclimatic reconstruction) is very uncertain (see Section 2.I.b.ii.), this may not be a genuine climate-related result. However, the direction of difference (larger sinuses in wetter climates) does mirror the relationship seen between relative sphenoidal sinus volumes and precipitation in the current thesis (see below).

In contrast to previous studies (as with the frontal sinus results), from this study finds no evidence that relative maxillary sinus volume in Mid-Late Pleistocene hominins is due to climatic adaptation of any kind. There is no significant relationship between relative maxillary sinus volume and any of the continuous climatic variables in recent *H. sapiens*, and there are no significant differences in relative maxillary sinus volumes between climate categories in the full sample. There is, therefore, no evidence from this thesis for either air conditioning or thermoregulatory functions in this sinus type.

Earlier studies with less geographically broad sample distributions have shown differences in recent *H. sapiens* maxillary sinus volumes between populations from different climates and concluded that population-level differences can be explained by climate (Fernandez, 2004b; Holton *et al.*, 2013). The lack of relationships between maxillary sinus volumes and climatic variables in the present thesis, following

analysis of a much larger, more climatically diverse sample, suggests this is a spurious conclusion; there may be differences between some populations (although those in the current sample did not reach significance), but it is unlikely that maxillary sinus volume is determined directly by climate. Given the long-standing nature of assumptions about the climatic function of sinuses, this addition to the body of evidence that neither frontal, nor maxillary sinuses are directly adapted to climate is a significant contribution to understanding the correlates of variation in hominin craniofacial morphology.

Holton *et al*. (2013) found a difference in recent *H. sapiens* maxillary sinus volumes between populations that they attributed to climate, yet there are problems with their sample. In addition to only comparing two populations, the sample is mainly composed of Americans, and both African and European Americans are likely to have admixture from different populations in their recent pasts. The combination of South Africans and African Americans may also confuse the results, if climatic adaptation is plastic to some degree (as suggested by experimental studies [Rae *et al.*, 2006]), although Holton *et al.* (2013) report that there was no significant difference between the African American group and the native South African group for any of the measurements.

The results from the current thesis are congruent with those of Butaric *et al.* (2010), who found no significant difference in maxillary sinus volume between climate groups, and no significant correlation between relative maxillary sinus volume and latitude. They did, however, record a non-significant, climate-related trend, such that

colder groups tended to show smaller relative sinus volumes. Butaric *et al*. (2010) based their climate categorisation on the same method as was used in the current thesis (following Kottek *et al.*, 2006; see Chapter 2), but there is one major difference: Butaric *et al.* (2010) place Peru in the Cold/Dry category, which does not fit with the climate data collected for the specimens in the current thesis, despite the fact that some of them are the same individuals from the Morton collection. In the current thesis, Peruvians are classified as Hot/Dry (see Section 2.I.b.i. and 2.IV.c.i.). Since it is not clear what criteria Butaric *et al.* (2010) used to assign their climatic categories, this difference cannot be accounted for. It may, however, explain why there seemed to be a trend for smaller relative maxillary sinus volumes in cold climates for Butaric *et al.* (2010), whilst this was not found in the present study, strengthening the argument that there is no direct link between climate and maxillary sinus volume across recent *H. sapiens* populations. Butaric *et al.* (2010) explained the differences between their results and Shea's (1977) by suggesting that latitudinal differences in maxillary sinus volume may be masked by noise when populations are combined, if that relationship differs between populations. As stated above with reference to frontal sinus volumes, this is still a possibility, given the results presented here, and this possibility could be investigated further with larger sample sizes and greater geographic distributions within each population. In accounting for the differences between their results and those from non-human species, Butaric *et al.* (2010) point out that macaque and rat maxillary sinuses may not be a good homologue for those of *H. sapiens*, since maxillary sinuses in macaques appear to be an evolutionary reversal, having been lost and regained in their evolutionary history (Rae *et al.*, 1999, 2002), and because morphological integration, such as the

relationship between nasal cavity and maxillary sinuses suggested as the driving force for climatic differences in maxillary sinus volume variation (Shea, 1977; Rae *et al.*, 2003; Rae *et al.*, 2006), is likely to be distinct in the retrognathic faces of *H. sapiens* (Butaric *et al.*, 2010).

The current thesis is the first to date to explicitly test the relationship between sphenoidal sinus volume and climatic variables. Both the full and the recent *H. sapiens* sample display relationships between relative sphenoidal sinus volume and precipitation, with relatively larger sphenoidal sinuses in individuals from wetter climates. Continuous and categorical climatic variables support this conclusion. The results from the two different types of variable support one another and extend the relationship between relative sphenoidal sinus volume and precipitation from recent *H. sapiens* to Mid-Late Pleistocene hominins in general (although few fossil taxa in the sample preserve sphenoidal sinuses, so this extrapolation is preliminary only). There is also a small, significant, positive relationship between relative sphenoidal sinus volume and maximum monthly temperature in the recent *H. sapiens* sample, but this is not supported by any corresponding differences in the categorical variables. It may be due to chance, as witnessed by its lack of robusticity to a Bonferroni correction, or it could be due to the strong covariation of temperature and precipitation (Noback *et al.*, 2011).

Neither the larger relative sphenoidal sinus volumes associated with greater precipitation in recent *H. sapiens*, nor the larger relative sphenoidal sinuses in the Wet category for the full sample supports the hypothesis that the sphenoidal sinuses

have an air conditioning or brain cooling function, since one would expect the sinuses to be larger in drier climates if this were the case. In agreement with Tillier's (1977) suggestion, in the current thesis, larger relative sphenoidal sinus volumes are associated with warmer temperatures, and though the size effect of this relationship is very small and not robust, this offers some (limited) support for the thermoregulatory hypothesis. Alternatively, the results presented here could point to sphenoidal sinus volume as a secondary adaptation to climatic influence on sphenoidal shape (see below). This issue requires further investigation with a larger fossil sample that preserves the sphenoidal sinus and also better palaeoprecipitation data, if these can be obtained. Given the paucity of any information regarding the ecological correlates of sphenoidal sinus volume, however, these data represent a useful starting point for such an investigation.

7.III.b. Could climatic variables affect the sinuses indirectly, via sinus-related morphology?

In the current thesis full sample, there is a small (but significant) difference in relative frontal sinus volumes among precipitation categories: the Wet category has larger relative frontal sinus volumes than the Dry category. There is also a much stronger relationship between frontal sinus volume-related craniofacial shape variables associated with smaller sinuses and hotter, wetter climates in the full sample. Given that the relationship between climate and frontal sinus-related craniofacial morphology is in the opposite direction to the relationship between climate and the relative frontal sinus volumes themselves, the former cannot be invoked as an explanation for the latter, via climate-adapted morphology and

spandrels. Nor can it support the validity of the precipitation-mediated difference in relative frontal sinus volumes against the likelihood that it is simply due to the (potentially error-prone) precipitation categorisation of one individual with an extremely large frontal sinus (see above).

In the current thesis there are large relationships between recent *H. sapiens* frontal sinus-related morphology and all of the continuous temperature and precipitation variables (except the relationship with minimum monthly precipitation, which is significant, but has a smaller effect size). Recent *H. sapiens* specimens are more likely to have craniofacial morphology linked to smaller sinuses in warmer and wetter climates. There is no direct relationship between relative frontal sinus volume and any of the continuous climatic variables; this suggests that a portion of the differences in relative frontal sinus volumes between recent *H. sapiens* specimens in the current thesis may be due to craniofacial shape differences related to climate, and supports the theory that the frontal sinuses are spandrels.

The frontal sinus volume-related shape variables for the recent *H. sapiens* population in the current thesis describe the association of a relatively narrower, more dolichocephalic neurocranium, anteroposteriorly flatter and mediolaterally broader face with larger frontal sinus volumes and with colder, drier climates. It has been shown repeatedly in previous work that the shapes of neurocrania in recent *H. sapiens* are related to temperature. Populations living in colder climates tend to have larger, more spherical, brachycephalic neurocrania, which has been interpreted as conformation to Allen's rule; a sphere being the shape with the least surface area and

so the optimal shape to minimise heat loss (Beals, 1972; Beals *et al.*, 1984). The most robust expression of this difference in neurocranial shape at different temperatures appears to be in measures of cranial breadth (Roseman, 2004; Hubbe *et al.*, 2009; Betti *et al.*, 2010; Nowaczewska *et al.*, 2011), although size also plays a part (Roseman, 2004; Harvati & Weaver, 2006a). The relationship between temperature and neurocranial globularity may largely be reliant on a few populations from extremely cold climates (Roseman, 2004; Harvati & Weaver, 2006b; Hubbe, *et al.*, 2009; Betti *et al.*, 2010; Foster & Collard, 2013). Despite this caveat, there is general agreement that extreme cold (at least) affects the shape of the neurocranium in correspondence with Allen's rule, particularly in measures of breadth. In previous analyses of overall craniofacial shape differences between geographically disparate populations of recent *H. sapiens*, the face has been shown to be particularly influenced by climate. Effects of climate have been inferred in the size of the maxilla (Evteev *et al.*, 2013), in the degree of facial projection, and in facial height and breadth (Hubbe *et al.*, 2009; Betti *et al.*, 2010). As with the shape of the neurocranium, differences in facial flatness are interpreted adapting the cranium to the nearest approximatio of a sphere to minimise surface area/heat loss. Some authors have found a relationship between facial shape and both temperature and precipitation (Hubbe *et al.*, 2009; Evteev *et al.*, 2013), whilst others found a relationship with temperature only (Harvati & Weaver, 2006a; Betti *et al.*, 2010). As with the neurocranial shape differences, the majority of these differences in face shape seem to be driven by populations from very cold climates, and the signal becomes weaker, or disappears if those samples are removed (Roseman, 2004; Harvati & Weaver, 2006a, b; Hubbe *et al.*, 2009; Betti *et al.*, 2010). Interestingly,

however, Evteev *et al*. (2013) have recently shown that reduction in prognathism at colder temperatures is also seen *within* an extreme cold-adapted group of recent *H. sapiens* (north Asians).

This is the first study to expand Zollikofer *et al*.'s (2008) analysis of sinus-related craniofacial shape (which concluded that frontal sinus volume could be explained by non-functional, opportunistic expansion dependent on craniofacial shape) to examine the correlates of those shape variables. In agreement with the studies cited above, in the results presented here, frontal sinus-related shape differences in neurocranial globularity, facial breadth, and projection are related to climate. Although changes in these same climate-sensitive dimensions are seen, the relationships between shape and climate presented here do not always follow the same direction as those described above. That is to be expected, since previous studies examined overall shape differences between populations, whereas it is only specific shape variables are of interest here; i.e., those that are associated with sinus volume. It should also be noted that, despite the general trend for more brachycephalic crania at cold temperatures, the Inuit have quite dolichocephalic crania; they also have very flat faces, which may (in part) drive the trend seen in the results presented here (as described above). The results of the current thesis suggest that craniofacial shapes associated with a cold, dry climate lead to larger frontal sinuses in recent *H. sapiens*. This is not a direct adaptation of frontal sinus size to climate, since there is no direct relationship between the two, which supports the hypothesis that the sinuses are non-functional and that sinus size is affected by partially climatically adapted craniofacial morphology.

In the results presented here there is a relationship in the full sample between small frontal sinus-related craniofacial morphology and hotter, wetter climates, in parallel with the relationship seen in the recent *H. sapiens* sample. This runs counter to the direct difference in frontal sinus volume found in the full sample, which showed that specimens in the Wet category had larger frontal sinuses. This suggests the substantive effect of the extremely large *H. heidelbergensis* frontal sinuses on that result. In the frontal volume analysis, there were four *H. heidelbergensis*, including Bodo and Petralona, which both have remarkable frontal pneumatisation; in the frontal sinus-related morphology analyses, there were only three *H. heidelbergensis*, and Bodo was not included (for reasons of preservation/quality of scan data). It seems likely that the difference between *H. heidelbergensis* and *H. sapiens* relative frontal sinus size is much greater than the difference between *H. heidelbergensis* and *H. sapiens* frontal sinus-related morphology and thus, *H. heidelbergensis* has a much greater effect in the former analysis, reversing the pattern in *H. sapiens*, whereas, in the latter analysis, *H. sapiens* dominate the sample, and so the relationship between sinus-related shape and climate is mainly *H. sapiens*-led and conforms to the pattern seen in the *H. sapiens*-only sample. This suggestion could be tested with a larger sample of putative *H. heidelbergensis*.

Across taxa, the frontal sinus volume-related shape variable identified in the current thesis shows that a longer, larger, more sloping frontal and superoinferiorly taller maxillary regions are associated with both larger frontal sinuses and colder, drier climates. Within recent *H. sapiens*, frontal bone curvature and breadth are two of the

few non-nasal cranial shape differences between populations that appear to be under selective pressure from temperature (Roseman & Weaver, 2004; Betti *et al.*, 2010). There are also reports of relevant differences in the size of the maxilla in recent *H. sapiens* from different temperature and precipitation conditions; north Asians have larger maxillae than east Asians (from warmer, wetter climates), once population history has been taken into account (Evteev *et al.*, 2013). Differences in maxillary height are linked with frontal sinus-related morphology in the current thesis and have previously been shown to be climate-sensitive in comparisons between populations of recent *H. sapiens*, when genetic drift is taken into account (Hubbe *et al.*, 2009). As previously suggested (see Chapter 3), maxillary height differences in shapes along the cross-taxon frontal sinus-related shape variable in the current thesis may actually be the result of differences in prognathism, which Hubbe *et al.* (2009) also found to be related to both temperature and precipitation. Hubbe *et al.*'s (2009) study shows that the relationships between morphology and climate are affected by sample composition, suggesting that it is only a robust association in populations from extremely cold environments. The authors also suggest that different cold-adapted populations have adapted in distinct ways, with northern Asians and extreme North Americans contributing to different shape changes from the northern Europeans sample in the overall results. Hubbe *et al.*'s (2009) results again highlight the importance of considering within-population variation in studies of the relationships between climate and morphology. Previous studies suggest that shape changes, found in the current thesis to be associated with differences in relative frontal sinus volumes, occur in cranial regions affected by climate. They therefore suggest that changes in these regions may contribute to the differences in relative frontal sinus

volumes presented here, if sinuses are spandrels. It is not clear what mechanism causes the relationship between cranial morphology adapted to warmer, wetter climates and smaller sinuses; this is an area ripe for future investigation.

Climate-related differences in maxillary sinus-related craniofacial shape across taxa are described in the current thesis, although there were no climate-related differences in the maxillary sinus volumes themselves. This suggests that craniofacial shape affected by climate may indirectly cause some of the variation in relative maxillary sinus volume in the current sample, as suggested by previous studies that found climate-linked differences in maxillary sinus volume (Shea, 1977; Rae *et al.*, 2003; Marquez & Laitman, 2008). In the results presented here, shape related to relatively large maxillary sinus volumes corresponds to a more dolichocephalic neurocranium with more pronounced glabella, a larger maxillary region, and more swept-back zygomatics; this morphology is also more likely to be found in specimens from warmer, wetter climates. Within recent *H. sapiens*, the evidence for a climatic effect on the shape of the neurocranial vault is well established, as discussed above. There are also climate-sensitive regions of the face; measures of bi-zygomatic breadth, in particular, are mentioned (where details are given) as measures of facial breadth that are found to have a strong relationship with both temperature and humidity (Hubbe *et al.*, 2009; Betti *et al.*, 2010). Mid-facial morphology is likely to be affected by nasal morphology, which is known to be one of the craniofacial regions most sensitive to climate (Harvati & Weaver, 2006b), and the maxillary landmark set might be expected to be the set most likely to pick up on nasal shape differences, since it is focused on the maxillary region. Many papers have shown how nasal

aperture (Weiner, 1954; Wolpoff, 1968; Carey & Steegmann, 1981; Franciscus & Long, 1991; Roseman, 2004; Roseman & Weaver, 2004; Hubbe *et al.*, 2009; Betti *et al.*, 2010; Evteev *et al.*, 2013) and nasal cavity (Noback *et al.*, 2011; Holton *et al.*, 2013) morphology differ with temperature and precipitation conditions and have related this to the main function of the nose: air conditioning (Negus, 1954). The differences in shape shown by the maxillary sinus-related shape variable identified in the current thesis are in regions previously shown to be particularly sensitive to climate, as summarised above. These shape changes identified by the current thesis may be integrated with nasal apparatus shape or volume (cf. Shea, 1977; Rae *et al.*, 2003; Noback *et al.*, 2011; Holton *et al.*, 2013). This could be investigated with an extension of the current shape analyses to the internal and external nasal region, preservation of specimens permitting. The relationship between craniofacial morphology associated with relative maxillary sinus volume, but not with the volumes themselves, suggests that the shape of the cranium, which is affected in part by climate, leads to the size of the maxillary sinus in Mid-Late Pleistocene hominins.

In the current thesis, significant differences across taxa are described in relative sphenoidal sinus volumes of specimens from different precipitation and climate categories and also between sphenoidal sinus-related morphology and both continuous and categorical climatic variables. The relationships between climatic variables and sphenoidal sinus-related morphology vary in strength, but some are considerably stronger than the direct relationship between relative sphenoidal sinus volume and precipitation/climate. In particular, the difference between sphenoidal sinus-related morphology in different climate categories is far stronger than the

difference in relative sphenoidal sinus volume between climate categories. However, as relative sphenoidal sinus volumes themselves are larger in warmer, wetter climates, yet the differences in sphenoidal sinus-related shape variables shows that morphology linked to larger relative sphenoidal sinuses is more likely in colder, drier environments, the latter cannot explain the former. The difference in these results is puzzling and may reflect inadequacies in the method, such as the small number of landmarks, or climatic imprecision. It must be remembered that both the relationship between sinus volume and climate and between sinus volume-related morphology and climate have relatively small effect sizes and the relationship between relative sphenoidal sinus volume and sphenoidal sinus volume-related shape also has a very small effect size. In combination, these results seem to suggest that there are many differing influences on sphenoidal sinus volume, of which one is potentially climate-affected craniofacial morphology.

The sphenoidal sinus-related shape variable identified in the current thesis shows that specimens with broader, superoinferiorly shorter neurocrania with a relative expansion of the anterior portion of the vault are linked to colder, drier climates in recent *H. sapiens*, and to larger relative sphenoidal sinus volumes. As described above, changes to neurocranial shape have been associated with cold climates in many studies (Beals, 1972; Beals *et al.*, 1984; Roseman, 2004; Hubbe *et al.*, 2009; Betti *et al.*, 2010; Nowaczewska *et al.*, 2011), although many more recent studies have added the caveat that this trend may be driven by a few populations from extremely cold climates (Roseman, 2004; Harvati & Weaver, 2006b; Hubbe *et al.*, 2009; Betti *et al.*, 2010; Foster & Collard, 2013). It is possible this extreme cold-adaptation also affects the shape relationships identified in the current thesis, as the

Inuit seem to show a slightly different relationship between sphenoidal sinus-related shape and continuous temperature variables from the rest of the sample (see Section 6.II.b.iii.). However, they actually reduce the relationship rather than causing it, and the shapes of another cold-adapted recent *H. sapiens* population in the sample (the Russians) do not behave in the same way. Since the crucial, cold-adapted populations (Russia and Greenland/Inuits) are represented in the current thesis by relatively small sample sizes, and the Russian population also combines individuals from a wide geographical area, an improved sample from these regions could clarify this point further.

Conclusion

In this thesis, sinus volume and sinus volume-related craniofacial shape in Mid-Late Pleistocene hominins have been compared in order to answer questions about the taxonomic and ecological correlates of paranasal pneumatisation. From the results presented here, it can be concluded that *H. heidelbergensis* has a hyperpneumatised frontal sinus compared to *H. neanderthalensis*, *H. sapiens*, and perhaps *H. erectus*, although it is not of homogenous size throughout the taxon. This characteristic may be an apomorphy with taxonomic utility for classifying putative members of the *H. heidelbergensis* hypodigm, and supporting the Euro-African species concept. Although there is a taxonomic difference in frontal sinus-related craniofacial morphology, in addition to the difference in relative frontal sinus volumes between taxa, the effect size of the former is smaller and therefore the difference in sinus volume cannot be explained by difference in craniofacial morphology. The suggestion that very large frontal sinuses cause supraorbital morphology in *H. heidelbergensis* (Seidler *et al.*, 1997; Bookstein *et al.*, 1999) cannot be refuted based on these results; it does seem unlikely, however, given the much smaller relative frontal sinus volumes in *H. neanderthalensis* and *H. erectus*, which also both have large supraorbital tori.

The results presented here augment the already considerable evidence that *H. neanderthalensis* is not hyperpneumatised in its frontal sinuses compared to *H.*

sapiens (see also Zollikofer *et al.*, 2008; Rae *et al.*, 2011); therefore, the difference between the two species in their supraorbital morphology cannot be attributed to frontal pneumatisation (contra Coon, 1962; Bookstein *et al.*, 1999; Wolpoff, 1999). The assertion that the unique mid-facial morphology in *H. neanderthalensis* is the product of hyperpneumatised maxillary sinuses is also not supported by the results of this thesis, at least in relation to the difference between the morphology of *H. neanderthalensis* and *H. heidelbergensis*, as there is no relative difference in maxillary sinus size between the two species. Conversely, the difference in maxillary pneumatisation morphology found here to distinguish *H. sapiens* from *H. neanderthalensis* and *H. heidelbergensis* seems to be partly explained by craniofacial morphology. The evidence is that the morphology shapes the maxillary sinuses, however, rather than the reverse. Between taxa, *H. sapiens* was found to *hypo*pneumatised compared to *H. heidelbergensis*/*H. neanderthalensis,* and this difference can be accounted for by stronger inter-taxonomic differences in craniofacial size and shape related to maxillary sinus volume.

H. sapiens is not the most variables species in relative sinus volume. This metric can, therefore, offer no support for the idea of a hyper-plastic adaptation in our species (as suggested by Wells & Stock, 2007; Stock, 2008). This may be due to the small sample size for *H. heidelbergensis*, the relatively invariable nature of the cranium in comparison with the rest of the skeleton across the primate order; (Buck *et al.*, 2010; Stock & Buck, 2010), or due to the low taxonomic level of the comparisons performed here.

In addition to the aim of contributing to the debate on taxonomic issues in Mid-Late Pleistocene hominins, it was the aim of this thesis to evaluate assertions of a function for paranasal pneumatisation in this group. The results presented here show no evidence for an unambiguous function of paranasal sinuses. They instead suggest that sinus volumes are determined by responses to selective pressures and neutral evolution, which shape the regions of the cranium they pneumatise, in combination with stochastic growth processes (Zollikofer & Weissmann, 2008) in the sinuses themselves. The results presented here suggest that, although they are integrated to some degree, the three different sinus types studied are not homologous; each responds to different factors depending on their cranial location.

Masticatory strain appears to affect the maxillary and sphenoidal sinuses indirectly, via craniofacial shape, resulting in relatively smaller sinuses in crania adapted to higher strain. A plausible mechanism for this relationship is epigenetic, plastic remodelling of the cranium in response to strain gradients via bone functional adaptation (Fitton *et al.*, 2010, 2013). The frontal sinus does not seem to be affected by this pressure on craniofacial morphology, which is consistent with the evidence that masticatory strains are low in this region (Endo 1965; Ross & Metzger, 2004; Chalk *et al.*, 2011).

Craniofacial adaptation to climate seems to affect all three sinus types. In the frontal and sphenoidal sinuses, there appears to be a connection between craniofacial shape adapted to colder, drier climates and relatively large sinuses; this may be via climate-mediated relationships with the degree of prognathism (Hubbe *et al.*, 2009; Betti *et*

al., 2010) and the shape of the neurocranium (Roseman, 2004; Roseman & Weaver, 2004; Harvati & Weaver, 2006b; Betti *et al.*, 2010; Nowaczewska *et al.*, 2011). Both of these shape differences potentially affect the length of the cranial base, which could be relevant for the development of the sphenoidal sinus, and the shape of the frontal bone, which could be relevant for the development of the frontal sinus. In the case of the maxillary sinus, smaller sinuses are linked morphology associated with colder, drier climates, and the relationships between the craniofacial shape linked to volume and climate seem to be mainly in the mid-face. This may reflect the adaptation of the nasal apparatus to differing requirements for air conditioning, as previously suggested by other authors (Shea, 1977; Rae *et al.*, 2003; Noback *et al.*, 2011; Holton *et al.*, 2013). The lack of a direct relationship between the sinus and climatic variables presented here is likely to be due to the greater geographic range, or to the small number of individuals from each population, in the present sample. Experimental studies of climatic adaptation, when genetic variation is controlled for, suggest that at least some of climatic adaptation leading to differences in sinus volumes described may be due to phenotypic plasticity (Steegmann & Platner, 1968; Rae *et al.*, 2006).

The maxillary sinus is less variable than the frontal or sphenoidal sinuses. This may suggest that the factors affecting the regions of the cranium that determine maxillary sinus volume, including pressures of masticatory strain and climate, and taxonomic differences in craniofacial morphology, result in more canalisation in this region than those pneumatised by the other sinuses. If this was the case, sinus development here would be more constrained.

The relationships between craniofacial shape and sinus volume uncovered in here do not explain differences in sinus volume in their entirety. In addition, there is some relationship between population history and frontal sinus-related craniofacial shape, but none directly between any of the sinus types and population history. This suggests that neutral evolution of cranial shape is another influence on frontal sinus volume; the lack of relationship between neutral differences in craniofacial morphology and the other sinus types may be due to greater canalisation in those regions, or to the failure of the sinus-specific landmark sets to capture more subtle shape differences, since the relationship with frontal sinus-specific shape was found in the full landmark set shape variable. Whilst some of the failure to account for more of the variation in sinus volume here may be due to methodological limitations, such as the necessarily low number of landmarks used to capture craniofacial shape, pneumatisation is also likely to be determined, in part, by other selective pressures on the skull that have not been considered here. It is likely that sinus volume also differs, within a range of optimal morphology determined by constraints on cranial form, due to stochastic development and may also be secondarily optimised to other factors, such as, perhaps, nitric oxide production (Marquez *et al.*, 2002; Lundberg, 2008).

The sinuses are a very ancient morphological trait in mammal evolutionary history (Witmer, 1999); the results of this thesis support the theory that paranasal sinuses are present in Pleistocene hominins due to shared evolutionary history (see also Rae & Koppe, 2014) and that their different size in different species, populations, and

individuals is shaped by the responses of crania to external pressures, such as diet and climate, as well as neutral evolution via mechanisms such as genetic drift and founder effect.

Bibliography

Abel, R. L., Laurini, C. R. and Richter, M., 2012. A palaeobiologist's guide to virtual micro-CT preparation. *Palaeontologica Electronica* 15: 17p.

Ackermann, R. R. and Cheverud, J. M., 2004. Detecting genetic drift versus selection in human evolution. *Proceedings of the National Academy of Sciences of the United States of America* 101: 17946-17951.

Adams, D. C., Rohlf, F. J. and Slice, D. E., 2004. Geometric morphometrics: ten years of progress following the 'revolution'. *Italian Journal of Zoology* 71: 5-16.

Alba, D. M., 2010. Cognitive inferences in fossil apes (Primates, Hominoidea): does encephalization reflect intelligence? *Journal of Anthropological Sciences* 88: 11-48.

Almécija, S., Tallman, M., Alba, D. M., Pina, M., Moyà-Solà, S., and Jungers, W. L., 2013. The femur of *Orrorin tugenensis* exhibits morphometric affinities with both Miocene apes and later hominins. *Nature communications* 4.

Antón, S. C., 1994. Mechanical and other perspectives on Neanderthal craniofacial morphology. In: Corruccini, R. S., Ciochon, R. L. *Integrative paths to the past: Palaeoanthropological advances in honor of F. Clark Howell*. Prentice Hall: Eagle Wood Cliffs. pp. 677-695.

Antón, S. C., 1996. Cranial adaptation to a high attrition diet in Japanese macaques. *International Journal of Primatology* 17: 401-427.

Antón, S. C., 2002. The natural history of *Homo erectus*. *Yearbook of Physical Anthropology* 46: 126-170.Baab, K. L., Friedline, S. E., Wang, S. L. and Hanson, T. 2009. Relationship of cranial robusticity to cranial form, geography and climate in *Homo sapiens. American Journal of Physical Anthropology* 141: 97-115

Baab, K. L. and McNulty, K. P. 2009. Size, shape, and asymmetry in fossil hominins: the status of the LB1 cranium based on 3D morphometric analyses. *Journal of Human Evolution* 57: 608-622.

Balzeau, A., 2005. *Spécificités des caractères morphologiques internes du squelette céphalique chez* Homo erectus. PhD thesis. Département de Préhistoire, Muséum national d'Histoire naturelle, Paris.

Balzeau, A. and Badawi-Fayad, J., 2005. La morphologie externe et interne de la région supra-orbitaire est-elle corrélée á des contraintes biomechaniques? Analyses structurales des populations d'*Homo sapiens* d'Afalou Bou Rhummel (Algérie) et de Taforalt (Maroc). *Bulletins et Mémoires de la Société d'anthropologie de Paris* 17: 185-197.

Balzeau, A. and Grimaud-Hervé, D., 2006. Cranial base morphology and temporal bone pneumatization in Asian *Homo erectus*. *Journal of Human Evolution* 51: 350-359.

Balzeau, A. and Rougier, H., 2010. Is the suprainiac fossa a Neandertal autapomorphy? A complementary external and internal investigation. *Journal of Human Evolution* 58: 1-22.

Bar-Matthews, M., Ayalon, A., Gilmour, M., Matthews, A. and Hawkesworth, C. J., 2003. Sea-land oxygen isotopic relationships from planktonic forminifera and speleotherms in the Eastern Mediterranean region and their implication for

paleorainfall during interglacial intervals. *Geochimica et Cosmochimica Acta* 67: 3181-3199.

Barron, E., van Andel, T. and Pollard, D., 2004. Glacial environments II: reconstructing the climate of Europe in the last glaciation. In: T. van Andel and W. Davies (Eds.). *Neanderthals and modern humans in the European landscape during the last glaciation.* McDonald Institute for Archaeological Research: Cambridge. pp. 57-78.

Barton, R. N. E., Bouzouggar, A., Hogue, J. T., Lee, S., Colcutt, S. N. and Ditchfield, P., 2013. Origins of the Iberomaurusian in NW Africa: new AMS radiocarbon dating of the Middle and Later Stone Age deposits at Taforalt Cave, Morocco. *Journal of Human Evolution* 65: 266-281.

Bastir, M. and Rosas, A., 2005. Hierarchical nature of morphological integration and modularity in the human posterior face. *American Journal of Physical Anthropology* 128: 26-34.

Beals, K. L., 1972. Head form and climatic stress. *American Journal of Physical Anthropology* 37: 85-92.

Beals, K. L., Smith, C. L. and Dodd, S. M., 1984. Brain size, cranial morphology, climate, and time machines. *Current Anthropology* 25: 301-330.

Berckheimer, F., 1933. Ein Menschen-Schädel aus den diluvialen Schottern von Steinheim a.d. Murr. *Annals of Anatomy* X: 318-32.

Betti, L., Balloux, F., Amos, W., Hanihara, T. and Manica, A., 2009. Distance from Africa, not climate, explains within-population phenotypic diversity. *Proceedings of the Royal Society B* 276: 809-814.

Betti, L., Balloux, F., Hanihara, T. and Manica, A., 2010. The relative role of drift and selection in shaping the human skull. *American Journal of Physical Anthropology* 141: 76-82.

Blain, H.-A., Bailon, S., Cuenca-Bescós, G., Arsuaga, J.-L., Bermúdez de Castro, J. M. and Carbonell, E., 2009. Long-term climate record inferred from early-middle Pleistocene amphibian and squamate reptile assemblages at the Gran Dolina Cave, Atapuerca, Spain. *Journal of Human Evolution* 56: 55-65.

Blain, H.-A., Gleed-Owen, C. P., López-García, J. M., Carrión, J. S., Jennings, R., Finlayson, G., Finlayson, C. and Giles-Pacheco, F., 2013. Climatic conditions for the last Neanderthals: herpetofaunal record of Gorham's Cave, Gibraltar. *Journal of Human Evolution* 64: 289-99.

Blake, C. C., 1864. On the alleged peculiar characters, and assumed antiquity of the human cranium from the Neanderthal. *Journal of the Anthropological Society of London* 2: cxxxix-clvii.

Blaney, S. P. A., 1990. Why paranasal sinuses? *Journal of Laryngology and Otology* 104: 690-693.

Blome, M. W., Cohen, A. S., Tryon, C. A., Brooks, A. S. and Russell, J., 2012. The environmental context for the origins of modern human diversity: A synthesis of regional variability in African climate 150,000–30,000 years ago. *Journal of Human Evolution* 62: 563-592.

Bogoras, W., 1904-9. *The Chuckchee*. E. J. Brill Ltd.: Leiden.

Bookstein, F. L. 1991. *Morphometric tools for landmark data; geometry and biology.* Cambridge University Press: Cambridge.

Bookstein, F., Schafer, K., Prossinger, H., Seidler, H., Fieder, M., Stringer, C., Weber, G. W., Arsuaga, J. L., Slice, D. E., Rohlf, F. J., Recheis, W., Mariam, A. J. and

Marcus, L. F., 1999. Comparing frontal cranial profiles in archaic and modern *Homo* by morphometric analysis. *Anatomical Record* 257: 217-24.

Brewster, C., Meiklejohn, C., von Cramon-Taubadel, N. and Pinhasi, R., 2014. Craniometric analysis of European Upper Palaeolithic and Mesolithic samples supports discontinuity at the Last Glacial Maximum. *Nature Communications* 5: 4094.

Bronk Ramsey, C., Higham, T. F. G., Owen, D. C., Pike, A. W. G. and Hedges, R. E. M., 2002. Radiocarbon dates from the Oxford AMS system (*Archaeometry* datelist 31). *Archaeometry* 44: 1-149.

Brose, D. S. and Wolpoff, M. H., 1971. Early Upper Paleolithic man and Late Middle Paleolithic tools. *American Anthropologist* 73: 1156-1194.

Brothwell, D. R., Molleson, T. and Metreweli, C., 1968. Radiological aspects of normal variation in earlier skeletons: an exploratory study. In: *The skeletal biology of earlier populations*. Pergammon Press: Oxford. pp. 149-172.

Bruner, E. and Manzi, G., 2005. CT-based description and phyletic evaluation of the archic human calvarium from Ceprano, Italy. *Anatomical Record* 285A: 643-658.

Buck, L. T., Stock, J. T. and Foley, R. A., 2010. Levels of intraspecific variation within the catarrhine skeleton. *International Journal of Primatology* 31: 779-795.

Buck, L. T. and Stringer, C. B., 2014. *Homo heidelbergensis*. *Current Biology* 24: R214-R215.

Buckland-Wright, J. C., 1970. A radiographic examination of frontal sinuses in early British populations. *Man* 5: 512-517.

Busk, G., 1861. Translation with comments of "On the crania of the most ancient races of man" by D. Schaafhausen. *Natural History Review* April 1861: 155-175.

Busk, G., 1865. On a very ancient human cranium from Gibraltar. In: *Report of the 34th Meeting of the British Association for the Advancement of Science (Bath 1864)*. pp. 91-92.

Butaric, L. N., McCarthy, R. C. and Broadfield, D. C., 2010. A preliminary 3D computed tomography study of the human maxillary sinus and nasal cavity. *American Journal of Physical Anthropology* 143: 426-436.

Butzer, K. W. and Isaac, G. L., 1975. Sorting of the muddle in the middle: an anthropologist's post-conference appraisal. In: K. W. Butzer and G. L. Isaac (Eds.). *After the Australopithecines.* Mouton: The Hague. pp. 495-542.

Cacho, I., Grimault, J. O., Canals, M., Sbaffi, L., Shackelton, N. J., Schönfeld, J. and Zahn, R., 2001. Variability of the western Mediterranean Sea surface temperature during the last 25,000 years and its connection with the Northern Hemisphere climatic changes. *Palaeoceanography* 16: 40-52.

Carbonell, E., Bermúdez de Castro, J., Parés, J. M., Pérez-González, A., Cuenca-Bescós, G., Ollé, A., Mosquera, M., Huguet, R., van der Made, J., Rosas, A., Sala, R., Vallverdú, J., García, N., Granger, D. E., Martinón-Torres, M., Rodríguez, X. P., Stock, G. R., Vergès, J. M., Allué, E., Burjachs, F., Cáaceres, I., Canals, A., Benito, A., Diez, C., Lozano, M., Mateos, A., Navazo, M., Rodríguez, J., Rosell, J. and Arsuaga, J. L., 2008. The first hominin of Europe. *Nature* 452: 465-469.

Cardini, A. and Elton, S., 2008. Variation in guenon skulls (I): species divergence, ecological and genetic differences. *Journal of Human Evolution* 54: 615-637.

Carey, J. W. and Steegmann, A. T., 1981. Human nasal protrusion, latitude, and climate. *American Journal of Physical Anthropology* 56: 313-319.

Carlson, N. R., 2001. *Physiology of behaviour*. Allyn and Bacon: Boston.

Caspari, R. and Radovčić, J., 2006. New reconstruction of Krapina 5, a male Neandertal cranial vault from Krapina, Croatia. *American Journal of Physical Anthropology* 130: 294-307.

Chalk, J. R., Ross, C.F., Strait, D.S., Wright, B.W., Spencer, M.A., Wang, Q. and Dechow, P.C., 2011. A finite element analysis of masticatory stress hypotheses. *American Journal of Physical Anthropology* 145: 1.

Cheverud, J. M., 1982. Phenotypic, genetic, and environmental morphological integration in the cranium. *Evolution* 36: 499-516.

Christensen, A. M., 2004. Assessing the variation in individual frontal sinus outlines. *American Journal of Physical Anthropology* 127: 291-295.

Churchill, S. E., 1998. Cold adaptation, heterochrony and Neandertals. *Evolutionary Anthropology* 7: 46-60.

Clark, J., 1983. *The aboriginal people of Tasmania*. Tasmanian Museum and Art Gallery: Hobart.

Clark, J. D., de Heizelin, J., Schick, K., Hart, W. K., White, T. D., WoldeGabriel, G., Walter, R. C., Suwa, W., Asfaw, B., Vrba, E. and Selassie, Y. H., 1994. African *Homo erectus*: old radiometric ages and young Oldowan assemblages in the Middle Awash Valley, Ethiopia. *Science* 264: 1907-1910.

Cobb, S. N. and O'Higgins, P., 2007. The ontogeny of sexual dimorphism in the facial skeleton of the African Apes. *Journal of Human Evolution* 53: 176-190.

Coon, C. S., 1962. *The origin of races.* Alfred A. Knopf: New York.

Dart, R. A., 1925. *Australopithecus africanus*: the man-ape of South Africa. *Nature* 115:195–199.

Davies, W. and Gollop, P., 2003. The human presence in Europe during the last glacial period II: climate tolerance and climate preferences of mid- and late glacial hominids. In: T. H. van Andel and W. Davies (Eds.). *Neanderthals and modern humans in the European landscape during the last glaciation.* MacDonald Institute for Archaeological Research: Cambridge. pp.

De Groote, I., 2011a. Femoral curvature in Neanderthals and modern humans: A 3D geometric morphometric analysis. *Journal of Human Evolution* 60: 540-548.

De Groote, I., 2011b. The Neanderthal lower arm. *Journal of Human Evolution* 61: 396-410.

De Groote, I., Lockwood, C. A. and Aiello, L. C., 2010. A new method for measuring long bone curvature using 3D landmarks and semilandmarks. *American Journal of Physical Anthropology.* 141: 658-664.

Dean, D., Hublin, J. J., Holloway, R. and Ziegler, R., 1998. On the phylogenetic position of the pre-Neandertal specimen from Reilingen, Germany. *Journal of Human Evolution* 34: 485-508.

Dean, M. C., 1988. Another look at the nose and the functional significance of the face and nasal mucous-membrane for cooling the brain in fossil hominids. *Journal of Human Evolution* 17: 715-718.

Demes, B., 1987. Another look at an old face: biomechanics of the Neandertal facial skeleton reconsidered. *Journal of Human Evolution* 16: 297-303.

Dennell, R. W., Martinón-Torres, M. and Bermúdez de Castro, J. M., 2011. Hominin variability, climatic instability and population demography in Middle Pleistocene Europe. *Quaternary Science Reviews* 30: 1511-1524.

Diehl, R. A., 1993. The Toltec horizon in Mesoamerica: new perspectives on an old issue. In: D. S. Rice (Eds.). *Latin American Horizons (Dumbarton Oaks Pre-Columbian symposia and colloquia).* Dumbarton Oaks Research Library and Collection: Washington D. C. pp. 263-294.

Douka, K., Bergman, C. A., Hedges, R. E. M., Wesselingh, F. P. and Higham, T. F. G., 2013. Chronology of Ksar Akil (Lebanon) and implications for the colonization of Europe by Anatomically Modern Humans. *Public Library of Science One* 8: e72931.

Dupont, L., 2011. Orbital scale vegetation change in Africa. *Quaternary Science Reviews* 30: 3589-3602.

Dryden, I. L.and Mardia, K. V. 1993. Multivariate shape analysis. *Sankya* 55: 460-480.

Endo, B., 1965. Distribution of stress and strain produced by the masticatory force. *The Journal of the Anthropological Society of Tokyo* 73: 123-136.

Evteev, A., Cardini, A. L., Morozova, I. and O'Higgins, P., 2013. Extreme climate, rather than population history, explains mid-facial morphology of northern Asians. *American Journal of Physical Anthropology* 153: 449-462.

Falk, D., Hildebolt, C., Smith, K., Morwood, M. J., Sutikna, T., Brown, P., Jatmiko, Saptomo, E. W., Brunsden, B. and Prior, F., 2005. The brain of LB1, *Homo floresiensis*. *Science* 308: 242-245.

Farah, M. J., 1996. Is face recognition 'special'? Evidence from neuropsychology. *Behavioural Brain Research* 76: 181-189.

Farke, A. A., 2010. Evolution and functional morphology of the frontal sinuses in Bovidae (Mammalia: Artiodactyla), and implications for the evolution of cranial pneumaticity. *Zoological Journal of the Linnean Society* 159: 988-1014.

Fediuk, K., 2000. *Vitamin in the Inuit diet: past and present*. Master of Science. School of Dietetics and Human Nutrition, McGill University, McGill University, Montreal

Fernandez, C. L., 2004a. Forensic ethnic identification of crania: the role of the maxillary sinus—a new approach. *American Journal of Forensic Medicine and Pathology* 25: 302-313.

Fernandez, C. L., 2004b. Volumetric analysis of maxillary sinuses of Zulu and European crania by helical, multislice computed tomography. *Journal of Laryngology and Otology* 118: 877-881.

Field, A., 2009. *Discovering statistics using SPSS*. Sage: London.

Finlayson, C., Giles Pacheco, F., Rodriguez-Vidal, J., Fa, D. A., Maria Gutierrez Lopez, J., Santiago Perez, A., Finlayson, G., Allue, E., Baena Preysler, J., Caceres, I., Carrion, J. S., Fernandez Jalvo, Y., Gleed-Owen, C. P., Jimenez Espejo, F. J., Lopez, P., Antonio Lopez Saez, J., Antonio Riquelme Cantal, J., Sanchez Marco, A., Giles Guzman, F., Brown, K., Fuentes, N., Valarino, C. A., Villalpando, A., Stringer, C. B., Martinez Ruiz, F. and Sakamoto, T., 2006. Late survival of Neanderthals at the southernmost extreme of Europe. *Nature* 443: 850-853.

Fitton, L. C., Shi, J., Liu, J., Fagan, M. J., and O'Higgins, P. 2010. Functional loading, facial remodelling and the formation of the maxillary sinus and maxillary fossa

in Macaca fascicularis and Cercocebus torquatus. *American Journal of Physical Anthropology*, 141: 105.

Fitton, L., Shi, J. and O'Higgins, P., 2013. Patterns of craniofacial pneumatisation: the consequence of skull shape and functional loading? *Third conference of the European Society for the Study of Human Evolution*. European Society for the Study of Human Evolution:Vienna. 85.

Flatt, T., 2005. The evolutionary genetrics of canalization. *The Quarterly Review of Biology* 80: 287-316.

Fletcher, W. J. and Sánchez-Goñi, M. F., 2008. Orbital- and sub-orbital-scale climate impacts on vegetation of the western Mediterranean basin over the last 48,000 yr. *Quaternary Research* 70: 451-464.

Foster, F. and Collard, M., 2013. A reassessment of Bergmann's rule in modern humans. *Public Library of Science ONE* 8: e72269.

Franciscus, R. G. and Long, J. C., 1991. Variation in human nasal height and breadth. *American Journal of Physical Anthropology* 85: 419-427.

Frayer, D. W., 1997. Perspectives on Neanderthal as ancestors. In: C. M. Willermet and G. A. Clark (Eds.). *Conceptual issues in modern human orgins research.* Aldine Transaction: Piscataway. pp. 202-234.

Friess, M., 2010a. Calvarial shape variation among Middle Pleistocene hominins: an application of surface scanning in palaeoanthropology. *Comptes Rendus Palevol* 9: 435-443.

Friess, M., 2010b. Parietal expansion during later hominin evolution, and the validity of *H. heidelbergensis* - a quantitative approach. *Bulletin der Schweizerischen Gesellschaft feur Anthropologie* 16: 55-61.

Frumkin, A., Bar-Yosef, O. and Schwarcz, H. P., 2011. Possible paleohydrologic and paleoclimatic effects on hominin migration and occupation of the Levantine Middle Paleolithic. *Journal of Human Evolution* 60: 437-451.

Fuller, D. Q., 2006. Agricultural origins and frontiers in South Asia: a working synthesis. *Journal of World Prehistory* 20: 1-86.

Garamszegi, L. Z., 2006. Comparing effect sizes across variables: generalization without the need for Bonferroni correction. *Behavioural Ecology* 17: 682-687.

García, L. V., 2004. Escaping the Bonferroni iron claw in ecological studies. *Oikos* 105: 657-663.

Gaudzinski, S., 2004. A matter of high resolution? The Eemian Interglacial (OIS 5e) in North-central Europe and Middle Palaeolithic subsistence. *International Journal of Osteoarchaeology* 14: 201-211.

Gerszten, P. C., 1993. An investigation into the practice of cranial deformation among the Pre-Columbian peoples of northern Chile. *International Journal of Osteoarchaeology* 3: 87-98.

Gilbert, W. H., Holloway, R. L., Kubo, D., Kono, R. T. and Suwa, G., 2008. Tomographic analysis of the Daka calvaria. In: W. H. Gilbert and B. Asfaw (Eds.). *Homo erectus: Pleistocene evidence from the Middle Awash, Ethiopia.* University of California Press: Berkeley. pp. 329-348.

Gomez, C., David, V., Peet, N. M., Vico, L., Chenu, C. and Malaval, L., 2007. Absence of mechanical loading *in utero* influences bone mass distribution and architecture but not innervation in Myod-Myf5-deficient mice. *Journal of Anatomy* 210: 259-271.

Gower, J. C. 1975. Generalised Procrustes analysis. *Psychometrika* 40: 33-50.

González-José, R., Ramírez-Rozzi, F., Sardi, M., Martínez-Abadías, N., Hernández, M. and Pucciarelli, H. M., 2005. Functional-cranial approach to the influence of economic strategy on skull morphology. *American Journal of Physical Anthropology* 128: 757-771.

Gómez-Robles, A., Martinón-Torres, M., Bermúdez de Castro, J. M., Prado, L., Sarmiento, S., and Arsuaga, J. L., 2008. Geometric morphometric analysis of the crown morphology of the lower first premolar of hominins, with special attention to Pleistocene *Homo*. *Journal of Human Evolution* 55: 627-638.

Goodship, A. E. and Cunningham, J. L., 2001. Pathophysiology of functional adaptation of bone in remodelling and repair *in vivo* In: S. C. Cowin (Eds.). *Bone mechanics handbook.* CRC Press: Boca Raton. pp. 1-31.

Gould, S. J., 1997. *The mismeasure of man*. Penguin: London.

Gould, S. J. and Lewontin, R. C., 1979. The spandrels of San Marco and the Panglossian paradigm: a critique of the adaptationist programme. *Proceedings of the Royal Society of London B* 205: 581-98.

Gray, H. G., 1997. *Gray's anatomy*. The Promotional Reprint Company Ltd.: London.

Green, R. E., Krause, J., Briggs, A. W., Maricic, T., Stenzel, U., Kircher, M., Patterson, N., Li, H., Zhai, W., Fritz, M. H.-Y., Hansen, N. F., Durand, E. Y., Malaspinas, A.-S., Jensen, J. D., Marques-Bonet, T., Alkan, C., Prüfer, K., Meyer, M., Burbano, H. n. A., Good, J. M., Schultz, R., Aximu-Petri, A., Butthof, A., Höber, B., Höffner, B., Siegemund, M., Weihmann, A., Nusbaum, C., Lander, E. S., Russ, C., Novod, N., Affourtit, J., Egholm, M., Verna, C., Rudan, P., Brajkovic, D., Kucan, Ž., Gušic, I., Doronichev, V. B., Golovanova, L. V., Lalueza-Fox, C., de la Rasilla, M., Fortea, J., Rosas, A., Schmitz, R. W., Johnson, P. L. F., Eichler, E. E., Falush, D., Birney, E., Mullikin, J. C., Slatkin, M., Nielsen, R., Kelso, J., Lachmann, M., Reich, D. and Pääbo, S., 2010. A draft sequence of the Neandertal genome. *Science* 328: 710-722.

Greene, D. L. and Scott, L., 1973. Congenital frontal sinus absence in the Wadi Halfa Mesolithic population. *Man* 8: 471-74.

Grün, R., 1996. A re-analysis of electron spin resonance dating results associated with the Petralona hominid. *Journal of Human Evolution* 30: 227-241.

Grün, R. and Stringer, C. B., 1991. Electron spin resonance dating and the evolution of modern humans. *Archaeometry* 33: 153-199.

Grün, R. and Stringer, C., 2000. Tabun revisited: revised ESR chronology and new ESR and U-series analyses of dental material from Tabun C1. *Journal of Human Evolution* 39: 601-612.

Grün, R., Stringer, C., McDermott, F., Nathan, R., Porat, N., Robertson, S., Taylor, L., Mortimer, G., Eggins, S. and McCulloch, M., 2005. U-series and ESR analyses of bones and teeth relating to the human burials from Skhul. *Journal of Human Evolution* 49: 316-334.

Gunz, P. and Harvati, K., 2007. The Neanderthal "chignon": Variation, integration, and homology. *Journal of Human Evolution* 52: 262-274.

Haddon, A. C., 1935. *Reports of the Cambridge Anthropological Expedition to Torres Straits*. Cambridge University Press: Cambridge.

Hadjikhani, N., Kveraga, K., Naik, P. and Ahlfors, S. P., 2009. Early (N170) activation of face-specific cortex by face-like objects. *Neuroreport* 20: 403-407.

Hamdy, R., M., and Abdel-Wahed, N., 2014. Three-dimensional linear and volumetric analysis of maxillary sinus pneumatization, *Journal of Advanced Research* 5: 387-395.

Hammer, Ø., Harper, D. A. T. and Ryan, P. D., 2001. PAST: Paleontological statistics software package for education and data analysis. *Palaeontologia Electronica* 4: 9.

Hanson, C. L. and Owsley, D. W., 1980. Frontal sinus size in Eskimo populations. *American Journal of Physical Anthropology* 53: 251-255.

Harlan, J. R., 1971. Agricultural origins: centres and noncentres. *Science* 174: 468-472.

Harrington, B., 2004-5. *Inkscape.* http://www.inkscape.org/.

Harvati, K., 2003. The Neanderthal taxonomic position: models of intra- and inter-specific craniofacial variation. *Journal of Human Evolution* 44: 107-132.

Harvati, K., 2007. 100 years of *Homo heidelbergensis* - life and times of a controversial taxon. *Mitteilungen der Gesellschaft für Urgeschichte* 16: 85-94.

Harvati, K., Frost, S. R. and McNulty, K. P., 2004. Neanderthal taxonomy reconsidered: Implications of 3D primate models of intra- and interspecific differences. *Proceedings of the National Academy of Sciences USA* 101: 1147-1152.

Harvati, K., Hublin, J. J. and Gunz, P., 2010. Evolution of middle-late Pleistocene human cranio-facial form: A 3-D approach. *Journal of Human Evolution* 59: 445-464.

Harvati, K. and Hubin, J.-J., 2012. Morphological continuity in the Late Middle and Late Pleistocene hominins from Northwestern Africa: a 3D geometric morphometric analysis. In: Hublin, J.-J. and McPherron, S. P. *Modern Origins: a North African Perspective*. Spring: Dordrecht. pp. 179-188.

Harvati, K. and Weaver, T., 2006a. Reliability of cranial morphology in reconstructing Neanderthal phylogeny. In: K. Harvati and T. Harrison (Eds.). *Neanderthals Revisited: New Approaches and Perspectives.* Springer: Berlin. pp. 239-254.

Harvati, K. and Weaver, T. D., 2006b. Human cranial anatomy and the differential preservation of population history and climate signatures. *Anatomical Record* 288: 1225-1233.

Hernández Fernández, M. and Vrba, E. S., 2006. Plio-Pleistocene climatic change in the Turkana Basin (East Africa): evidence from large mammal faunas. *Journal of Human Evolution* 50: 595-626.

Hicks, F., 1982. Tetzcoco in the early 16th century: The State, the City, and the "Calipolli". *American Ethnologist* 9: 230-249.

Hodder, I., 2006. *The leopard's tale: revealing the mysteries of Çatalhöyük*. Thames and Hudson: London.

Holliday, T. W., 1997. Postcranial evidence of cold adaptation in European Neandertals. *American Journal of Physical Anthropology* 104: 245-258.

Holliday, T. W. and Trinkaus, E., 1991. Limb/trunk proportions in Neandertals and early anatomical modern humans. *American Journal of Physical Anthropology* Suppl 12: 93-94.

Holton, N., Yokley, T. and Butaric, L., 2013. The morphological interaction between the nasal cavity and maxillary sinuses in living humans. *Anatomical Record* 296: 414-426.

Holton, N. E., Yokley, T. R. and Franciscus, R. G., 2011. Climatic adaptation and Neandertal facial evolution: A comment on Rae *et al*. (2011). *Journal of Human Evolution* 61: 624-627.

Howell, H. P., 1917. Voice production form the standpoint of the laryngologist. *Annals of Otology, Rhinology and Laryngology* 26: 643-655.

Hubbe, M., Hanihara, T. and Harvati, K., 2009. Climate signatures in the morphological differentiation of worldwide modern human populations. *Anatomical Record* 292: 1720-1733.

Hublin, J.- J., 1998. Climatic changes, paleogeography and the evolution of the Neanderthals. In: T. Akazawa, K. Aoki and O. Bar-Yosef (Eds.). *Neanderthals and modern humans in western Asia.* Plenum Press: New York. pp. 295-310.

Hublin, J. -J., 2007. What can Neanderthals tell us about modern human origins? . In: Mellars, P., Boyle, K. Bar-Yosef, O. and Stringer, C. (Eds.). *Rethinking the human revolution.* McDonald Institute Monographs.: Cambridge. pp. 235-248.

Hublin, J.-J. and Roebroeks, W., 2009. Ebb and flow or regional extinctions? On the character of Neandertal occupation of northern environments, *Comptes Rendus Palevol* 8: 503-509.

Humphrey, L., Bello, S. M., Turner, E., Bouzouggar, A. and Barton, N., 2012. Iberomaurusian funery behaviour: evidence from Grotte des Pigeons. *Journal of Human Evolution* 62: 261-273.

Humphrey, L. and Bocaege, E., 2008. Tooth evulsion in the Maghreb: chronological and geographical patterns. *African Archaeological Review* 25: 109-123.

Humphrey, L. T., De Groote, I., Morales, J., Barton, N., Collcutt, S., Bronk Ramsey, C. and Bouzouggar, A., 2014. Earliest evidence for caries and exploitation of starchy plant foods in Pleistocene hunter-gatherers from Morocco. *Proceedings of the National Academy of Sciences USA* 111: 954-959.

Hylander, W. L., 1975. The adaptive significance of Eskimo craniofacial morphology. In: A. A. Dahlberg and T. M. Graber (Eds.). *Orofacial growth and development.* Walter De Gruyter Inc.: Berlin. pp. 129–169.

IBM Corp., 2010. *IBM SPSS Statistics for Windows, Version 19.0*. Armonk, NY: IBM Corp.

Ingicco, T., Amano, N., Ochoa, J., and Détroit, F., 2014. An allometric study of *Macaca fascicularis* from the Late Pleistocene deposits at the Ille site (Philippines): a possible model for Southeast Asian Dwarf Hominins. *Bulletins et Mémoires de la Société Anthropologie de Paris* 1-7.

Irmak, M. K., Korkmaz, A. and Erogul, O., 2004. Selective brain cooling seems to be a mechanism leading to human craniofacial diversity observed in different geographical regions. *Medical Hypotheses* 63: 974-979.

Jahns, S., Hüls, M. and Sarnthein, M., 1998. Vegetation and climate history of west equatorial Africa based on a marine pollen record of Liberia (site GIK 16776) covering the last 400,000 years. *Review of Palaeobotany and Palynology* 102: 277-288.

James, F. C. and McCulloch, C. E., 1990. Multivariate analysis in ecology and systematics: panacea or Pandora's box? *Annual Review of Ecology and Systematics* 21: 129-166.

Jankaukas, R., 1998. On the epidemiology of medieval European populations. *Kongress der Gesellschaft fuer Anthropologie e.V.* In: C. Czaja, S. Dessi and C. Maelicke. (Eds.) Cuvillier Verlag, Goettingen: Goettingen. pp. 235-241.

Jolly, C. J., 1970. The Seed-Eaters: A new model of hominid differentiation based on a baboon analogy. *Man* 5: 5-26.

Jolly, C. J., 2001. A proper study of mankind: analogies from the papionin monkeys and their implications for human evolution. *Yearbook of Physical Anthropology* 44: 177-204.

Jolly, C. J., 2009. Mixed signals: reticulation in human and primate evolution. *Evolutionary Anthropology* 18: 275-281.

Jolly, C. J., Woolley-Barker, T., Beyene, S., Disotell, T. R. and Phillips-Conroy, J. E., 1997. Intergeneric hybrid baboons. *International Journal of Primatology* 18: 597-627.

Kay, R. F. and Kirk, E. C., 2000. Osteological evidence for the evolution of activity pattern and visual acuity in primates. *American Journal of Physical Anthropology* 113: 235-262.

Keir, J. 2009. Why do we have paranasal sinuses? *The Journal of Laryngology and Otology* 123: 4-8.

Kenyhercz, M. W., Klales, A. R., and Kenyhercz, W. E., 2014. Molar size and shape in the estimation of biological ancestry: A comparison of relative cusp location using geometric morphometrics and interlandmark distances. *American Journal of Physical Anthropology*, 153: 269-279.

Kent, J. T. 1994. The complex Bingham distribution and shape analysis. *Journal of the Royal Statistical Society Series B* 56: 285-299.

Kerttula, A. M., 2000. *Antler on the sea: the Yup'ik and Chuckhi of the Russian Far East*. Cornell University Press: Ithaca.

Klein, R. G., 1973. Geological antiquity of Rhodesian Man. *Nature* 244: 311-312.

Klein, R. G., 1999. *The human career: human biological and cultural origins*. University of Chicago Press: Chicago.

Klingenberg, C. P., 2013. Visualizations in geometric morphometrics: how to read and how to make graphs showing shape changes. *Hystrix: the Italian Journal of Mammalogy* 24: 15-24.

Klingenberg, C. P., and Marugán-Lobón, J., 2014. Evolutionary covariation in geometric morphometric data: analyzing integration, modularity, and allometry in a phylogenetic context. *Systematic Biology* 62: 591-610.

Klingenberg, C. P. and Monteiro, L. R., 2005. Distances and directions in multidimensional shape spaces: implications for morphometric applications. *Systematic Biology* 54: 678-688.

Koertvelyessy, T., 1972. Relationships between frontal sinus and climatic conditions – a skeletal approach to cold adaptation. *American Journal of Physical Anthropology* 37: 161-172.

Koppe, T. and Nagai, H., 1999. Factors in the development of the paranasal sinuses. In: T. Koppe, H. Nagai and K. W. Alt (Eds.). *The paranasal sinuses of higher primates: development, function and evolution.* Quintessence: Chicago. pp. 133-149.

Koppe, T., Nagai, H. and Rae, T. C., 1999a. Factors in the evolution of the primate paranasal sinuses. In: T. Koppe, H. Nagai and K. W. Alt (Eds.). *The paranasal sinuses of higher primates: development, function and evolution.* Quintessence Publishing Co. Inc.: Chicago. pp. 151-175.

Koppe, T., Rae, T. C. and Swindler, D. R., 1999b. Influence of craniofacial morphology on primate paranasal pneumatization. *Annals of Anatomy* 181: 77-80.

Kottek, M., Griser, J., Beck, C., Rudolf, B. and Rubel, F., 2006. World map of the Köppen-Geiger climate classification updated. *Meterologische Zeitschrift* 15: 259-263.

Kühl, N. and Litt, T., 2007. Quantitative time-series reconstructions of Holsteinian and Eemian temperatures using botanical data. In: F. Sirocko, M. Claussen, M. F. Sáchez-Goñi and T. Litt (Eds.). *The climates of past interglacials.* Elsevier: Amsterdam. pp. 239-347.

Kupczik, K., Dobson, C. A., Crompton, R. H., Phillips, R., Oxnard, C. E., Fagan, M. J. and O'Higgins, P., 2009. Masticatory loading and bone adaptation in the supraorbital torus of developing macaques. *American Journal of Physical Anthropology* 139: 193-203.

Kuykendall, K. L. and Rae, T. C., 2008. Presence of the maxillary sinus in fossil Colobinae (*Cercopithecoides williamsi*) from South Africa. *Anatomical Record* 291: 1499-1505.

LaBarbera, M. 1989. Analyzing body size as a factor in ecology and evolution. *Anuual Review of Ecological Systematics* 20: 97-117.

Larransoaña, J. C., Roberts, A. P. and Rohling, E. J., 2013. Dynamics of green Sahara periods and their role in hominin evolution. *Public library of science ONE* 8: e76514.

Larsen, C. S., 1997. *Bioarchaeology: interpreting behaviour from the human skeleton*. Cambridge University Press: Cambridge.

Lartet, L.1868. Une Sépulture des Troglodytes du Périgord. *Bulletin de la Société d'Anthropologie de Paris*, 2e Série, 3:335-349.

Lawrence, D. and Reeves Lawrence, H., 2004. Torres Strait: the region and its people. In: R. Davis (Eds.). *Woven Histories and Dancing Lives: Torres Straits Islanders Identity, Culture and History.* Aboriginal Studies Press: Canberra. pp. 15-29.

Le, H., Kendall, D. G. 1993. The Riemannian structure of Euclidean shape spaces. A novel environment for statistics. *Annals of Statistics* 21: 1225-1271.

Lee, R. B. and Hitchcock, R. K., 2001. African hunter-gatherers: survival, history, and the politics of identitity. *African Study Monographs* S26: 257-280.

Lieberman, D. E., 1996. How and why humans grow thin skulls: experimental evidence for systematic cortical robusticity. *American Journal of Physical Anthropology* 101: 217-236.

Lieberman, D. E., 1998. Neanderthal and early modern human mobility patterns: comparing archaeological and anatomical evidence. In: T. Akazawa, K. Aoki and O. Bar-Yosef (Eds.). *Neanderthals and modern humans in western Asia.* Plenum Press: New York. pp. 263-275.

Lieberman, D. E., 2008. Speculations about the selective basis for modern human craniofacial form. *Evolutionary Anthropology* 17: 55-68.

Lieberman, D. E., 2011. *The evolution of the human head*. The Belknap Press of Harvard University Press: Cambridge, MA.

Lieberman, D. E., Krovitz, G., Yates, F. W., Devlin, M. J. and St. Claire, M., 2004. Effects of food processing on masticatory strain and craniofacial growth in a retrognathic face. *Journal of Human Evolution* 46: 655-677.

Lieberman, D. E., McBratney, B. M. and Krovitz, G., 2002. The evolution and development of cranial form in *Homo sapiens*. *Proceedings of the National Academy of Sciences of the United States of America* 99: 1134-1139.

Lisiecki, L. E. and Raymo, M. E., 2005. A Pliocene-Pleistocene stack of 57 globally distributed benthic $d^{18}O$ records. *Palaeoceanography* 20: PA 1003.

Lockwood, C. A., Lynch, J. M. and Kimbel, W. H., 2002. Quantifying temporal bone morphology of great apes and humans: an approach using geometric morphometrics. *Journal of Anatomy* 201: 447-464.

Lund, V. J., 1988. The maxillary sinus in the higher primates. *Acta Oto-Laryngologica* 105: 163-171.

Lundberg, J. O., 2008. Nitric oxide and the paranasal sinuses. *Anatomical Record* 291: 1479-1484.

McNulty, K. P. 2005. A geometric morphometric assessment of the Hominoid supraorbital region: affinities of the Eurasian Miocene Hominoids *Dryopithecus*, *Graecopithecus*, and *Sivapithecus*. In: D. E. Slice. *Modern morphometrics in physical anthropology.* University of Chicago Press: Chicago. pp. 349-373.

Magori, C. C. and Day, M. H., 1983. Laetoli hominid 18: an early *Homo sapiens* skull. *Journal of Human Evolution* 12: 747-753.

Mallegni, F., Carnieri, E., Bisconti, M., Tartarelli, G., Ricci, S., Biddittu, I., and Segre, A. (2003). *Homo cepranensis sp. nov*. and the evolution of African-European Middle Pleistocene hominids. *Comptes Rendus Palevol* 2: 153-159.

Manica, A., Prugnolle, F. and Balloux, F., 2005. Geography is a better determinant of human genetic differentiation than ethnicity. *Human Genetics* 118: 366-371.

Manning, K., 2010. A developmental history for early West African agriculture. In: P. Allsworth Jones (Eds.). *African archaeology: new developments, new perspectives.* British Archaeological Reports: Oxford. pp. 43-52.

Manzi, G., 2004. Human evolution at the Matuyama-Brunhes boundary. *Evolutionary Anthropology* 13: 11-24.

Manzi, G., Magri, D., Milli, S., Palombo, M. R., Margari, V., Celiberti, V., Barbieri, M., Barbieri, M., Melis, R. T., Rubini, M., Ruffo, M., Saracino, B., Tzedakis, P. C., Zarattini, A. and Biddittu, I., 2010. The new chronology of the Ceprano calvarium (Italy). *Journal of Human Evolution* 59: 580-585.

Manzi, G., Mallegni, F. and Ascenzi, A., 2001. A cranium for the earliest Europeans: Phylogenetic position of the hominid from Ceprano, Italy. *Proceedings of the National Academy of Sciences of the United States of America* 98: 10011-10016.

Marcus, L. F., Corti, M., Loy, A., Naylor, G. J. P., Slice, D. (eds). 1996. *Advances in Morphometrics*. Plenum Press: New York.

Marquez, S., Gannon, P. J., Lawson, W., Reidenberg, J. S. and Laitman, J. T., 2002. Were Neanderthals full of "NO" gas? The relationship between paranasal sinus morphology and nitric oxide production. *American Journal of Physical Anthropology* 117: 107.

Marquez, S., 2008. The paranasal sinuses: the last frontier in craniofacial biology. *Anatomical Record* 261: 1350-1361.

Marquez, S. and Laitman, J. T., 2008. Climatic effects on the nasal complex: a CT imaging, comparative anatomical, and morphometric investigation of *Macaca mulatta* and *Macaca fascicularis*. *Anatomical Record* 291: 1420-1445.

Mataskovna Gouchinova, E.-B., 2006. *The Kalmyks (Caucasus World: People of the Caucasus)*. Routledge: London.

Maureille, B. and Tillier, A. M., 2008. Répartition géographique et chronologique des sépultures néandertaliennes. In: J.-L. Silicani, P. Courtaud, H. Duday and A.

Turq (Eds.). *Première humanité : Gestes funéraires des Néandertaliens.* Musée National de Préhistoire: Les Eyzies-de-Tayac. pp. 66-74.

McBrearty, S. and Brooks, A. S., 2000. The revolution that wasn't: a new interpretation of the origin of modern human behaviour. *Journal of Human Evolution* 39: 453-563.

McDermott, F., Stringer, C., Grün, R., Williams, C. T., Din, V. K. and Hawkesworth, C. J., 1996. New Late-Pleistocene uranium-thorium and ESR dates for the Singa hominid (Sudan). *Journal of Human Evolution* 31: 507-516.

McGregor, D. P., 2007. *Nā Ku'āina: living Hawaiian culture*. University of Hawai'i Press: Honolulu.

McNulty, K. P., 2005. A geometric morphometric assessment of the Hominoid supraorbital region: affinities of the Eurasian Miocene Hominoids *Dryopithecus*, *Graecopithecus*, and *Sivapithecus*. In: D. E. Slice (Eds.). *Modern morphometrics in physical anthropology.* University of Chicago: Chicago. pp. 349-373.

Meyer, H., Schirrmeister, L., Yoshikawa, K., Opel, T., Wetterich, S., Hubberten, H.-W. and Brown, J., 2010. Permafrost evidence for severe winter cooling during the Younger Dryas in northern Alaska. *Geophysical Research Letters* 37: L03501.

Michczynski, A., Eeckhout, P., Pazdur, A. and Pawlyta, J., 2007. Radiocarbon dating of the Temple of the Monkey - the next step towards a comprehensive absolute chronology of Pachacamac, Peru. *Radiocarbon* 49: 565-578.

Mitchell, P., 2006. *Peoples and cultures of Africa: West Africa*. Chelsea House Publishers: New York.

Montgomery, P. Q., Williams, H. O. L., Reading, N. and Stringer, C. B., 1994. An assessment of the temporal bone lesions of the Broken Hill cranium. *Journal of Archaeological Science* 21: 331-337.

Moran, M. D., 2003. Arguments for rejecting the sequential Bonferroni in ecological studies. *Oikos* 100: 403-405.

Morton, S. G., 1839. *Crania Americana; or, a comparative view of the skulls of various aboriginal nations of North and South America.* J. Dobson: Philadelphia.

Morvan, G., Mathieu, P., Vuillemin, V., Guerini, H., Bossard, P., zeiton, F., and Wybier, M. 2011. Standardized way for imagining of the sagittal spinal balance. *European Spine Journal* 20: 602-608.

Moss, M. L., 1962. The functional matrix. In: B. S. Kraus and R. A. Reidel (Eds.). *Vistas in orthodontics.* Lea and Febiger: Philadelphia. pp. 85-98.

Moss, M. L. and Young, R. W., 1960. Functional approach to craniology. *American Journal of Physical Anthropology* 18: 281-292.

Moss Salentijn, L., 1997. Melvin L. Moss and the functional matrix. *Journal of Dental Research* 76: 1814-1817.

Mounier, M. A., 2009. *Validity of the taxon* Homo heidelbergensis *Schoetensack, 1908*. PhD thesis. Facultie de médecine, Université de la Mediterranée, Marseille.

Mounier, A., Condemi, S. and Manzi, G., 2011. The stem species of our species: a place for the archaic human cranium from Ceprano, Italy. *Public library of science ONE* 6: e18821.

Mounier, A., Marchal, F. and Condemi, S., 2009. Is *Homo heidelbergensis* a distinct species? New insight on the Mauer mandible. *Journal of Human Evolution* 56: 219-246.

Movius, H. L., 1969. The Abri de Cro-Magnon, Les Eyzies (Dorgogne), and the probable age of the contained burials on the basis of the evidence of the nearby Abri Pataud. *Anuario de Estudios Atlanticos* 15: 323-344.

Nakagawa, S., 2004. A farewell to Bonferroni: the problems of low statistical power and publication bias. *Behavioural Ecology* 15: 1044-1045.

Nansen, F., 1893. *Eskimo life*. Longmans, Green and Co.: London.

Negus, V. E., 1954. The function of the paranasal sinuses. *Acta Oto-Laryngologica* 44: 408-426.

Noback, M. L., Harvati, K. and Spoor, F., 2011. Climate-related variation of the human nasal cavity. *American Journal of Physical Anthropology* 145: 599-614.

Noback, M. L. 2014. *Diet- and climate-related variation of the human cranium*. PhD dissertation. Senkenberg Centre for Human Evolution and Palaeoenvironment, Eberhard Karls Universität, Tübingen.

Nowaczewska, W., Dabrowski, P. and Kuzminski, L., 2011. Morphological adaptation to climate in modern *Homo sapiens* crania: the importance of basicranial breadth. *Collegium Antropologicum* 35: 625-636.

Oakley, K. P., Campbell, B. G., and Molleson, T. I., 1967. *Catalogue of fossil hominids. Part III: Americas, Asia, Australasia*. The British Museum (Natural History): London.

O'Connor, C. F., Franciscus, R. G. and Holton, N. E., 2005. Bite force production capability and efficiency in Neandertals and modern humans. *American Journal of Physical Anthropology* 127: 129-151.

O'Higgins, P., 2000. The study of morphological variation in the hominid fossil record: biology, landmarks and geometry. *Journal of Anatomy* 197: 103-120.

O'Higgins, P., Bastir, M. and Kupczik, K., 2006. Shaping the human face. *International Congress Series* 1296: 55-73.

O'Higgins, P. and Jones, N., 1998. Facial growth in *Cercocebus torquatus*: An application of three dimensional geometric morphometric techniques to the study of morphological variation. *Journal of Anatomy* 193: 251-272.

Palubeckaité, Z., 2001. Patterns of linear enamel hypoplasia in Lithuanian Iron Age population. *Variability and Evolution* 9: 75-87.

Pan, R. and Oxnard, O. E., 2002. Craniodental variation among Macaques (*Macaca*), nonhuman primates. *Evolutionary Anthropology* 2: 10-22.

Paschetta, C., de Azevedo, S., Castillo, L., Martinez-Abadias, N., Hernandez, M., Lieberman, D. E. and Gonzalez-Jose, R., 2010. The influence of masticatory loading on craniofacial morphology: a test case across technological transitions in the Ohio Valley. *American Journal of Physical Anthropology* 141: 297-314.

Passey, B. H., Levin, N. E., Cerling, T. E., Brown, F. H. and Eiler, J. M., 2010. High-temperature environments of human evolution in East Africa based on bond ordering in paleosol carbonates. *Proceedings of the National Academy of Sciences of the United States of America* 107: 11245-11249.

Pearce, E. and Dunbar, R., 2012. Latitudinal variation in light levels drives human visual system size. *Biology Letters* 8: 90-93.

Pearson, O. M., 2008. Statistical and biological definitions of "anatomically modern" humans: suggestions for a unified approach to modern morphology. *Evolutionary Anthropology* 17: 38-48.

Pearson, O. and Lieberman, D. E., 2004. The aging of Wolff's "Law". Ontogeny and responses to mechanical loading in cortical bone. *Yearbook of Physical Anthropology* 47: 63-99.

Perdue, P. C., 1998. Boundaries, maps, and movement: Chinese, Russian, and Mongolian empires in early modern Central Eurasia. *The International History Review* 20: 263-286.

Pérez-Barbería, J., Shultz, S. and Dunbar, R., 2007. Evidence for intense coevolution of sociality and brain size in three orders of mammals. *Evolution* 61: 2811-2821.

Pettitt, P., 2011. *The Palaeolithic origins of human burial*. Routledge: New York, USA.

Pettitt, P. B., 2002. The Neanderthal dead: exploring mortuary variability in Middle Palaeolithic Eurasia. *Before Farming: The Anthropology of Hunters-gatherers* 1: 1-19.

Piperno, D. R., 2011. The origins of plant cultivation and domestication in the new world tropics: patterns, process, and new developments. *Current Anthropology* 52: S453-S470.

Plavcan, J. M., 2000. Inferring social behaviour from sexual dimorphism in the fossil record. *Journal of Human Evolution* 39: 327-344.

Plavcan, J. M., 2001. Sexual dimorphism in primate evolution. *Yearbook of Physical Anthropology* 44: 25-53.

Plavcan, J. M., 2002. Taxonomic variation in the patterns of craniofacial dimorphism in primates. *Journal of Human Evolution* 42: 579-608.

Plomley, N. J. B., 1983. *The Baudin expedition and the Tasmanian Aborigines 1802*. Blubberhead Press: Hobart.

Preuschoft, H., Witte, H. and Witzel, U., 2002. Pneumatized spaces, sinuses and spongy bones in the skulls of primates. *Annals of Anatomy* 60: 67-79.

Prossinger, H., Bookstein, F., Schafer, K. and Seidler, H., 2000. Reemerging stress: supraorbital torus morphology in the mid-sagittal plane? *Anatomical Record* 261: 170-172.

Prossinger, H., Seidler, H., Wicke, L., Weaver, D., Recheis, W., Stringer, C. and Müller, G., 2003. Electronic removal of encrustations inside the Steinheim cranium reveals paranasal sinus features and deformations, and provides a revised endocranial volume estimate. *Anatomical Record* 273B: 132-142.

Prüfer, K., Racimo, F., Patterson, N., Jay, F., Sankararaman, S., Sawyer, S., Heinze, A., Renaud, G., Sudmant, P. H., de Filippo, C., Li, H., Mallick, S., Dannemann, M., Fu, Q., Kircher, M., Kuhlwilm, M., Lachmann, M., Meyer, M., Ongyerth, M., Siebauer, M., Theunert, C., Tandon, A., Moorjani, P., Pickrell, J., Mullikin, J. C., Vohr, S. H., Green, R. E., Hellmann, I., Johnson, P. L. F., Blanche, H., Cann, H., Kitzman, J. O., Shendure, J., Eichler, E. E., Lein, E. S., Bakken, T. E., Golovanova, L. V., Doronichev, V. B., Shunkov, M. V., Derevianko, A. P., Viola, B., Slatkin, M., Reich, D., Kelso, J. and Paabo, S., 2014. The complete genome sequence of a Neanderthal from the Altai Mountains. *Nature* 505: 43-49.

Pucciarelli, H. M., Ramirez Rozzi, F. V., Mune, M. C. and Sardi, M. L., 2006. Variation of functional cranial components in six Anthropoidea species. *Zoology* 109: 231-243.

Rae, T. C., 1999. The maxillary sinus in primate paleontology and systematics. In: T. Koppe, H. Nagai and K. W. Alt (Eds.). *The paranasal sinuses of higher primates.* Quintessence Books Co. Inc.: Chicago. pp. 177-189.

Rae, T. C., 2008. Paranasal pneumatization in extant and fossil Cercopithecoidea. *Journal of Human Evolution* 54: 279-86.

Rae, T., Hill, R., Hamada, Y. and Koppe, T., 2003. Clinal variation of maxillary sinus volume in Japanese macaques (*Macaca fuscata*). *American Journal of Primatology* 59: 153-158.

Rae, T. C. and Koppe, T., 2000. Isometric scaling of maxillary sinus volume in hominoids. *Journal of Human Evolution* 38: 411-423.

Rae, T. C. and Koppe, T., 2004. Holes in the head: evolutionary interpretations of the paranasal sinuses in catarrhines. *Evolutionary Anthropology* 13: 211-223.

Rae, T. C. and Koppe, T., 2008. Independence of biomechanical forces and craniofacial pneumatization in *Cebus*. *Anatomical Record* 291: 1414-1419.

Rae, T. C. and Koppe, T., 2014. Sinuses and flotation: Does the aquatic ape theory hold water? *Evolutionary Anthropology* 23: 60-64.

Rae, T. C., Koppe, T., Spoor, F., Benefit, B. and McCrossin, M., 2002. Ancestral loss of the maxillary sinus in Old World monkeys and independent acquisition in *Macaca*. *American Journal of Physical Anthropology* 117: 293-296.

Rae, T. C., Koppe, T. and Stringer, C. B., 2011. The Neanderthal face is not cold adapted. *Journal of Human Evolution* 60: 234-239.

Rae, T. C., Viðarsdóttir, U. S., Jeffery, N. and Steegmann, A. T., 2006. Developmental response to cold stress in cranial morphology of *Rattus*: implications for the interpretation of climatic adaptation in fossil hominins. *Proceedings of the Royal Society B* 273: 2605-2610.

Rak, Y., 1986. The Neandertal – a new look at an old face. *Journal of Human Evolution* 15: 151-164.

Ramachandran, S., Deshpande, O., Roseman, C. C., Rosenberg, N. A., Feldman, M. W. and Cavalli-Sforza, L. L., 2005. Support from the relationship of genetic and geographic distance in human populations for a serial founder effect originating in Africa. *Proceedings of the National Academy of Sciences USA* 102: 15942-15947.

Ravosa, M. J., Vinyard, C. J. and Hylander, W. L., 2000. Stressed out: masticatory forces and primate circumorbital form. *Anatomical Record* 261: 173-175.

Reddy, D. P., Harvati, K. and Kim, J., 2005. An alternative approach to space curve analysis using the example of the Neanderthal occipital bun. In: D. E. Slice (Eds.). *Modern morphometrics in physical anthropology.* Kluwer Academic/Plenum Publishers: New York. pp. 99-116.

Relethford, J. H., 2010. Population-specific deviations of global human craniometric variation from a neutral model. *American Journal of Physical Anthropology* 142: 105-111.

Reynolds, A. J. 2006., *Keeping culture*. National Museum of Australia Press: Hobart.

Rhŷs Evans, P., 1992. The paranasal sinuses and other enigmas: an aquatic evolutionary theory. *The Journal of Laryngology and Otology* 106: 214-225.

Rightmire, G. P., 1996. The human cranium from Bodo, Ethiopia: Evidence for speciation in the Middle Pleistocene? *Journal of Human Evolution* 31: 21-39.

Rightmire, G. P., 1998. Human evolution in the Middle Pleistocene: the role of *Homo heidelbergensis. Evolutionary Anthropology* 6: 218-227.

Rightmire, G. P., 2001. Comparison of middle Peistocene hominids from Africa. In: L. Barham and K. Robson-Brown (Eds.). *Human roots: Africa and Asia in the*

middle Pleistocene. Western Academic and Specialist Press Ltd.: Bristol. pp. 123-133.

Rightmire, G. P., 2008. *Homo* in the Middle Pleistocene: hypodigms, variation, and species recognition. *Evolutionary Anthropology* 17: 8-21.

Rightmire, G. P., 2013. *Homo erectus* and Middle Pleistocene hominins: Brain size, skull form, and species recognition. *Journal of Human Evolution* 65: 223-252.

Rink, W. J., Schwarcz, H. P., Smith, F. H. and Radovčić, J., 1995. ESR ages for Krapina hominids. *Nature* 378:

Roberts, C. A., 2007. A bioarcheological study of maxillary sinusitis. *American Journal of Physical Anthropology* 133: 792-807.

Rosas, A. and Bermúdez de Castro, J. M., 1997. The Mauer mandible and the evolutionary significance of *Homo heidelbergensis*. *Geobios* 31: 687-697.

Roseman, C. C., 2004. Detecting interregionally diversifying natural selection on modern human cranial form by using matched molecular and morphometric data. *Proceedings of the National Academy of Sciences USA* 101: 12824-12829.

Roseman, C. C. and Weaver, T. D., 2004. Multivariate apportionment of global human craniometric diversity. *American Journal of Physical Anthropology* 125: 257-63.

Ross, C. F. and Metzger, K. A., 2004. Bone strain gradients and optimization in vertebrate skulls. *Annals of Anatomy* 186: 387-396.

Ruff, C., Holt, B. and Trinkaus, E., 2006. Who's afraid of the big bad Wolff?: "Wolff's Law" and bone functional adaptation. *American Journal of Physical Anthropology* 129: 498.

Sánchez-Goñi, M. F., Chacho, I., Turon, J.-L., Guinot, J., Sierro, F. J., Peypouquet, J.-P., Grimault, J. O. and Shackelton, N. J., 2002. Synchroneity between marine and terrestrial responses to millenial scale climate variability during the last glacial period in the Mediterranean region. *Climate Dynamics* 19: 95-105.

Sanchez-Quinto, F., Botigue, L. R., Civit, S., Arenas, C., Avila-Arcos, M. C., Bustamente, C. D., Comas, D. and Lalueza-Fox, C., 2013. North African populations carry the signature of admixture with Neandertals. *Public library of science ONE* 7: e47765.

Sardi, M. L., Novellino, P. and Pucciarelli, H. M., 2006. Craniofacial morphology in the Argentine Centre-West: consquences of the transition to food production. *American Journal of Physical Anthropology* 130: 333-343.

Schmit, M. W. and Hertzberg, J. E., 2011. Abrupt climate change during the last Ice Age. *Nature Education Knowledge* 3: 11-19.

Schmitz, R. W., Serre, D., Bonani, G., Feine, S., Hillgruber, F., Krainitzki, H., Pääbo, S. and Smith, F. H., 2002. The Neandertal type site revisited: Interdisciplinary investigations of skeletal remains from the Neander Valley, Germany. *Proceedings of the National Academy of Sciences USA* 99: 13342-13347.

Schoetensack, O., 1908. *Der Unterkiefer des Homo heidelbergensis aus dem Sanden von Mauer bei Heidelberg: ein Beitrag zur Paläontologie des Menschen.* Wilhelm Engelmann: Leipzig.

Schultz, S. and Maslin, M., 2013. Early human speciation, brain expansion and dispersal influenced by African climate pulses. *Public library of science ONE* 8: e76750.

Schwarcz, H. P., Bietti, A., Buhay, W. M., Stiner, M. C., Grun, R. and Segre, A., 1991. On the reexamination of Grotta Guattari: uranium-series and electron-spin-resonance dates. *Current Anthropology* 32: 313-316.

Schwartz, J. H. and Tattersall, I. 2002. *The human fossil record: craniodental morphology of genus* Homo *volume two (Africa and Asia).* Wiley-Liss: Hoboken

Schwartz, J. H., Tattersall, I. and Teschler-Ncola, M., 2008. Architecture of the nasal complex in Neanderthals: comparison with other hominids and phylogenetic significance. *Anatomical Record* 291: 1517-1534.

Seidler, H., Falk, D., Stringer, C., Wilfing, H., Muller, G. B., zur Nedden, D., Weber, G. W., Reicheis, W. and Arsuaga, J. L., 1997. A comparative study of stereolithographically modelled skulls of Petralona and Broken Hill: Implications for future studies of middle Pleistocene hominid evolution. *Journal of Human Evolution* 33: 691-703.

Shaw, C. N. and Stock, J. T., 2009. Habitual throwing and swimming correspond with upper limb diaphyseal strength and shape in modern human athletes. *American Journal of Physical Anthropology* 140: 160-172.

Shea, B. T., 1977. Eskimo craniofacial morphology, cold stress and maxillary sinus. *American Journal of Physical Anthropology* 47: 289-300.

Sherwood, R. J., Ward, S. C. and Hill, A., 2002. The taxonomic status of the Chemeron temporal (KNM-BC 1). *Journal of Human Evolution* 42: 153-184.

Singleton, M., 2002. Patterns of cranial shape variation in the Papionini (Primates: Cercopithecinae). *Journal of Human Evolution* 42: 547-578.

Singleton, M., 2004. Geometric morphometric analysis of functional divergence in mangabey facial form. *Journal of Archaeological Science* 82: 29-46.

Singleton, M., 2005. Functional shape variation in the cercopithecine masticatory complex. In: D. E. Slice (Eds.). *Modern morphometrics in physical anthropology.* Kluwer Academic/Plenum Publishers: New York. pp. 319-348.

Slice, D. E., 2007. Geometric morphometrics. *Annual Review of Anthropology* 36: 261-281.

Smith, F. H., 1976a. Behavioral interpretation of changes in craniofacial morphology across the archaic/modern *Homo sapiens* transition. In: E. Trinkaus (Eds.). *The Mousterian Legacy.* Archaeopress: Oxford. pp.

Smith, F. H., 1976b. On anterior tooth wear at Krapina and Ochoz. *Current Anthropology* 17: 167-168.

Smith, H. F., Terhune, C. E. and Lockwood, C. A., 2007a. Genetic, geographic, and environmental correlates of human temporal bone variation. *American Journal of Physical Anthropology* 134: 312-322.

Smith, T. D., Rossie, J. B. and Bhatnagar, K. P., 2007b. Evolution of the nose and nasal skeleton in primates. *Evolutionary Anthropology* 16: 132-146.

Sokal, R. R. and Rohlf, F. J., 1995. *Biometry: the principals and practice of statistics in biological*
research. W. H. Freeman: New York.

Spoor, F. and Stringer, C., 1998. Rare temporal bone pathology of the Singa calvaria from Sudan. *American Journal of Physical Anthropology* 107: 41-50.

Stannard, D. E., 1989. *Before the horror: the population of Hawai'i on the eve of Western contact*. Social Science Research Institute, University of Hawaii: Honolulu.

Steegmann, A. T. and Platner, W. S., 1968. Experimental cold modification of cranio-facial morphology. *American Journal of Physical Anthropology* 28: 17-30.

Stewart, J. R., 2004. Neanderthal – modern human competition? A comparison between the mammals associated with middle and Upper Palaeolithic industries in Europe during OIS 3. *International Journal of Osteoarchaeology* 14: 178-189.

Stewart, J., R., 2005. The ecology and adaptation of Neanderthals during the non-analogue environment of Oxygen Isotope Stage 3. *Quaternary International* 137: 35-46.

Stock, J. T., 2006. Hunter-gatherer postcranial robusticity relative to patterns of mobility, climatic adaptation and selection for tissue economy. *American Journal of Physical Anthropology* 131: 194-204.

Stock, J. T., 2008. Are humans still evolving? *EMBO Reports* 9: ss1-ss4.

Stock, J. T. and Buck, L. T., 2010. Canalization and plasticity in humans and primates: implications for interpreting the fossil record. In: A. Perote Alejandre and A. Mateos Cachorro (Eds.). *150 años después de Darwin: evolución, future o crisis? Lecciones sobre evolución humana.* Instituto Tomás Pascual Sanz, Centro Nacional de Investigación sobre la Evolución Humana: Madrid. pp. 91-102.

Street, M., Terberger, T. and Orschiedt, J., 2006. A critical review of the German Paleolithic hominin record. *Journal of Human Evolution* 51: 551-579.

Stringer, C., 1974. Population relationships of later Pleistocene hominids: a multivariate study of available crania. *Journal of Archaeological Science* 1: 317-342.

Stringer, C., 1979. A re-evaluation of the fossil human calvaria from Singa, Sudan. *Bulletin of the British Museum (Natural History), Geology Series* 32: 77-83.

Stringer, C. B., 1983. Some further notes on the morphology and dating of the Petralona hominid. *Journal of Human Evolution* 12: 731-742.

Stringer, C., 1984. The definition of *Homo erectus* and the existence of the species in Africa and Europe. *Courier Forschungsunstitut Senckenberg* 69: 131-144.

Stringer, C., 1985. Middle Pleistocene hominid variability and the origin of late Pleistocene humans. In: E. Delson (Eds.). *Ancestors: the hard evidence.* Alan R. Liss: New York. pp. 289-295.

Stringer, C. B., 1994. Out of Africa - a personal history. In: M. Nitecki and D. V. Nitecki (Eds.). *Origins of Anatomically Modern Humans.* Plenum Press: New York. pp. 151-172.

Stringer, C. B., 1996. Current issues in modern human origins. In: W. E. Meikle, F. C. Howell and N. Jablonski (Eds.). *Contemporary Issues in Human Evolution.* California Academy of Sciences Memoir: pp. 115-134.

Stringer, C. B., 2002b. Modern human origins: progress and prospects. *Philosophical Transactions of the Royal Society B: Biological Sciences* 357: 563-79.

Stringer, C., 2011. The chronological and evolutionary postion of the Broken Hill cranium. *American Journal of Physical Anthropology* 144: 287.

Stringer, C., 2012a. Evolution: what makes a modern human. *Nature* 485: 33-35.

Stringer, C., 2012b. *Lone survivors*. Times Books: New York.

Stringer, C., 2012c. The status of *Homo heidelbergensis* (Schoetensack, 1908). *Evolutionary Anthropology* 21: 101-107.

Stringer, C., 2012d. What makes a modern human. *Nature* 485: 33-35.

Stringer, C. B. and Buck, L. T., 2014. Diagnosing *Homo sapiens* in the fossil record. *Annals of Human Biology* 41: 312-322.

Stringer, C. B., Finlayson, J. C., Barton, R. N. E., Fernández-Jalvo, Y., Cáceres, I., Sabin, R. C., Rhodes, E. J., Currant, A. P., Rodríguez-Vidal, J., Giles-Pacheco,

F. and Riquelme-Cantal, J. A., 2008. Neanderthal exploitation of marine mammals in Gibraltar. *Proceedings of the National Academy of Sciences USA*105: 14319-14324.

Stringer, C. B., Hublin, J.-J. and Vandermeersch, B., 1984. The origin of anatomically modern humans in Western Europe. In: F. Smith and F. Spencer (Eds.). *The origins of modern humans.* Liss: New York. pp. 51-135.

Ströhle, A. and Hahn, A., 2011. Diets of modern hunter-gatherers vary substantially in their carbohydrate content depending on ecoenvironments: results from an ethnographic analysis. *Nutrition Research* 31: 429-435.

Swindler, D. R., 1999. Maxillary sinuses, dentition, diet and arch form in some anthropoid primates. In: T. Koppe, H. Nagai and K. W. Alt (Eds.). *Paranasal sinuses in higher primates: development, function and evolution.* Quintessence: Chicago. pp. 91-206.

Systat Software. 2013. *SigmaPlot 12.5*. San Jose: Systat Software.

Tattersall, I., 2007. Neanderthals, *Homo sapiens*, and the question of species in paleoanthropology. *Journal of Anthropological Sciences* 85: 139-146.

Tattersall, I. and Schwartz, J. H., 1998. Morphology, paleoanthropology, and Neanderthals. *Anatomical Record* 253: 113-117.

Tattersall, I. and Schwartz, J. H., 2006. The distinctiveness and systematic context of *Homo neanderthalensis*. In: K. Harvati and T. Harrison (Eds.). *Neanderthals revisited: New approaches and perspectives.* Springer: Berlin. pp. 9-22.

Tillier, A. M., 1975. *Les sinus craniens chez les hommes actuels et fossiles: essai d'interpretation*. Doctorat de 3eme Cycle. Univerisite de Paris VI, Paris.

Tillier, A. M., 1977. La pneumatisation du massif cranio-facial chez les hommes actuels et fossiles (suite). *Bulletins et Mémoires de la Société d'anthropologie de Paris* 4: 287-316.

Trauth, M. H., Deino, A. L., Bergner, A. G. N. and Strecker, M. R., 2003. East African climate change and orbital forcing during the last 175 kyr BP. *Earth and Planetary Science Letters* 206: 297-313.

Trinkaus, E., 1981. Neanderthal limb proportions and cold adaptation. In: C. B. Stringer (Eds.). *Aspects of Human Evolution.* Taylor and Francis: London. pp. 187-224.

Trinkaus, E., 1983. Functional aspects of Neandertal pedal remains. *Foot and Ankle International* 3: 377-390.

Trinkaus, E., 1986. The Neandertals and modern human origins. *Annual Review of Anthropology* 15: 193-218.

Trinkaus, E., 1987. The Neandertal face: evolutionary and functional perspectives on a recent hominid face. *Journal of Human Evolution* 16: 429-443.

Trinkaus, E., 2003. Neandertal faces were not long; modern human faces are short. *Proceedings of the National Academy of Sciences of the United States of America* 100: 8142-8145.

Trinkaus, E., 2006. Modern human versus Neandertal evolutionary distinctiveness. *Current Anthropology* 47: 597-620.

Tückmantel, S., Röllin, A., Müller, A. E. and Soligo, C., 2009. Facial correlates of frontal bone pneumatisation in strepsirrhine primates. *Mammalian Biology* 74: 25-35.

Twine, R., 2002. Physiognomy, phrenology and the temporality of the body. *Body and Society* 8: 67-88.

Ungar, P. S., Fennell, K. J., Gordon, K. and Trinkaus, E., 1997. Neandertal incisor beveling. *Journal of Human Evolution* 32: 407-421.

van Andel, T. H., Davies, W. and Weninger, B., 2003. The human presence in Europe during the last glacial period I: human migrations and the changing climate. In: T. H. van Andel and W. Davies (Eds.). *Neanderthals and modern humans in the European landscape during the last glaciation.* McDonald Institute for Archaeological Research: Cambridge. pp. 31-56.

van Andel, T. H. and Tzedakis, P. C., 1996. Palaeolithic landscapes of Europe and environs 150,000-25,000 years ago: an overview. *Quaternary Science Reviews* 15: 481-500.

van Vark, G., 1995. The study of hominid skeletal remains by means of statistical methods. In: N. T. Boaz and L. D. Wolfe (Eds.). *Biological Anthropology: the state of the science.* International Institute for Human Evolutionary Research: Bend. pp. 71-90.

Vandersmeersch, B., 1985. The origin of the Neandertals. In: E. Delson (Eds.). *Ancestors: the hard evidence.* Alan R. Liss: New York. pp. 306-309.

Vialet, A., Guipert, G., Alçiçek, M. C. and de Lumley, M.-A., 2014. La calotte crânienne de l'*Homo erectus* de Kocabaş (Bassin de Denizli, Turquie). *L'Anthropologie* 118: 74-107.

Vialet, A., Guipert, G., Jianing, H., Xiaobo, F., Zune, L., Youping, W., Tianyuan, L., de Lumley, M. A. and de Lumley, H., 2010. *Homo erectus* from the Yunxian and Nankin Chinese sites: anthropological insights using 3D virtual imaging techniques. *Comptes Rendus Palevol* 9: 331-339.

Viguier, B., 2004. Functional adaptations in the craniofacial morphology of Malagasy primates: shape variations associated with the family Cheirogaleidae. *Annals of Anatomy* 186: 495-500.

Vinyard, C. J. and Smith, F. H., 1997. Morphometric relationships between the supraorbital region and frontal sinus in Melanesian crania. *Homo* 48: 1-21.

Vlček, E., 1967. Die Sinus frontales bei Europaeischen Neandertalen. *Annals of Anatomy* 30: 166-189.

von Cramon-Taubadel, N., 2009. Congruences of individual cranial bone morphology and neutral affinity patterns in modern humans. *American Journal of Physical Anthropology* 140: 205-215.

von Cramon-Taubadel, N. 2011. The relative efficiency of functional and developmental cranial modules for reconstructing global human population history. *American Journal of Physical Anthropology* 146: 83-93.

Waddington, C. H., 1942. Canalisation of development and the inheritance of acquired characters. *Nature* 150: 563-565.

Wagner, G. A., Krbetschek, M., Degering, D., Bahain, J.-J., Shao, Q., Falguères, C., Voinchet, P., Dolo, J.-M., García, T. and Rightmire, G. P., 2010. Radiometric dating of the type-site for *Homo heidelbergensis* at Mauer, Germany. *Proceedings of the National Academy of Sciences USA* 107: 19726-19730.

Wang, Q., Wright, B. W., Smith, A., Chalk, J. and Byron, C. D., 2010. Mechanical impact of incisor loading on the primate midfacial skeleton and its relevance to human evolution. *Anatomical Record* 293: 607-617.

W. B. G., 2013. World Bank Group. *Climate Change Knowledge Portal*. http://sdwebx.worldbank.org/climateportal/index.cfm?page=global_map. Accessed 11/2013-01/2014.

Weaver, T. D., 2009. The meaning of neandertal skeletal morphology. *Proceedings of the National Academy of Sciences of the United States of America* 106: 16028-33.

Weaver, T. D., Roseman, C. C. and Stringer, C. B., 2007. Were Neandertal and modern human cranial differences produced by natural selection or genetic drift? *Journal of Human Evolution* 53: 135-45.

Weber, G. W., Schafer, K., Prossinger, H., Gunz, P., Mitterocker, P. and Seidler, H., 2001. Virtual anthropology: the digital evolution in anthropological sciences. *Journal of Physiological Anthropology and Applied Human Science* 20: 69-80.

Webster, D. B., 1966. Ear structure and function in modern mammals. *American Zoologist* 6: 451-466.

Weidenreich, D., 1943. *The skull of* Sinanthropus pekinensis*; a comparative study on a new primitive hominid skull*. Geological Survey of China: Pehpei, Chungking.

Weidenreich, D., 1951. *Morphology of Solo Man*. The American Museum of Natural History: New York.

Weiner, J. S., 1954. Nose shape and climate. *American Journal of Physical Anthropology* 12: 615-8.

Wells, J. C. K. and Stock, J. T., 2007. The biology of the colonising ape. *Yearbook of Physical Anthropology* 50: 191-222.

White, T. D. and Folkens, P. A., 2005. *The human bone manual*. Elsevier Academic Press: Burlington, MA.

Willis, K. J. and MacDonald, G. M., 2011. Long-term ecological records and their relevance to climate predictions for a warmer world. *Annual Review of Ecology, Evolution and Systematics* 42: 267-287.

Witmer, 1999. The phylogenetic history of paranasal sinuses. In: T., Koppe, H., Nagai and K. W., Alt. *The paranasl sinuses of higher primates: development, function, and evolution.* pp. 21-34

Wolpoff, M. H., 1968. Climatic influence on the skeletal nasal aperture. *American Journal of Physical Anthropology* 29: 405-424.

Wolpoff, M. H., 1999. *Paleoanthropology*. McGraw-Hill: New York.

Woodward, A. S. 1921. A new cave man from Rhodesia, South Africa. *Nature* 108: 371-372.

Woltering, M., Johnson, T. C., Werne, J. P., Schouten, S. and Sinninghe Damasté, J. S., 2011. Late Pleistocene temperature history of Southeast Africa: a TEX_{86} temperature record from Lake Malawi. *Palaeogeography, Palaeoclimatology, Palaeoecology* 303: 93-102.

Wood, B. and Lieberman, D. E., 2001. Craniodental variation in *Paranthropus boisei*: a developmental and functional perspective. *American Journal of Physical Anthropology* 116: 13-25.

Wu, X. and Poirier, F. E., 1995. *Human evolution in China: A metric description of the fossils and a review of the sites.* Oxford University Press: Oxford.

Zelditch, M. L., Swiderski, D. L. and Sheets, H. D., 2004. *Geometric morphometrics for biologists: a primer.* Academic Press: San Diego, CA.

Zhao, Z., 2011. New archaeobotanic data for the study of the origins of agriculture in China. *Current Anthropology* 52: S295-S306.

Zizumbo-Villarreal, D. and Colunga-GarcíaMarín, P., 2010. Origin of agriculture and plant domestication in West Mesoamerica. *Genetic Resources and Crop Evolution* 57: 813-825.

Zollikofer, C. P. E., Ponce de León, M. S. and Martin, R. D., 1998. Computer-assisted paleoanthropology. *Evolutionary Anthropology* 6: 41-54.

Zollikofer, C., Ponce de León, M., Schmitz, R. and Stringer, C., 2008. New insights into Mid-Late Pleistocene fossil hominin paranasal sinus morphology. *Anatomical Record* 291: 1506-1516.

Zollikofer, C. P. and Weissmann, J. D., 2008. A morphogenetic model of cranial pneumatization based on the invasive tissue hypothesis. *Anatomical Record* 291: 1446-1454.